

STRUCTURE AND CHEMISTRY OF
RETINYLIDENE IMINIUM SALTS AND
RELATED SYSTEMS

By

GEORGE RICHARD ELIA

A Thesis

Submitted to the School of Graduate Studies

in Partial Fulfilment of the Requirements

for the Degree

Doctor of Philosophy

McMaster University

April, 1993

**STRUCTURE AND CHEMISTRY OF
RETINYLIDENE IMINIUM SALTS AND
RELATED SYSTEMS**

DOCTOR OF PHILOSOPHY (1993)

MCMASTER UNIVERSITY
Hamilton, Ontario

TITLE: Structure and Chemistry of Retinylidene Iminium Salts and Related Systems

AUTHOR: George Richard Elia, B.Sc. (McMaster University)

SUPERVISOR: Professor R. F. Childs

NUMBER OF PAGES: xvii, 224

ABSTRACT

This thesis embodies an investigation into the structure and thermal isomerizations of retinylidene iminium salts and related systems. Over the past three decades there has been a tremendous amount of interest surrounding the structurally related natural pigments rhodopsin and bacteriorhodopsin. Studies of these compounds have had a large impact in the fields of bioenergetics and visual photochemistry. Both of these proteins consist of a protonated Schiff base linkage between the retinal chromophore and the protein.

A series of retinylidene iminium salts were synthesized and characterized both in solution and the solid state. A unique combination of x-ray crystallography, solid state ^{13}C NMR, FTIR and UV spectroscopic techniques were used in order to address the mechanism by which the protein can modify the electronic properties of the retinal chromophore in the ground state. One important conclusion of this study was that wavelength and positive charge delocalization in retinylidene iminium salts can primarily be modified by varying the distance between the anion and the proton bonded to the Schiff base nitrogen atom. It was also found that most of the positive charge in these systems is located on the nitrogen atom and the proton to which it is bonded.

The thermal *cis-trans* isomerization about the C11-C12 bond of a series of retinylidene iminium salts was investigated by high field ^1H NMR spectroscopy at ambient temperatures. It was found that the isomerizations proceeded via nucleophilic

catalysis by the counterion present in the salt. No 11-*cis* isomer was detected at thermodynamic equilibrium for all of the salts examined.

The thermal reactivity of the isoelectronic protonated poly-unsaturated aldehydes were also examined by high field ¹H NMR spectroscopy. In contrast to the observed iminium salt chemistry, it was found that these species cyclized completely in superacidic media to form cyclopentene ring moieties. It was found that the rate determining step in these reactions involves additional protonation on the oxygen atom to form a dication.

ACKNOWLEDGEMENTS

I would like to extend sincere gratitude to my research supervisor Dr. R. F. Childs. Despite his hectic schedule, his interest and enthusiasm through the course of this work was unceasing. His guidance and support during the experimental work and during the writing of this thesis is greatly appreciated.

The members of the NMR facility at McMaster, Dr. Don Hughes, Brian Sayer and Ian Thompson, provided exceptional assistance on the many NMR experiments conducted, and for this I am grateful. I would also like to thank Dr. Jim Britten, Dr. Daniel Yang and Dr. Bernie Santarsiero for their expertise in the crystallographic determinations.

The light-hearted atmosphere in the lab provided a very enjoyable environment. I would particularly like to thank my friends Brad, John and Teresa- those chili con carne nights will never be forgotten.

I am forever thankful to Mom, Dad and Mike for their incessant support and encouragement from the beginning. Their belief in the merits of education made everything worthwhile.

Finally, I would like to extend a very special and sincere thank you to Marianne, my wife. Having recently gone through it all herself, she truly understood the trials and tribulations of these past few years. Her constant love, encouragement and good advice played an important part in the completion of this work.

for Marianne,
and for Mom, Dad and Mike

TABLE OF CONTENTS

	<u>Page</u>
Descriptive Note	ii
Abstract	iii
List of Tables	xi
List of Figures	xiv
List of Abbreviations	xvi
<u>CHAPTER 1</u> - Introduction - Part I	1
Bacteriorhodopsin	3
Photochemical/Thermal Cycle	3
Conformation of Retinal in Bacteriorhodopsin	7
Structure of the Protein	10
Absorption Studies	13
External Point Charge Model	16
Thermal Chemistry	20
Statement of Problem	28
Introduction - Part II	
Protonated Unsaturated Carbonyl Compounds	32
Reactions of Protonated Unsaturated Carbonyl Compounds	35
Statement of Problem	40

TABLE OF CONTENTS (con't)

RESULTS AND DISCUSSION

CHAPTER 2 - The Structure of Retinylidene Iminium Salts 42

RESULTS

Preparation of Iminium Salts	43
¹ H NMR Spectroscopy	48
Solution ¹³ C NMR Spectroscopy	48
Solid State ¹³ C NMR Spectroscopy	51
Absorption Spectroscopy	
Solution Spectra	53
Solid State Spectra	53
X-ray Crystallographic Structure Determinations	55

DISCUSSION

X-ray Crystallography	70
Cation/Anion Interactions	76
Location of the Anion	77
Effect of Anion on ¹³ C NMR Spectra	83
Conformation	89
Effect of Cation/Anion Placement on UV/VIS Absorption Spectra	91
Summary	93

TABLE OF CONTENTS (con't)

<u>CHAPTER 3</u> - Thermally Induced Isomerizations of Retinylidene Iminium Salts	95
<u>RESULTS</u>	
Preparation and Characterization	96
<i>Cis/Trans</i> Isomerization of Retinylidene Iminium Salts	102
Thermodynamic Equilibria	104
<u>DISCUSSION</u>	
Thermal Isomerization	106
Thermal Equilibria	111
Summary	112
<u>CHAPTER 4</u> - Thermal Isomerizations of Unsaturated Iminium Salts and Corresponding Protonated Poly-Unsaturated Aldehydes	115
<u>RESULTS</u> - Part I - Octatrienyl Iminium Salts	
Preparation and Characterization	115
Kinetics of <i>Cis/Trans</i> Isomerization	124
<u>DISCUSSION</u>	
Mechanism of Isomerization	126
<u>RESULTS</u> - Part II - Protonated Poly-Unsaturated Aldehydes	
Preparation and Characterization	133
Thermal Isomerizations	139

TABLE OF CONTENTS (con't)

Kinetic Measurements	141
 <u>DISCUSSION</u>	
Mechanism of Cyclization	143
Summary	151
 <u>CHAPTER 5 - Experimental Methods</u>	
Materials	156
Instrumentation	
¹ H NMR Spectroscopy	156
Solution State ¹³ C NMR Spectroscopy	157
Solid State ¹³ C NMR Spectroscopy	157
Infrared Spectra	158
Centrifugal Chromatography	158
Synthesis	158
3-methyl-2,4,6-octatrienal, 44	159
N-t-butyl-3-methyl-2,4,6-octatrienyldene imine, 45	159
N-t-butyl-3-methyl-2,4,6-octatrienyldene iminium triflate, 46	160
N-n-butyl-retinyldene iminium triflate, 50	160
N-t-butyl-retinyldene iminium perchlorate, 51	160

TABLE OF CONTENTS (con't)

N-t-butyl-retinylidene iminium triflate, 52	160
N,N-dimethyl-3-methyl-2,4,6-octatrienylidene iminium perchlorate, 47	160
N,N-dimethyl-retinylidene iminium perchlorate, 54	160
N-methyl-N-phenyl-retinylidene iminium perchlorate, 53	161
2,4,6-octatrienal, 95	161
Preparation of Protonated Unsaturated Aldehydes	162
Irradiations	162
H _ν Measurements	162
Kinetic Measurements	163
Single Crystal X-ray Crystallography	
Crystal Selection and Handling	164
Data Collection, Structure Solution and Refinement	
N-t-butyl-retinylidene iminium perchlorate, 51	165
N-t-butyl-retinylidene iminium triflate, 52	166
<u>APPENDIX</u> - Supplementary Crystallographic Data for 51 and 52	171
<u>REFERENCES</u>	213

LIST OF TABLES

Table 1-1:	Absorption maxima for chromophores (SBH+) and pigments.	17
Table 2-1:	¹ H NMR Chemical Shift Data (ppm) for 3-methyl-2,4,6-octatrienylidene iminium salts.	46
Table 2-2:	¹ H, ¹ H coupling Constant data (Hz) for 3-methyl-2,4,6-octatrienylidene iminium salts.	46
Table 2-3:	¹ H NMR Chemical Shift Data (ppm) for retinylidene iminium salts.	47
Table 2-4:	¹ H, ¹ H Coupling Constant Data (Hz) for retinylidene iminium salts.	47
Table 2-5:	¹³ C NMR Chemical Shift Data (ppm) for 3-methyl-2,4,6-octatrienylidene iminium salts.	49
Table 2-6:	¹³ C NMR Chemical Shift Data (ppm) for retinylidene iminium salts.	50
Table 2-7:	Solid State ¹³ C NMR Chemical Shift Data (ppm) for retinylidene iminium salts.	52
Table 2-8:	Absorption Spectral Data (nm) for iminium salts 46, 47 and 50-53.	54
Table 2-9:	Selected Bond Lengths (Å) for 51 and 52.	56
Table 2-10:	Selected Bond Angles (°) for 51 and 52.	57
Table 2-11:	Torsion or Conformational Angles for 51 and 52.	59
Table 2-12:	Selected Least Squares Planes Data for 51 and 52.	61
Table 2-13:	Intermolecular Contact Distances (Å) and Angles (°) for 51 and 52.	79
Table 3-1:	Isomeric Purity of Iminium Salts on Preparation.	98

LIST OF TABLES (con't)

Table 3-2:	¹ H NMR Chemical Shift Data (ppm) for retinylidene iminium salts and their Primary Photoproducts.	99
Table 3-3:	¹ H, ¹ H Coupling Constant Data (Hz) for retinylidene iminium salts and their Primary Photoproducts.	99
Table 3-4:	Rates of Isomerization about the 11-cis bond.	103
Table 3-5:	Concentration Dependence of Half Life on the Isomerization of 79 to 54.	103
Table 3-6:	Isomer Composition at Thermodynamic Equilibrium.	105
Table 4-1:	¹ H NMR Chemical Shift Data (ppm) for 46, 47 and their Primary Photoproducts.	118
Table 4-2:	Coupling Constant Data (Hz) for 46, 47 and their Primary Photoproducts.	118
Table 4-3:	Isomeric Composition (%) of Iminium Salts 46 and 47 Under Various Conditions.	123
Table 4-4:	Rate constants and Activation Parameters of the <i>cis/trans</i> Isomerization of 86 and 87.	126
Table 4-5:	¹ H NMR Chemical Shift Data of Cations.	135
Table 4-6:	¹³ C NMR Chemical Shifts of 1-hydroxyallyl Cations and Corresponding Aldehydes.	137
Table 4-7:	Isomeric Composition of Aldehydes and Corresponding 1-hydroxyallyl Cations.	138
Table 4-8:	Rate Constants and Activation Parameters for the Isomerization of 96 to 98.	142
Table 6-1:	Atomic Coordinates for 51.	168

LIST OF TABLES (con't)

Table 6-2:	Atomic Coordinates for 52.	169
Table 6-3:	Crystallographic Data for 51 and 52.	170
Table A-1:	Bond Lengths (Å) Involving Hydrogen Atoms in 51 and 52.	172
Table A-2:	Hydrogen Atom Coordinates and Isotropic Thermal Parameters for 51.	173
Table A-3:	Hydrogen Atom Coordinates and Isotropic Thermal Parameters for 52.	174
Table A-4:	Anisotropic Temperature Factors for the Non-Hydrogen Atoms in 51.	175
Table A-5:	Anisotropic Temperature Factors for the Non-Hydrogen Atoms in 52.	176
Table A-6:	Observed and Calculated Structure Factors for 51.	177
Table A-7:	Observed and Calculated Structure Factors for 52.	198

LIST OF FIGURES

Figure 1-1: The seven α -helices of the polypeptide chain in bR.	12
Figure 1-2: Primary interaction between an anion and a ternary iminium salt.	27
Figure 2-1: The Conformation of 51.	62
Figure 2-2: Stereoscopic View of Unit Cell Contents for 51.	63
Figure 2-3: Unit Cell Packing in 51- View along z-Axis.	64
Figure 2-4: Unit Cell Packing in 51- View along y-Axis.	65
Figure 2-5: The Conformation of 52.	66
Figure 2-6: Stereoscopic View of Unit Cell Contents for 52.	67
Figure 2-7: Unit Cell Packing in 52- View along x-Axis.	68
Figure 2-8: Unit Cell Packing in 52- View along y-Axis.	69
Figure 2-9: Bond Length Alternation in 51 and 52.	74
Figure 2-10: Bottom View of Hydrogen Bonding Interactions in 52.	81
Figure 2-11: Side View of Hydrogen Bonding Interactions in 52.	82
Figure 2-12: Differences in ^{13}C NMR Chemical Shift Between 51 and 52 Solution and Solid States.	84
Figure 2-13: Differences in ^{13}C NMR Chemical Shift Between bR and 51/52 in the Solid State.	86
Figure 3-1: ^1H NMR Spectrum of 51 in CD_2Cl_2 After Irradiation at 350 nm.	100
Figure 3-2: Destabilizing Interactions in 7- <i>cis</i> , 9- <i>cis</i> , 11- <i>cis</i> and 13- <i>cis</i> isomers.	113

LIST OF FIGURES (con't)

Figure 4-1:	Chemical Shift Trends for Each Mono <i>cis</i> isomer of 46.	119
Figure 4-2:	¹ H NMR Spectrum of 46 in CD ₂ Cl ₂ After Irradiation at 350 nm.	120
Figure 4-3:	¹ H NMR Spectra of 96 and 97 in FSO ₃ H at -60°C.	136

LIST OF ABBREVIATIONS

CPMAS	Cross Polarization Magic Angle Spinning
LCAO	Linear Combination of Atomic Orbitals
Me	Methyl
ph	Phenyl
MO	Molecular Orbital
NMR	Nuclear Magnetic Resonance
OMe	Methoxy
ppm	Parts per million
SCF	Self Consistent Field
uv	Ultraviolet
bR	Bacteriorhodopsin
bO	Bacterioopsin
ATP	Adenosine triphosphate
FTir	Fourier Transform Infrared
ir	Infrared
NOE	Nuclear Overhauser Effect
Lys	Lysine
Asp	Aspartate
Arg	Arginine

LIST OF ABBREVIATIONS (con't)

Trp	Tryptophan
vis	Visible
λ_{\max}	Absorption Maximum
MeOH	Methanol
MNDOC	Modified Neglect of Diatomic Overlap Correlation
MNDO	Modified Neglect of Diatomic Overlap
TFA	Trifluoroacetic Acid
HPLC	High Performance Liquid Chromatography

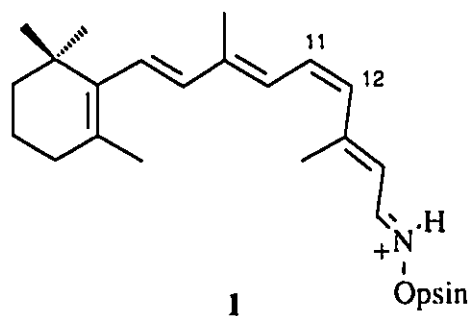
Chapter 1

PART I

Introduction

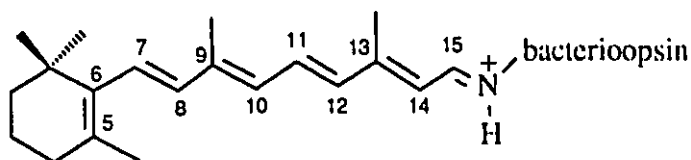
The discovery of bacteriorhodopsin (bR), the protein pigment of the purple membrane of the halophilic microorganism *Halobacterium halobium*¹, has had a large impact on the field of bioenergetics and on the understanding of the structure and chemistry of the visual pigment, rhodopsin.² The pigments bacteriorhodopsin and rhodopsin, are similar in that both contain retinal as their active chromophores. However, aside from the primary event involving the absorption of a photon of light, the remaining steps of their dark reactions, the chemistry of these proteins and their biological purposes are considerably different.

The protein rhodopsin, 1, consists of the 11-*cis* isomer of retinal linked to an apoprotein opsin via a protonated Schiff base linkage. The polypeptide chain in this



protein was found to contain 348 amino acids. In nature, the purpose of this pigment is to form the link between the physical phenomenon of light and the biological act of visual

perception. In contrast, bacteriorhodopsin is comprised of all-*trans* retinal connected via a protonated Schiff base linkage to a protein consisting of 248 amino acids, 2. Interest in this pigment stems from the insight provided in the study of the mechanisms of photophosphorylation and the production of energy-rich fuel molecules which are needed to drive thermodynamically unfavourable reactions in the cell.



2

Common to both rhodopsin and bacteriorhodopsin are the questions of their structures and mechanisms of action. In light of the forthcoming research presented in this thesis, the following introduction will focus on the structure and chemistry of bacteriorhodopsin.

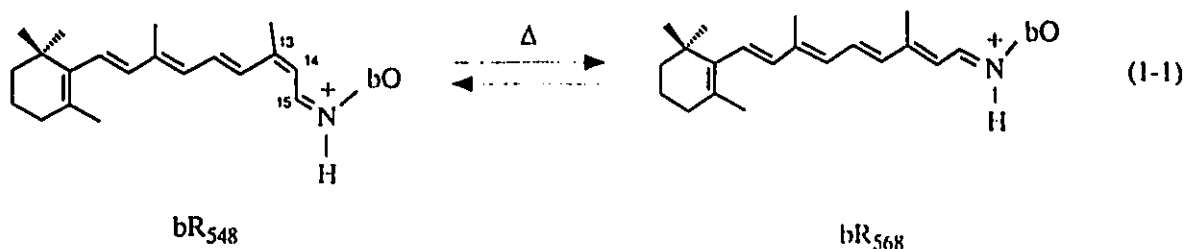
Bacteriorhodopsin

Halobacterium halobium has been the focus of a tremendous amount of research over the past two decades. The functions of this bacterium are both interesting and ecologically important. It can survive not only in solutions containing at least 12% NaCl, but can also survive in saturated salt solutions.³ Under conditions of oxygen depletion

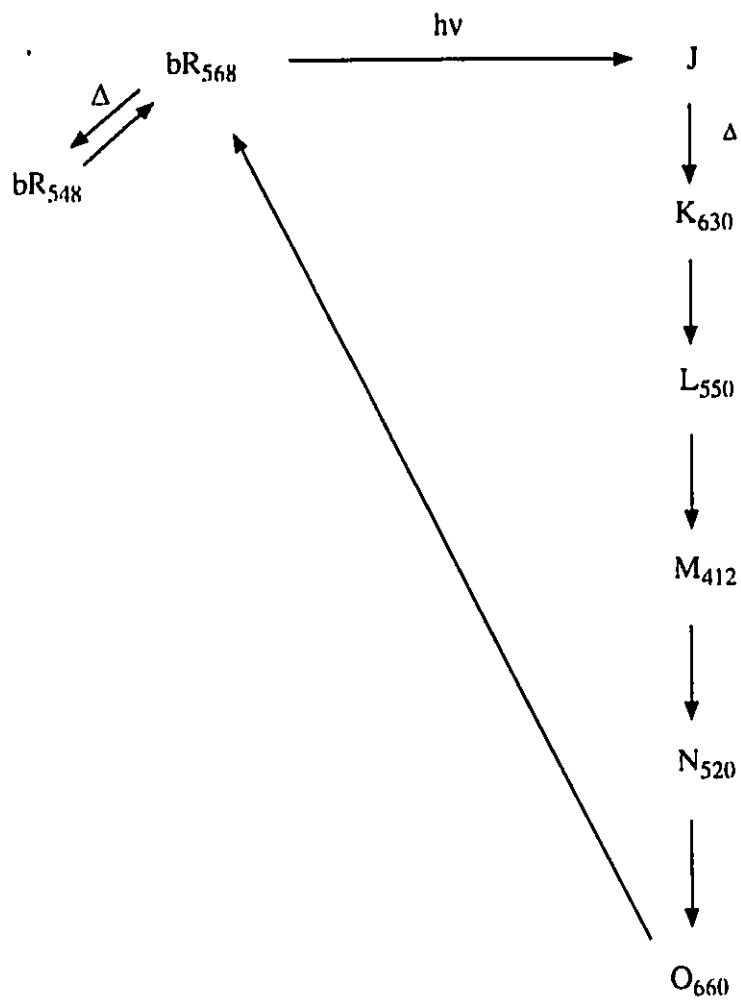
when the normal source of metabolic energy is cut off, this organism can use light energy. The light energy is initially converted into an electrochemical gradient of hydrogen ions across the cell membrane which is used to synthesise ATP and, subsequently, to energize many of the normal functions of the cell. The segment within the cell membrane which functions as the light-driven proton pump is known as the purple membrane or bacteriorhodopsin. It is composed of one molecule of retinal covalently bound to the ϵ -amino group of the lysine residue 216 of the surrounding protein via a protonated Schiff base linkage.⁴

Photochemical/Thermal Cycle

Bacteriorhodopsin can exist in light adapted and dark adapted forms. Through solid state ^{13}C NMR spectroscopy it was found that dark adapted bR contains roughly equal proportions of 13-*cis*, 15-*cis* (bR_{348}) and all-*trans*, 15-*trans* (bR_{568}) protonated Schiff bases in thermal equilibrium⁵ (equation 1-1). In response to the absorption of light, this protein undergoes a photocycle which produces a number of intermediates. These intermediates were named according to their order of appearance, as well as, optical absorption.^{6,7} The current picture of the bR photocycle is represented in Scheme 1-1. Upon absorption of light, bR_{348} is converted to the all-*trans* isomer, bR_{568} . The all-*trans* species, bR_{568} , is the reactive species that undergoes the cyclical sequence of an initial photoreaction followed by a series of dark reactions terminating in the regeneration of the parent pigment.

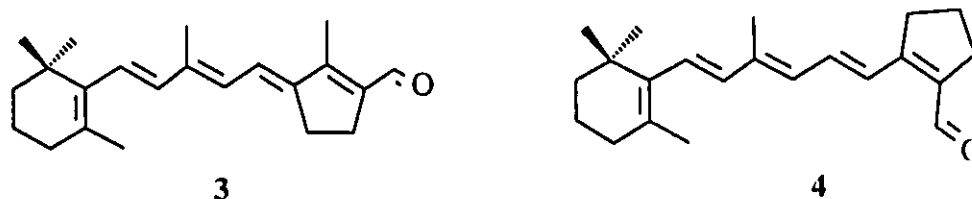


Recently, femtosecond optical measurement techniques were used to directly observe the primary photoprocess which involves an isomerization about the C13-C14 bond of the bound all-*trans* retinal protonated Schiff base chromophore.⁸ The initial photoproduct, J, is formed in about 500 fs and relaxes to K₆₃₀ on a 3 ps time scale.⁹ Earlier picosecond flash photolysis studies have shown that K₆₃₀ is formed with a quantum yield of about 0.3.¹⁰ The results of resonance Raman studies indicate that K₆₃₀ contains a 13-*cis* chromophore with a *trans* configuration about the C=N bond.^{11,12} Decay of K₆₃₀ produces L₅₅₀, which has also been shown to possess a 13-*cis* bond.^{12,13} Further relaxation of the 13-*cis* chromophore and protein structure gives way to M₄₁₂ which is deprotonated as evidenced by its short absorption maximum. This intermediate also contains a 13-*cis*, 15-*trans* configuration.¹⁴ The chromophore is reprotonated during the M₄₁₂-N₅₂₀ transition¹⁵ and thermally isomerizes back to an all-*trans* isomer during the formation of O₆₆₀.¹⁶ It was suggested that this *trans* chromophore has a distorted conformation about single bonds which must then relax as bR₅₄₈ is formed.



Scheme 1-1: The Bacteriorhodopsin Photocycle.

Proton translocation during the bacteriorhodopsin photocycle is thought to be associated with changes in both the protonation of the Schiff base as well as changes in retinal geometry. Bacteriorhodopsins derived from synthetic retinals **3** and **4** both fail to pump protons on irradiation showing that C13-C14 bond isomerization is a necessity for proton transport.¹⁷ Similarly, bR analogues containing modified retinals having built-in steric hindrance inhibiting the all-*trans*/13-*cis* isomerizations do not allow proton pumping to occur.¹⁸



Other attempts have been made to pinpoint the relationship between proton pumping and the photocycle intermediates of bR. Ebrey et al., using resonance Raman spectroscopy have shown that as the intermediate M_{412} is formed, the Schiff base becomes deprotonated.¹⁹ This suggested that protons which are pumped across the cell membrane may be from the pigment's protonated Schiff base and that proton translocation should couple with the formation of the M_{412} intermediate. However, Ort and Parson have found that the kinetics of proton release and uptake do not match the kinetics of M_{412} formation and decay.²⁰ While proton release and uptake are single exponential processes, the rise

and decay of M_{412} is the sum of at least two exponential processes, M^{slow} and M^{fast} .²¹ Ebrey studied the effects of proton pumping and the amounts of photocycle intermediates M_{412} and O_{660} by varying either pH or temperature.²¹ Their results showed a striking correspondence between pH dependence of the amplitude of M^{slow} and the number of protons that are pumped across the membrane cells. A similar correspondence is seen in the temperature dependence of the amount of M^{slow} and the number of protons released.

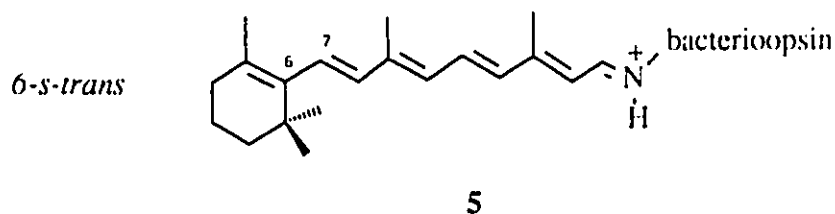
Conformation of Retinal in Bacteriorhodopsin

In order to explain the chemistry exhibited by bR it is important to know the structure of the retinylidene backbone. The unsaturated carbon chain contains a number of formal single and double bonds which can adopt a variety of conformations. The geometry about the single bonds is of great concern since the propensity for rotation about single bonds is greater than that for double bonds. An exact structure of the retinal chromophore in bR is still unknown. Much of the problem lies in the difficulty in crystallizing such a large membrane protein. However, resonance Raman, NMR and chemical extraction studies have all contributed to showing that the chromophore in bR₅₆₈ is an all-*trans* protonated Schiff base.^{12,23,24,25}

It was shown by Smith²³ and Curry²⁶ that the resonance Raman spectrum of bR₅₆₈ is significantly different from that of an *in vitro* all-*trans* retinal protonated Schiff base. This observation suggests that these differences are due to the increased delocalization of the conjugated π -system upon binding to the protein. As π -electrons become more

delocalized, the C-C single bonds gain more double bond character and their ir stretching bands are seen to shift to higher frequency. Through resonance Raman studies it was found that all of the "single bonds" from C8 to C15 are *s-trans*.²⁷

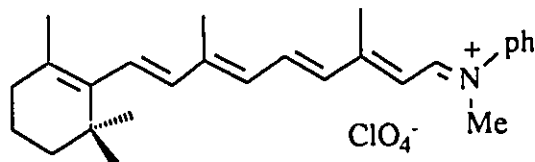
A crystal structure of all-*trans* retinal has shown the polyene chain to be all-*trans* with the exception of the *s-cis* orientation about the C6-C7 bond.²⁸ The dihedral angle between the β -ionone ring and the polyene chain was 62°. This compound was found to be curved in the plane containing the alternating single and double bonds and bowed normal to this plane. Solution studies using NOE experiments²⁹ have shown the torsion angle about the C6-C7 bond to be about 32°. Quantum chemical calculations have also found the C6-C7 bond to be 6-*s-cis* however the torsion angle was predicted³⁰ to be about 83°. Harbison et al. presented an extensive solid state ¹³C NMR study of retinals, retinal Schiff bases and other carotenoids.²⁵ Using the ¹³C NMR C5 chemical shift as a probe of the ring-chain conformation, these workers suggested that the 6-*s-trans* conformer is present in bacteriorhodopsin.²⁵



Theoretical calculations done by Tavan and Schulten³⁰ on protonated Schiff bases

of retinal have shown that the pattern of alternating long and short bonds exhibited clearly by the Schiff base was altered once the Schiff base becomes protonated; the short π -bonds become longer and the formal single bonds in the polyene chain become shorter. This tendency was so pronounced as one proceeded toward the nitrogen that the C13-C14 double bond was even longer than the adjacent C14-C15 single bond. The weakening of double bonds and the corresponding strengthening of single bonds is evidenced by a partial migration of π -electronic charge from the terminal nitrogen to the polyene fragment. Overall, most of the positive charge was born by N(H), C15, C13 and C11 while most of the negative charge was located on C12, C14 and N.

Recently, the crystal structure of N-methyl-N-phenyl-retinylidene iminium perchlorate, **6**, was obtained by Childs et al.³¹ Since no reliable x-ray structure of a retinylidene iminium salt had ever been reported in the open literature, this structure provided a wealth of information into the structure of the retinal chromophore in an iminium salt. All of the bonds including the C6-C7 bond in the polyene fragment were shown to be *trans*. The polyene chain of **6** was essentially planar (all torsion angles $\approx 0^\circ$ or $\approx 180^\circ$) while exhibiting significant in-plane curvature. As was predicted by



calculation, the C-C single bonds in **6** were shortened and the C-C double bonds lengthened when compared to all-*trans* retinal or those calculated for the N-methyl imine of all-*trans* retinal. This effect was more pronounced with bonds close to the terminal nitrogen atom. Since progressively larger bond alternations were observed further away from N, it follows that delocalization of positive charge also falls away with distance from N. It is interesting to note that although theoretical calculations have shown similar trends as seen for **6**, they tended to overestimate the C-C bond lengths along the polyene chain.

Structure of the Protein

Chemical analysis of isolated purple membrane shows 75% protein and 25% lipid content. Bacteriorhodopsin was shown to consist of one polypeptide containing 248 amino acids having a molecular weight of 26,000. Khorana elucidated the complete amino acid sequence in 1979.³² One molecule of all-*trans* retinal is covalently linked to Lys-216 via a protonated Schiff base linkage. Over the years x-ray diffraction and electron microscopy studies have provided a wealth of information pertaining to the 3D structure of bR.

Since membrane proteins cannot be induced to form 3D crystals, x-rays are weakly diffracted in passing through such thin crystals. However, electrons which interact with atomic nuclei, are scattered much more strongly than x-rays and can yield a diffraction pattern. By subjecting purple membranes to electron doses low enough to preserve their

intrinsic structure, Unwin and Henderson were able to record electron diffraction patterns that displayed the hexagonal lattice structure of purple membrane.³³ The polypeptide chain of bR consists of seven α -helices approximately 40 Å long and 10 Å apart that extend across the membrane roughly perpendicular to its plane, Figure 1-1. There are three helices almost perpendicular to the plane of the membrane and four angled from 10° to 20° from the plane. Solid state ¹³C NMR structural analysis of bR showed the polypeptide backbone to be rigid on the ¹³C NMR time scale even at 40°C.³⁴ No motions with angular excursions > 10° and faster than $\approx 100 \text{ s}^{-1}$ were detected.

Recently, through electron microscopy studies by Henderson et al., interactions between Asp-85, Asp-212 and Arg-82 and the protonated Schiff base were shown to be critically important for the formation and uv/vis absorption maximum of bR.³⁵ They proposed a structural model for bR in which the side chains of Asp-85 and Asp-212 were approximately equidistant ($\approx 4 \text{ Å}$) from the protonated Schiff base with both residues appearing to be deprotonated in the ground state. A complete atomic model for bR was assembled between amino acid residues 8 and 225. There are between 20 and 27 amino acids contributed by each of the seven helices. It was determined within the uncertainty due to resolution, that 21 amino acid residues in all form the retinal binding pocket. The proton path or channel is formed by 26 residues contributed by 5 helices.

Khorana has concluded on the basis of pK_a measurements and absorption studies that the retinylidene Schiff base counterion in bR is Asp-85.³⁶ Mutants of Asp-85 caused a decrease of > 3.5 units in pK_a , while substitution of Asp-212 produced only

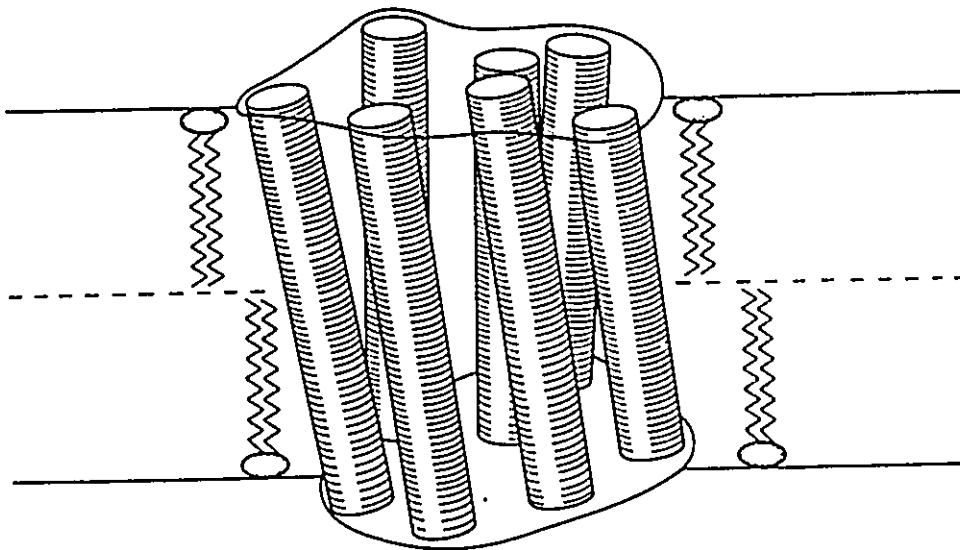


Figure 1-1: The seven α -helices of the polypeptide chain in hR.

< 1.2 decrease in pK_a relative to "wild type" hR. Substitutions of Asp-85 showed large red shifts in the absorption spectrum that were partially reversed upon addition of organic and inorganic ions Cl^- , Br^- , I^- , ClO_4^- , $ClCH_2CO_2^-$ and $Cl_2CHCO_2^-$. Mutants of Asp-212 displayed only minor red or blue shifts.

Absorption Studies

During the last two decades a large amount of work has been directed toward a better understanding of the spectroscopic problems related to bacteriorhodopsin and the visual pigments. In particular, much work has been focussed on determining the factors controlling the bathochromic shift and wavelength regulation characteristics of these pigments. The retinal chromophore in a hydrocarbon solvent absorbs at about 370 nm³⁷ yet when combined to form a pigment, the chromophore can absorb at wavelengths as high as 570 nm. Two avenues have been explored to account for this very large red shift. The first of these involves an understanding of the nature of the molecular interactions between the protein and the retinal chromophore. Secondly, the intrinsic structural properties of retinal chromophore have been examined in order to determine how it can be modified to allow this molecule to absorb at these large wavelengths. A number of model studies have been performed to address these two fundamental problems.

Early examinations of the λ_{max} of N-retinylidene-n-butylamine iminium salts with selected solvents indicated a leveling effect. Solvents such as methanol, ethanol and

tetrahydrofuran did not allow the character of the anion to be expressed. The salts exhibited an identical λ_{\max} in each of these solvents.³⁷ It was also noted that in a nonleveling solvent there is a relationship between the acid strength and the absorption maximum of the salt. For example, the decreasing order of maxima of N-retinylidene-n-butylamine HA salts in CHCl_3 is: $\text{ClO}_4^- > \text{Br}^- > \text{HSO}_4^- > \text{NO}_3^- > \text{Cl}^-$. With the exception of NO_3^- and Cl^- , the order of absorption maxima of these salts matches the relative strengths of the acids from which they are derived.

Although the acid strength correlation is intuitive and plausible it does not provide the basic underlying reasons for the λ_{\max} changes. Blatz et al., showed there was a linear relationship between the reciprocal of the square of the anion radius and the energy difference between the ground state and the first excited state, ΔE .³⁷ Hence, the chloride salt had the shortest λ_{\max} and the perchlorate salt the longest. However, in order to reproduce the λ_{\max} for hR, their model required a centre-to-centre distance between charges of approximately 10 Å.

Another way to shift the absorption spectra further is through solvent effects. It has been demonstrated by infrared studies that hydrogen bonding occurs between halide anions and solvents such as CHCl_3 and CHBr_3 .³⁸ The change in C-H stretching frequency is sensitive to anion identity in the expected order; $\text{F}^- > \text{Cl}^- > \text{Br}^- > \text{I}^-$. Blatz investigated the effect of solvent on the absorption of n-butyl-N-retinylidene halide salts.³⁹ Plots were made for the chloride, bromide and iodide in which the absorption maxima of the salts were plotted against the dipole moment of the pure solvents. It was shown

that there is a linear relationship over the range of dipoles examined for solvents of a single structural type. For all three salts, the absorption maximum increased as the dipole moment of the solvent decreased. Hence, for the chloride salt, the shortest absorption maximum (443 nm) was seen in bromoethane ($D = 2.02$) while the longest absorption (469 nm) maximum was seen in bromoform ($D = 0.90$). Those solvents that exhibited a linear relationship between dipole moment and wavelength can participate in hydrogen bonding while solvents such as CCl_4 and CH_2Cl_2 , which cannot hydrogen bond, deviated markedly from linearity. While the absorption spectra of protonated Schiff bases have been shown to be sensitive to solvent effects, the shifts in the absorption maxima are limited and it has been impossible on this basis to devise a model system that can reproduce λ_{max} observed for bR.

Theoretical calculations have shown it possible to regulate pigment spectra through interaction of charges or polar groups placed around the chromophore by the protein. Honig and Ebrey concluded through a theoretical study that a favourable chromophore-protein interaction is one in which the protonated Schiff base is closely associated with its counterion and where an additional negative charge or polar group is positioned at the ring-end of retinal.⁴⁰ Although this study was able to demonstrate that a spectral red shift can be produced by suitable placement of a negative charge, the exact nature and location of the charge is still not known.

External Point Charge Model

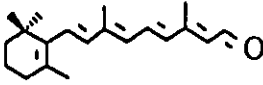
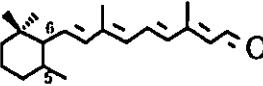
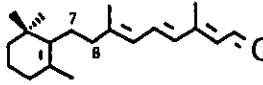
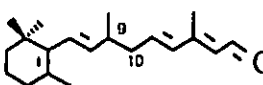
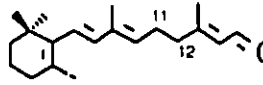
This model was proposed by Nakanishi and coworkers in an effort to clarify the type of interaction between the apoprotein, bacterioopsin, and the protonated retinylidene Lysine chromophore.^{41,42} It is this interaction which shifts the absorption maximum of an *in vitro* protonated Schiff base (SBH+) from about 450 nm to the 570 nm absorption maximum of the light adapted form of bacteriorhodopsin. The extent of this shift is a measure of the influence of the binding site. Hence the "opsin shift" is the difference between λ_{\max} of SBH+ (in cm^{-1}) and λ_{\max} of the pigment bR (in cm^{-1}).

Nakanishi and coworkers showed that the large opsin shift for bacteriorhodopsin is due to electrostatic interactions between the protonated chromophore and the charged or polar groups located on the protein near the β -ionone ring of retinal. A series of synthetic dihydroretinals were bound to the apoprotein and the absorption maxima of these "pigments" were compared to those of the respective SBH+, Table 1-1. The largest opsin shift (4870 cm^{-1}) was obtained with the longest chromophore with six double bonds. The opsin shift decreases as the saturated bond is moved further away from the ring. The magnitude of the shift induced by the external charges depends on their proximity to the polyene system. Hence, the maximum effect that can be realized is induced by a charge in the vicinity of the β -ionone ring on a chromophore with six double bonds. This effect would successively decrease as the location of the bond that was saturated approached the iminium function.

It is known both experimentally and theoretically that the Schiff base nitrogen

Table 1-1

Absorption Maxima^a for chromophores (SBH')^a and pigments (bR)^b.

Retinal	SBH' (nm)	bR (nm)	Opsin Shift $\Delta\nu$ (cm ⁻¹)
	440 (460) ^c	560 (576)	4870 (4400)
	425 (441)	476 (485)	2500 (2100)
	385 (398)	400 (415)	1000 (1000)
	322 (342)	325 (347)	300 (420)
	270	-	-

^a Protonated n-butyl Schiff base in MeOH.^b Bacteriorhodopsin analogues.^c Calculated values.

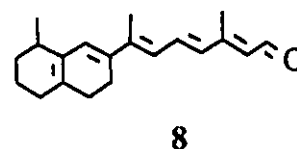
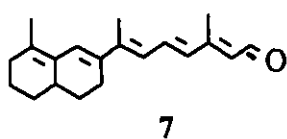
becomes more basic in the excited state.^{40,43,44} Negative charge accumulates on the nitrogen while positive charge migrates into the unsaturated chain toward the ring. Hence, a charge located near the β -ionone ring could, in principle, stabilize the excited state resulting in a spectroscopic red shift.

Using the Pariser-Parr-Pople (PPP) scheme which was parameterized to yield results in good agreement with model polyene spectra,⁴⁴ Nakanishi et al., carried out π -electron calculations in an effort to model their experimental results.⁴¹ The transition energies were calculated for the various SBH⁺ containing a counterion separated 3 Å from the terminal nitrogen to represent the environment of SBH⁺ in solution. For the model compounds containing shortened π -systems, the calculated shifts corresponded well to those found from experiment. It was concluded that a negative charge is located in the vicinity of the C5-C6 double bond.

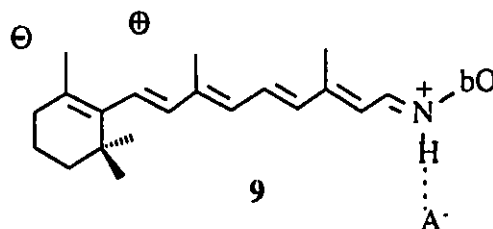
Solid state ¹³C NMR experiments by Harbison have supported the proposal that there is a negative charge near C5,C6.⁴⁵

More recently, the 5,6- and 7,8-dihydroretinal data were re-examined by Lugtenburg and coworkers.⁴⁶ While the 5,6-dihydroretinal spectra were in agreement with Nakanishi's work, the measured opsin shift for the 7,8-dihydroretinal derivative (3500 cm⁻¹) is larger than the originally published value. It was suggested that in addition to a negative charge near C5,C6 there is also a positive charge near C7. In the 5,6-dihydro derivative, the interaction of the conjugated chain with the negative charge is essentially eliminated and the opsin shift falls to 2500 cm⁻¹. However, in this derivative

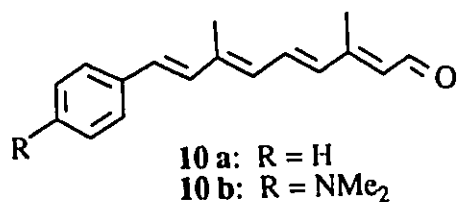
the positive charge near C7 would still interact effectively with the conjugated chain and should contribute to a reduction of the opsin shift. When the polyene chain is shortened in the 7,8-dihydro derivative, the opsin shift increases to 3500 cm^{-1} . These data with dihydro systems provided evidence that there is a pair of opsin charges near the β -ionone ring in bR. Lugtenburg showed that bR requires the retinal to be in a 6-*s-trans* conformation to produce the bathochromic shift.⁴⁷ Thus, while **7** reacted rapidly with bacterioopsin to form a bR analogue with λ_{max} 564 nm, incubation of **8** with bacterioopsin lead to a severely decreased proton pumping ability and no light-dark adaptation. These



results fully agree with Harbison's solid state ^{13}C NMR studies.⁴⁵ Hence, the currently accepted model for bR contains a negative charge near C5, a positive charge near C7 and a negative charge about 3 \AA removed from the terminal nitrogen.



This model was corroborated by Nakanishi when model retinals 10a and 10b were synthesized having structural differences at the ring end of the chromophore.⁴² Both of these chromophores, when incubated with bacterioopsin, exhibited absorbance maxima far removed from that of natural bR. Since the electronic and steric properties of the aromatic ring are drastically different from trimethyl cyclohexene, the effect of the point charge near C5 is greatly reduced.

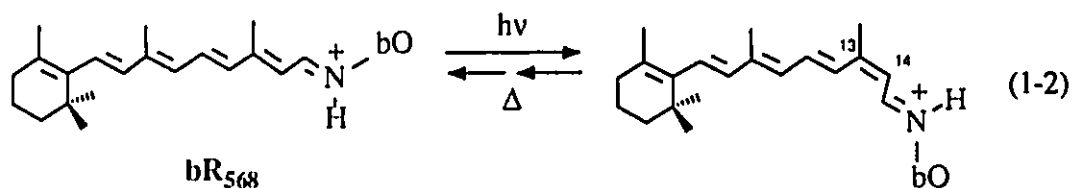


Retinal analogues with built-in point charges have also been synthesised in an effort to mimic the electronic spectrum of the natural pigment.^{48,49}

Thermal Chemistry

The primary event in the bR photocycle involves the absorption of light by light adapted bR (bR₅₆₈) and results in the femtosecond *trans* to 13-*cis* isomerization of the protonated Schiff base of retinal. The remaining steps of the photocycle are completed in less than 10 ms at room temperature and when it is finished, all-*trans* bR is regenerated in its original form, equation 1-2. Hence the thermal 13-*cis* to *trans*

isomerization occurs in less than 10 ms.⁶ The rapid thermal isomerization which occurs during the photocycle of bR is critical for the efficient functioning of the protein. A slower thermal isomerization of the protonated Schiff base would slow down the regeneration of light-adapted bR and retard the rate at which bR could absorb light and



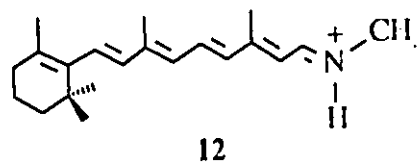
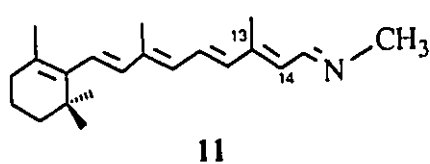
pump protons. In the absence of light, light-adapted bR isomerises in ≈ 20 min to a dark adapted form containing a 1:1 mixture of all-*trans*, 15-*trans* and 13-*cis*, 15-*cis* chromophores at thermal equilibrium, equation 1-1.⁵⁰ It is known that 13-*cis* bR does not pump protons upon absorption of light and that it isomerizes to the photoactive all-*trans* bR with a quantum yield of less than 0.05.⁵¹ At low light levels the all-*trans* to 13-*cis* thermal isomerization decreases proton pumping activity. At higher light fluxes, the 13-*cis* to all-*trans* photoisomerization occurs at a greater rate than the thermal back isomerization and the quantum yield of proton pumping is also greater.

In order to function as an appropriate photocatalyst within the bacterium, thermal isomerization of the protonated Schiff base in bR must occur efficiently. While the

nature of the intermediates important in proton pumping have been the subject of extensive investigation during the last two decades, strangely, the details of the thermal isomerizations in bR have been much less studied.

Typically, thermally induced rotations about C=C and C=N bonds involve activation energies of ≈ 50 kcal/mole³⁰ and ≈ 70 kcal/mole³², respectively. Conversely, single C-C bonds exhibit low barriers of typically ≈ 5 kcal/mole. A strong perturbation of the polyene bond pattern is therefore necessary to facilitate the rapid ($k \approx 10^7$ s⁻¹) thermal isomerization of 13-*cis* to all *trans* retinal during the dark phase of the bR photocycle.

Tavan and coworkers have shown through MNDOC calculations that protonation of the Schiff base nitrogen lowers the isomerization barriers for double bond rotation.³⁰



For example, protonation of model compound 11 was calculated to lower the activation barrier for rotation about the C13-C14 bond from 47 kcal/mole to 11.5 kcal/mole in 12.

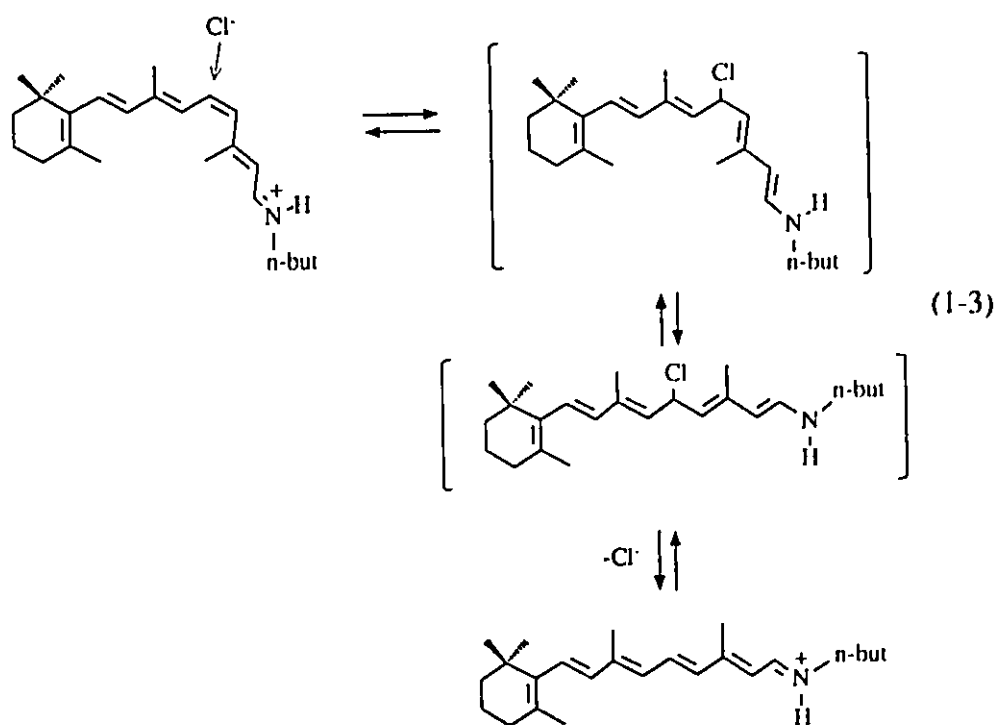
Interaction of the cation with a negative ion can also serve to alter isomerization barriers. Negative ions near the protonated nitrogen cause isomerization barriers to

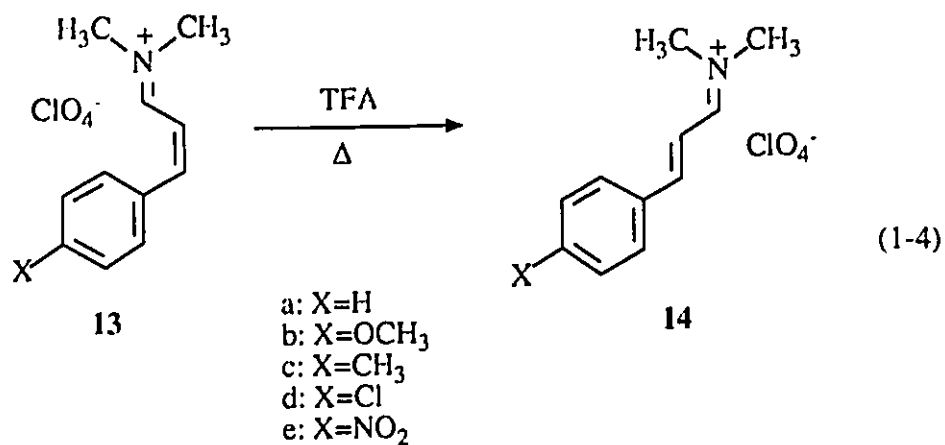
increase while positioning ions near the β -ionone ring have the opposite effect. Tavan has calculated that the C13-C14 isomerization barrier increases to 25.2 kcal/mole when a F^- ion is positioned 3 Å from the proton on the Schiff base nitrogen. Adding a second ion 3 Å above C5 lowered the barrier to 5.8 kcal/mole. MNDO calculations by Seltzer⁵³ showed the energy barrier for rotation about C13-C14 to decrease from 15.8 kcal/mole to 11.6 kcal/mole when a negative charge is placed 2.5 Å away from C13 and by removing negative charge from the vicinity of N.

MNDOC and MNDO calculations done by Tavan and Seltzer have provided some insight pertaining to the structural and electronic effects induced by protonation and external point charges on a retinal Schiff base. However, it is useful to use the numbers derived from these studies in a relative sense since it was shown earlier that, in the case of structure, the level of calculation used tended to overestimate the C-C bond lengths in a retinylidene iminium salt. A lowering of the activation barrier to below 20 kcal/mole would allow isomerization to proceed at ambient temperatures. In this vein, a number of studies have been reported on model compounds to investigate the mechanisms of C=C and C=N bond isomerizations. Rando and Lukton reported that the isomerization of 11-*cis* retinal proceeded at 65°C with a rate constant of $2.4 \times 10^{-6} \text{ s}^{-1}$ in heptane.⁵⁴ Schiff base formation enhanced the rate of thermal isomerization by a factor of three, but the reaction was still slow at room temperature.

In a separate experiment, it was found that triethyl amine decreased the rate of isomerization of the *n*-butyl Schiff base of 13-*cis* retinal in chloroform from 1.5×10^{-5}

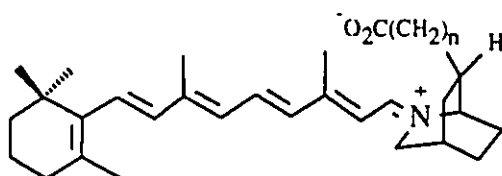
s^{-1} to $1.7 \times 10^{-6} s^{-1}$.⁵⁵ It was suggested that this inhibitory effect of the added amine was due to the neutralization of trace amounts of acid in the medium. At $25^\circ C$ HCl was shown to catalyse the rates of isomerization of the n-butyl Schiff base of retinal by a factor of 10^4 over the uncatalysed reaction. The order of reactivity of the various bonds was shown to be 13-*cis* > 11-*cis* > 9-*cis*. Trifluoroacetic acid proved to be a much weaker catalyst than HCl. From these results, Rando suggested that the rates of isomerizations in retinylidene iminium salts appeared to be dependent on the strength of the conjugate bases and that catalysis was occurring via a nucleophilic addition mechanism, equation 1-3. A detailed mechanistic investigation of the stereomutations of 3-aryl-2-propenylidene iminium salts 13 a-e supported the view that thermally induced *cis/trans* isomerization of unsaturated iminium salts may proceed via a nucleophilic addition mechanism.⁵⁶



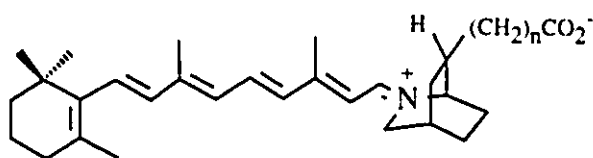


In a more recent study, Seltzer synthesized ternary iminium salts of retinal with variable length carboxylate anions to interact with the polyene system.⁵⁷ These salts were used as models to mimic aspartate-212 and lysine-216 in the retinal binding pocket of bR. The longer arm in the *syn* isomer, **15b**, could allow a closer interaction of the carboxylate with C13 than the nitrogen atom thereby providing greater catalysis for the isomerization than that observed for **15a**.

Although Seltzer's MNDO calculations predicted a lowering of the energy



15 syn a: n=1
b: n=3



16 anti a: n=1
b: n=3

barrier to isomerization about C13-C14 when an anion is placed 2.5 Å above C13, the experimental results showed only a modest threefold increase of the rate of isomerization of 15b versus 15a. Seltzer suggested that the primary interaction of the carboxylate is still with the nitrogen. However, Childs and Shaw⁵⁸ have shown that the primary interaction between a ternary iminium salt and its counteranion is at the aldiminium carbon atom, Figure 1-2. In this regard it is interesting that the calculations on all-*trans*-retinylpyrrolidiniminium perchlorate reported by Birge indicated two equilibrium positions for the perchlorate anions.⁵⁹ These involved positioning of the perchlorate anions above and below the polyene chain at either C15 or at C15 and C13.

It was unfortunate that no solid state ¹³C NMR or uv/vis absorption data were reported in Seltzer's work because these techniques have been shown to be particularly sensitive to changes in electron distribution in retinylidene iminium salts.^{5,45,60,61,62} If a closer interaction existed between the carboxylate anion and C13 of the cation in 15b than that of 15a then a corresponding downfield shift of C13 in 15b relative to 15a should be observed in their corresponding solid state ¹³C NMR spectra. In addition, a closer interaction of an anion at C13 should effect a greater ground state stabilization in 15b than in 15a.⁶⁰ Thus the solid state uv/vis spectrum of 15b should exhibit a shorter λ_{max} than that of 15a.

The first order rate constants for isomerization of 16a and 16b are essentially the same but both are $\approx 10^2$ greater than those observed for the *syn* compounds. Seltzer suggested that the carboxylate ion for both *anti* compounds were essentially at "infinity"

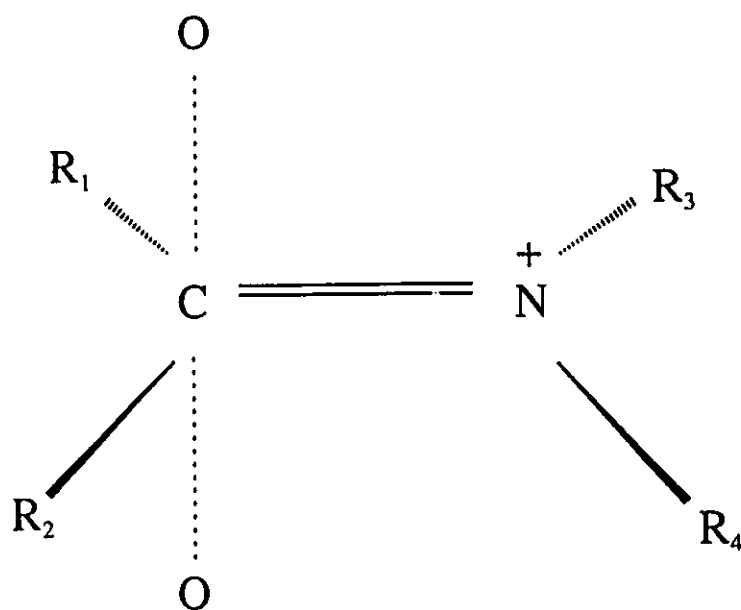


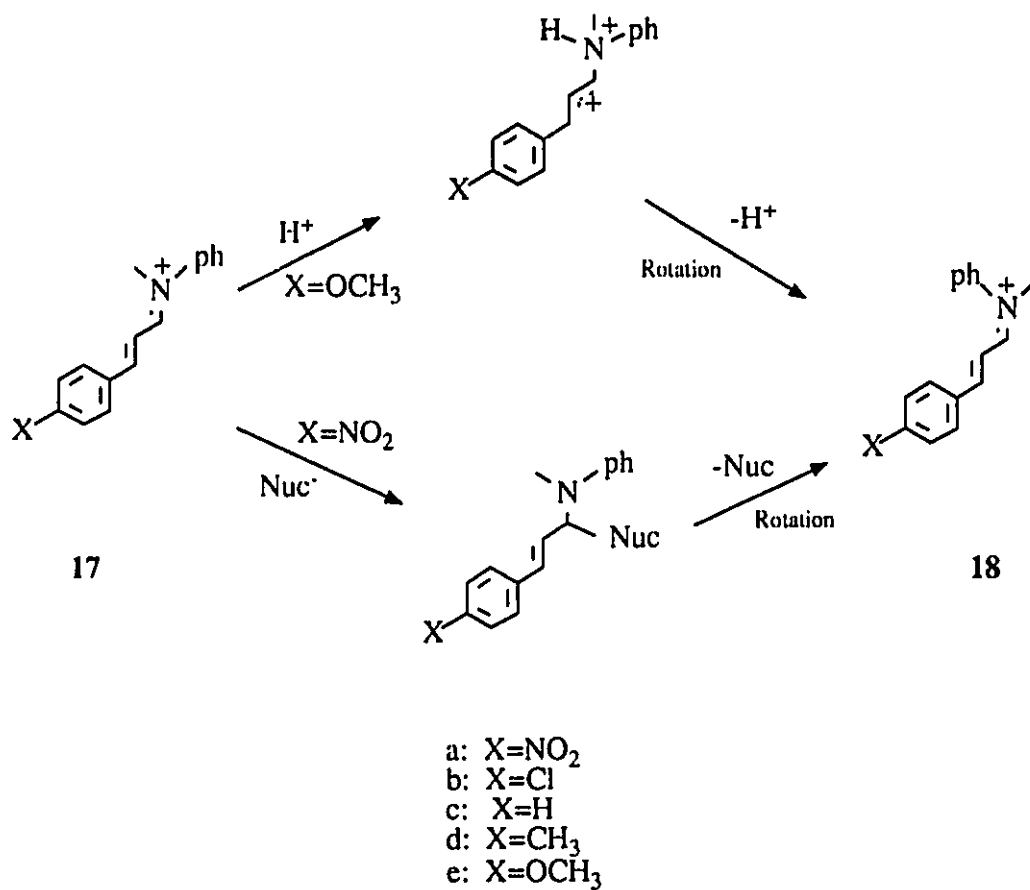
Figure 1-2: Primary interaction between an anion and a ternary iminium salt.

thereby increasing charge delocalization and creating a greater propensity for isomerization.

Pankratz and Childs investigated the thermal isomerizations about the C=N⁺ bond of a series of N-aryl-3-arylpropenylidene iminium perchlorate salts **17 a-c** in acid solutions.⁶³ This study showed that two different mechanisms operate depending on the substituents on the 3-aryl ring, Scheme 1-2. Electron donating substituents induced acid catalysed isomerization mechanisms with protonation occurring on nitrogen. Electron withdrawing groups on the 3-aryl ring caused isomerization to proceed via a nucleophilic addition mechanism. Pankratz and Childs suggested that in less acidic media or in solvents where a larger concentration of nucleophiles exist, isomerization of highly conjugated molecules such as bacteriorhodopsin should proceed via a nucleophile catalysed addition mechanism.

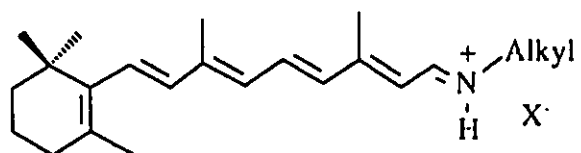
Statement of Problem

While there has been a tremendous amount of attention focussed on the structure and thermal reactivity of retinylidene iminium salts, considerable uncertainty still exists with respect to the structure of these chromophores and the relationship of their structure with their charge delocalization and uv/vis absorption. In particular, the nature and role of cation/anion interactions in retinylidene iminium salts need to be clarified including their effects on ¹³C NMR spectra and how they are able to attenuate the ground state



Scheme 1-2: Nucleophile and acid catalysed mechanisms for isomerization about the C=N bond in iminium salts.

The most direct technique for the determination of the structure of a retinylidene ion is through x-ray crystallography. Although the structure of **6** has been elucidated by Childs and James³¹, this salt is not a good model for the natural pigment since both N-substituents are carbon bearing. No crystallographic methods have been successfully employed to unequivocally determine the structure of a retinylidene iminium salt containing a proton and an alkyl group bonded to the nitrogen atom, **19**. It is the intent of this work to crystallize retinylidene iminium salts having the same substituents on nitrogen but differing counterions and to determine their structures by single crystal x-ray diffraction methods. It is intended to couple the use of x-ray crystallography with



the powerful solid state techniques of ¹³C NMR, FTIR and uv/vis absorption spectroscopic techniques in order to probe the effects of different interactions between a retinylidene cation and its counterion. It is hoped that this approach will allow definition of the different interactions and to use them to explain differences in charge delocalization and absorption maxima in various retinylidene systems.

Related to this structural study is one which addresses the mechanism of thermal C=C isomerization of retinylidene iminium salts. Previous studies have suggested that C=C bond isomerization in retinylidene iminium salts proceeds via external nucleophilic

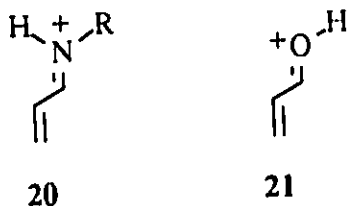
catalysis. Others have suggested that isomerization is effected by the counterion in an intramolecular process. It is intended that systematic kinetic studies in this area will serve to clarify some of the apparent confusion surrounding the thermal chemistry of retinylidene iminium salts. Of interest is the design of model systems that can be thermally isomerized at ambient temperatures and can mimic the *in vivo* system.

PART II

Protonated Unsaturated Carbonyl Compounds

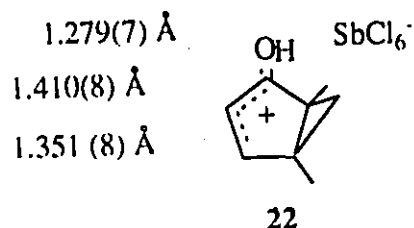
Introduction

Closely related to conjugated iminium salts are the isoelectronic protonated unsaturated carbonyl compounds. Both classes of compounds, 20 and 21, are relatively stable, easy to generate and are present in many biological systems.^{1,2,64} As such, the chemistry of protonated carbonyl compounds parallels that of iminium salts.

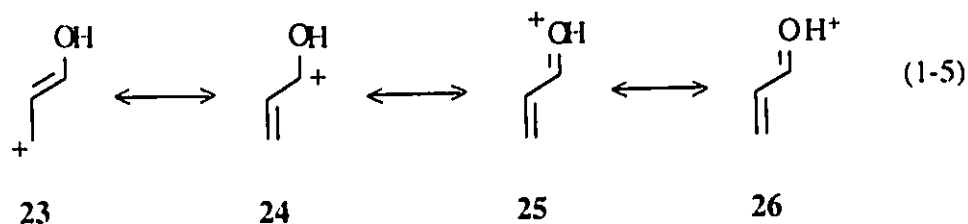


Protonated unsaturated carbonyl compounds are studied as both reactive intermediates and as observable species in strong acid solution. Several reports have detailed the isolation of some of these compounds and in several cases the structures of these compounds have been determined through x-ray crystallography.⁶⁵ In many of these structures it is clear that the C1-O bond and any conjugated double bonds are elongated and single bonds are shortened when compared to neutral unsaturated compounds. These observations are consistent with positive charge delocalization throughout the carbon framework of the molecule.

Childs et al., have elucidated the structure of a bicyclo [3.1.0] hexenyl cation as its SbCl_6^- salt.⁶⁵ The C-O bond distance observed within this cation is intermediate



between the length of a typical carbonyl bond, 1.22 Å and a C-O single bond, 1.37 Å. Similarly, the C-C bond distances in the polyene fragment are intermediate between the lengths of formal C-C single bonds and double bonds. These observations can be represented by resonance structures 23, 24 and 25. Resonance structure 26 is also important and cannot be neglected. Childs has shown through the crystal structures of



protonated benzophenones⁶⁵ and protonated cyclopropyl ketones^{66,67} that the separation between the counterion and the proton bonded to the carbonyl oxygen is less than the sum of the Van der Waal's radii for those atoms. Not only do these structures indicate a strong in-plane hydrogen bonding interaction, but they also reinforce theoretical studies

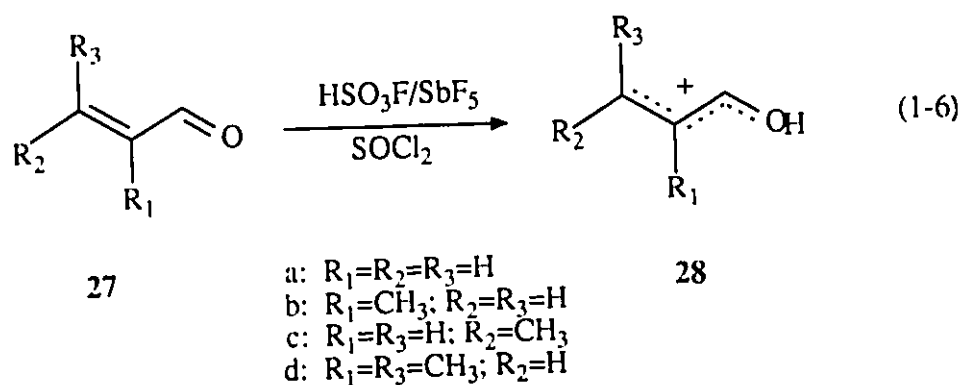
which suggest that the OH proton is acidic and that a considerable fraction of the total positive charge resides on this proton. In almost every case examined, there are also two counteranions situated about 3 Å above and below the carbonyl plane.

Recently, the crystal structures of a series of substituted protonated cyclopropyl ketones have been determined by Childs and Kostyk.⁶⁷ It was shown that the structures of these cations are dramatically distorted from those corresponding to their neutral analogues. These studies have indicated that the degree of bond length and angle distortions observed is proportional to the degree of involvement of the carbon framework in charge delocalization and substituent charge stabilization ability. In one study the crystal structures of a series of substituted protonated cyclopropyl ketones were correlated with atomic charge populations generated by high level *ab initio* calculations.⁶⁸ This study enabled quantitative correlation between systematic geometry changes with variable electronic distributions in these systems. It was shown that increasing cyclopropyl group distortions is the structural result of increased cyclopropyl group participation in positive charge stabilization and that the degree of cyclopropyl group distortion observed is proportional to the amount of positive charge available for delocalization.

It is important to note that in several cases where solid state ¹³C NMR spectra have been obtained,^{65,69} these spectra directly correspond to those spectra obtained in solution. Thus, the carbenium ion structures that were found in the crystalline state should, in general, be reflected by those in solution.

Reactions of Protonated Unsaturated Carbonyl Compounds

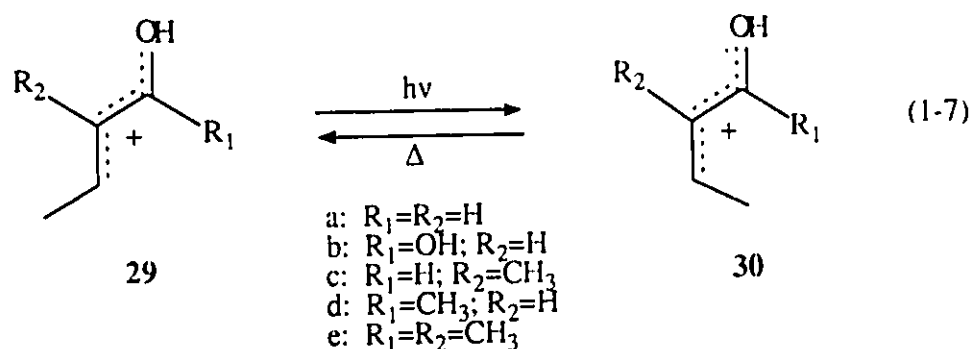
Positive charge delocalization can be an important factor in the understanding of the chemical reactivity of protonated carbonyl compounds. Hence, a number of studies dealing with the thermal and photoisomerization reactions of many simple protonated α,β -unsaturated carbonyl compounds have been reported. Initial reports by Olah described some α,β -unsaturated aldehydes and ketones studied in 1:1 $\text{HSO}_3\text{F}/\text{SbF}_5$ in SO_2ClF solution.⁷⁰ ^1H and ^{13}C NMR studies indicated that the site of protonation was the carbonyl oxygen and that the ions were hydroxyallyl in nature. The resonance of the proton on the oxygen indicated that it was highly deshielded and compared well to resonances observed from the acidic proton on carboxylic acids. ^{13}C NMR spectra of protonated versus unprotonated unsaturated species indicated that positive charge density is greater



at C3 than C1 and that there is practically no charge at C2. In all of the protonated α,β -unsaturated aldehydes, the proton on the oxygen exhibited *anti* stereochemistry. The

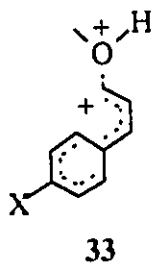
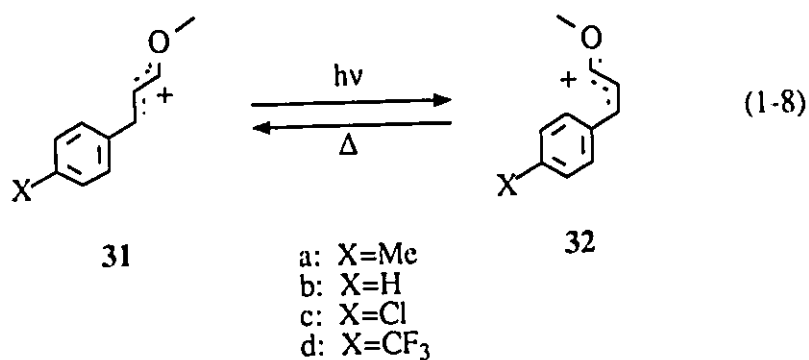
corresponding protonated α,β -unsaturated ketones behaved differently. Some cases exhibited both *anti* and *syn* conformations about the C=O'H bond while in others only one isomer was detectable. Compounds that were methyl substituted at C2 or disubstituted at C3 precluded formation of the *syn* isomer.

The group of Childs investigated the thermal and photochemical stereomutations of 1-hydroxyallyl cations **29 a-e** in FSO_3H .⁷¹ These cations were found to be thermally stable at fairly high temperatures. The 2-*cis* isomers were generated photochemically from their starting all-*trans* isomers. Since the lowest energy excited states of protonated carbonyl compounds are of π,π^* character, photoreactions characteristic of n,π^* states such as hydrogen atom abstraction do not occur in the protonated species.^{72,73} The magnitude of the coupling constants between the two protons attached to the C2-C3 partial double bond were indicative of the *cis* configuration (11 Hz).



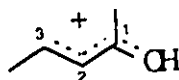
The *cis* isomers were thermally unstable and quantitatively reverted to the *trans*

isomer: upon heating with a free energy of activation in the range 20 - 26 kcal/mole at 50°C. Addition of SbF₅ (25%) to FSO₃H caused a decrease in the rate constants of the isomerization of 30a and 30c by a factor of 10². Since addition of this Lewis acid to FSO₃H is known to increase the acidity and thus reduce the nucleophilicity in solution,⁷⁴ it was proposed that the mechanism for thermal *cis-trans* isomerization in the case of 30a and 30c involved nucleophilic addition at C3, rotation and subsequent reionization. Conversely, a comparable increase in the acidity of the reaction medium increased the rates of 30d and 30e by a small amount. Blackburn and Childs showed that the thermally induced *cis* to *trans* isomerization of 3-aryl-1-methoxyallyl cations in super acidic media proceeded via an oxygen protonated dication.⁷⁵ A good correlation with



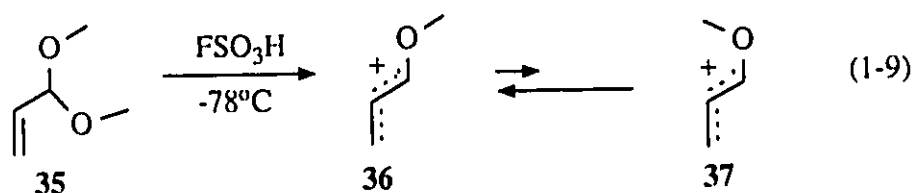
Hammett σ' values gave $\rho = -5.6$ at -5°C . It was clear that the conversion of **32** to **31** involved a mechanism in which positive charge on the aryl ring was substantially increased in the transition state as compared to the starting cations. This isomerization was shown to be more rapid in $\text{FSO}_3\text{H}:\text{SbF}_5$ (4:1) and slower in $\text{CF}_3\text{SO}_3\text{H}$. The magnitude of the acid strength dependence indicated that the stereomutations involved protonation in the rate determining step. Since no deuterium incorporation was seen on C2 or C3, clearly the mechanism of isomerization of **32-31** does not involve protonation on carbon. It was proposed that the mechanism involved protonation on oxygen to form a dication **33**.

Investigations pertaining to the dynamics and conformation about the C1-C2 partial single bond are few. However, on the basis of the expected size of the substituents $\text{Me} > \text{OH} > \text{H}^{76}$ on C1, it is likely that the *s-trans* configuration predominates with the protonated aldehydes. It has been shown by the group of Müllen⁷⁷ that rotation about the C1-C2 bond of protonated enones such as **34** may be slowed sufficiently at -85°C that non-averaged ^{13}C NMR spectra can be obtained for the *s-cis* and *s-trans* conformers. Compounds substituted at C3 failed to exhibit any dynamic processes about the C1-C2 bond and were shown to exist in a single stereoisomeric form.

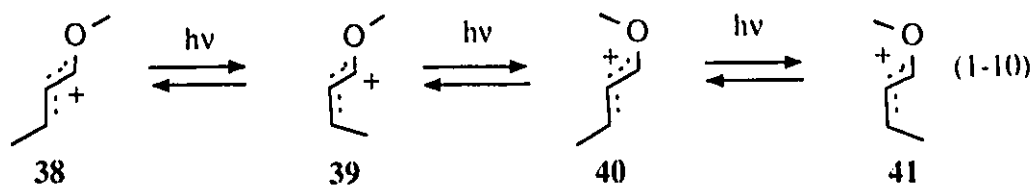


34

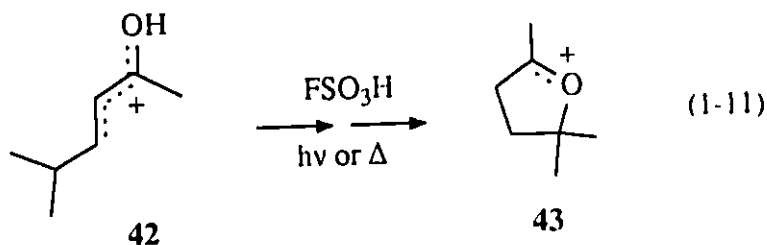
Although stereoisomerizations about the C1-O bond have been established, exchange of the proton on oxygen with the acid medium renders the isomerizations about this bond undetectable. To eliminate this problem, Childs and Hagar began to work with the corresponding O-methyl derivatives.⁷⁸ Dissolution of the dimethyl acetal of acrolein in FSO₃H gave a thermodynamic equilibrium mixture of the ions 36, 96% and 37, 4%.



Irradiation of the thermodynamic mixture of 36 and 37 at 254 nm lead to isomerization about the C1-O bond ($\phi = 0.13 \pm 0.03$ at -68°C). A photostationary state was established consisting of 73% of 36 and 23% of 37. Irradiation of a mixture of mostly 38 lead to the formation of three additional ions. Warming the FSO₃H solution to -20°C caused isomerization about the C1-O bonds. A thermodynamic equilibrium was reached with 38 (83%) and 40 (13%) at 38°C . It was further illustrated that the stereomutation about the C1-O bond was medium independent and involved a rotation mechanism.^{79,80} The free energy barrier for such a process was found to be about 18-20 kcal/mole. Substitution of a methyl group at C3 had a small effect on the rate indicating that there is no major change in charge distribution during the isomerization about the C1-O bond.



Extension of the alkyl chain results in a completely different reaction forming the tetrahydrofuryl cation. The protonation of **42** and subsequent thermal isomerization to **43** has been reported by Brower⁸¹ and by Childs.⁸² This reaction was also seen to occur photochemically.⁸²



Statement of Problem

Unlike the large number of studies that have been reported on poly-unsaturated iminium salts, the thermal chemistry of extensively conjugated protonated carbonyl compounds have not been previously reported. The lack of studies in this area is

particularly interesting in view of the fact that these species have been found to participate in mutagenic activities.⁶⁴ Most chemical carcinogens and mutagens are described as electrophilic agents and have shown to be increasingly reactive with progressively more conjugated species. It is intended that a detailed study of protonated poly-unsaturated aldehydes will enhance the current understanding of the thermal reactivity of this class of carbenium ions.

Chapter 2

The Structure of Retinylidene Iminium Salts

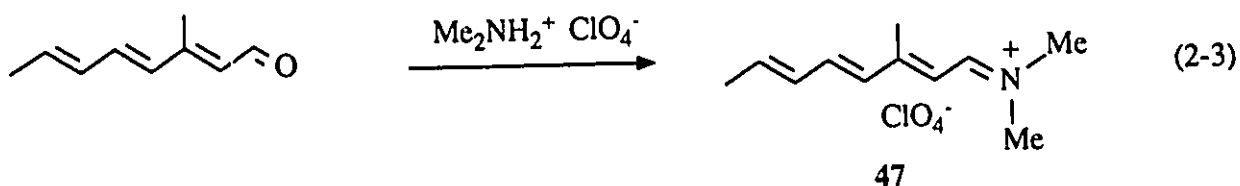
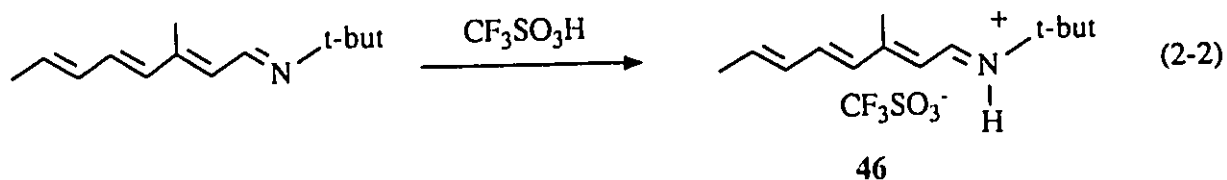
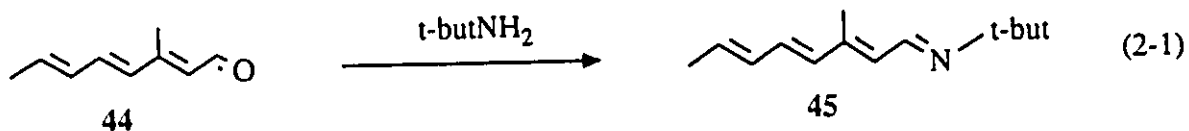
The most direct method that can be used in determining the structure of retinylidene iminium salts is x-ray crystallography. In this work, the x-ray structures of two salts have been obtained with good precision. Other techniques such as ^1H NMR, ^{13}C NMR and uv spectroscopy in both solution and the solid state have been used in an integrated manner to probe the structure of retinylidene iminium salts.

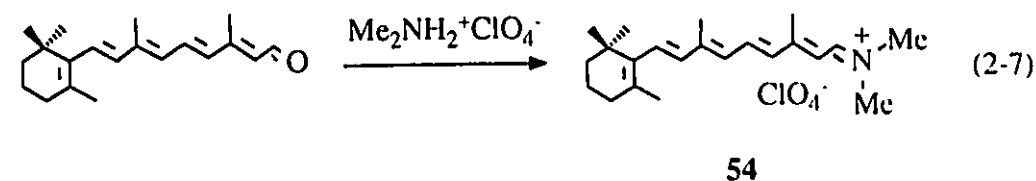
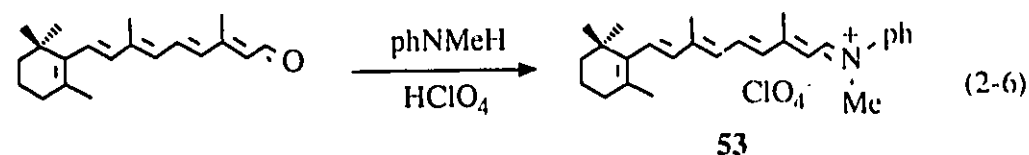
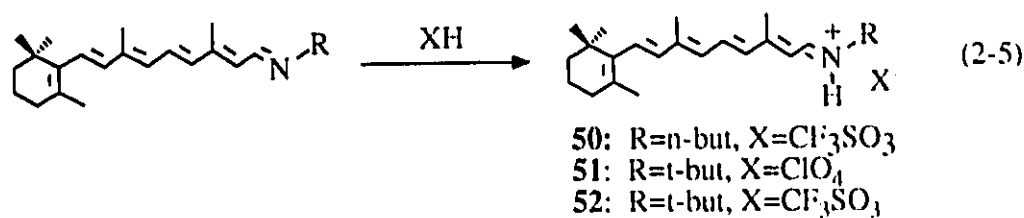
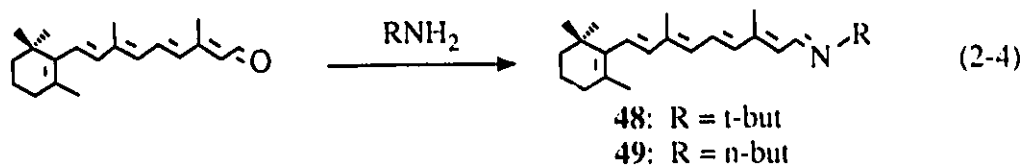
The goal of the work presented in this chapter is to investigate the effect that differing counteranions exert on the structure and charge delocalization of the retinylidene iminium cation. In the previous chapter it was shown that the position of the counteranion has a large effect on both charge delocalization in these compounds and also their thermal barriers to isomerization. The use of x-ray crystallography has not only provided the position of the counteranions but also their closest contacts to the retinylidene cation and their effects on structure. The use of both solution and solid state ^{13}C NMR, absorption and infrared spectroscopies in conjunction with x-ray crystallography has provided a measure for the extent of charge delocalization as a function of differing counteranions. These studies also include the effects of nitrogen substitution and chain length on structure and charge delocalization in these important compounds.

Results

Preparation of Iminium Salts

3-methyl-2,4,6-octatrienal, **44**, was prepared using a modified procedure of Weedon and Woods.⁴³ The synthesis of the n-butyl and t-butyl imines **45**, **48** and **49** was accomplished by the condensation of the appropriate aldehyde and either n-butyl or t-butyl amine. The imines were protonated using a dilute ethereal solution of trifluoromethane sulfonic acid or perchloric acid to give **46**, **50**, **51** and **52**. Dimethyl iminium salts **47** and **54** were prepared by reacting dimethyl ammonium perchlorate with a suitable aldehyde.⁴⁴ The N-phenyl-N-methyl retinylidene iminium perchlorate salt, **53**, was prepared by stirring an equimolar amount of retinal with N-methyl aniline in the presence of perchloric acid. The isomeric compositions resulting from the preparation





of salts 46 and 47 are given in Table 4-3 and those corresponding to the preparation of salts 50-54 are given in Table 3-1.

¹H NMR Spectroscopy

All ¹H NMR spectra were acquired at 500 MHz using CD₂Cl₂ as a solvent. The chemical shifts and coupling constants of the iminium salts are listed in Tables 2-1, 2-2, 2-3 and 2-4. The assignments were based on first order coupling constant information and by comparison to previous work in the literature.^{85,86} In iminium salts 46, 50, 51 and 52 the aldiminium proton appears as a doublet of doublets. The largest of the two

coupling constants results from coupling across the C=N bond to the proton on the nitrogen (ca. 16 Hz).^{86,87} This is indicative of protonation on nitrogen and an anti C=N configuration.⁸⁸ Since CD₂Cl₂ is a relatively non-nucleophilic solvent, exchange of the N-H proton is extremely slow on the NMR time scale and allows this coupling constant to be observed. In general, protonation induces odd numbered vinylic protons to resonate at lower fields than even numbered protons.

Table 2-1

¹H NMR Chemical Shift Data (ppm) for 3-methyl-2,4,6-octatrienyliidene Iminium Salts.^a

Position	Compound	
	47	46
C(1)H	8.62	8.23
C(2)H	6.37	6.84
C(3)H	-	-
C(4)H	6.53	6.43
C(5)H	7.12	7.00
C(6)H	6.37	6.33
C(7)H	6.37	6.25
C(8)H	1.95	1.90
C(9)H	2.40	2.26
N(H)	-	11.2
C(1')H	3.75	-
C(1'')H	3.50	-
C(2')H	-	1.50

^a referenced in CD₂Cl₂ at 5.32 ppm. Measured at 22°C.

Table 2-2

¹H,¹H Coupling Constant Data (Hz) For 3-methyl-2,4,6-octatrienyliidene Iminium Salts.

	Compound	
	47	46
J _{1,2}	11.5	11.1
J _{4,5}	15.4	16.0
J _{5,6}	9.3	10.5
J _{6,7}	15.2	14.9
J _{7,8}	5.5	6.2

Table 2-3: ¹H NMR Chemical Shift Data (ppm) For Retinylidene Iminium Salts.^{ab}

Position	Compound			
	50	51	52	53
C(2)H	1.49t	1.50t	1.49t	1.42t
C(3)H	1.63m	1.61m	1.62m	1.55m
C(4)H	2.06t	2.06t	2.06t	2.02t
C(7)H	6.54d	6.46d	6.53d	6.64d
C(8)H	6.26d	6.23d	6.26d	6.31d
C(10)H	6.32d	6.30d	6.33d	6.64d
C(11)H	7.47dd	7.44dd	7.46dd	7.67dd
C(12)H	6.54d	6.58d	6.56d	6.79d
C(14)H	6.78d	6.67d	6.89d	6.42d
C(15)H	8.21dd	8.26dd	8.26dd	8.43dd
C(16)H	1.05s	1.05s	1.05s	1.00s
C(17)H	1.05s	1.05s	1.05s	1.00s
C(18)H	1.74s	1.74s	1.74s	1.74s
C(19)H	2.10s	2.10s	2.10s	2.13s
C(20)H	2.31s	2.31s	2.31s	2.43s
NH	10.7bs	10.9bs	11.7bs	-
C(1')H	3.66t	-	-	-
C(1'')H	-	-	-	3.88s
C(2')H	1.78m	1.50s	1.50s	7.57d
C(3')H	1.42m	-	-	7.46dd
C(4')H	0.97t	-	-	7.53dd

^a s = singlet, t = triplet, dd = doublet of doublets,
bs = broad singlet, m = multiplet.

^b referenced to CD₂Cl₂ at 5.32 ppm. Measured at 22°C.

Table 2-4: ¹H, ¹H Coupling Constant Data (Hz) For Retinylidene Iminium Salts.

	Compound			
	50	51	52	53
J _{7,8}	16.1	15.9	16.1	15.9
J _{10,11}	11.8	11.8	11.7	11.7
J _{11,12}	14.9	14.9	14.8	14.5
J _{14,15}	11.4	11.2	11.1	11.7
J _{15,NH}	15.4	15.4	15.8	-

Solution ^{13}C NMR Spectroscopy

The ^{13}C NMR data for 46, 47 and 50-53 are shown in Tables 2-5 and 2-6. Assignment of the carbon atoms was accomplished by ^1H - ^{13}C hetero shift correlations, J-modulated spin echo experiments and comparison with literature data.^{61,66} All spectra were acquired at ambient temperatures except for 53 whose propensity for thermal isomerization about the C=N bond required spectral acquisition at -60°C . Comparison of the spectra with those of the imines⁶¹ shows that protonation of the imines produces a general downfield shift of the odd numbered olefinic carbons and a slight upfield shift of the even numbered carbons.

Table 2-5

¹³C NMR Chemical Shift data (ppm) For 3-methyl-2,4,6-octatrienyldene Iminium Salts.^a

Position	Compound	
	47	46
C1	165.3	159.9
C2	117.5	120.3
C3	166.5	165.0
C4	132.4	132.6
C5	145.8	143.3
C6	132.4	131.9
C7	142.8	141.7
C8	20.4	19.6
C9	15.3	15.9
C1'	49.9	59.8
C1''	40.9	-
C2	-	29.0

^a referenced to CD₂Cl₂ at 53.8 ppm. Measured at 22°C.

Table 2-6

¹³C NMR Chemical Shift Data (ppm) For Retinylidene Iminium Salts.^a

Position	Compound			
	50	51	52	53 ^b
C1	34.6	34.3	34.8	34.3
C2	40.1	40.1	39.9	39.3
C3	19.5	19.3	19.6	19.0
C4	33.7	33.4	33.8	33.6
C5	132.4	132.1	132.5	133.5
C6	137.9	137.6	138.1	136.7
C7	132.4	132.6	132.9	134.5
C8	137.1	137.1	137.5	136.7
C9	147.1	146.9	147.1	151.3
C10	129.9	129.8	129.9	134.1
C11	139.2	139.1	139.1	143.8
C12	133.6	133.4	133.7	135.0
C13	165.5	164.8	164.7	171.3
C14	119.6	119.6	119.8	118.1
C15	164.8	158.8	159.3	160.6
C16	29.1	28.6	29.0	28.8
C17	29.1	28.6	29.0	28.8
C18	21.9	21.7	21.9	22.1
C19	14.6	13.2	13.4	13.7
C20	14.8	14.4	14.7	13.7
C1'	52.6	59.5	59.6	145.0
C1''	-	-	-	41.8
C2'	31.4	28.4	28.6	130.5
C3'	19.9	-	-	122.6
C4'	13.5	-	-	130.5

^a referenced to CD₂Cl₂ at 53.8 ppm. Measured at 22°C.^b measured at -60°C.

Solid State ^{13}C NMR Spectroscopy

Solid state ^{13}C NMR spectra of the retinylidene iminium salts were obtained using cross polarization magic angle spinning (CPMAS) methods. All spectra were consistent with the presence of only one iminium salt isomer in accordance with ^1H NMR and solution ^{13}C NMR findings. The ^{13}C NMR chemical shifts of these compounds are listed in Table 2-7. Identification of the quaternary and methyl carbons was facilitated using a delay without coupling sequence which suppresses CH and CH_2 resonances.⁸⁹ The remainder of the resonances were assigned by comparison with solution spectra and literature data.⁶⁰

Table 2-7

Solid State ^{13}C NMR Chemical Shift Data (ppm) For Retinylidene Iminium Salts.^a

Position	Compound			
	50	51 ^c	52	53
C1	34.3	36.7	34.1	34.6
C2	39.3	45.2	44.2	44.0
C3	19.7	19.9	20.3	20.0
C4	34.3	34.8	36.8	36.1
C5	130.2	136.8	137.0	136.9
C6	138.9	140.1	138.0	140.2
C7	130.2	134.3	133.1	133.0
C8	138.6	136.8	136.9	139.3
C9	144.7	147.6	143.9	148.1
C10	130.4	129.7	128.8	130.3
C11	138.6	140.1	137.9	141.6
C12	130.2	133.4	133.1	133.0
C13	165.9	167.2	161.8	170.7
C14	119.3	120.3	121.5	121.4
C15	164.8	161.0	158.0	159.1
C16	29.6	29.9	27.5	29.5 ^b
C17	29.6	29.9	27.5	31.3 ^b
C18	23.3	22.3	20.3	21.7
C19	13.5	12.8	11.1	13.2
C20	13.5	15.5	14.2	13.2
C1'	52.2	60.3	61.2	143.0
C1''	-	-	-	41.6
C2'	29.6	32.2	30.4	133.3
C3'	19.7	-	-	133.3
C4'	13.5	-	-	133.3

^a referenced to adamantane, 29.5 and 38.6 ppm. Measured at 22°C.^b assignment may be reversed.^c included for ease of comparison.

Absorption Spectroscopy

Solution Spectra

The absorption spectra of the iminium salts were measured at ambient temperatures in CH_2Cl_2 . Absorption maxima and extinction coefficients are listed in Table 2-8. All of the spectra exhibited a broad and intense peak characteristic of a $\pi\text{-}\pi^*$ transition in iminium salts.

Solid State Spectra

Solid state absorption spectra are listed in Table 2-8. Solid state absorption spectroscopy is not a common technique in organic chemistry but it can yield valuable structural information pertaining to ground state cation/anion interactions and conformational changes on moving from solution to the solid state. Spectra were obtained by simply smearing micro crystalline fragments onto a glass or quartz slide⁹⁰ using a HP photodiode spectrometer. The resulting absorption peaks were typically broader than those obtained from solution but still Gaussian in shape. The error in the absorption maximum for each spectrum was approximately ± 2 nm.

Table 2-8

Absorption Spectral Data (nm) For Iminium Salts 46, 47 and 50-53.^a

Compound	λ_{\max} (nm)	ϵ_{\max} ($\times 10^4$)	λ_{\max} (solid) (nm)
46	378	3.55	370
47	392	3.12	375
50	476	4.36	444
51	472	4.18	504
52	465	4.51	445
53	564 ^b	4.25	505

^a in CH₂Cl₂ at 22°C.^b at -70°C.

X-ray Crystallographic Structure Determinations

Single crystals of **51** and **52** suitable for x-ray crystallographic studies were generated by slow diffusion of diethyl ether into acetonitrile solutions of each compound. Crystals large enough for crystallographic analysis were exceedingly difficult to grow. The work reported here represents the first examples of secondary retinylidene iminium salts containing an N-alkyl substituent to be successfully analyzed by x-ray crystallography. The crystals were found to be stable to light and moisture at room temperature. Experimental details pertaining to data collection and the solution of the structures can be found in the Experimental section and the Appendix.

Bond lengths, angles, torsion angles and least squares planes of the two salts are given in Tables 2-9 to 2-12. Plots for **51** illustrating the geometry of the cation, stereoscopic view of unit cell contents and packing diagrams are shown in Figures 2-1 to 2-4. Those for **52** are shown in Figures 2-5 to 2-8.

Table 2-9: Selected Bond Lengths (Å) For 51 and 52.

Bond	Compound	
	51	52
C1-C2	1.528(8)	1.51(1)
C1-C16	1.532(8)	1.55(1)
C1-C17	1.539(8)	1.51(2)
C2-C3	1.473(9)	1.46(2)
C3-C4	1.487(10)	1.54(2)
C4-C5	1.509(8)	1.50(2)
C5-C6	1.356(7)	1.33(1)
C5-C18	1.496(9)	1.50(1)
C6-C1	1.542(8)	1.55(1)
C6-C7	1.437(7)	1.45(1)
C7-C8	1.355(7)	1.32(1)
C8-C9	1.448(7)	1.46(1)
C9-C10	1.333(7)	1.34(1)
C9-C19	1.493(8)	1.48(1)
C10-C11	1.458(7)	1.43(1)
C11-C12	1.326(7)	1.33(1)
C12-C13	1.434(7)	1.43(1)
C13-C14	1.346(7)	1.36(1)
C13-C20	1.519(8)	1.47(1)
C14-C15	1.402(7)	1.40(1)
N-C15	1.266(6)	1.27(1)
N-C21	1.506(6)	1.46(1)
C21-C22	1.501(7)	1.55(1)
C21-C23	1.527(8)	1.50(1)
C21-C24	1.519(8)	1.49(1)
Cl-O1	1.402(8)	-
Cl-O2	1.371(14)	-
Cl-O3	1.408(9)	-
Cl-O4	1.390(8)	-
S-O1	-	1.415(7)
S-O2	-	1.443(7)
S-O3	-	1.409(7)
S-C25	-	1.78(1)
F1-C25	-	1.32(1)
F2-C25	-	1.28(1)
F3-C25	-	1.31(1)

Table 2-10: Selected Bond Angles (°) For 51 and 52.

Angle	Compound	
	51	52
C15-N-C21	129.5(5)	130.7(8)
C2-C1-C16	105.0(5)	111(1)
C6-C1-C16	111.4(5)	111(1)
C16-C1-C17	109.5(5)	110(1)
C2-C3-C4	109.5(6)	110(1)
C3-C4-C5	114.1(5)	111(1)
C4-C5-C18	112.8(5)	112(1)
C1-C6-C5	120.0(5)	122(1)
C5-C6-C7	119.2(5)	118(1)
C7-C8-C9	126.4(5)	128.9(9)
C8-C9-C19	119.8(5)	116.1(9)
C9-C10-C11	128.6(5)	127.6(9)
C11-C12-C13	127.4(5)	125.8(9)
C12-C13-C20	118.4(5)	118(1)
C13-C14-C15	127.1(5)	126.4(9)
N-C21-C22	107.0(4)	105.9(8)
N-C21-C24	105.8(4)	107.3(8)
C22-C21-C24	111.7(5)	112(1)
C2-C1-C6	112.2(5)	111(1)
C2-C1-C17	108.9(5)	103(1)
C6-C1-C17	109.8(5)	110(1)
C1-C2-C3	113.6(6)	112(1)
C23-C21-C24	111.4(5)	113(1)
C4-C5-C6	123.1(6)	124(1)
C6-C5-C18	124.1(5)	124(1)
C1-C6-C7	120.8(5)	119.8(9)
C6-C7-C8	130.1(5)	132(1)
C8-C9-C10	117.3(5)	119.0(9)
C10-C9-C19	122.9(5)	125(1)
C10-C11-C12	122.1(5)	121.7(9)
C12-C13-C14	119.9(5)	118.7(8)
C14-C13-C20	121.7(5)	123(1)
N-C15-C14	124.1(5)	124.5(9)
N-C21-C23	110.1(4)	112.0(9)
C22-C21-C23	110.6(5)	106.4(8)
O1-C1-O2	108.5(9)	-
O1-C1-O3	114.1(8)	-

Table 2-10 (continued)

Angle	51	52
O1-C1-O4	110.4(6)	-
O2-C1-O3	100(1)	-
O2-C1-O4	109.3(9)	-
O3-C1-O4	114.2(7)	-
O1-S-O2	-	115.7(5)
O1-S-O3	-	113.3(5)
O1-S-C25	-	101.7(5)
O2-S-O3	-	115.5(5)
O2-S-C25	-	104.9(6)
O3-S-C25	-	103.7(6)
S-C25-F1	-	114(1)
S-C25-F2	-	112(1)
S-C25-F3	-	109(1)
F1-C25-F2	-	108(1)
F1-C25-F3	-	107(1)
F2-S-F3	-	107(1)

Table 2-11

Torsion or Conformation Angles For 51 and 52.

Torsion Angle	Compound	
	51	52
N-C(15)-C(14)-C(13)	-175.1(5)	-179(1)
C(1)-C(6)-C(5)-C(4)	-2.2(8)	2(2)
C(1)-C(6)-C(7)-C(8)	5.5(9)	-3(2)
C(2)-C(1)-C(6)-C(7)	170.6(5)	-171(1)
C(3)-C(2)-C(1)-C(6)	42.9(9)	-46(2)
C(3)-C(2)-C(1)-C(17)	-78.8(8)	-163(1)
C(3)-C(4)-C(5)-C(18)	165.5(6)	-167(1)
C(5)-C(6)-C(1)-C(16)	-128.0(5)	-111(1)
C(5)-C(6)-C(7)-C(8)	-173.3(5)	174(1)
C(7)-C(6)-C(1)-C(16)	53.3(7)	66(1)
C(7)-C(6)-C(5)-C(18)	-5.4(8)	7(2)
C(7)-C(8)-C(9)-C(19)	-2.4(9)	3(2)
C(9)-C(10)-C(11)-C(12)	176.7(6)	-179(1)
C(11)-C(10)-C(9)-C(19)	-3(1)	1(2)
C(11)-C(12)-C(13)-C(20)	4.7(9)	-4(2)
C(14)-C(15)-N-C(21)	176.0(5)	-176.1(9)
C(15)-N-C(21)-C(23)	-19.6(8)	18(2)
C(15)-C(14)-C(13)-C(20)	-9.6(9)	8(2)
C(1)-C(2)-C(3)-C(4)	-61.5(9)	64(2)
C(1)-C(6)-C(5)-C(18)	175.8(5)	-177(1)
C(2)-C(1)-C(6)-C(5)	-10.6(8)	13(2)
C(2)-C(3)-C(4)-C(5)	46.8(9)	-46(2)
C(3)-C(2)-C(1)-C(16)	164.1(7)	78(2)
C(3)-C(4)-C(5)-C(6)	-16.3(9)	14(2)
C(4)-C(5)-C(6)-C(7)	176.6(5)	-174(1)
C(5)-C(6)-C(1)-C(17)	110.6(6)	126(1)
C(6)-C(7)-C(8)-C(9)	-179.5(5)	178(1)
C(7)-C(6)-C(1)-C(17)	-68.2(7)	-57(1)
C(7)-C(8)-C(9)-C(10)	176.9(5)	-176(1)
C(8)-C(9)-C(10)-C(11)	178.1(5)	-179(1)
C(10)-C(11)-C(12)-C(13)	172.3(5)	-173(1)
C(11)-C(12)-C(13)-C(14)	-173.9(6)	172(1)
C(12)-C(13)-C(14)-C(15)	168.9(5)	-168(1)
C(15)-N-C(21)-C(22)	100.7(6)	133(1)
C(15)-N-C(21)-C(24)	-140.1(6)	-106(1)

Table 2-11 (continued)

Torsion Angle	Compound	
	51	52
F1-C25-S-O1	-	-56(1)
F1-C25-S-O2	-	-176.5(9)
F1-C25-S-3	-	62(1)
F2-C25-S-O1	-	67(1)
F2-C25-S-O2	-	-54(1)
F2-C25-S-O3	-	-175(1)
F3-C25-S-O1	-	-175(1)
F3-C25-S-O2	-	64(1)
F3-C25-S-O3	-	-57(1)

Table 2-12: Selected Least Squares Planes Data For 51 and 52.

Atom	Distance (\AA) of Atoms From Plane ^{ab}			
	A		B	
	51	52	51	52
N	0.023	0.023	-1.42	-1.61
C1	-2.54	-2.50	0.00	0.00
C2	-2.78	-2.71	0.30	0.35
C3	-3.72	-3.65	-0.42	-0.39
C4	-3.16	-3.06	-0.00	-0.00
C5	-2.63	-2.50	0.01	0.01
C6	-2.35	-2.25	-0.01	-0.01
C7	-1.92	-1.82	-0.07	-0.11
C8	-1.79	-1.62	-0.22	-0.26
C9	-1.25	-1.14	-0.26	-0.32
C10	-1.04	-0.94	-0.35	-0.41
C11	-0.62	-0.49	-0.44	-0.49
C12	-0.38	-0.31	-0.47	-0.55
C13	-0.12	-0.01	-0.71	-0.78
C14	-0.020	-0.02	-0.82	-0.99
C15	0.017	0.02	-1.26	-1.45
C16	-1.28	-3.70	1.11	-1.36
C17	-3.73	-1.24	-1.36	1.14
C18	-2.40	-2.21	0.09	0.07
C19	-1.02	-0.91	-0.18	-0.28
C20	0.010	0.21	-0.87	-0.88
C21	-0.020	-0.02	-1.97	-2.16
C22	1.35	-1.08	-0.83	-3.15
C23	-0.55	-0.49	-2.77	-2.95
C24	-0.94	1.34	-2.84	-1.01
Cl	1.18	-	0.43	-
O1	0.28	0.57	-0.42	-0.31
O2	0.89	0.09	0.54	-1.08
O3	2.50	-0.15	1.78	-0.44
O4	1.07	-	-0.08	-
S	-	0.49	-	-0.30

^a Plane A: plane of the atoms N C14 C15 C21

Plane B: plane of the atoms C1 C4 C5 C6

^b the angle between Planes A and B for both 51 and 52 is 20°.

Figure 2-1: The Conformation of 51.

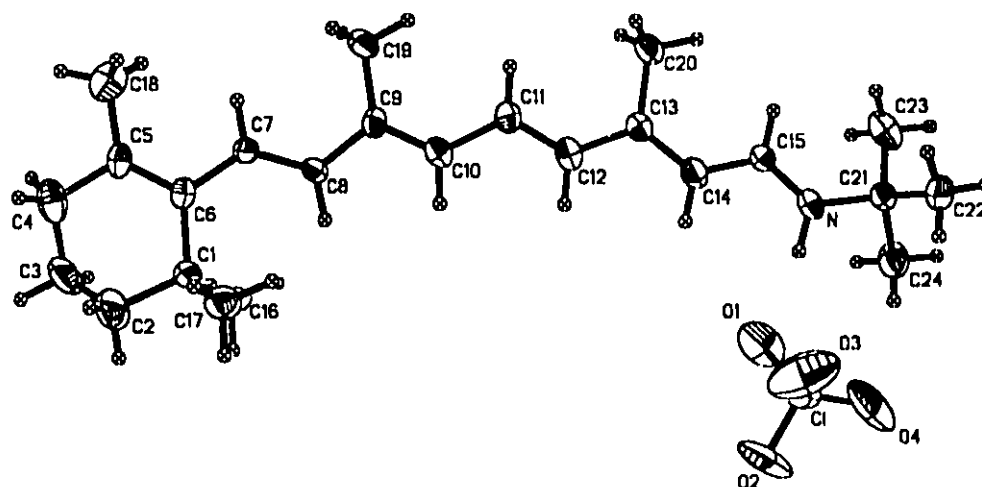
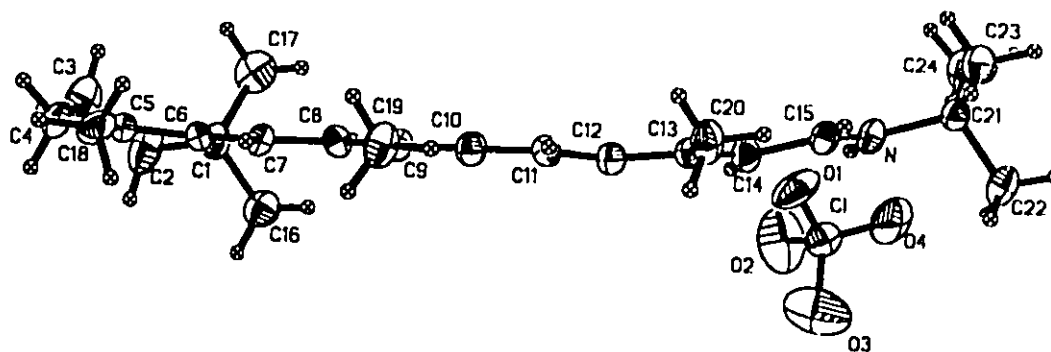
a. Top View of 51.b. Edge View of 51.

Figure 2-2: Stereoscopic View of Unit Cell Contents for 51.

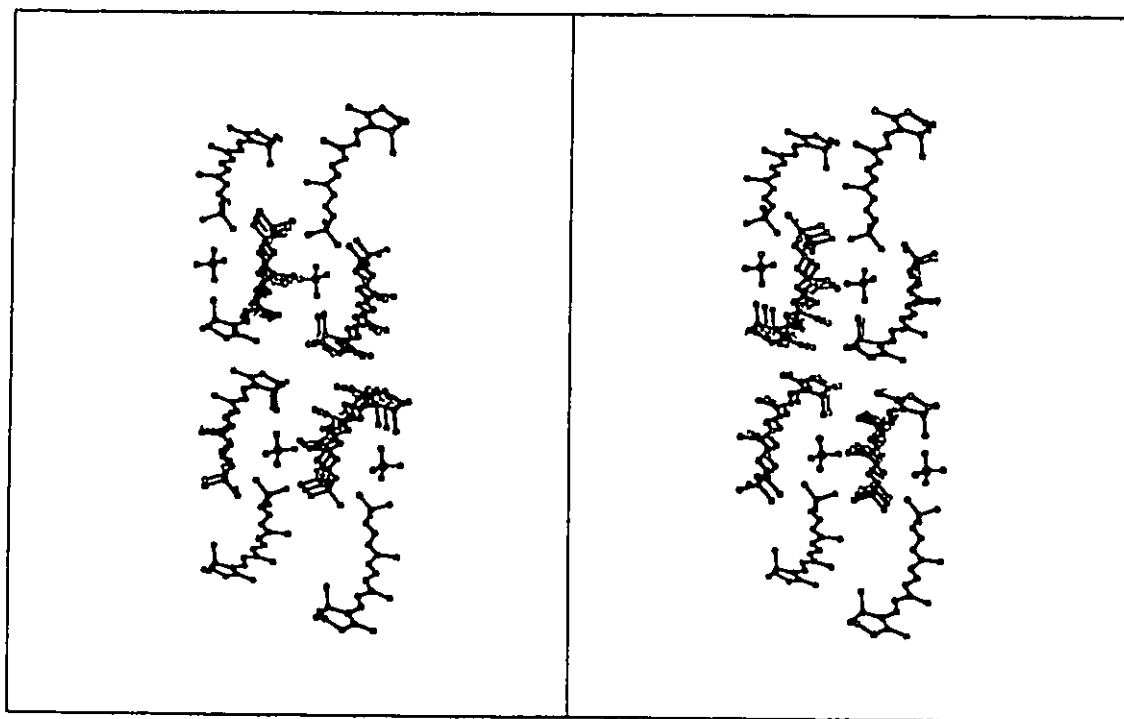


Figure 2-3: Unit Cell Packing in 51 - View Along z-Axis.

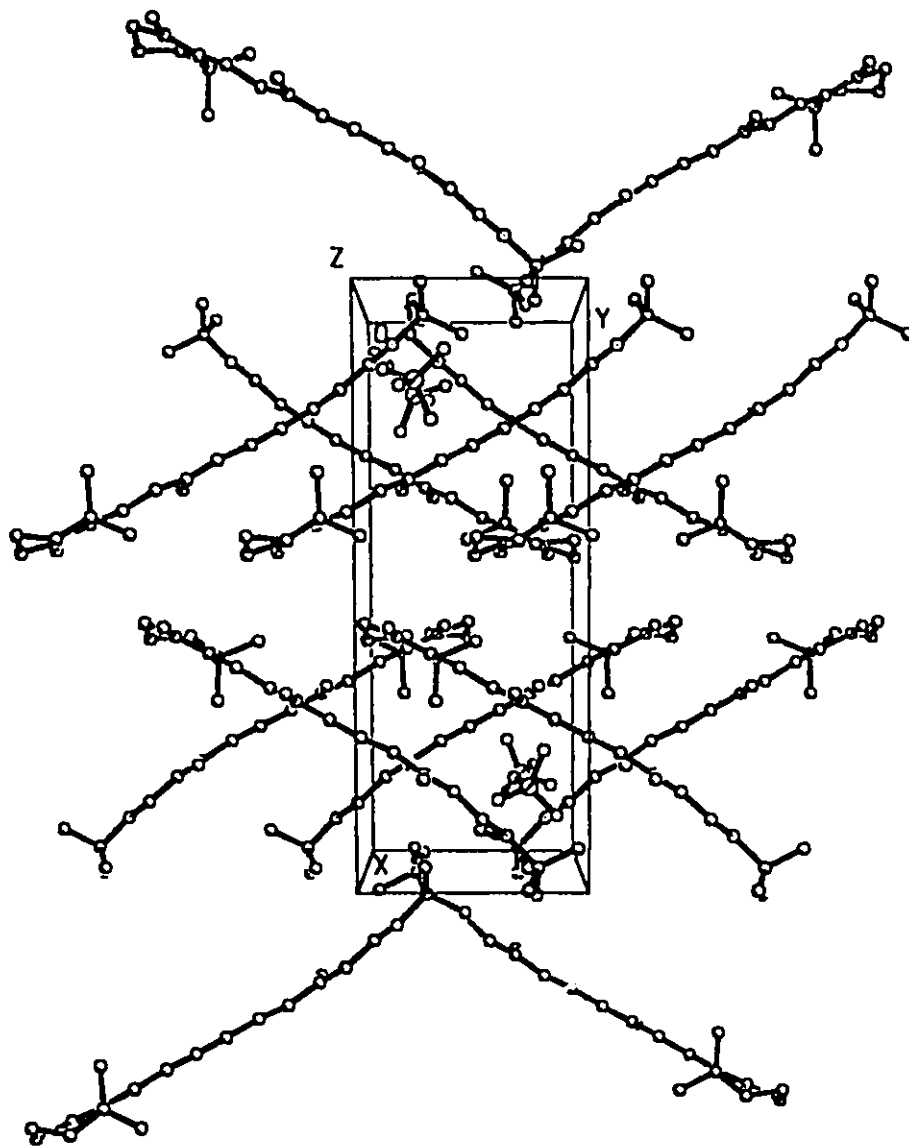


Figure 2-4: Unit Cell Packing in 51 - View Along y-Axis.

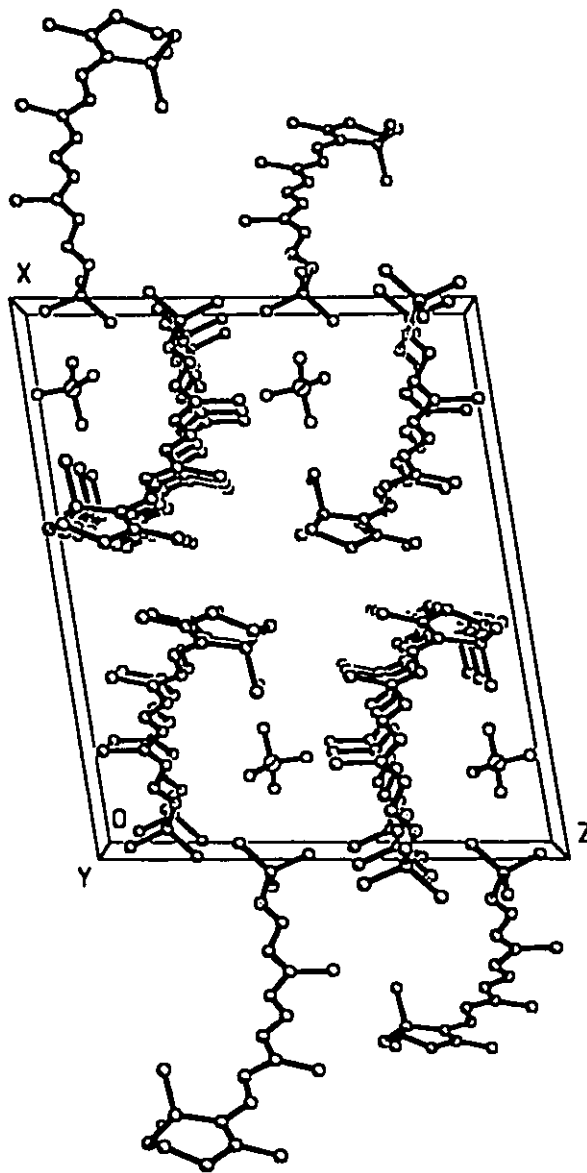


Figure 2-5: The Conformation of 52.

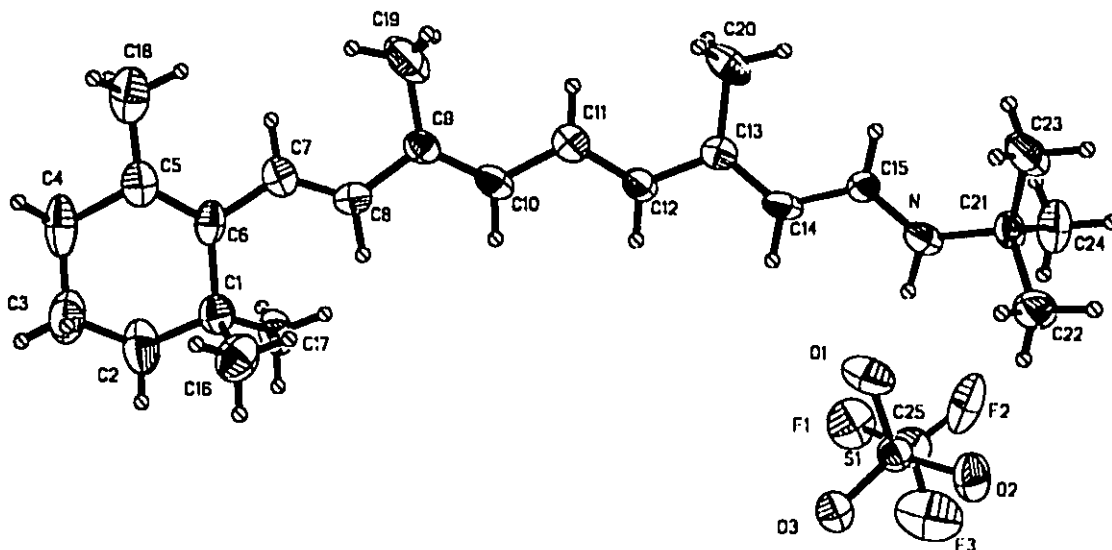
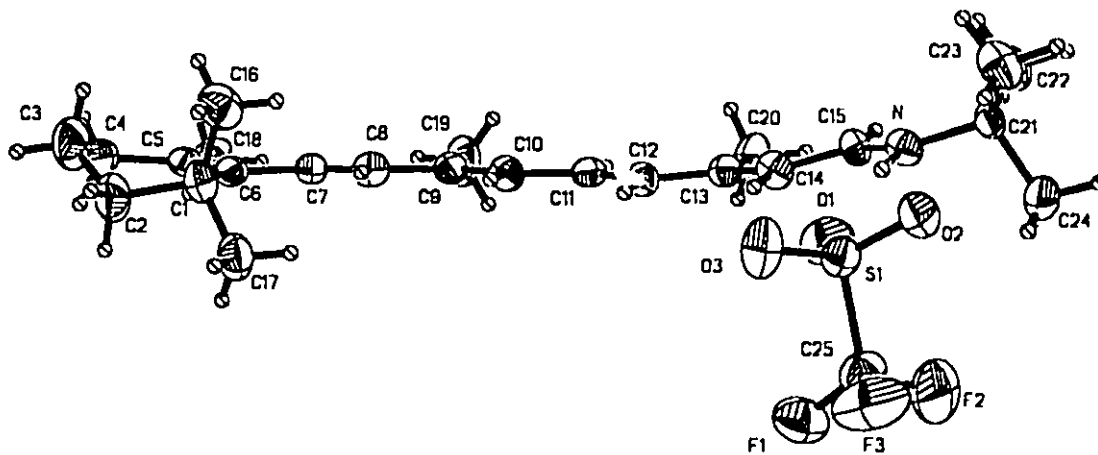
a. Top View of 52.b. Edge View of 52.

Figure 2-6: Stereoscopic View of Unit Cell Contents for 52.

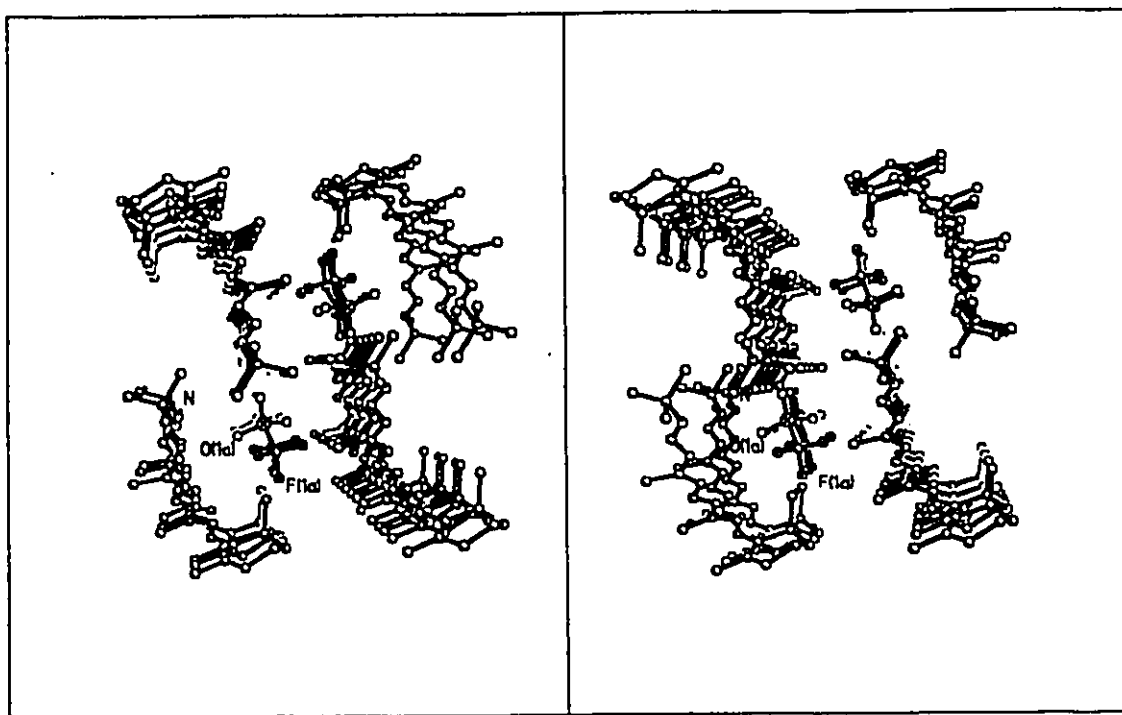


Figure 2-7: Unit Cell Packing in 52 - View Along x-Axis.

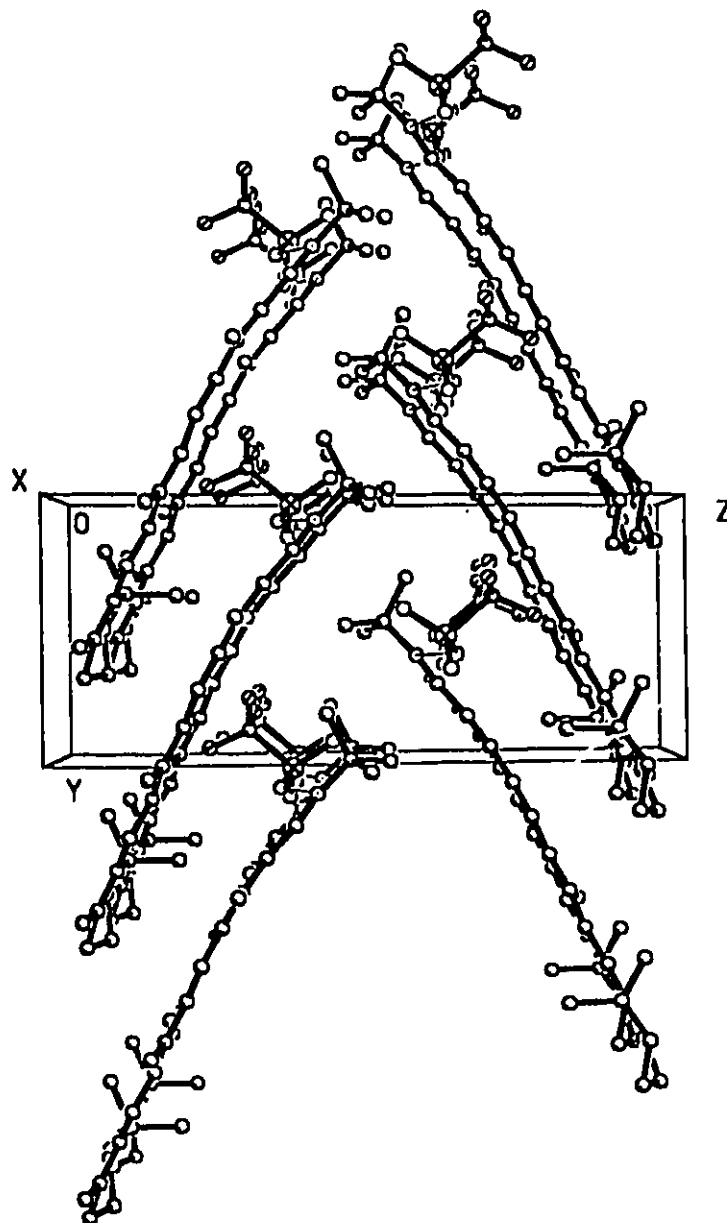
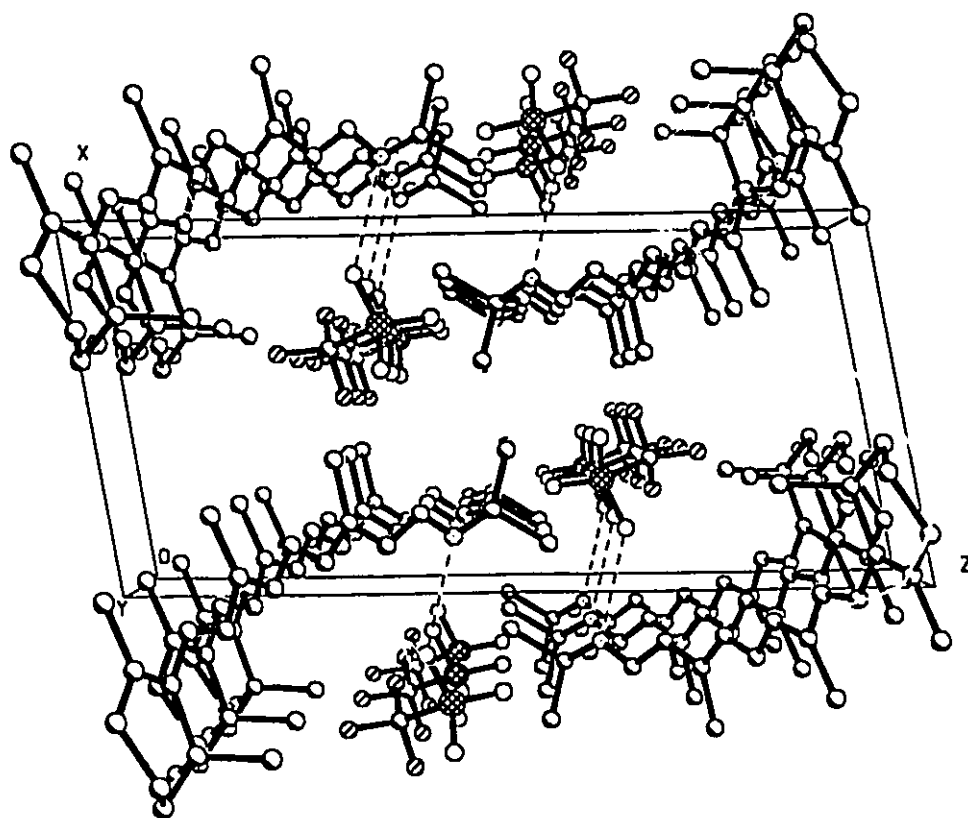


Figure 2-8: Unit Cell Packing in 52 - View Along y-Axis.



Discussion

X-Ray Crystallography

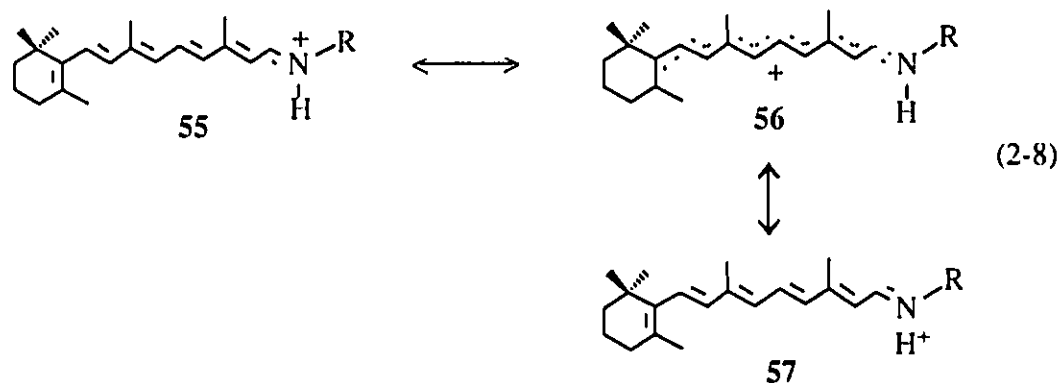
The structures of **51** and **52** are shown in Figures 2-1 and 2-5. These molecules differ only by the presence of the perchlorate anion in **51** and the trifluoromethanesulfonate (triflate) anion in **52**. With the exception of the C20-C13 bond lengths, all bond lengths (Table 2-9) and angles (Table 2-10) are the same within experimental error.

Both cations contain a *trans* configuration about each of the C-C single and double bonds of their unsaturated chains. In particular, it should be noted that **51** and **52** both have *s-trans* configurations about the C6-C7 bond with C5-C6-C7-C8 torsion angles (Table 2-11) of 173.3(5)° and 174(1)°, respectively. The C6-C7-C8 bond angles of 130.1(5)° for **51** and 132(1)° for **52** are large as a result of the steric interactions between the methyl groups at C1 and the hydrogen atom at C8. Other relatively large bond angles are found at C7-C8-C9, C9-C10-C11, C11-C12-C13 and C13-C14-C15.

Each cation is bowed in the plane defined by atoms N, C14, C15 and C21 and bent normal to this plane, Figures 2-1 and 2-5. The angle of intersection of the plane defined by C1,C4,C5,C6 and N, C14, C15, C21 is 20° for both **51** and **52**.

The bond lengths found in **51** and **52** should give some indication of the degree of positive charge delocalization. In a localized system such as **55** where the positive charge is placed on the nitrogen atom, "normal" single and double bond lengths are expected to predominate. An alternating bond pattern should be exhibited as in the parent

retinals or retinoic acids where the single bonds are much larger than the double bonds. As charge is delocalized through the system this alternation is expected to decrease with the former single bonds adopting some double bond character and vice versa, equation 2-8. Thus the single bonds are expected to contract and the double bonds are expected to lengthen. Ideally, with full positive charge delocalization an intermediate C-C distance would be achieved near that of an aromatic C-C bond at 1.384(13)Å.⁹¹



The C=N+ bond lengths in 51 and 52 are 1.266(6) Å and 1.27(1) Å, respectively. The average of these two bond lengths (1.268(6) Å) is not significantly different when compared to C=N bond lengths found for simple neutral imines¹,

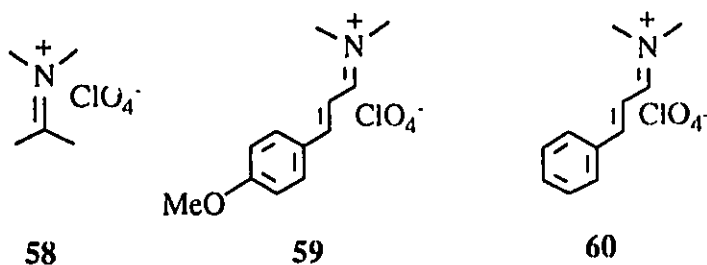
¹ The statistical treatment used in this chapter to determine the difference between two directly comparable bond length or angle values $n_1(\sigma_1)$ and $n_2(\sigma_2)$ is as follows:

$$\sigma = [(\sigma_1)^2 + (\sigma_2)^2]^{1/2}$$

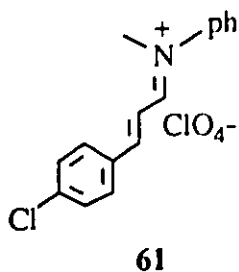
where σ_1 and σ_2 are the standard deviations of the two observed values being compared, n_1 and n_2 , and σ is the standard deviation associated with the difference between the two values. The values of n_1 and n_2 are significantly different at the 99% confidence level if the following inequality holds:

$$| n_1 - n_2 | > 3\sigma$$

1.279(8) Å.⁹¹ One would expect that upon protonation the C=N⁺ bond would elongate as a result of positive charge delocalization into the polyene chain. This did not occur in the case of 51 and 52. Using the statistical treatment available from Allen, the C=N⁺ bond length (1.291(8) Å average) of 58 (1.30(2) Å)⁹², 59 (1.284(9) Å)⁹³ and 60 (1.290(6) Å)⁹³ are the same within experimental error (difference 2.3σ) as the average C=N⁺ bond



length in 51 and 52. The lack of variation in C=N⁺ bond lengths between these two groups indicates that a dramatic change in the polyene side chain from retinylidene to simple methylidene has no detectable structural effect on the delocalization of positive charge in dialkyl- or mono-alkyl iminium salts. Substitution of a phenyl and methyl group on the nitrogen atom, as evidenced by 61 (C=N, 1.325(8) Å)⁹⁴ and 53 (C=N, 1.324(6) Å)⁹¹ (1.325(5) Å average) significantly increases the C=N⁺ bond length from



the average reported for 58, 59 and 60 (difference 3.6σ). Thus, a large change in nitrogen substitution results in variation in the C=N' bond length in iminium salts whereas a dramatic change in polyene chain length has no detectable effect.

Examination of the C-C double bond lengths within the polyene structure of 51 and 52 (Table 2-9) reveals these bond lengths to be more representative of those found in simple butadiene derivatives ($1.330(14) \text{ \AA}$)⁹¹ and hexatriene derivatives ($1.345(12) \text{ \AA}$).⁹¹ Although it appears that positive charge is not extensively delocalized into the polyene chain for 51 and 52 there appears to be a slight diminution of positive charge delocalization as distance from the nitrogen atom increases. This can be seen on examination of the data presented in Figure 2-9 where progressively larger alternations in bond distances are observed as the bond in question is further removed from the nitrogen atom. The effect is more pronounced in the formal single bonds. A more dramatic pattern has previously been shown for 53. The individual differences in the C-C and C=C bond lengths in 53 were found to be greater than the experimental errors.³¹ The progressive bond distance changes are in accord with ¹³C data to be discussed later.

From the results available from this work, it can be inferred that positive charge in retinylidene iminium salts is borne largely by the nitrogen atom with comparatively little charge migrating into the polyene fragment. Since little positive charge is delocalized to the aldiminium carbon atom, structural distortions in the polyene chain are relatively small. As shown in equation 2-8, resonance structure 55 more accurately illustrates the nature of the C=N' bond in retinylidene iminium salts as having more

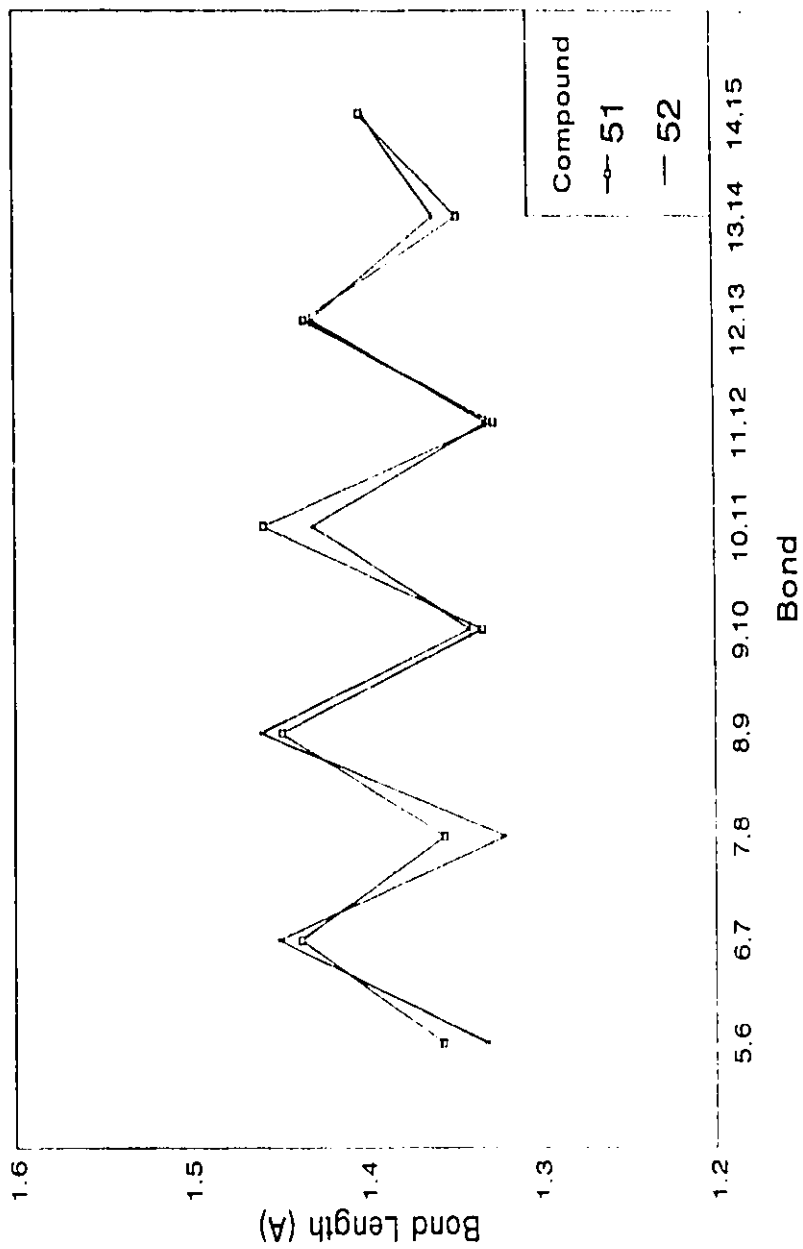
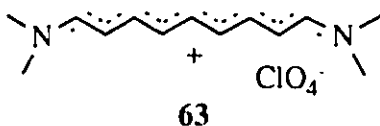
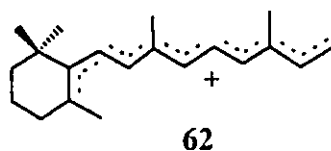


Figure 2-9: Bond Length Alternation in 51 and 52.

double bond character.

In contrast to the small structural distortions observed in the polyene C-C bond lengths of **51** and **52**, compound **62** is expected to have very large structural distortions in its polyene framework. Compound **62**, with no perturbing heteroatom substituents has been reported to absorb at 610 nm (toluene/ $\text{Cl}_3\text{CCO}_2\text{H}$)⁹⁵ as compared to **51** at 472 nm (CH_2Cl_2) and **52** at 465 nm (CH_2Cl_2). Replacement of both the terminal carbon atoms of an undecapentenyl cation by nitrogen has little effect on the absorption maximum. For example, the λ_{max} of the polymethine dye **63** is at 625 nm (CH_2Cl_2).⁹⁶ The large bathochromic shifts exhibited by **62** and **63** over **51** and **52** suggests that most of the positive charge in **62** and **63** is delocalized over the entire unsaturated system with little or no C-C bond alternation. Thus, **62** and **63** serve as good examples of cations containing complete positive charge delocalization throughout the polyene framework.



If **56** were a good model for retinylidene iminium salts then it is expected that the

absorption maximum for these salts would be greater than 600 nm. As a result of their relatively short absorption maxima (Table 2-8) it is inferred that positive charge is not completely delocalized in retinylidene iminium salts. Hence, the absence of structural distortions within these salts is in agreement with their observed absorption spectra.

Cation/Anion Interactions

To this point the structures of retinylidene salts 51 and 52 have been discussed with no reference to the effect of the counteranion. As has been stated earlier, there are few significant differences in the structure of the two cations 51 and 52. However, upon examination of the solid state ^{13}C NMR and uv spectra summarized in Tables 2-7 and 2-8 it is apparent that the anion has a large impact on the spectroscopic properties of these systems.

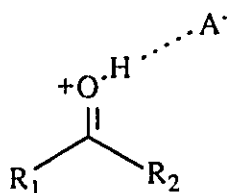
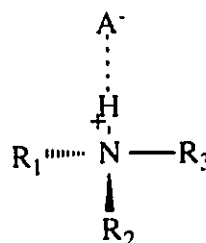
Examination of Figures 2-3 and 2-7 indicates that even though the packing within the crystalline lattice in 51 and 52 is different as a result of differing counterions, the retinylidene cations in each system lie on top of one another in a very similar π - π stacking fashion. The anionic spacial arrangement in both systems is also very similar. The polar ends of the cations in 51 and 52 are all directed toward one another while the relatively non-polar β -ionone rings are grouped together. There is no apparent reason why the spectroscopic differences observed for 51 and 52 can be attributed to the stacking arrangements of the cation or general placement of the anion. Rather, it would appear that the unique spectroscopic properties exhibited by 51 and 52 are primarily a

result of the differential N-H---O interactions in both systems and, to a lesser extent, to the weaker C-H---O and C-H---F interactions. In order to understand this it is important to examine how the anion interacts with the retinylidene cation.

Location of the Anion

Within each of the crystalline lattices of the two salts 51 and 52, significant contacts between the cations and an atom of the counter-anion are observed. The closest such contacts in 51 and 52 are hydrogen bonding interactions between the iminium proton of the cations and an oxygen atom of the ClO_4^- or CF_3SO_3^- counterions. The N-H and H-O internuclear distances are imprecise owing to the uncertainty associated with crystallographically determined hydrogen atom positions. However, the corresponding N---O internuclear distances are determined with good precision. The closest N---O interactions in the lattices for 51 (2.939(7) Å) and 52 (2.85(1) Å) are significantly different (7σ difference). The N---O contact in 52 is shorter than the sum of the Van der Waals radii of the respective neutral atoms (2.90 Å). Upon examination of the N-O-H angles in Table 2-13, it is clear that in both 51 and 52 linear or near linear hydrogen bonds exist between the proton on the nitrogen and an oxygen atom on the anion. In general, it has been found from previous x-ray crystallographic determinations of salts of organic cations with an OH or NH group bonded to a positively charged system that there is always an anion located nearby such that a linear hydrogen bond exists between the anion and the heteroatom bearing the proton. For example, this has been found to

be the case in every reported structure of protonated ketones^{65,66,67}, **64**. Similarly, in crystal structures of ammonium salts^{97,98,99}, **65**, the anion is always found to form a linear hydrogen bond with the acidic proton on the nitrogen.

**64****65**

The shorter N---O distance in **52** as compared to **51** would suggest a stronger hydrogen bonding interaction is present in the former salt. This is corroborated by the observation that the ¹H NMR chemical shift of the N(H) proton in **52** is 0.8 ppm further downfield from the analogous proton in **51**. This suggests that the proton accepting capability of CF₃SO₃⁻ in **52** is greater than ClO₄⁻ in **51**.

The observation of an abnormally short C13-C20 bond length of 1.47(1) Å in **52** versus 1.519(8) Å in **51** lead to a detailed investigation of secondary interactions involving C(20)-H---O and C(20)-H---F hydrogen bonds. Table 2-13 lists all the important interactions occurring within **51** and **52**. In the present work stronger hydrogen bonds involving C20 were found in **52** which has a triflate counteranion. Two of the protons on C20 were found to be participating in hydrogen bonding, each with a

Table 2-13: Intermolecular Contact Distances (Å) And Angles (°) For 51 and 52.

		Distance (Å)	Angles (°)			
			θ		ϕ	
51	O1-N	2.939(7)	N-O1-H1	3.4	N-H1-O1	169.5
	O1-H1	1.999	C14-O1-H14	11.0	C14-H14-O1	137.1
	O1-C14	3.421(8)	C20-O2-H202	5.0	C20-H202-O2	159.4
	O1-H14	2.668				
	O2-C20	3.800(8)				
	O2 H202	2.911				
52	O1-N	2.85(1)	N-O1-H1	5.4	N-H1-O1	164.8
	O1-H1	1.92	C14-O1-H14	12.2	C14-H14-O1	133.2
	O1-C14	3.35(1)	C20-F3-H201	9.7	C20-H202-O3	163.7
	O1-H14	2.64	C20-O3-H202	4.6	C20-H201-F3	146.5
	O3-C20	3.34(1)				
	O3-H202	2.42				
	F3-C20	3.22(2)				
	F3-H201	2.36				

separate anion, Figures 2-10 and 2-11. Internuclear distances are F3---C20 at 3.22(2) Å and O3---C20 at 3.34(1) Å. Although these distances are outside the sum of the Van der Waals radii for fluorine and carbon (3.05 Å) and oxygen and carbon (3.10 Å), they are much closer than the analogous interactions in 51. The closest C-H---O interaction in 51 is O2---C20 at 3.800(8) Å which is about 0.5 Å further removed than the analogous interaction in 52. Since an activated C-H bond is polarized C(δ^-)-H(δ^+), interaction of an anion at C20 would be expected to induce a shortening of the C13-C20 single bond since C13 bears a partial positive charge. Taylor and Kennard have shown in their extensive study¹⁰⁰ that C-H---O contacts are electrostatic and that they occur within certain distances (C---O, 3.0-4.0 Å) and angles ($\phi \sim 90$ -180°). It is useful to note that there is a growing consensus that C-H---O bonds have significant implications in many diverse areas of structural chemistry.¹⁰¹ There are numerous examples of C-H---O bonds in the literature and several reports show that these interactions contribute significantly to the stability and tertiary structures of biomolecules such as nucleosides and amino acids.^{100,101,102}

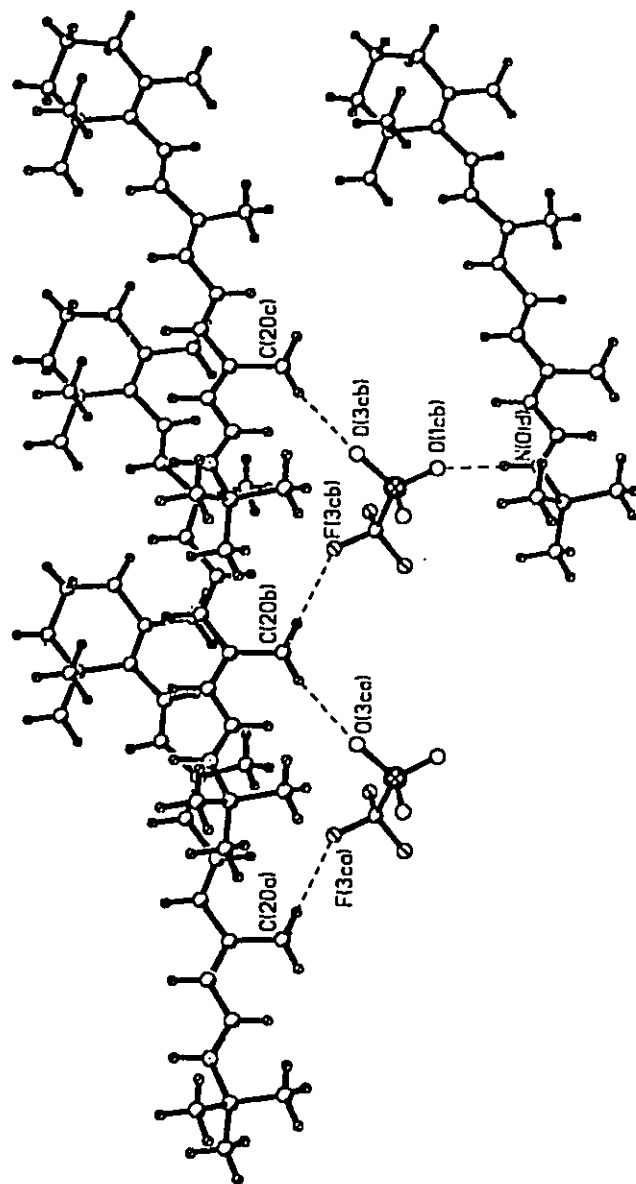


Figure 2-10: Bottom View of Hydrogen Bonding Interactions in 52.

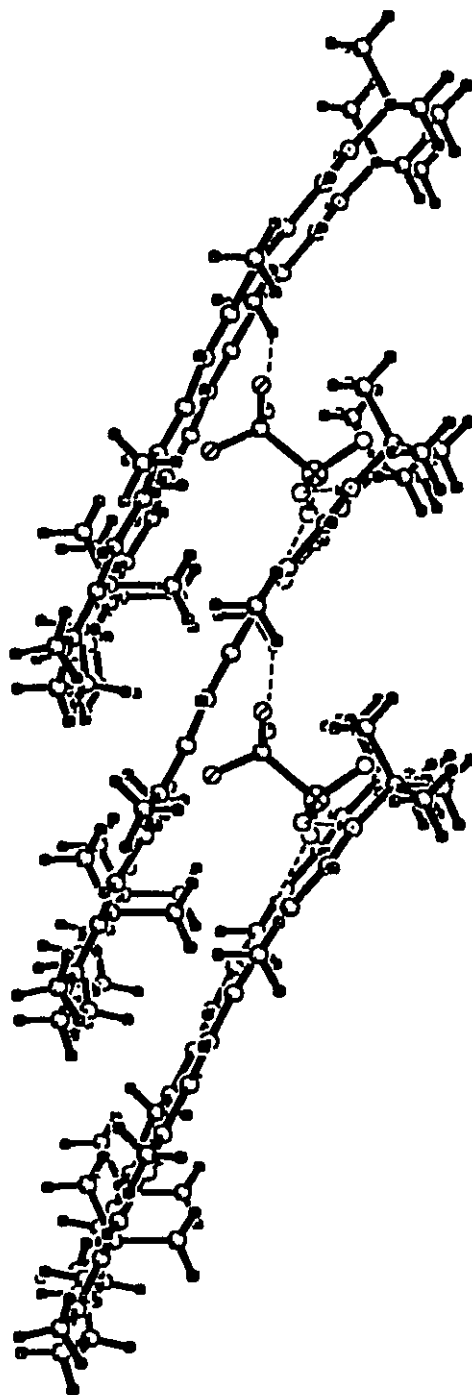


Figure 2-11: Side View of Hydrogen Bonding Interactions in 52.

Effect of Anion on ^{13}C NMR Spectra

The solution state ^{13}C NMR spectra obtained for compounds 51 and 52 are virtually identical. This is not unexpected given that similar results have been reported by Vocelle.⁶¹ In contrast to the solution studies, relatively dramatic differences in ^{13}C NMR chemical shifts were seen for the series of salts in the solid state. Examination of the data summarized in Figure 2-12 reveals that in the case of 51 and 52, the solid state ^{13}C NMR spectra for these compounds differ significantly for C15, C13, C11 and C9 and that the differences decrease with increasing distance from the nitrogen atom. As was mentioned earlier, the odd-numbered carbons are particularly sensitive to π -electron distribution along the polyene chain of these iminium salts. The consistent pattern in the differences in chemical shift for the odd-numbered carbons in the solid state spectra of 51 and 52 would indicate less positive charge is delocalized over the polyene carbon atoms in 52 as compared to 51. Since the primary difference in the two structures is the N-H...O distance, the differences in the solid state ^{13}C NMR shifts can then be related directly to the relative strengths of the hydrogen bonding interactions involving the nitrogen atom on the cation with an oxygen atom on the anion. Since the triflate counterion in 52 interacts more strongly with the N(H) proton than the perchlorate in 51, less positive charge is induced on the polyene chain. The weakening of the N-H bond in 52 through a greater hydrogen bonding interaction with the triflate counterion results in a reduced positive charge induction on the carbon framework. As a result, the ^{13}C NMR chemical shifts of C15, C13, C11 and C9 in 52 resonate at higher fields compared

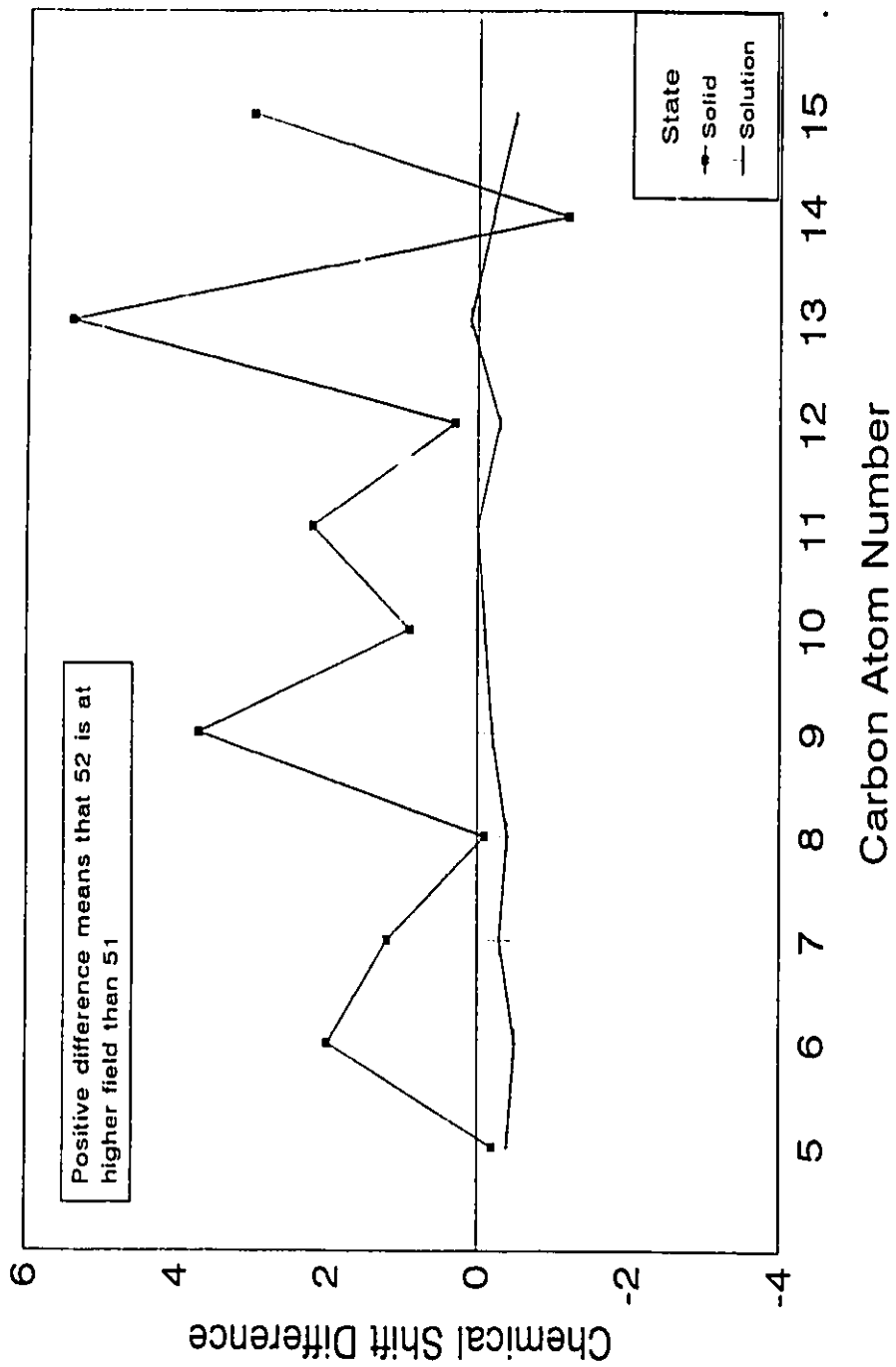


Figure 2-12: Differences in ¹³C NMR Chemical Shift Between 51 and 52 in Solution and Solid States.

to those found in 51. In the case of 51 where the N-H...O1 interaction is much weaker than in 52, more positive charge is born by the odd-numbered carbons in the polyene chain.

Another way of viewing the importance of these different interactions of an anion with the N-H proton is to remember the importance of resonance structure 57 in equation 2-8. A certain fraction of the total positive charge in these cations formally resides on the N-H proton. The fraction of the positive charge on the N-H proton can be regulated by interaction of the counterion with this proton.

The solid state ^{13}C NMR chemical shifts for C15, C13, C11 and C9 in bR were reported by Harbison to be 163.2, 169.0, 139.1 and 146.4 ppm, respectively.¹⁰¹ The corresponding solid state ^{13}C NMR chemical shifts for 51 are 161.0, 167.2, 140.1, 147.6 ppm and for 52, 158.0, 161.8, 137.9 and 143.9 ppm. The ^{13}C NMR chemical shift differences between bR and 51/52 are illustrated in Figure 2-13. The chemical shift values for C15 and C13 in bR are each shifted downfield by approximately 2 ppm compared to 51, and 5 ppm and 7 ppm compared to 52. This indicates that bR contains slightly more positive charge at C15 and C13 than do the comparable atoms in 51 and much more than those in 52.

FTir experiments corroborate the solid state ^{13}C NMR work in that the C=C stretching frequencies for bR^{105,109}, 51 and 52 are 1530 cm^{-1} and 1539 cm^{-1} and 1553 cm^{-1} , respectively. The lower stretching frequency exhibited by bR is a result of a decreased C=C bond strength which is caused by more extensive positive charge delocalization in

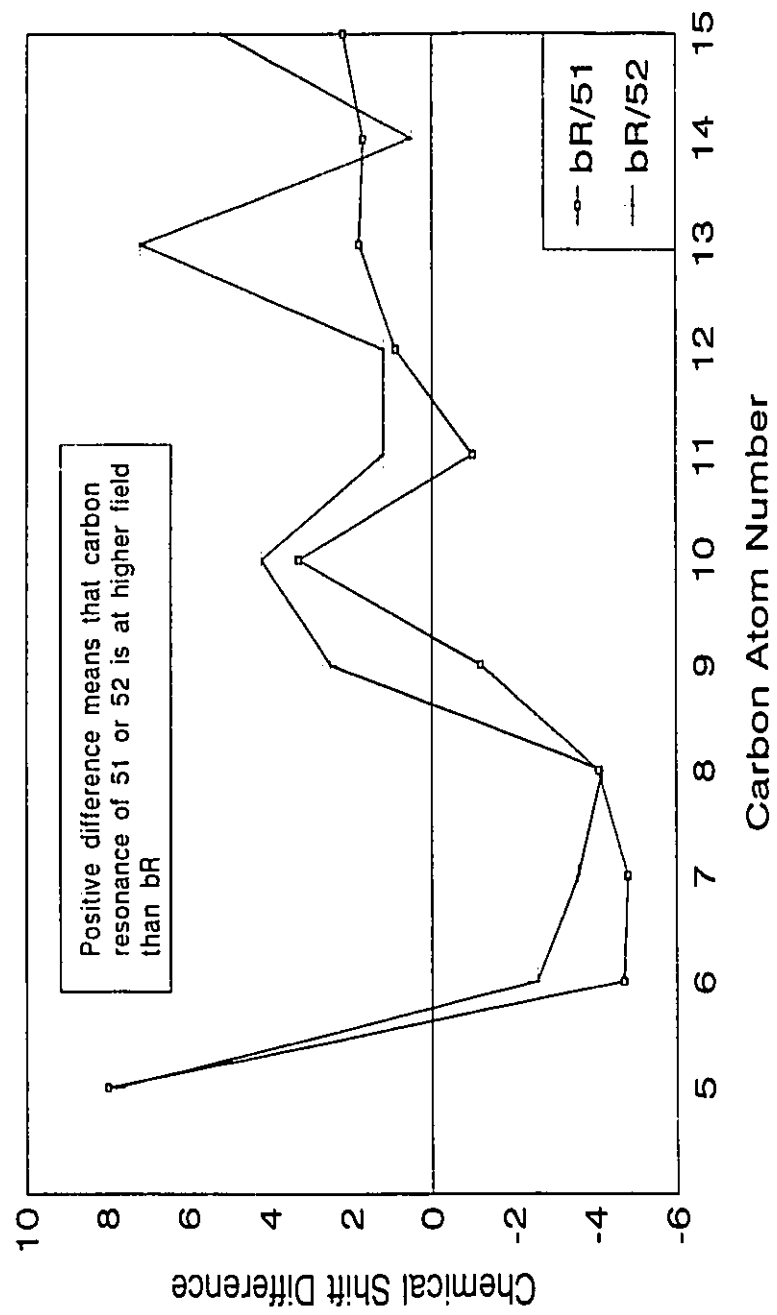
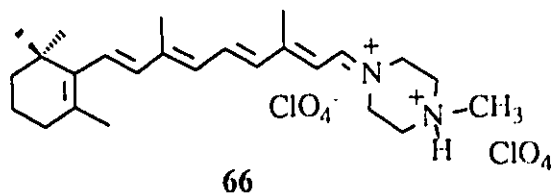


Figure 2-13: Differences in ^{13}C NMR Chemical Shift Between bR and 51 and 52 in the Solid State.

its polyene chain.

The solid state ^{13}C NMR chemical shifts of C13 and C11 in **53** are shifted further downfield by 3.5 and 1.5 ppm, respectively, relative to **51**. In compound **53** where the nitrogen atom is doubly substituted, the perchlorate counterion cannot participate in hydrogen bonding which causes more positive charge to be delocalized by the polyene carbons and results in the ^{13}C NMR chemical shifts of the odd-numbered carbons to shift downfield.

Recent solution work by Sheves⁶² has shown that the introduction of a positive charge in the vicinity of the Schiff base linkage in retinylidene iminium salts results in further downfield ^{13}C NMR chemical shifts of the odd-numbered polyene carbon atoms. Electrostatic interaction induced by the positive charge in the vicinity of the Schiff base linkage repulses the positive charge located primarily on nitrogen and causes more π -electron delocalization along the polyene chain. Interaction between the positive charges in **66** is enhanced through the use of fluorinated alcohols (ie. hexafluoroisopropanol) since this class of solvents has been shown to solvate poorly positively charged systems.¹⁰⁴



Examination of the chemical shift differences of carbons C6-C8 between **51/52**

and bR in Figure 2-13 reveals that these carbon atoms are substantially shifted to lower field in 51/52 than the corresponding carbon atoms in bR. This effect has been shown by Harbison⁶⁰ and Sheves⁶² to be due to the presence of a nonconjugated positive charge in the vicinity of C7-C9. However, in the recent bR structure³⁵, there are no obvious positive charges near these carbon atoms. The effect of the protein on ¹³C NMR chemical shifts in bR may be due to the interaction of the polyene chain with four tryptophan residues (Trp86, Trp138, Trp 182 and Trp189) which line the retinal pocket. It is possible that such an interaction with aromatic ring currents may be responsible for the observed effects. Through crystallographic studies of compounds 51 and 52 it has been found that a small increase in N---O1 distance from 2.85(1) Å in 52 to 2.939(7) Å in 51 produces relatively large downfield shifts of the odd-numbered polyene carbons in their solid state ¹³C NMR spectra and a lower ir C=C stretching frequency. As evidenced by solid state ¹³C NMR and FTir studies, bR has been shown to possess a slightly greater amount of positive charge delocalized over the polyene carbons than 51 and 52.

Although the greatest modulation in positive charge delocalization in retinylidene iminium salts involves the interaction of a heteroatom on the anion with the proton bonded to the Schiff base nitrogen atom, secondary hydrogen bonded interactions involving C20 could serve to assist further delocalization through electron release to C13 resulting in the ¹³C NMR chemical shift of this atom to be shifted slightly to higher field. Bader has shown through theoretical calculations that if a hyperconjugative mechanism is operational at C20, then the C13-C20 bond should possess some π -character¹⁰⁷ and

consequently result in a downfield shift of C20. Since no downfield shift was seen for C20 in **52** the hybridization of C20 is sp^3 .

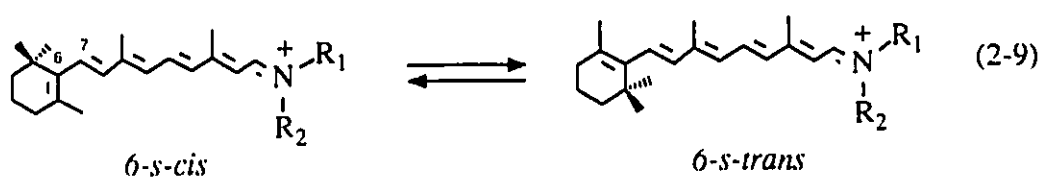
The ^{13}C NMR chemical shifts of the polyene carbons close to the Schiff base linkage are also influenced by the nature of nitrogen substitution. Compounds **50** and **52** have the same triflate counterion but exhibit different ^{13}C NMR chemical shifts for the unsaturated carbons near the iminium function. For example, the n-butyl group in **50** shifts the ^{13}C NMR chemical shift of C15 and C13 downfield by 6.8 and 4.1 ppm relative to the t-butyl group in **52**. This effect might be attributed to the exact location of the anion relative to the $\text{C}=\text{N}^+$ bond or to the greater ability of the t-butyl group to donate charge.

Conformation

A comparison of the solution state ^{13}C NMR spectra to the solid state spectra of **50**, **51**, **52** and **53** reveals that with the exception of C2, C5, C6, C9, C13 and C15, the majority of the resonances lie within 1 ppm of one another. The changes in ^{13}C resonances near the iminium function are likely due to the differences in packing between solution and solid states. In the solid state there is a tight anion/cation packing whereas in solution, solvent separated ion pairs are expected to predominate.

In terms of the conformation of the retinylidene iminium ions in solution, a number of nuclear Overhauser experiments (NOE) have been reported and the results from these experiments have indicated that these cations exist in the all-*trans*

configuration with a predominantly *s-cis* conformation about the C6-C7 bond^{60,108}, equation 2-9. This is not surprising since in retinal itself a twisted 6-*s-cis* conformation is calculated to be 2.5 kcal/mole more stable than the 6-*s-trans* conformation.¹⁰⁹



In compounds 51, 52 and 53 the ¹³C NMR chemical shift in the solid state for C5 is about 137 ppm. This is shifted 4 ppm downfield relative to that found in solution (132.5 ppm). Compound 50 exhibited a chemical shift for C5 at 130.2 ppm in the solid state as compared to 132.4 ppm in solution.

Harbison has shown, through an extensive solid state ¹³C NMR study of carotenoids, retinoid derivatives and retinylidene iminium salts that the chemical shift of C5 is a sensitive indicator of the conformation about the C6-C7 bond.²⁵ In 6-*s-cis* conformers, the resonance attributed to C5 is found at 128 ppm whereas that attributed to 6-*s-trans* conformers is found at about 136 ppm. The chemical shifts of C5 for 51, 52 and 53 in the solid state are exactly in the range reported by Harbison to be representative of the 6-*s-trans* conformer while the chemical shift for C5 in 50 is representative of the 6-*s-cis* conformer. Since at the time of Harbison's work no x-ray

crystallographic study had been successfully completed for a retinylidene iminium salt, there was no definitive structural evidence available to base this conclusion. However, the recently reported crystal structure of 53 and the current structures of 51 and 52 confirm Harbison's results.

Effect of Cation/Anion Placement on UV/VIS Absorption Spectra

The solution (CH_2Cl_2) absorption maxima of retinylidene iminium salts 51 (472 nm) and 52 (465 nm) are very similar. In contrast, their solid state absorption maxima differ by 59 nm (2631 cm^{-1}). Compound 51 exhibited an absorption maximum at 504 nm while 52 absorbed at 445 nm. It has been suggested earlier that this difference is consistent with a conformational change about the C6-C7 single bond.⁶⁰ As Honig and Ebrey have indicated that twisting about the C6-C7 bond could alter the absorption maximum by about 50 nm⁴⁰, the relatively short wavelength of 445 nm for 52 could have been due to the lack of conjugation of the C5-C6 double bond with the rest of the retinylidene chromophore. The absorption maximum of a 6-*s-cis* retinylidene iminium salt with a 60° torsion angle about the C6-C7 bond is expected to be about 450 nm. Conversely, a planar 6-*s-trans* conformer is expected to possess an absorption maximum of about 500 nm.⁴⁰

The crystal structures of 51 and 52 show that both cations have 6-*s-trans* conformations in the solid state. As was shown for the solid state ¹³C NMR spectra for 51 and 52, the 2631 cm^{-1} (7.5 kcal/mole) difference in the absorption maxima for these

compounds in the solid state is primarily the result of a variation in internuclear distance between N and O1. The shorter hydrogen bonded interaction between O1 in CF_3SO_3^- with N-H will have the effect of stabilizing (lowering) the ground state energy of **52** as compared to **51**. Since most of the positive charge in retinylidene cations is located on the Schiff base nitrogen atom, modulation of the N---O1 distance can induce large wavelength shifts, as evidenced from the absorption maxima of **51** and **52**. Hence, the red shifted absorption maximum observed for bR can be achieved by just increasing the distance between the positively charged nitrogen atom and its counterion.

Recent solution work by Sheves has shown that a red shift in the absorbance spectrum of retinylidene iminium salts is accompanied by downfield ^{13}C NMR chemical shifts of the odd-numbered polyene carbons.⁶² It was suggested that weakening of the Schiff base - counterion interaction leads to significant π -electron delocalization along the polyene chain and is responsible for the observed spectroscopic properties. The work described here demonstrates unequivocally the correctness of this suggestion.

Thus, it is possible to approach long wavelength absorption maxima of retinylidene ions without requiring a nonconjugated negative charge in the vicinity of the β -ionone ring. It has been shown through FTIR studies that Asp 115, the closest potential negative charge to the β -ionone ring according to the recent bR structure³⁵, is protonated in the ground state and cannot function as an external negative point charge.¹¹⁰

The solid state absorption maxima of all but one of the retinylidene iminium salts are blue shifted from that measured in solution. The greatest blue shift in the secondary

iminium salts (1514 cm^{-1}) occurred in **50**. In contrast, **51** absorbed at a longer wavelength in the solid state (504 nm) than in solution (472 nm) by 1345 cm^{-1} . The changes in absorption maxima between solution and solid state can best be analyzed by changes in cation/anion interactions in each state. This has been extensively studied for a series of alkali metal cations having triphenylmethanide, fluorenyl and cyclopentadienide as the carbanions.^{111,112} In solution, the minimum distance between an anion and a cation is attained when both exist as a contact ion pair where this distance is close to the Van der Waals radii for each ion. It was shown that the distance between anion and cation is increased by the use of polar solvents or by decreasing the temperature. This results in solvent separated ion pairs. The absorption spectra of these two types of ion pairs are noticeably different. The contact ion pair is normally blue shifted from its corresponding solvent separated ion pair.

Hogen-Esch and Smid have shown the absorption maxima of a series of fluorenyl salts to undergo a blue shift as the counterion's radius decreases.¹¹¹ Blatz and co-workers have also shown the absorption maxima of a series of retinylidene iminium salts to decrease as the polarity of a series of non-protic solvents decreased. They found that there was a good linear relationship between the anion/cation distance (or anion radius) and the absorption maximum.³⁹

Summary

The crystal structure determinations of **51** and **52** have provided the first direct

experimental evidence for the structures of secondary retinylidene iminium salts directly related to bacteriorhodopsin. It was found that with the exception of the C13-C20 bond length all bond lengths and angles between these two cations are the same. The conformation about the C6-C7 bond was found to be *s-trans* in both cases. Both cations exhibit relatively large bond alternations which indicated that positive charge in these ions is primarily located on the nitrogen atom and its proton. The only difference in the structures of 51 and 52 is their anionic contacts. Although both 51 and 52 contained near linear hydrogen bonds involving the Schiff base nitrogen atom, O1 in CF_3SO_3^- was found to have a much closer internuclear distance with N than O1 in ClO_4^- . This difference was dramatically reflected in the solid state ^{13}C NMR studies, where the odd numbered polyene carbons in 51 were found to be substantially shifted downfield than those in 52, and in the solid state absorption spectra where the absorption maximum of 51 was substantially red shifted relative to 52. Hence, the N-H---O interaction was found to be the dominant interaction in the regulation of positive charge delocalization and wavelength of absorption in retinylidene iminium salts.

Chapter 3

Thermally Induced Isomerizations of Retinylidene Iminium Salts

As was outlined in chapter 1, the efficient thermal isomerization of the protonated Schiff base of retinal in bR is essential for the appropriate functioning of the protein. The purpose of the work detailed in this section is to determine the various pathways of isomerization available to *in vitro* retinylidene iminium salts. While thermal isomerizations of Schiff bases of retinal have been studied in dilute acidic media by a variety of groups, these studies have led to conflicting results.^{35,113,114} The problem appears to lie in the analytical methods used in the detection of the various isomers. In previous experiments, HPLC and absorption spectroscopy have been used.^{35,113} These methods are indirect since some call for the conversion of the isomers into their corresponding oximes prior to analysis. The extraction of structural information using these techniques can be misleading.

In this work, high field ¹H NMR spectroscopy has been used to characterize and quantitatively measure the products of thermal isomerization of retinylidene iminium salts. This technique also allows the determination of the rate of isomerization of retinylidene ions. The kinetics and thermodynamic equilibria of a series of retinylidene iminium salts were examined in neutral and nucleophilic media. The results obtained are used to explain the effects of differential nitrogen substitution, counterion and the use of external nucleophiles on the rates of isomerization and conformational equilibria of retinylidene iminium salts. These results are of interest in the understanding of the properties of the

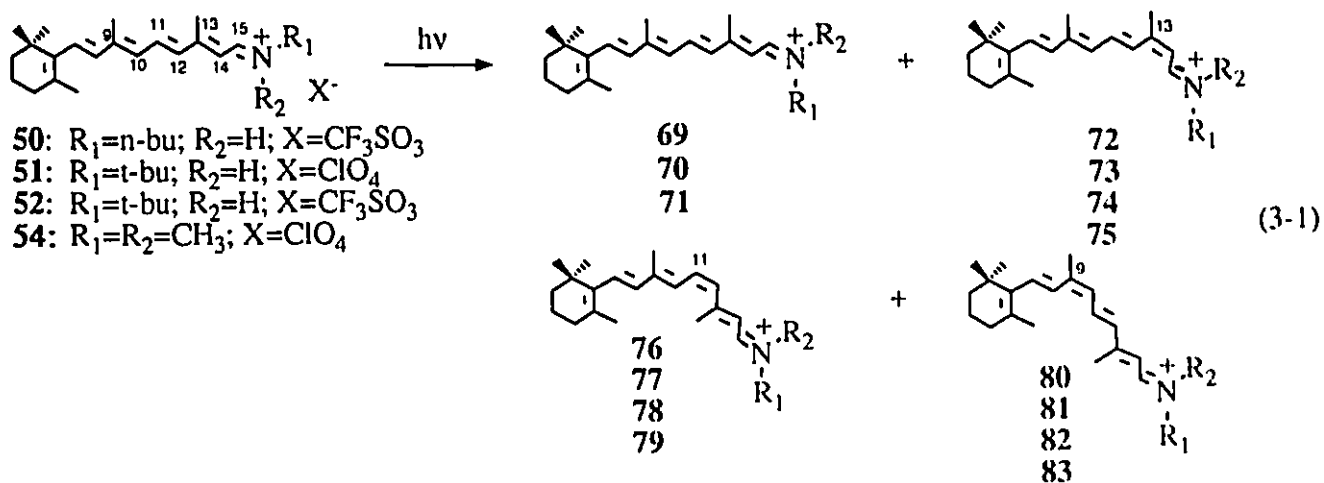
natural pigment bacteriorhodopsin.

Preparation and Characterization

The all-*trans* retinylidene iminium salts 50, 51, 52 and 53 were prepared and characterized by ^1H NMR, ^{13}C NMR and absorption spectroscopy as described in the previous chapter. Compound 54 was prepared in the same manner to that previously described.⁶⁰

Each iminium salt was found to contain a small amount of isomeric impurity formed on preparation of the ions, Table 3-1. Identification of the minor isomer of 50-52 and 54 was made by examination of the high field ^1H NMR spectra of solutions of each compound. In each case the minor isomer was identified as the 13-*cis* isomer by comparison of chemical shifts and coupling constants with previously reported data.¹¹⁵ Chemical shifts and coupling constants for each of the parent compounds and their 11-*cis* primary photoproducts are reported in Tables 3-2 and 3-3. Irradiation at 350 nm for periods greater than two hours yielded three of the four possible mono-*cis* isomers as well as di-*cis* isomers in appreciable amounts^{86,115}, equation 3-1 (note: 50 gives 69, 72, 76 and 80). At this point the ^1H NMR spectra became extremely complex and complete assignment of all resonances was not possible.

The ^1H NMR spectrum shown in Figure 3-1 was obtained upon irradiation of 51 at 350 nm in deuterated methylene chloride. Examination of this spectrum shows that a second major isomer, not present in the starting material, had been formed on irradiation.



In this spectrum, the resonances for C(15)H for both major isomers are located at 8.26 ppm and appeared as a broadened doublet of doublets. The similarity in chemical shift of C(15)H in the two isomers suggests that the isomerized bond is quite removed from C(15)H. The very similar doublet of doublet coupling pattern exhibited by C(15)H in both isomers indicates that the configuration about the C=N bond is the same in both isomers. The magnitude of the larger of the coupling constants, $J_{15,\text{NH}} = 15.4$ Hz shows that the configuration about C=N is *anti*.

Table 3-1
Isomeric Purity^{ab} of Iminium Salts on Preparation.

Compound	Isomer Percentage		
	All- <i>trans</i>	15- <i>cis</i>	13- <i>cis</i>
50	97.4	nd ^c	2.6
51	96.8	nd	3.2
52	98.8	nd	1.2
53 ^d	95.5	4.5	nd
54	88.5	nd	11.5

^a Assayed by ¹H NMR. CD₂Cl₂, solvent, 22°C.

^b Errors are ± 5%.

^c Not detected.

^d Acquired at -60°C.

Table 3-2: ¹H NMR Chemical Shift Data (ppm) for Retinylidene Iminium Salts and their Primary Photoproducts.

Position	Compound							
	50	76	51	77	52	78	54	79
C(2)H	1.49t	1.49t	1.50t	1.49t	1.49t	1.49t	1.49t	1.49t
C(3)H	1.63m	1.63m	1.61m	1.62m	1.62m	1.62m	1.63m	1.63m
C(4)H	2.06t	2.06t	2.06t	2.06t	2.06t	2.06t	2.08t	2.08t
C(7)H	6.54d	6.54d	6.46d	6.46d	6.53d	6.53d	6.64d	6.59d
C(8)H	6.26d	6.27d	6.23d	6.30d	6.26d	6.27d	6.28d	6.30d
C(10)H	6.32d	6.75d	6.30d	6.75d	6.33d	6.73d	6.34d	6.75d
C(11)H	7.47dd	6.98t	7.44dd	7.02t	7.46dd	7.00t	7.56dd	7.08d
C(12)H	6.54d	6.18d	6.58d	6.18d	6.56d	6.19d	6.62d	6.24d
C(14)H	6.78d	6.31d	6.67d	6.83d	6.89d	6.89d	6.62d	6.41d
C(15)H	8.21dd	8.21dd	8.26dd	8.26dd	8.26dd	8.25dd	8.55d	8.58d
C(16)H	1.05s	1.05s	1.05s	1.05s	1.05s	1.05s	1.05s	1.05s
C(17)H	1.05s	1.05s	1.05s	1.05s	1.05s	1.05s	1.05s	1.05s
C(18)H	1.74s	1.74s	1.74s	1.74s	1.74s	1.74s	1.74s	1.74s
C(19)H	2.10s	2.06s	2.10s	2.05s	2.10s	2.05s	2.12s	2.08s
C(20)H	2.31s	2.42s	2.31s	2.46s	2.31s	2.45s	2.43s	2.53s
NH	10.7bs	10.7bs	10.9bs	10.9bs	11.7bs	11.7bs	-	-
C(1')H	3.66t	3.69t	-	-	-	-	3.71s	3.73s
C(1'')H	-	-	-	-	-	-	3.45s	3.45s
C(2')H	1.78m	1.80m	1.50s	1.51s	1.50s	1.50s	-	-
C(3')H	1.42m	1.44m	-	-	-	-	-	-
C(4')H	0.97t	0.97t	-	-	-	-	-	-

^a s=singlet, t=triplet, dd=doublet of doublets, bs=broad singlet, m=multiplet

^b referenced to CD₂Cl₂ at 5.32 ppm. Measured at 22°C.

Table 3-3: ¹H, ¹H Coupling Constant Data (Hz) For Retinylidene Iminium Salts and their Primary Photoproducts.

	Compound							
	50	76	51	77	52	78	54	79
J _{7,8}	16.1	16.1	15.9	16.1	16.1	16.0	16.1	16.2
J _{10,11}	11.8	13.5	11.8	12.4	11.7	13.2	11.5	12.5
J _{11,12}	14.9	11.9	14.9	11.8	14.8	11.8	14.6	11.5
J _{14,15}	11.4	11.4	11.2	11.1	11.1	11.2	11.5	11.5
J _{15,NH'}	15.4	15.1	15.4	15.4	15.8	15.8	-	-

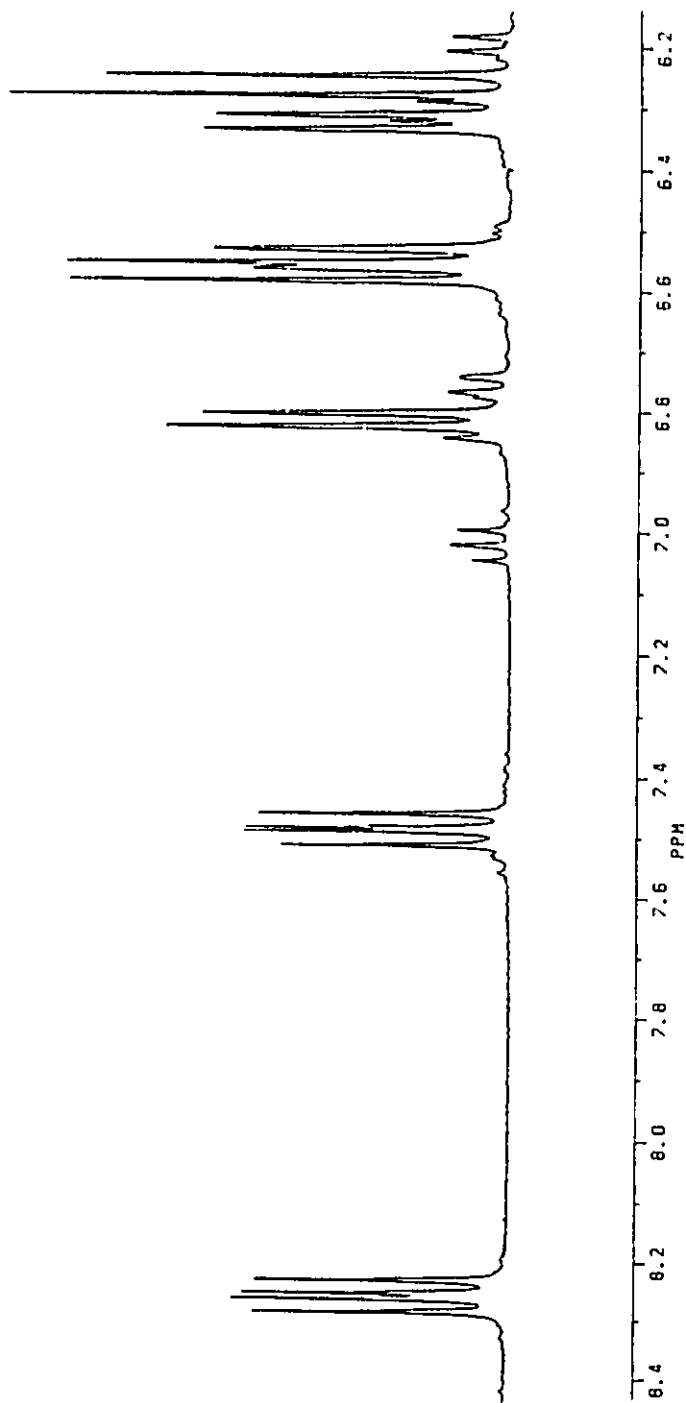


Figure 3-1: ¹H NMR Spectrum of 51 in CD₂Cl₂ after Irradiation at 350 nm.

The C(11)H coupling pattern corresponding to the second isomer was critical in determining its structure. The triplet centered at 7.02 ppm was assigned to C(11)H and provides conclusive evidence that the photoproduct resulting from the irradiation of 51 is the 11-*cis* isomer. The characteristic coupling constant of 11.8 Hz for $J_{11,12}$ is typical of a *cis* configuration about the C11-C12 double bond. This resonance occurs 0.42 ppm to higher field from C(11)H in 51. Accompanying the upfield shift of C(11)H was the expected downfield shift of C(10)H and upfield shifts of C(12)H and C(14)H. The C(20)H resonance has been shown by Childs and Shaw to be a good marker for the 11-*cis* isomer.¹¹⁵ This resonance occurs at 2.46 ppm in 77 as compared to 2.31 ppm in 51. This is consistent with previously reported ¹H NMR values for C(20)H in 11-*cis* isomers.¹¹⁵

Similarly, the C(20)H resonance is used to determine the relative amounts of the 9-*cis*, 13-*cis* and 15-*cis* isomers present in these mixtures. In the case of 51 the C(20)H chemical shift for the 9-*cis* isomer resonates at 2.32 ppm while the C(20)H chemical shift for the 13-*cis* isomer resonates at 2.30 ppm.

Cis/trans Isomerization of Retinylidene Iminium Salts

This study was conducted to evaluate the effects of nitrogen atom substitution, counterion and external nucleophiles on the isomerization about the C11-C12 bond in retinylidene iminium salts.

Solutions (CD_2Cl_2) containing about 30%, respectively, of the 11-*cis* isomers of 50, 51, 52 and 54 were obtained by irradiation at 350 nm at -78°C in sealed NMR tubes. Examination of the NMR spectrum of these solutions showed that the photoproducts underwent thermally induced isomerization at room temperature. The rates of disappearance of the 11-*cis* isomers of 51, 52 and 54 were studied quantitatively using high field ^1H NMR spectroscopy. Good first order kinetics ($r > 0.99$) were obtained for each isomerization, Table 3-4. Dimethyl ammonium bromide was introduced into solutions of the 11-*cis* isomers of 52 and 54 and the isomerization monitored by ^1H NMR. In each case the addition of this salt was found to accelerate the isomerization rate.

The half-life of the isomerization of 79 to 54 was determined for two different concentrations of 79, Table 3-5. Variation in concentration by nearly a factor of three had no significant effect on the observed rate of isomerization.

Table 3-4

Rates of Isomerization about the 11-*cis* Bond.^{ab}

Compound	Substituent		Anion X	Rate Constant	
	R ₁	R ₂		Uncatalyzed (kx10 ³ , s ⁻¹)	Catalyzed ^c (kx10 ³ , s ⁻¹)
79	Me	Me	ClO ₄	1.2	6.8
77	t-but	H	ClO ₄	0.84	-
78	t-but	H	CF ₃ SO ₃	0.14	0.49

^a CD₂Cl₂, solvent. Temperature, 21°C.

^b Errors in rate constants ± 5%.

^c Concentration of retinylidene iminium salts was ~4 x 10² mol l⁻¹ with dimethylammonium bromide at ~8 x 10² mol l⁻¹.

Table 3-5

Concentration Dependence of Half Life on the Isomerization^a of 79 to 54.

Concentration (x 10 ² /mol l ⁻¹)	t _{1/2} (hrs)
1.2	9.9 ± 0.5
0.45	10.1 ± 0.6

^a Solvent CD₂Cl₂. Temperature 26°C.

Thermodynamic Equilibria

CD_2Cl_2 solutions of the iminium salts **50**, **51**, **52** and **54** were kept at 21°C for prolonged periods of time with periodic monitoring of their composition. Each cation was found to undergo isomerization about the C9-C10, C11-C12 and C13-C14 double bonds with the eventual formation of an equilibrium mixture, equation 3-2. The relative concentrations of each isomer at thermodynamic equilibrium (21°C) are given in Table 3-6.

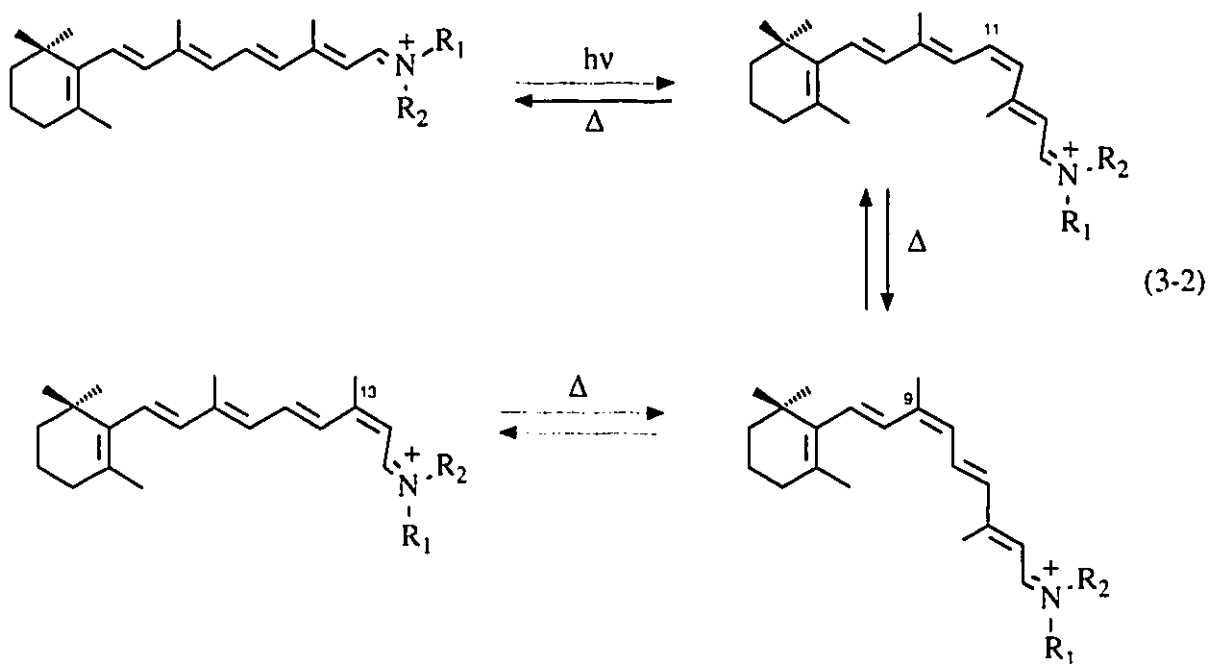


Table 3-6

Isomer Composition at Thermodynamic Equilibrium.^{ab}

Compound	Substituent			Isomer Composition (%)				
	R ₁	R ₂	X	AT ^c	15- <i>cis</i>	13- <i>cis</i>	11- <i>cis</i>	9- <i>cis</i>
50	n-but	H	CF ₃ SO ₃	57.4	31.2	2.3	nd ^d	9.1
51	t-but	H	ClO ₄	78.9	nd	4.4	nd	16.7
52	t-but	H	CF ₃ SO ₃	84.9	nd	2.7	nd	12.4
54	Me	Me	ClO ₄	73.2	nd	14.4	nd	12.4

^a CD₂Cl₂, solvent. Temperature 21°C.^b Errors are ± 5%.^c AT = all-*trans*.^d nd = not detected

The isomer compositions varied considerably depending on the substitution on the nitrogen atom and to a less extent on counterion. Only in the case of **50** was the presence of two isomers about the C=N bond detectable.

Discussion

Thermal Isomerization

CD₂Cl₂ was found to be the least polar medium in which sufficient amounts of the iminium salts were dissolved to permit high quality, unobstructed ¹H NMR spectra to be obtained. This solvent has the added advantage that it is relatively non-nucleophilic and as a result allows the study of the retinylidene iminium salts without solvent intervention.¹⁵ Ethanol, isopropyl alcohol and acetonitrile are leveling solvents that have been shown to cancel the effect of the counterion on the positively charged nitrogen atom.³² In contrast, methylene chloride should serve as a model system for the hydrophobic environment present in a large membrane protein.

Mowery and Storckenius have reported the observation of striking rate enhancements for the isomerization of retinals on formation of neutral retinal Schiff bases relative to retinal itself.¹³ Lukton and Rando have recently disputed this contention suggesting that the observed rate enhancements could have been due to trace amounts of acid present in the chloroform which was used as a solvent in these reactions.³⁵ The observation that Schiff base formation does not lead to substantial isomerization rate enhancements relative

to that of retinal is expected since the transition state for thermal isomerization of a Schiff base of retinal would, as in the case of retinal itself, presumably possess some diradical character. It is not clear why substitution of the oxygen atom of retinal by an NR group should lower the barrier to isomerization.

The situation is different with protonated or N-alkylated Schiff bases. Protonated Schiff bases isomerize considerably more rapidly than their unprotonated counterparts. The 11-*cis* n-butyl Schiff base of retinal ($\lambda_{\text{max}}=380$ nm in CH_3OH) isomerizes to all-*trans* in n-heptane with a rate constant $8.0 \times 10^6 \text{ s}^{-1}$ at 65°C .³⁵ The rate constant for the isomerization of **77** ($\lambda_{\text{max}}=472$ nm in CH_2Cl_2) is $8.37 \times 10^6 \text{ s}^{-1}$ at 21°C .

Recently, the rate of the thermal isomerization about the 13-*cis* double bond of n-butyl-retinylidene iminium salts was correlated with their corresponding absorption maxima CDCl_3 .¹¹⁶ A linear relationship was found between $\log(k)$ and λ_{max} for three compounds. It was concluded that the facile 13-*cis* to *trans* isomerization in bR was due, in large part, to increased π -electron delocalization which decreases bond alternation and decreases the strength of the double bonds.

In this work, the most facile isomerization about the 11-*cis* bond in **77**, **78** and **79** was observed for **79** (Table 3-4). The first order rate constant for **79** is greater than that for **77**. Since there are two methyl groups substituted on the nitrogen atom, there is no possibility for stabilization of positive charge by hydrogen bonding of the counterion to the proton on the nitrogen atom. This allows a more rapid isomerization in **79** compared to **77** and **78**. As was shown by the solid state studies of **51** and **52** in Chapter 2,

stabilization of positive charge is facilitated by close interaction of an oxygen atom on the anion with the N-H proton. An increase in internuclear distance between N and O results in a red shift in the uv absorption spectrum and the ^{13}C NMR downfield shift of the odd-numbered polyene carbon atoms suggesting that more charge is delocalized over these atoms.

In CD_2Cl_2 stabilization will be afforded largely by the solvent. Thus, the dramatic effects observed in the solid state ^{13}C NMR and uv absorption spectra are not seen in solution as a result of long N-O internuclear distances. A comparison of the solution ^{13}C NMR spectra of 51, 52 and 54 reveals that there is a general downfield shift of the odd-numbered carbon resonances in 54 compared to 51 and 52. Since the solvent cannot stabilize charge in 54 through hydrogen bonding as it can in 51 and 52 more charge is borne by the polyene chain in 54 resulting in a lower barrier to rotation and a greater rate of isomerization about the C11-C12 double bond.

In the case of 51 and 52, the solution uv absorption spectra (Table 2-8) are very similar while the ^1H (Table 2-3) and solution state ^{13}C NMR (Table 2-6) spectra are virtually identical. This suggests that the delocalization of positive charge in the ground state of 51 and 52 in CD_2Cl_2 solution is the same. However, the rate of isomerization of the corresponding 11-*cis* isomers 77 and 78 in CD_2Cl_2 are completely different. The salt 77 isomerizes almost six times faster than 78.

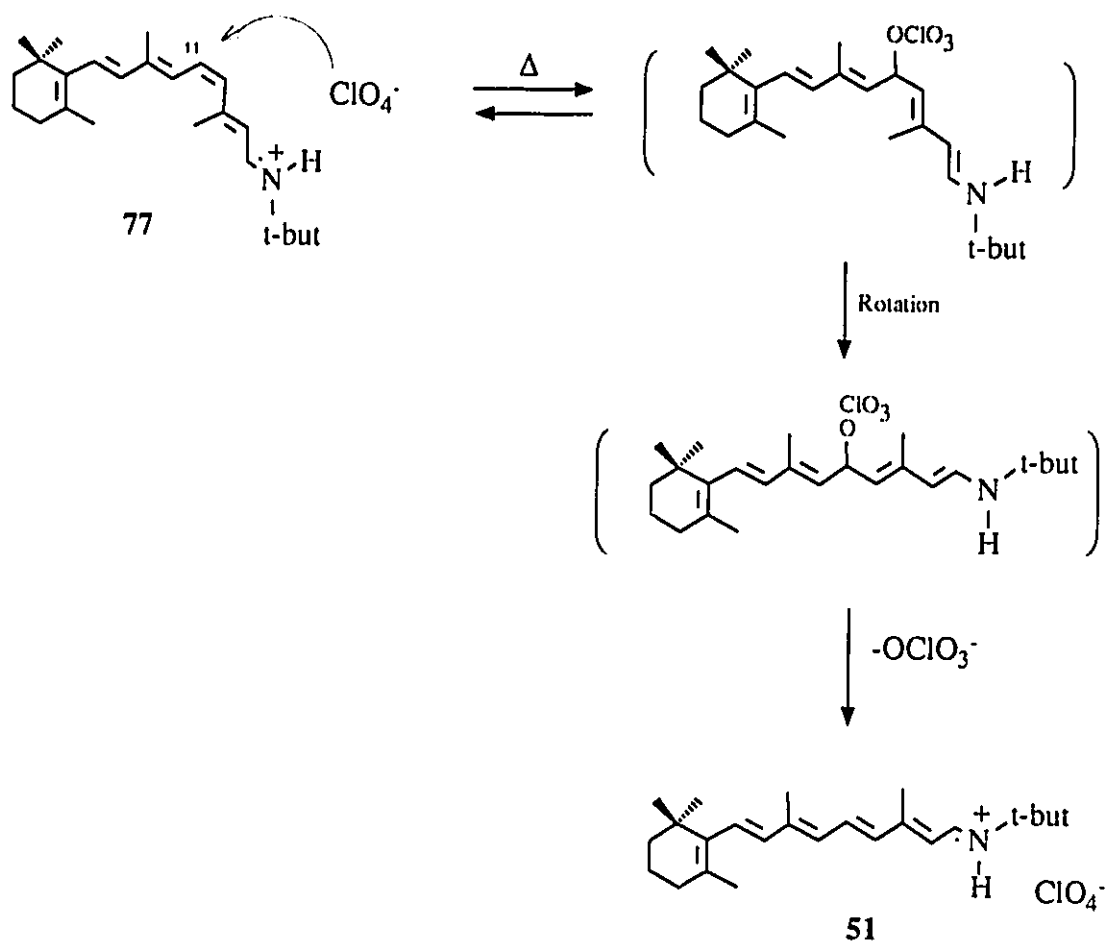
In this context it is important to note that the $t_{1/2}$ of a first order reaction should be independent of concentration.¹¹⁸ The $t_{1/2}$ of reactions of higher order are concentration

dependent. In the case of **79** the half-life of 11-*cis* to *trans* isomerization was found to be independent of concentration (Table 3-5).

Thermal isomerization of the 11-*cis* isomers to the corresponding all-*trans* isomers can be thought of as occurring through an "intramolecular" nucleophilic addition mechanism where catalysis is induced by the movement of the counterion from the positively charged nitrogen atom to the C11 of retinal (Scheme 3-1). Support for the nucleophile catalyzed isomerization is evident from the data given in Table 3-4. Isomerizations of **78** and **79** to the corresponding all-*trans* isomers are about 3.5-6 times more rapid in the presence of added bromide than those for the analogous isomerizations of the salts themselves in CD₂Cl₂. It has been previously shown that for simple iminium salts, catalysis using halide ions proceeds by a second order rate law.⁸⁶

The greater isomerization rate for **77** is attributed to the greater nucleophilicity of ClO₄⁻ versus CF₃SO₃⁻. As HClO₄ is a weaker acid than CF₃SO₃H¹¹⁷, it follows that the conjugate base ClO₄⁻ is a stronger nucleophile than CF₃SO₃⁻.

Nucleophilic addition at C11, rotation and subsequent reionization to give the all-*trans* isomer provides a mechanistic pathway for the regiospecific isomerization in bR. *Cis/trans* isomerization of the protonated retinal Schiff base in bacteriorhodopsin may be brought about by its interaction with the carboxylate of the Asp 85 counterion which would provide suitable catalysis to effect the isomerization. Such a movement would increase the fraction of positive charge on the unsaturated system as well as providing a nucleophilic catalyst. This in effect serves to reduce the relative bond orders of the



Scheme 3-1: Mechanism of 11-*cis* to *trans* thermal isomerization of retinylidene iminium salts.

former double bonds which lowers the barrier to rotation thereby facilitating rotation about former double bonds. Recent MNDO calculations done by Seltzer provide evidence for a decrease in activation energy from 15.8 kcal mole⁻¹ to 11.6 kcal mole⁻¹ for a C=C isomerization when such an interaction occurs.⁵³

Thermal Equilibria

In all of the retinylidene iminium salts examined in Table 3-6, the 11-*cis* isomers are undetectable by high field ¹H NMR in solutions which have been allowed to reach thermodynamic equilibrium. The destabilising interaction in the 11-*cis* isomer involves an intramolecular steric repulsion between the hydrogen atom at C10 and the methyl group at C13, Figure 3-2. Likewise the 7-*cis* isomer is predicted to be unstable due to severe steric crowding between the methyl groups at C5 and C9. Both the 9-*cis* and 13-*cis* isomers are relatively more stable since they are comparatively free of this problem.

The nature of nitrogen substitution and counterion does not seem to have a drastic effect on the equilibrium position of the 9-*cis* isomer in each case. This is not surprising considering the remoteness of the nitrogen substituents and the counterion from the C9-C10 double bond. Some variation in composition is observed in the equilibrium position of the 13-*cis* isomers. The highest 13-*cis* concentration was observed in **54** due to the sterically small methyl groups substituted to the nitrogen atom which serve to increase the stability of the 13-*cis* isomer in solution.

The relatively low equilibrium 13-*cis* concentrations for each of the remaining salts is due to the comparatively more bulky n-butyl and t-butyl nitrogen substituents which

greatly limit the formation of this isomer.

The only salt which possesses a detectable equilibrium concentration of the 15-*cis* isomer was **50**. Since an n-butyl group is sterically less bulky and has more degrees of freedom than a t-butyl group, the tendency for rotation about the C=N bond is higher in compound **50** compared to **51** and **52**.

The effect of the anion on equilibrium can be assessed on comparison of the relative position of thermodynamic equilibrium between **51** and **52**. Examination of Table 3-6 reveals that, at equilibrium, **51** has 39% more 13-*cis* concentration and 26% more 9-*cis* concentration than **52**. Explanation for the higher 13-*cis* isomer concentrations in **51** appears to originate from the relatively smaller steric size of the nitrogen substituents in **51** compared to **52**. The size of the iminium function would seem to affect the relative equilibrium concentrations of the 13-*cis* isomer more than the 9-*cis* isomer due to the close proximity of the former to the iminium end. Although both **51** and **52** are substituted with a t-butyl group at the nitrogen atom, the counterions influence the overall steric bulk of the iminium function since they form loose hydrogen bonds with the N-H proton. Since it is known that CF_3SO_3^- is a larger anion than ClO_4^- , the overall size of the iminium function in **52** is larger than in **51**. Thus the equilibrium concentration of the 13-*cis* isomer in **51** is higher than in **52** as a result of its greater stability.

Summary

The equilibrium composition of retinylidene iminium salts is slightly effected by the

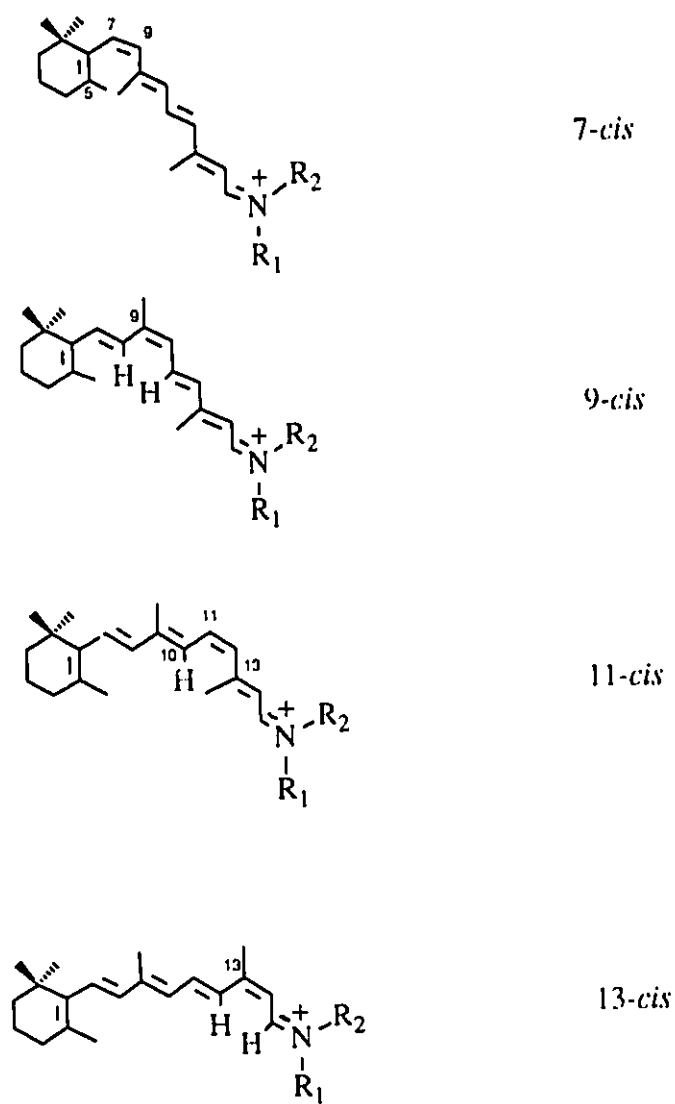


Figure 3-2: Destabilizing interactions in 7-cis, 9-cis, 11-cis and 13-cis isomers.

type of counterion. However, with the exception of the 9-*cis* isomer, the concentration of the 15-*cis* and 13-*cis* isomers varies considerably with differential nitrogen substitution. There are no 7-*cis* or 11-*cis* isomers at thermodynamic equilibrium due to their relatively large thermal instabilities. *Cis* to *trans* isomerization about the C11-C12 bond in **77**, **78** and **79** is effected by the counterion in an "intramolecular" bimolecular process. The isomerization is catalyzed by movement of the anion from its position near the protonated Schiff base nitrogen atom to the retinal's C11 where it exerts its catalytic effect. It is suggested that such a process is viable in bacteriorhodopsin where the carboxyl group of Asp 85 can act as the nucleophile.

Chapter 4

Thermal Isomerizations of Unsaturated Iminium Salts and Corresponding Protonated Poly-Unsaturated Aldehydes

As was discussed in chapter 1, unsaturated iminium salts are similar in structure to their isoelectronic protonated oxygen analogues. Several studies have reported thermal isomerizations of relatively simple iminium salts and protonated enones and enals in acid solution. This chapter details the thermal isomerizations of poly-unsaturated iminium salts and protonated poly-unsaturated aldehydes in acidic media. These studies were conducted in order to provide a further understanding of the isomerizations of retinylidene iminium salts.

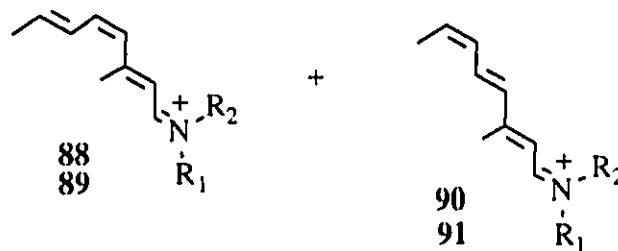
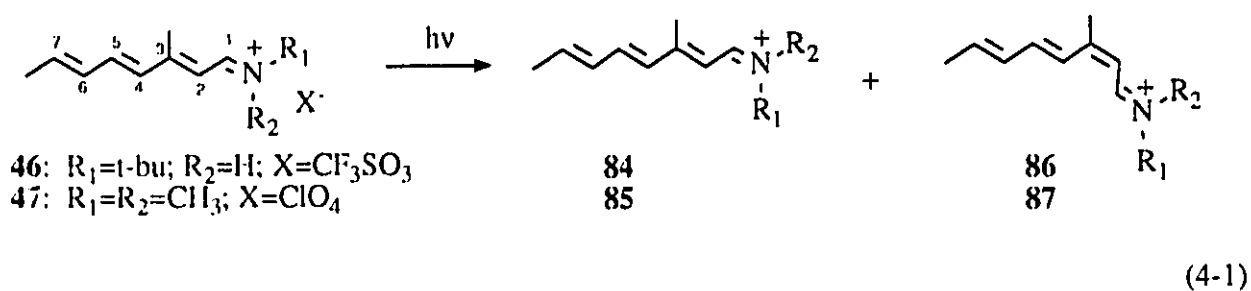
Part I

Octatrienylidene Iminium Salts

Preparation and Characterizations

The all-*trans* iminium salts **46** and **47** were prepared and characterized by ¹H NMR, ¹³C NMR and absorption spectroscopy as described in the previous chapter. Minor isomers were generated in appreciable amounts from the photolysis (Table 4-3) of iminium salts **46** and **47**, equation 4-1, and identified by an analysis of the ¹H NMR spectra of the mixtures. Identification of each isomer was based on their observed coupling constants and previously reported chemical shift information. The relative

amounts of the isomers were obtained by comparison of the peak heights associated with the C(1)H resonances.



The ^1H NMR chemical shift and coupling constant data for **46** and **47** and their primary photoproducts are reported in Tables 4-1 and 4-2. Unequivocal assignment of all resonances arising from each of the minor isomers was impossible due to peak overlapping and low concentrations. However in each case, the largest change in chemical shift occurred near the site of isomerization, Figure 4-1. The $^1\text{H}/^1\text{H}$ coupling

constants across C(1)H-NH, C(4)H-C(5)H and C(6)H-C(7)H bonds were diagnostic of *cis/trans* conformations about these bonds. Typically, it is found that a C-C double bond having a *cis* configuration exhibits a ¹H/¹H coupling constant 3-4 Hz smaller than the corresponding *trans* isomer.

The t-butyl iminium ion, **46**, displayed a typical doublet of doublets coupling pattern for C(1)H at 8.23 ppm, C(5)H at 7.00 ppm and C(6)H at 6.33 ppm. The position of the resonances and the nature of the H,H coupling confirmed the all-*trans* configuration of **46**. Upon irradiation of **46** at 350 nm at -78°C, the ¹H NMR spectrum shown in Figure 4-2 was obtained. This spectrum shows that a second major isomer, not present in the starting material, has been generated in addition to the starting *trans* isomer **46**. Examination of the aldiminium region of the ¹H NMR spectrum, 8-8.5 ppm, revealed that the new isomer contained a resonance at 8.43 ppm with a similar doublet of doublet coupling pattern as **46**. The magnitude of the larger coupling constant, 16.1 Hz, corresponded to $J_{1,NH}$. This coupling constant is well within the range reported for an anti C=N bond configuration, typically 15-17 Hz.⁸⁸

Table 4-1: ¹H NMR Chemical Shift Data^{a,b} (ppm) for 46, 47 and their Corresponding Primary Photoproducts.

Position	Compound			
	46	86	47	87
C(1)H	8.23dd	8.43dd	8.62d	8.79d
C(2)H	6.84d	6.70d	6.37d	6.20d
C(4)H	6.43d	6.80d	6.53d	7.11d
C(5)H	7.00dd	6.92dd	7.12dd	6.99dd
C(6)H	6.33dd	6.33dd	6.37dd	6.37dd
C(7)H	6.25m	6.25m	6.37m	6.37m
C(8)H	1.90d	1.91d	1.95d	1.95m
C(9)H	2.26s	2.27s	2.40s	2.36s
N(H)	11.2bs	11.2bs	-	-
C(1')H	-	-	3.75s	3.76s
C(1'')H	-	-	3.50s	3.48s
C(2')H	1.50s	1.50s	-	-

^a s=singlet, d=doublet, dd=doublet of doublets, m=multiplet, bs=broad singlet.

^b Referenced to CD₂Cl₂ at 5.32 ppm. Measured at 22°C.

Table 4-2: Coupling Constant Data (Hz) for 46, 47 and their Primary Photoproducts.

	Compound			
	46	86	47	87
J _{1,8(11)}	16.0	16.1	-	-
J _{1,2}	11.1	11.1	11.5	11.5
J _{4,5}	15.3	15.0	15.4	15.2
J _{5,6}	10.5	10.4	9.3	9.3
J _{6,7}	14.9	14.9	15.2	15.2
J _{7,8}	6.2	6.2	5.5	5.5

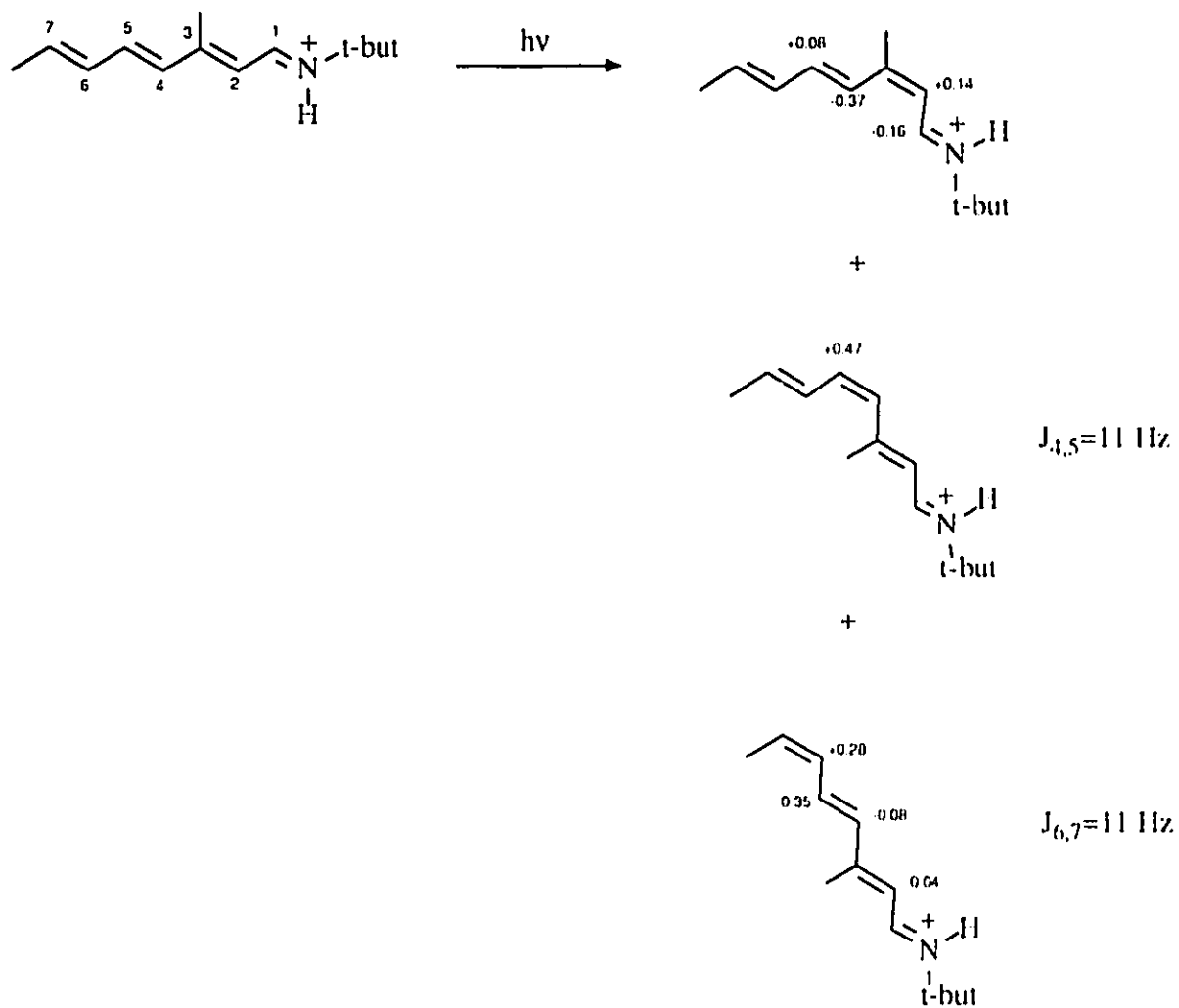


Figure 4-1: Chemical Shift trends for each mono *cis* isomer of 46.

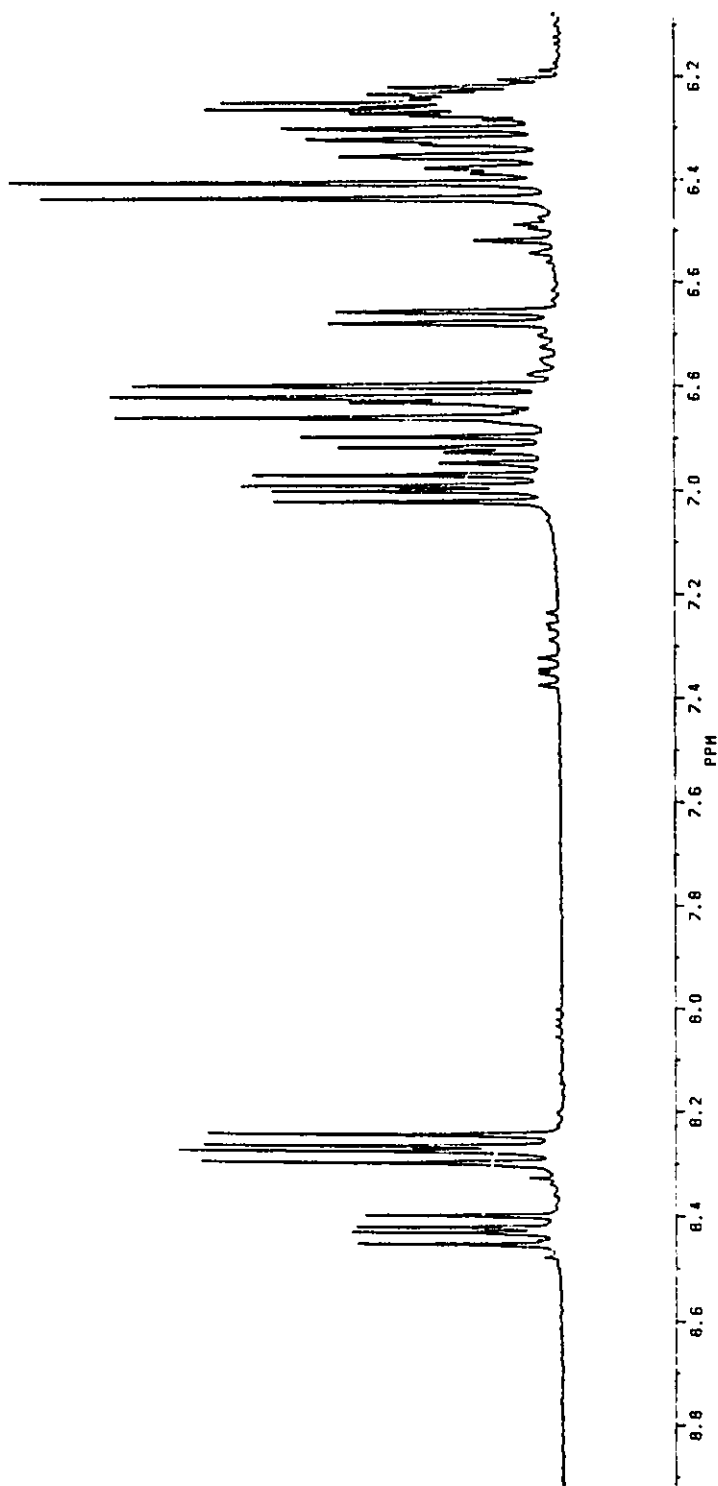


Figure 4-2: ^1H NMR Spectrum of 46 in CD_2Cl_2 , After Irradiation at 350 nm.

The resonance appearing at 6.92 ppm in the ^1H NMR spectrum shown in Figure 4-2 was assigned to C(5)H. The doublet of doublet pattern with the larger of the two coupling constants, $J_{4,5}$, having a magnitude of 15.0 Hz indicated that the configuration about the C4-C5 bond was *trans*. However, irradiation of the C(1)H peak at 8.39 ppm lead to a large NOE enhancement at C(4)H which corresponded to the C2-C3 bond existing in a *cis* fashion. Thus, the isomer generated from photolysis was the 2-*cis* iminium salt, **86**.

The 4-*cis* isomer, not present prior to irradiation, was photochemically generated in very low concentration (Table 4-3) and was difficult to measure accurately. The triplet appearing at 6.53 ppm was assigned to C(5)H. The presence of the triplet pattern indicates the presence of two protons with similar coupling constants of about 11 Hz. This value is consistent with a 5-*s-trans* configuration as found in the starting material. The remaining coupling constant is attributed to a 4-*cis* configuration across the C4-C5 double bond, typically 9-12 Hz.

The 6-*cis* isomer, **90**, was also present in the spectrum shown in Figure 4-2 but in a much smaller quantity than **46** or **86**. This isomer was present before irradiation and was characterized by its doublet of doublet coupling pattern of the C(1)H resonance which was located between C(1)H for **46** and **86**. The close proximity of the C(1)H resonance for the 6-*cis* isomer to C(1)H for **46** is expected given the remoteness of the 6-*cis* double bond from C(1)H. The chemical shift difference of a proton (C(1)H) used in characterizing two particular isomers becomes smaller the further away the *cis* bond

in question is from the proton used in the assay.

The photoisomerization of **47** followed a similar course to that of **46** with isomerization about the C2-C3 bond occurring to give the primary photoproduct 2-*cis* isomer, **87**. The identification of this isomer was made in an analogous manner to **86**. Again the downfield shift of C(1)H is characteristic of the presence of this isomer. Due to the symmetric substitution about the nitrogen atom, isomerization about C=N could not be detected.

Both **46** and **47** possessed small amounts of isomeric impurities formed on preparation. The composition of these isomers is listed in Table 4-3. Listed also in Table 4-3 is the isomer composition after one hour of irradiation and position of thermodynamic equilibrium.

Table 4-3

Isomeric Composition^a (%) of Iminium Salts **46** and **47** Under Various Conditions.

Compound	Conditions ^b	AT	2- <i>cis</i>	4- <i>cis</i>	6- <i>cis</i>
46	A	91.8	nd ^c	nd	8.2
	B	55.1	35.9	4.6	4.4
	C	64.6	24.4	nd	11.0
47	A	84.5	12.7	nd	2.8
	B	58.2	34.9	2.9	4.0
	C	68.1	20.1	nd	11.8

^a Assayed by ¹H NMR. CD₂Cl₂ solvent, 22°C.^b A - on preparation; B - after one hour irradiation at -80°C at 350 nm; C - at thermodynamic equilibrium (22°C).^c Not detected.

The solvent chosen as the reaction medium, trifluoroacetic acid, is a medium strength acid having an H_0 reported to be between -4.4 and -2.8. This variation is thought to be due to the presence of minute amounts of HCl in the acid.¹¹⁹ The TFA used in the current work was found to have an H_0 of -4.21. The isomerization of **86**, **87** was also examined in TFA/H₂SO₄ mixtures. The acidity of TFA is increased by the addition of sulfuric acid. In the present case a mixture with an H_0 of -4.86 was used.

Table 4-4

Rate constants and Activation Parameters of the *cis/trans* Isomerizations of 86 and 87.

Compound	Temp T, °C	Acid System	Rate Constant kx10 ⁴ , s ⁻¹	ΔH [‡] kcal mole ⁻¹	ΔS [‡] cal mole ⁻¹ K ⁻¹
87	55	TFA	1.01 ± 0.06	-	-
87	65	TFA	2.42 ± 0.16	18 ± 2	-25 ± 2
87	75	TFA	5.06 ± 0.33	-	-
87	55	H ₂ SO ₄ /TFA	7.88 ± 0.44	-	-
86	50	TFA	5.49 ± 0.32	-	-
86	60	TFA	10.3 ± 0.6	15 ± 2	-26 ± 2
86	70	TFA	23.3 ± 1.6	-	-
86	50	H ₂ SO ₄ /TFA	20.8 ± 1.4	-	-

Discussion

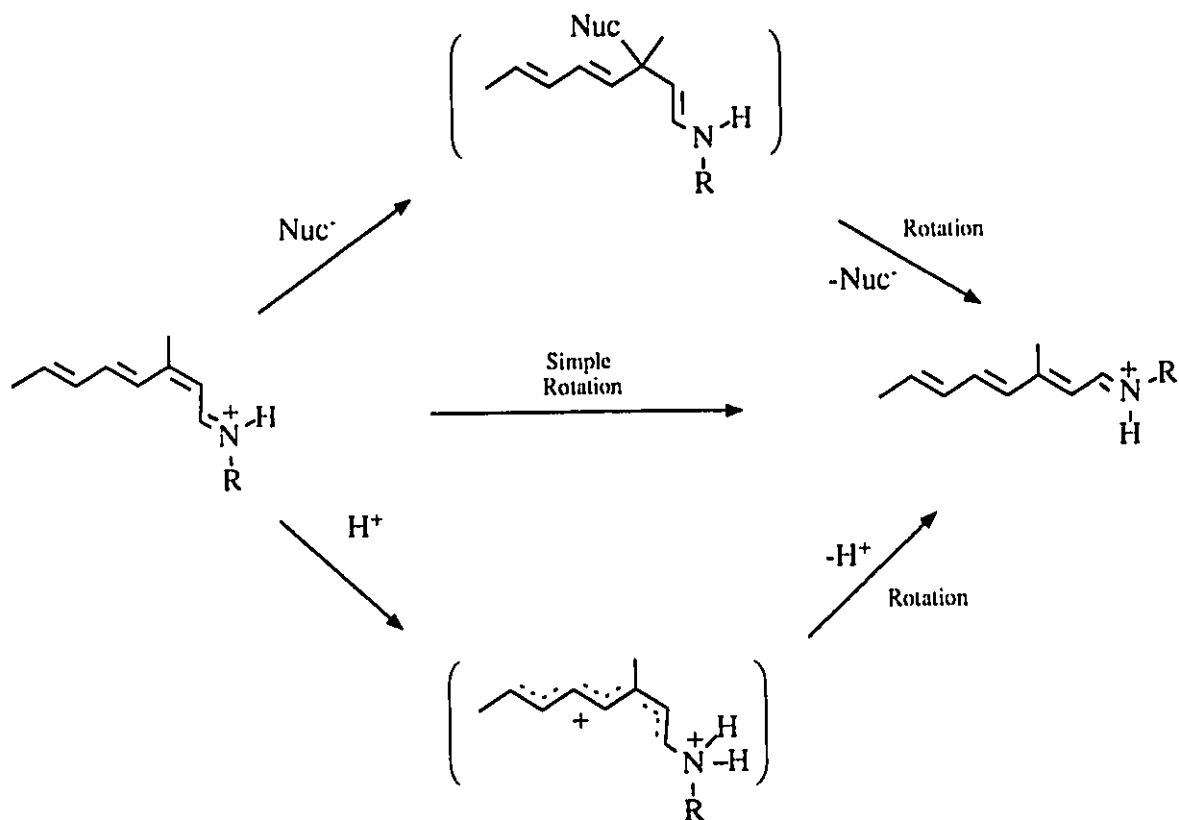
Mechanism of Isomerization

There are a number of mechanisms that have been proposed to account for the *cis/trans* isomerizations of iminium salts. The various mechanistic pathways are shown in Scheme 4-1. They involve simple rotation, nucleophilic catalysis and catalysis through protonation.

Two approaches were used to differentiate between these different mechanistic possibilities. The first involves variation in the acidity of the medium. The second involves measurement of the activation parameters associated with these reactions.

The addition of sulfuric acid to TFA enhances the acidity of the medium and should correspondingly decrease its nucleophilicity.^{56,63} The acid strengths of TFA and H₂SO₄ in TFA used in these studies were measured on the H₀ scale using 2,4-dinitroaniline as an indicator. Values of -4.21 and -4.86 were found for TFA and 0.01 M H₂SO₄/TFA respectively. The value obtained for H₂SO₄/TFA is lower than that previously reported. However, the important point is that the H₂SO₄/TFA medium is a stronger acid and has a lower nucleophilicity than TFA. It should be noted that as kinetic studies were done at temperatures greater than 50°C, the absolute values for H₀ will undoubtedly be different from those measured at 22°C.

Kinetic data obtained for the isomerization of salts **86** and **87** in 0.01 M H₂SO₄/TFA are summarized in Table 4-4. As can be seen from this data, the rate constants for the isomerization of both **86** and **87** are increased in the stronger acid



Scheme 4-1: Mechanistic Pathways to Isomerization of Unsaturated Iminium Salts.

medium by factors of 4 and 8 respectively. Such a result is inconsistent with a simple rotation mechanism where changes in acidity should have little effect on the rate of isomerization. The effect of an increase in rate as a function of increased acidity also rules out nucleophilic addition. Alternatively, the involvement of a protonation mechanism in which the acid participates in the reaction is consistent with the observed medium effects.

These observations point to a mechanism in which a proton is added to the iminium ion in such a way that in the transition state, positive charge is enhanced to facilitate C-C double bond isomerization. It was shown in chapter 2 that positive charge is poorly delocalized through the polyene framework in retinylidene iminium salts. However a perturbation such as additional protonation could serve to decrease C=C bond orders and facilitate C=C bond rotations. In principle, in systems such as **46** and **47**, protonation on nitrogen leads to a diprotonated transition state which can be regarded as a heptatrienyl cation with an electronegative non π -donor substituent. Through semiempirical SCF-LCAO-MO calculations, Baird has calculated the C2-C3 rotation barrier for the heptatrienyl cation to be $\Delta H^\ddagger = 18 \text{ kcal mole}^{-1}$.¹²⁰ This is in good agreement with the observed enthalpies of activation for **86** and **87** to be 15 ± 2 and $18 \pm 2 \text{ kcal mole}^{-1}$, respectively.

As exemplified by **92** and **93**, there are several possible protonation sites on the iminium salt. However, protonation on nitrogen leads to the most stable of the possible dications with the positive charge being delocalized over the polyene skeleton. Previous

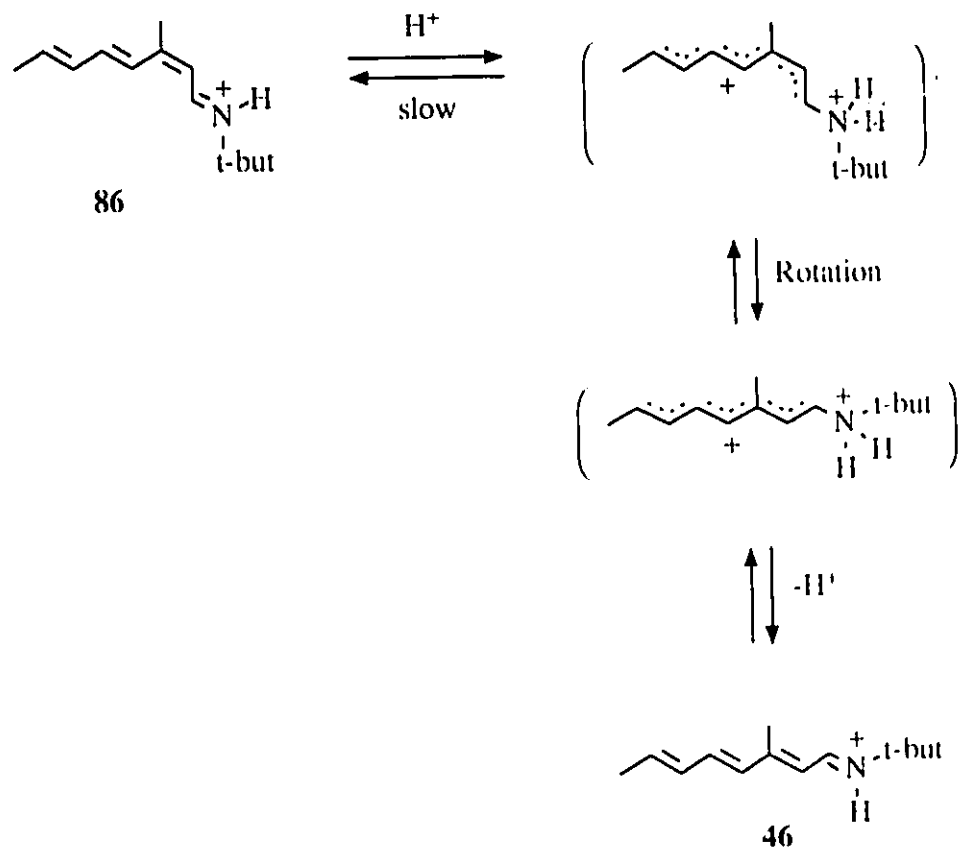
work at McMaster has shown no deuterium incorporation to take place in the polyene fragment of related species during similar acid catalyzed isomerizations.^{56,63,88} There is growing evidence to indicate that a number of reactions of heteroatom substituted cations



involve further protonation on the heteroatom to produce a transient dication. The mechanism suggested here for the *cis/trans* isomerization of **86** and **87** represents a further example (Scheme 4-2).^{63,75,121}

Although no direct evidence for the formation of a diprotonated intermediate was found by ¹H NMR, the activation parameters of the isomerization of **86** and **87** are fully consistent with a diprotonated transition state. The entropies of activation, -26 ± 2 cal K^{-1} mole⁻¹ at 60°C for **86** and -25 ± 2 cal K^{-1} mole⁻¹ at 65°C for **87**, are typical values associated with an ordered activated complex.¹²²

Lukton and Rando have reported a medium effect in the isomerization of the 11-*cis* isomer of the n-butylamine Schiff base of retinal.⁵⁵ The isomerization rate was observed to be much slower in excess TFA/chloroform than in excess HCl/hexane (both acid solutions were equivalent in concentration). The authors suggested that this result



Scheme 4-2: Mechanism of thermal isomerization of **86** to **46** in TFA.

was consistent with the isomerization proceeding by nucleophilic attack of the conjugate base on the protonated Schiff base. Since chloride ion is known to be a better nucleophile than trifluoroacetate, then it was expected that the rate of isomerization should also increase. While chloride ion is a better nucleophile it should also be remembered that HCl is a stronger acid than TFA.¹¹⁹ Since both experiments were done in excess acid it is possible that the isomerization of the retinylidene iminium salts examined by Lukton and Rando involved acid catalysis in which the nitrogen atom becomes diprotonated in the rate determining step.

The acid media used in the studies conducted by Lukton and Rando were considerably more dilute than those used in this work. However, the rate constants for retinylidene 11-*cis* to *trans* isomerization were about two orders of magnitude greater than those reported here for the octatrienylidene iminium salts. It would be expected that retinylidene iminium salts would be more basic thus more readily protonated to form a dication than their simpler relatives. It should be noted that the media used in the studies contained in this work are relatively more acidic than those present under physiological conditions. Thus, in less acidic media containing greater nucleophilicity, the nucleophile catalyzed isomerization pathway would be expected to predominate.

Part II

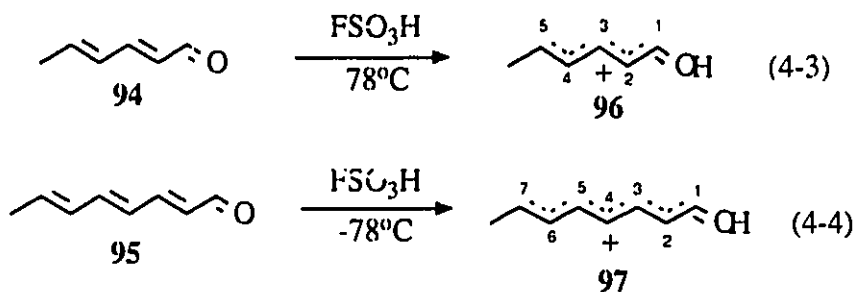
Owing to the similarity in structures of the poly-unsaturated iminium salts and protonated aldehydes, one might expect similar thermal chemistry to be exhibited by these two systems. However, contrary to the extensive investigations devoted to the structure and chemistry of the nitrogen containing iminium salts, comparatively little work has been done on their poly-unsaturated oxygen analogues. In particular, the chemistry of 1-hydroxy-pentadienyl or higher polyenyl cations have not previously been investigated and, given the importance of this type of functionality in a variety of natural systems⁶⁴ its chemical anonymity is surprising. To this light, the focus of the following section is directed to a detailed investigation of the mechanism of thermal isomerization of two such systems.

Protonated Poly-Unsaturated Aldehydes

Preparation and Characterization

The cations selected for study were **96** and **97**. These cations were prepared by the protonation of the corresponding carbonyl compounds **94** and **95** (equations 4-3 and 4-4). The ions were characterized by their low temperature ¹H and ¹³C NMR spectra which were consistent with their assigned structures, Tables 4-5 and 4-6. The chemical shifts of the various proton resonances and coupling constants corresponded to those reported for protonated enones⁷¹ and cyclic dienones.¹²³ The *trans* conformation about the

formal double bonds was clearly shown by the characteristic 14 Hz coupling constant observed between the two protons *trans* to each other on the formal double bonds.



Careful examination of the ^1H NMR spectra of these ions (Figure 4-3) showed in each case that a minor isomer was present. These minor isomers were shown to be the 4-*cis* isomer in the case of **96** and the 6-*cis* isomer in the case of **97**. In each case the $^1\text{H}/^1\text{H}$ coupling constant across the *cis* bond was found to be about 11 Hz; a value characteristic of a *cis* configuration in comparable cations.⁷¹ Both of these *cis* isomers were shown to be present in the neutral aldehydes prior to protonation, Table 4-7. As can be seen from the data in Table 4-7, in the case of **95** partial isomerization about the various C=C bonds to form the all-*trans* isomer occurred on protonation and NMR characterization of the cation. The all-*trans* isomer **97** is expected to be the

Table 4-5

¹H NMR Chemical Shift Data of Cations.

Position	Compound ^{ab}						
	96 ^c	100 ^c	97 ^c	102 ^c	101 ^d	98	99
C(1)H	8.82d	9.34d	8.60d	8.70d	-	-	-
C(2)H	6.83dd	6.66t	6.85dd	7.08t	3.93m	-	-
C(3)H	8.45dd	7.46t	8.44dd	8.96t	6.12m	8.90bs	8.58bs
C(4)H	7.03dd	8.41dd	7.00dd	7.26dd	6.10m	3.34m	3.45m
C(5)H	7.67dq	7.64dq	7.86dd	7.67dd	4.05m	3.26m	3.84m
C(6)H	2.23d	2.24d	6.81dd	6.86dd	1.50d	2.17s	7.15d
C(7)H	-	-	7.21dq	7.08dq	-	-	9.25d
C(8)H	-	-	2.21d	2.21d	-	-	2.17s

^a In ppm relative to CD₂Cl₂ (at 5.32 ppm) in FSO₃H/CD₂Cl₂; d = doublet, t = triplet, dq = doublet of quartets, m = multiplet, s = singlet, bs = broad singlet, dd = doublet of doublets. Measured at 21°C.

^b Coupling constants for 96, 100, 97 and 102 were very similar.
 $H, H_{trans} = 14.0 \pm 0.4$ Hz; $H, H_{cis} = 11.1 \pm 0.3$ Hz; Vinyl $H, CH_3 = 7.2 \pm 0.1$ Hz.

^c Measured at -60°C.

^d Measured at -40°C.

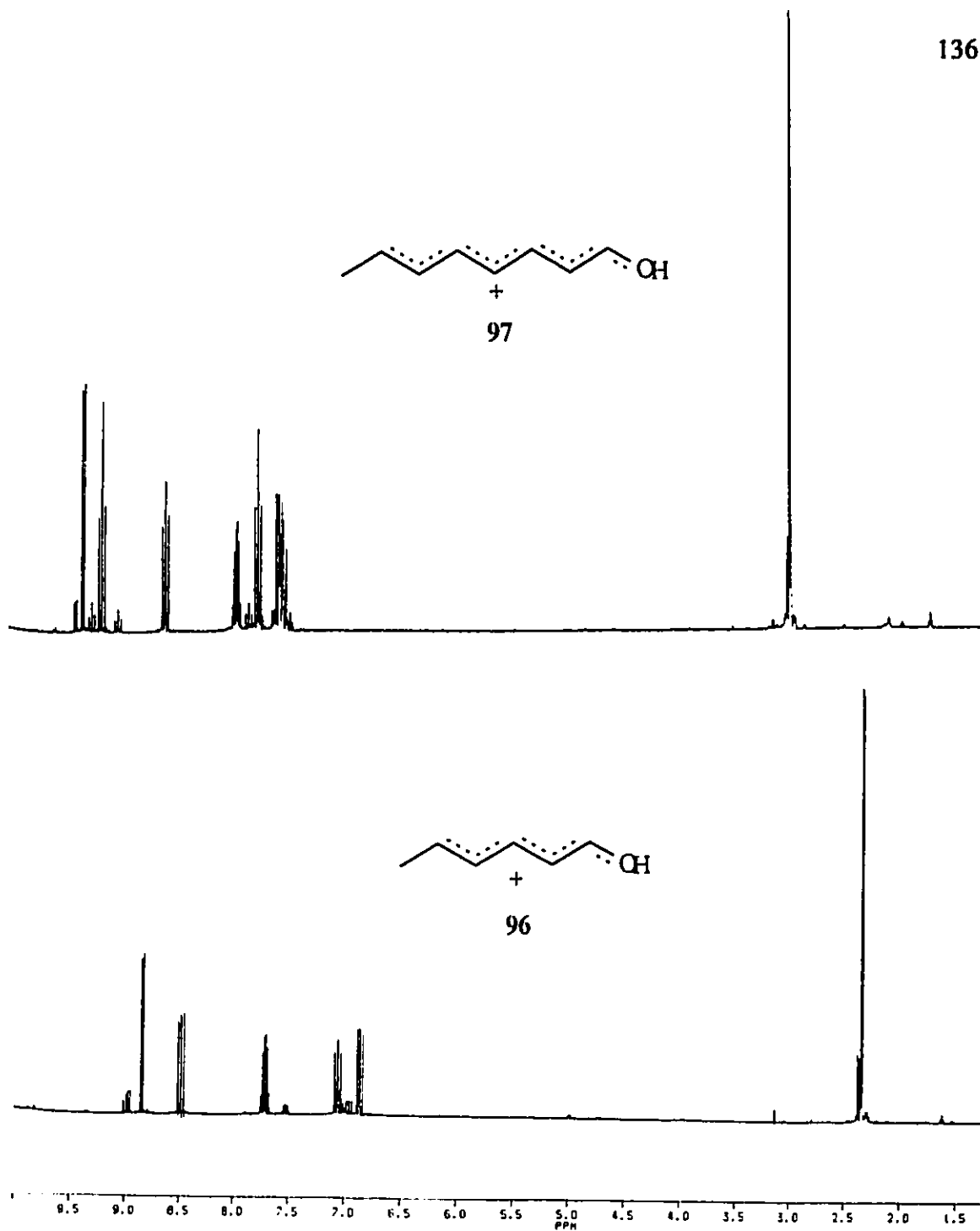


Figure 4-3: ^1H NMR spectra of 96 and 97 in FSO_3H at -60°C .

Table 4-6.

¹³C NMR Chemical Shifts of 1-hydroxyallyl Cations and Corresponding Aldehydes

Position	Compound ^a			
	94 ^b	96 ^c	95 ^b	97 ^c
C1	193.8	198.2	193.2	190.9
C2	129.8	122.9	130.5	132.1
C3	152.6	184.9	152.3	183.5
C4	130.0	134.6	127.4	122.2
C5	141.9	175.0	142.9	171.9
C6	18.9	22.2	131.0	134.4
C7	-	-	136.9	164.1
C8	-	-	19.1	21.0

^a In ppm.^b Referenced to CDCl₃ at 77.3 ppm. Measured at 21°C.^c Referenced to CD₂Cl₂ at 53.8 ppm in FSO₃H/CD₂Cl₂. Measured at -60°C.

Table 4-7

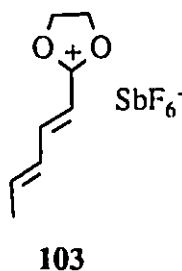
Isomeric Composition (%) of Aldehydes and Corresponding 1-hydroxyallyl Cations.

Compound	AT ^a	2- <i>cis</i>	4- <i>cis</i>	6- <i>cis</i>
94	85.5	nd ^b	14.5	-
96	87.4	nd	12.6	-
95	68.5	2.7	11.0	17.8
97	88.9	nd	nd	11.1

^a AT = all-*trans*^b nd = not detected

most thermodynamically stable conformer of this cation.

Rotational barriers about the formal C-C single bonds of cations comparable to **96** and **97** are expected to be low and as such rotation about these bonds will be fast on the NMR time scale at temperatures above -100°C .¹²⁰ The thermodynamically preferred conformations about the "single" bonds of **96** and **97** are also expected to be *trans*. This has been previously shown for protonated α,β -unsaturated aldehydes and conjugated iminium salts through low temperature ^{13}C NMR studies.^{72,124} A crystallographic study of a dioxolynium cation (**103**) corresponding to **96** has shown it has a *trans* configuration about each of the formal C-C and C=C bonds.¹²⁵

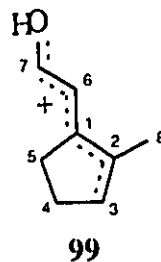
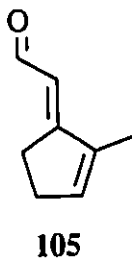
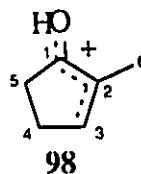
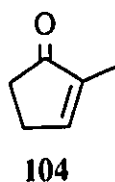


Thermal Isomerizations

The 1-hydroxy cations **96** and **97** were stable in FSO_3H at -60°C for several hours. Thermal stability at higher temperatures was assessed using ^1H NMR and monitoring the resulting spectrum as the temperature was increased. The samples were maintained at

each temperature for about 30 minutes while spectra were being acquired. From these spectra it was evident that **96** isomerized to form a second species as the temperature was increased above 30°C. The cation **97** was found to undergo a more facile reaction with it forming another species at temperatures as low as -20°C. In both cases the isomerizations proceeded quantitatively.

The thermal products of **96** and **97** were identified as the protonated



cyclopentenone, **98**, and the cation, **99**, respectively, on the basis of their ¹H NMR spectra, Table 4-5. In the case of the isomerization of **96**, a key feature in the spectrum used in the identification of **98** was the disappearance of all but one of the vinylic proton resonances. The presence of two methylene groups was evident from the two mutually coupled resonances appearing at 3.26 ppm and 3.34 ppm.

Elucidation of the structure of **99** proved to be a more difficult task than in the case of **98**. The presence of the cyclopentene ring moiety was evidenced by ^1H NMR signals arising from two adjacent methylene groups as in the case of **98**. The doublet at 9.25 ppm, characteristic of an aldehydic proton coupled to an adjacent vinyl proton, indicated that ring closure occurred between C3 and C7. A NOE confirmed that the protonated carbonyl group was *trans* to the methyl group substituted on the cyclopentene ring. The acid solutions of **98** and **99** were neutralized in order to retrieve the cyclopentene derivatives **104** and **105**. This proved to be a facile task in the case of **104**, which was recovered and purified by gas chromatography. The identification of **104** was confirmed through an independent synthesis following the method of Ho and Liu.¹²⁶ Protonation of 2-methyl-2-cyclopentenone in FSO_3H afforded a cation with the identical ^1H NMR spectrum to that of **98** derived from the isomerization of **96**. Neutralization of a FSO_3H solution containing the cation **99** led to the formation of a mixture of compounds. The major product was identified as 2-methyl-2-cyclopentylidene acetaldehyde by its ^1H NMR spectrum although isolation of a pure sample of this material proved to be difficult. The major product had an identical ^1H NMR spectrum to that described by Gilbert and Smith for **105**.¹²⁷

Kinetic Measurements

The rates of cyclization for **96** were measured at 50°C, 60°C and 70°C. Solutions of **94** in FSO_3H or $\text{CF}_3\text{SO}_3\text{H}$ were heated and analyzed at regular intervals by ^1H NMR

Table 4-8

Rate Constants and Activation Parameters for the Isomerization of 96 to 98.

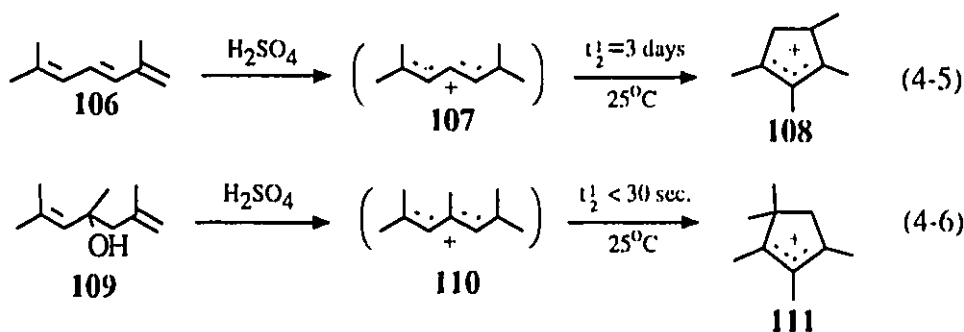
Temp (°C)	Acid	$k \times 10^4$ (s ⁻¹)	ΔS^\ddagger (cal K ⁻¹ mol ⁻¹)	E_a (kcal mol ⁻¹)	ΔG^\ddagger (kcal mol ⁻¹)
60	CF ₃ SO ₃ H	3.01 ± 0.23	-	-	25 ± 1
50	FSO ₃ H	3.59 ± 0.23			
60	FSO ₃ H	4.53 ± 0.04	-45 ± 3	10 ± 1	25 ± 2
70	FSO ₃ H	9.25 ± 0.16			

to determine the concentrations of the starting isomer and the final product. The analysis permitted the determination of the rate constants which are listed in Table 4-8. The isomerizations followed first order kinetics in all cases.

Discussion

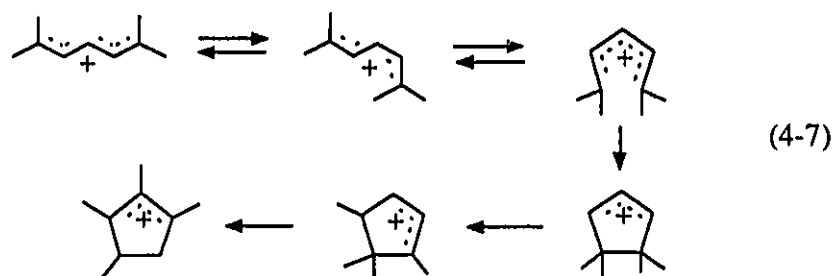
Mechanism of Cyclization

The mechanism of ring closure for **96** and **97** can be discussed in light of the chemistry of polyenyl carbocations that have been studied thoroughly by Deno¹²⁸ and Sorensen.¹²⁹ The characteristic reaction of this important class of carbenium ions consists of a 4π -electron electrocyclic ring closure of a pentadienyl fragment to form a substituted cyclopentenyl cation. Reactions representative of these ions are shown in equations 4-5 and 4-6. In the case of **109** the cation **110** was not detected even at temperatures as low as -30°C .¹³⁰



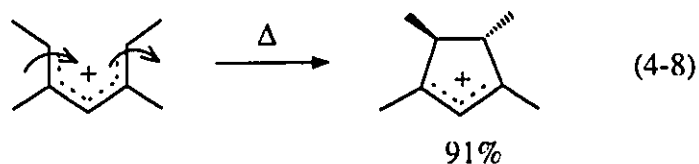
The actual mechanism of these reactions probably contains a large number of

steps, equation 4-7.



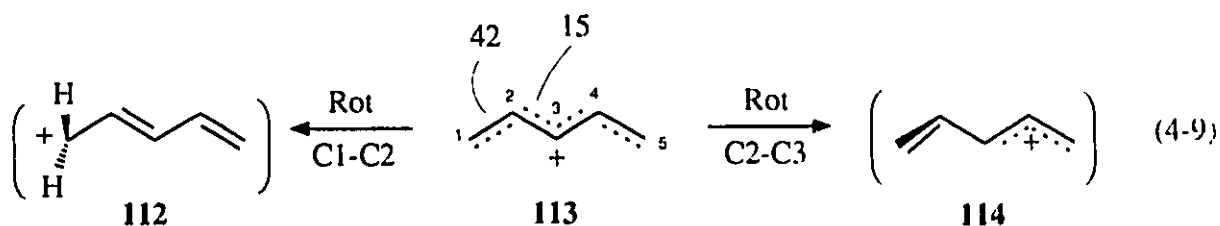
The rates of these cyclizations seem to be controlled to a large extent by steric factors. Sorensen suggested that the presence of the added methyl group at C3 in 110, aside from being in a stabilizing position destabilizes the all-*trans* conformation shown for 110 (equation 4-6).

Studies done by Woodward and Hoffmann¹³¹ and by Sorensen¹³² have shown the cyclization in pentadienyl cations to be highly stereoselective, proceeding in a conrotatory manner as predicted by the Woodward-Hoffmann rules (equation 4-8). It has been suggested that the small amount of product formed in these cyclizations that appears to

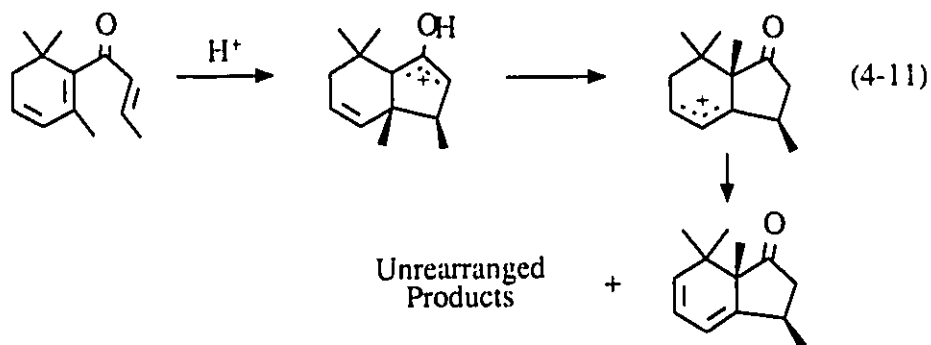
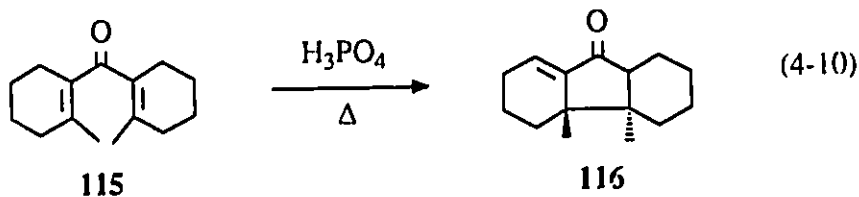


be derived from the "forbidden" pathways in fact is derived by the loss of geometric

integrity in the starting pentadienyl cation. Through the use of NNDO π -electron calculations, Baird has reported the rotational barriers (kcal/mole) for a series of polyenyl cations.¹²⁰ In the case of pentadienyl cations a much smaller energy barrier was observed for the C2-C3 partial double bond than the C1-C2 bond, equation 4-9. The small energy barrier for rotation about C2-C3 is readily understood by the extent of positive charge delocalization in the twisted conformations 112 and 114. The presence of methyl groups at C1, C3 or C5 should substantially reduce rotational barriers in these systems.



In contrast to the extensive studies done on polyenylic carbocations there have been far fewer studies pertaining to the thermal cyclizations of cross-conjugated ketones which are more closely related to the species described in the present work. One important well documented example is the very useful Nazarov reaction for the preparation of cyclopentenones.¹³³ Studies done by Kurkland¹³⁴ and Lehr¹³⁵ have shown that 115 is converted to 116 in the presence of an acid catalyst. The predicted conrotatory cyclization is followed as predicted by the Woodward-Hoffmann rules. Alkyl migrations can occur at the hydroxyallyl cation stage, equation 4-11.¹³⁶



The overall steps in the isomerization of **96** would most reasonably involve *trans* to *cis* isomerization about both the C2-C3 formal double and C3-C4 single bonds of the starting cation, Scheme 4-3. The intermediary 2-*cis* isomer **100** could then undergo cyclization and subsequent hydride shifts¹³⁷ to give **98**. In order to test this suggested mechanism the 2-*cis* isomer **100** was prepared by photoisomerization of **96**.^{71,138}

A FSO₃H solution of **96** was irradiated at 300 nm at low temperature for about 6 hours. A single isomer of the starting protonated aldehyde was formed in about 30% yield which was identified as **100** on the basis of its ¹H NMR spectrum, Table 4-5. The spectrum of **100** exhibited a 11.2 Hz coupling constant between the two protons attached to the C2-C3 partial double bond, clearly indicating the *cis* configuration of this bond.

On continued irradiation beyond this point the ^1H NMR spectrum of the mixture of cations became more complex suggesting the formation of other isomers such as the di-*cis* isomers. These cations were not identified.

The thermal isomerization of **100** was examined by following the reactions by ^1H NMR. Heating a mixture of **96** (70%) and **100** (30%) to -40°C caused the latter isomer to cyclize to give **101**. The new cation was identified as **101** on the basis of its ^1H NMR spectrum, Table 4-5. On further heating the reaction mixture to -10°C , the cation **101** was found to isomerize to give **98**. It is clear from these results that the isomerization of **96** could proceed via the formation of the thermodynamically less stable 2-*cis* isomer **100**. Given the thermal lability of **100** and its ring closure product **101**, these isomers would not be detected at temperatures required for the isomerization of **96**. The intermediacy of **101** and its subsequent transformation to the thermodynamically most stable ion **98** parallels the report of Olah and colleagues on the protonation of 3-cyclopentenone.⁷⁰

Further information on the mechanism of the thermal isomerization of **96** was obtained by examining the reaction in media of different acidity. The rate constants for the isomerization of **96** to the cyclopentenone cation **98** were measured in both FSO_3H and $\text{CF}_3\text{SO}_3\text{H}$. The isomerizations in each acid followed first order kinetics. The rate constants and activation parameters for the isomerizations are given in Table 4-8. As can be seen from these data in Table 4-8, the isomerization of **96** to **98** is significantly faster in FSO_3H compared to $\text{CF}_3\text{SO}_3\text{H}$.

FSO_3H is a stronger acid than $\text{CF}_3\text{SO}_3\text{H}$.¹¹⁷ The faster rate of isomerization in the stronger acid medium suggests that the reaction is acid catalyzed. The large negative entropy of activation ($-45 \pm 3 \text{ cal K}^{-1} \text{ mol}^{-1}$ at 60°C) measured for the isomerization of **96** to **98** is fully consistent with the transition state involving protonation to form a dication, Scheme 4-3. It is not clear whether it is the dication which undergoes ring closure or whether proton loss to form **100** occurs prior to cyclization.

As was shown in the previous section, the results obtained from the *cis/trans* isomerization of the octatrienylidene iminium salts also revealed the presence of a dication. Earlier work in this group has shown that the *cis/trans* isomerizations of 3-aryl-1-methoxyallyl⁷⁵ and N-aryl-3-arylpropenylidene⁶³ iminium salts can involve protonation on the heteroatom to form a dication.

The surprising feature of the isomerization of **97** is the regioselectivity of the process. The other product which could have formed is **117**¹³⁹, however, no such product could be detected in the ^1H NMR spectrum of the reaction mixture during the isomerization. In order to examine this regioselectivity the 2-*cis* isomer of **97** was prepared by irradiation.

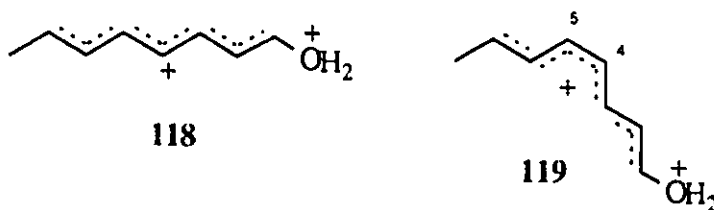


The cation **97** exhibited a uv spectrum with a long wavelength band at 425 nm.

Irradiation of a FSO_3H solution of **97** at low temperature for about 6 hours led to the formation of **102** (45% conversion). The photoproduct was identified as the corresponding 2-*cis* isomer **102** on the basis of its ^1H NMR spectra, Table 4-5. On continued irradiation of the **97/102** mixture, the vinyl region in the ^1H NMR spectrum for both cations became complex suggesting the formation of the di-*cis* isomers. These cations were not identified.

Warming the FSO_3H mixture of **102** (45%) and **97** (55%) to -50°C caused the former ion to revert completely to **97**. No cyclic products were formed under these conditions. The all-*trans* isomer **97** was stable in the acid solution at -50°C and did not isomerize to **99** until the solution was heated to -20°C . It is clear from these results that while **102** might well be thermally accessible from **97**, this isomer does not undergo a ring closure reaction.

The formation of **99** from **97** would seem to proceed via the 4-*cis* isomer **119**. As **97** is expected to be more basic than **96**, isomerization about the formal $\text{C}=\text{C}$ bonds of **97** will again involve protonation on oxygen to form the dication **118**. This dication can be considered to be a substituted heptatrienal cation. As noted earlier Baird has shown by calculation that the barriers to rotation about the central partial double bonds



of heptatrienyl cations are lower than those of the terminal partial double bonds.

This is in contrast to **97** where barriers to rotation increase as the bond in question is further removed from the protonated carbonyl. This is evident upon examination of the ^{13}C NMR chemical shifts of **95** and **97**. The difference in chemical shift between these systems is a measure of the extent of charge delocalization through the carbon framework. As was shown in chapter 2 for retinylidene iminium salts, charge delocalization falls off with distance from the protonated carbonyl. This effect is reflected in the relative concentration of minor isomers in **97** in Table 4-7. On protonation, the minor isomers present in **95** isomerize to the corresponding all-*trans* isomers with the exception of the 6-*cis* isomer which only partly isomerizes. Hence it would be expected that the barrier to rotation in **97** decreases in the order C6-C7 > C4-C5 > C2-C3.

In a solution of **97** in FSO_3H where there is a low concentration of **118** it would be expected that **119** could be produced preferentially. The lowest energy cyclization process available to **119** is C3-C7 bonding to form eventually **99** rather than a C1-C5 bonding reaction.

Summary

The cyclizations of **96** and **97** in strong acid media were found to be acid catalyzed with protonation occurring on oxygen to form a dication in the transition state. Although the mode of ring closure was different in each case, cyclization occurred at the

end of the polyene chains with both products exhibiting the 2-methyl-2-cyclopentene ring. Conversely, the isoelectronic iminium salts 46 and 47 did not cyclize but were found to undergo acid catalysed C=C isomerizations.

Chapter 5

Conclusions and Future Work

In this thesis, the powerful solid state techniques of x-ray crystallography, ^{13}C NMR, FTIR spectroscopy and UV absorption spectroscopy were successfully utilized in an integrated manner to probe the nature of the different interactions between a series of retinylidene cations and their associated anions. Through the combined use of these techniques it can be concluded that modulation of the extent of charge delocalization and corresponding absorption maxima positions in N-alkyl retinylidene iminium salts is an integral function of the distance between the counterion and the proton bonded to the Schiff base nitrogen atom in these salts. However, changes in the absorbance maxima and ^{13}C NMR chemical shifts as a function of counterion in a series of retinylidene iminium salts are not structurally manifested in terms of detectable C-C or C=C bond length differences in these systems.

Crystallographic analysis of compound **50** would provide valuable information as to the placement of the CF_3SO_3^- counterion with respect to the sterically smaller n-butyl group. It would also be interesting to extend the work herein described to systems which contain additional perturbations in the vicinity of the Schiff base nitrogen atom in retinylidene iminium salts. Sheves has suggested that a positive charge in the vicinity of the Schiff base linkage can repulse the positive charge formally located on the Schiff base nitrogen atom resulting in more positive charge delocalization along the polyene chain. Compound **66** has an absorption maximum at 550 nm in hexafluoro-2-propanol and

exhibits corresponding solution ^{13}C NMR chemical shifts considerably downfield shifted from the retinylidene salts contained in this work and bR itself.⁶² Determination of the x-ray structure of **66** in conjunction with solid state ^{13}C NMR, FTIR and UV absorption spectra for this compound will allow a definitive measure of the extent of positive charge delocalization in compounds having a positive charge in the vicinity of the Schiff base nitrogen atom.

It is suggested from the results of the solution studies detailed in this thesis that *cis-trans* isomerization in retinylidene iminium salts occurs via nucleophilic catalysis. In solution, movement of the counterion from the vicinity of the Schiff base nitrogen atom to a catalytic position at C11 not only increases the delocalization of positive charge from the nitrogen atom to the polyene carbon atoms, but also decreases the C11-C12 rotational barrier.

Further examination of the dynamics of *cis-trans* isomerization about the C11-C12 bond in retinylidene iminium salts would be facilitated by the determination of activation parameters for this process via a temperature dependent kinetic study. Previous work has shown that the activation energy for C11-C12 bond isomerization in retinal is about 25 kcal/mole.⁵⁵ However, the activation energy and the entropy of activation of the corresponding retinylidene iminium salts is still unknown. Knowledge of the activation parameters for the thermal C11-C12 bond isomerization would provide a more detailed description of the transition state for this process.

Curiously, the thermal chemistry exhibited by iminium salts is radically

different than that found for the analogous protonated poly-unsaturated aldehydes. Perhaps the bulky substituents borne by the nitrogen atom in these iminium salts prevents cyclization although 6π -electron electrocyclic reactions have recently been reported for the Schiff bases of 13-*cis* retinal.¹⁴⁰ Substitution of a n-butyl group resulted in a slow cyclization however the t-butyl Schiff base cyclization was negligible.¹⁴⁰ These two examples reflect the difficulty in cyclization as a result of the presence of bulky groups at the termini of the polyenes. In light of these results, it is not surprising that the analogous iminium salts examined in this work do not undergo similar cyclizations as a result of the sterically larger protonated or alkylated nitrogen termini.

In view of the relative ease of cyclization of the protonated poly-unsaturated aldehydes described in this work, it would be interesting to determine whether methoxy or ethoxypolyenyl cations cyclize to form a five membered rings or whether the increased steric bulk at the carbonyl end precludes cyclization.

Chapter 6

Experimental Methods

Materials

CH_2Cl_2 was refluxed over P_2O_5 and distilled under a dry N_2 atmosphere prior to its use. Similarly, diethyl ether was distilled from LiAlH_4 , CH_3CN from P_2O_5 and CaH_2 . Dry solvents were stored over 4\AA molecular sieves in a glove bag which was continuously purged with N_2 in the presence of solid P_2O_5 . Tertiary butylamine, n-butylamine and N-methyl aniline were distilled and kept over 4\AA molecular sieves. Superacids FSO_3H and $\text{CF}_3\text{SO}_3\text{H}$ were distilled twice under N_2 before use and stored in sealed glass ampules. Trifluoroacetic Acid (TFA), CD_2Cl_2 (purchased in sealed 1 gram ampules) and CDCl_3 were used without further purification.

2,4-hexadienal (Aldrich) was distilled prior to use whereas all-trans retinal (Aldrich) was used without further purification. Dimethyl ammonium perchlorate was prepared from dimethylamine and perchloric acid⁶⁴ and stored in a dessicator prior to use.

Instrumentation

^1H NMR Spectroscopy

^1H NMR spectra were obtained using Varian EM390 (90 MHz), Bruker AC200 (200 MHz) and Bruker AM500 (500 MHz) spectrometers. All solution spectra were referenced with CD_2Cl_2 ; the residual CH_2Cl_2 present appeared as a triplet centered at 5.32 ppm or CDCl_3 at 7.25 ppm. Spectra were acquired at variable temperatures as

individually noted. Nuclear Overhauser experiments as well as homo (^1H - ^1H) and hetero (^{13}C - ^1H) correlated shift experiments were done in order to simplify spectral assignments in the vinyl regions.

Solution State ^{13}C NMR Spectroscopy

All solution state ^{13}C NMR spectra were obtained with use of either a Bruker AC200 (50 MHz) or a Bruker AM500 (125.8 MHz) spectrometer. Unless otherwise noted spectra were acquired at room temperature. CD_2Cl_2 (quintet at 53.8 ppm) or CDCl_3 (triplet at 76.9 ppm) were used as internal standards. Spin-sort and (^{13}C - ^1H) hetero correlated shift experiments were performed when needed to aid in resonance assignments.

Solid State ^{13}C NMR Spectroscopy

Room temperature solid state ^{13}C NMR spectra of crystalline samples were obtained by cross polarization magic angle spinning (CPMAS) techniques with the use of a Bruker MSL100 (25 MHz) spectrometer. Spinning rates were approximately 4000 Hz. Methyl and quaternary carbon resonances were assigned using a delay without decoupling pulse sequence. Samples were mixed with NaCl, finely ground and densely packed into alumina rotors under a dry N_2 atmosphere. Adamantane was used as an external reference, and displayed resonances at 29.5 ppm (CH) and 38.6 ppm (CH_2) relative to tetramethylsilane.¹⁴¹

Solution and Solid State UV Absorption Spectra

UV absorption spectra were recorded on a Hewlett Packard 8451A spectrophotometer. Solutions of the various compounds contained in this work (about 10^{-5} M) were placed in 1 cm quartz cells to record their absorption spectra.

Solid state absorption spectra were obtained from crystalline samples smeared onto a glass or quartz slide. A similar slide was used as a reference.

Infrared Spectra

Infrared spectra were recorded on a Biorad FTIR spectrometer. The samples were prepared as thin KBr discs.

Centrifugal Chromatography

Centrifugal chromatography on 3-methyl-2,4,6-octatrienal and 2,4,6-octatrienal was carried out on silica (Merck Kieselgel 60PF₂₅₄) coated plates (coating 2 or 4 mm) spinning in a Chromatotron Model 7924T apparatus.

Synthesis

All imines were synthesized using a modified procedure of Blatz et al.³⁹ The corresponding iminium salts were prepared by addition of an ethereal solution of the desired acid to the imine dissolved in ether at room temperature under a N₂ atmosphere. The iminium salts 47 and 54 were prepared according to the method of Leonard and

Paukstelis.³⁴

3-methyl-2,4,6-octatrienal, 44.

This trienal was prepared according to the procedure of Weedon and Woods.³¹ It consisted of a Reformatsky reaction of ethylbromoacetate and activated zinc with crotonylidene acetone followed by dehydration with *p*-toluene sulphonic acid. Reduction of the resulting ester was accomplished by LiAlH₄ at -40°C. Oxidation to produce the aldehyde **44** was done by MnO₂ oxidation at room temperature (overall yield, 10%).

¹H NMR (CD₂Cl₂): δ 1.82 ppm (d, J=7 Hz, H₈, 3H), 2.30 ppm (s, H₉, 3H), 5.89 ppm (d, J=9 Hz, H₂, 1H), 6.21 ppm (m, H₆, H₇, 2H), 6.34 ppm (d, J=15 Hz, H₄, 1H), 6.75 ppm (dd, J=11 Hz, 15 Hz, H₃, 1H), 10.15 ppm (d, J=9 Hz, H₁, 1H).

N-t-butyl-3-methyl-2,4,6-octatrienylidene imine, 45.

Tertiary butylamine (4.40 g, 60.2 mmol) was added to a solution of 3-methyl-2,4,6-octatrienal (810 mg, 5.95 mmol) in dry ether (40 ml) under a N₂ atmosphere and in the absence of light. The reaction mixture was stirred for 24 hours over 4 Å molecular sieves. The mixture was filtered and ether and excess amine were removed under vacuum. The imine was rinsed three times with dry ether (5 ml) and the flask evacuated to ensure complete removal of amine (excess amine would interfere in the subsequent protonation). The yield was 1.05 g, 93 %. The imine was not characterized and was used immediately in the following step.

All of the retinylidene imines were prepared in a similar fashion.

N-t-butyl-3-methyl-2,4,6-octatrienyldene iminium triflate, 46.

The freshly prepared imine, 45, was dissolved in dry ether (50 ml) inside a glove bag under a N₂ atmosphere. To this an ethereal solution of CF₃SO₃H was added dropwise until precipitation was complete. The resulting solid was filtered and recrystallized from CH₂Cl₂/ether at -20°C to yield bright yellow crystals (450 mg, 25%). ¹H NMR, ¹³C NMR and uv spectra for 46 are reported in Tables 2-1, 2-5 and 2-8.

Retinylidene iminium salts 50, 51 and 52 were prepared in this fashion. Recrystallization was accomplished using CH₃CN/ether mixtures at -20°C. ¹H NMR, ¹³C NMR and uv absorption spectra of 51 and 52 are similar to those reported previously. ¹H NMR, ¹³C NMR and uv spectra of 50 are reported in Tables 2-3, 2-6 and 2-8.

N,N-dimethyl-3-methyl-2,4,6-octatrienyldene iminium perchlorate, 47.

N,N-dimethyl iminium perchlorate (520 mg, 3.6 mmol) was dissolved in 2 ml of dry methanol and quickly added to 3-methyl-2,4,6-octatrienal (480 mg, 3.5 mmol). After stirring for 24 hours under a N₂ atmosphere and in the absence of light, a minimum amount of dry ether was added to induce precipitation and the flask was cooled to -20°C. The resulting yellow solid was filtered, recrystallized from CH₂Cl₂/ether and dried under vacuum (yield 480 mg, 52%). ¹H NMR, ¹³C NMR and uv spectra of 47 are reported in Tables 2-1, 2-5 and 2-8.

The retinylidene iminium salt **54** was prepared similarly from N,N-dimethyl ammonium perchlorate and all-trans retinal. The ¹H NMR spectrum of **54** is similar to that reported previously.⁸⁶

N-methyl-N-phenyl-retinylidene iminium perchlorate, 53.

Freshly distilled N-methyl aniline (75 mg, 0.7 mmol) in dry ether (5 ml) was cooled in an ice bath. A slight excess of perchloric acid (110 mg of 70% HClO₄, 0.8 mmol) was added dropwise. A solution of all-trans retinal (200 mg, 0.7 mmol) in dry ether (2 ml) was added and the mixture stirred and allowed to stand until the salt precipitated from solution within about ten minutes. The product was filtered, washed with dry ether, recrystallized from CH₃CN/ether and dried under vacuum (yield 250 mg, 75%). ¹H NMR, ¹³C NMR and uv absorption spectra of **53** are reported in Tables 2-3, 2-6 and 2-8.

2,4,6-Octatrienal, 95.

A Mixture of butenal (11.0 g, 160 mmol), glacial acetic acid (1.5 ml, 25 mmol) and piperidine (0.15 ml, 1.5 mmol) was heated over a steam bath for 10 minutes under an N₂ atmosphere and subsequently cooled in an ice bath. The entire contents of the flask were distilled under 0.05 mmHg pressure and the fraction boiling at 65°C removed. A centrifugal chromatography separation using 10% ether/hexanes as solvent was carried out and the second band (R_f = 0.2) taken. The solvent was removed to give **95** as the

major product with a small amount of cis isomers representing the minor products. ^1H NMR (CD_2Cl_2) δ 1.80 (d, $J = 7$ Hz, CH_3 , 3H), 6.05(m, H_2 , H_7 , 2H), 6.18 (dd, $J = 11$ Hz, 15 Hz, H_6 , 1H), 6.33 (dd, $J = 11$ Hz, 15 Hz, H_4 , 1H), 6.66 (dd, $J = 11$ Hz, 15 Hz, H_5 , 1H), 7.14 (dd, $J = 11$ Hz, 15 Hz, H_3 , 1H), 9.46 (d, $J = 8$ Hz, H_1 , 1H).

Preparation of Protonated Unsaturated Aldehydes

FSO_3H (1 ml) was cooled to -78°C in a dry ice-acetone bath and added slowly down the sides of a medium walled NMR tube into a CD_2Cl_2 solution of the appropriate aldehyde (40-50 mg) also at -78°C . $\text{CF}_3\text{SO}_3\text{H}$ was cooled to -5°C and added in a similar manner.

Irradiations

All photoisomerizations were carried out using a photoreactor which consisted of ten reactor lamps (Southern New England Ultraviolet Co., RPR 3000A or 3500 A) arranged in a circle around a quartz dewar. The samples were placed inside the dewar and cooled using a FTS Systems Flexi-cooler refrigeration system and methanol. The photoisomerizations were monitored by ^1H NMR.

H. Measurements

The acidity of the acids used in the octatrienylidene iminium salt studies was determined by the Hammett indicator method using 2,4-dinitroaniline.¹⁴² The values

found were TFA, -4.21; 0.01 M H₂SO₄/TFA, -4.43.

Kinetic Measurements

The rate constants for the isomerization of iminium salts **86** and **87** were determined in duplicate at the previously indicated temperatures using a constant temperature bath ($\pm 0.1^\circ\text{C}$). In each case the iminium salt (10 mg) was dissolved in 0.75 ml of TFA or TFA/H₂SO₄ in a medium walled NMR tube. The sample was then irradiated at 350 nm until equal amounts of the 2-cis and all-trans isomer were present as assayed by ¹H NMR. The peak heights of the H₁ resonance were used to quantitate the reaction. After a given timed interval, the reaction was quenched by rapidly cooling the samples in an ice bath and the reaction assayed using ¹H NMR at 22°C.

The rates of isomerization were determined using equation 6-1.¹⁴³

$$\ln(x_0 - x_c / x - x_c) = (k_f + k_r)t \quad (6-1)$$

x = concentration of 2-cis isomer at time t .

x_0 = initial concentration of 2-cis isomer.

x_c = equilibrium concentration of 2-cis isomer.

k_f , k_r = rate constants for the forward and back reactions, respectively.

A plot of $\ln(x_0 - x_c / x - x_c)$ versus time gave the sum of the forward and reverse rate constants as the slope. Each rate constant can be determined using equation 6-2.

$$x_c / y_c = k_f / k_r \quad (6-2)$$

y_c = equilibrium concentration of all-trans isomer.

The error in rate constants was less than 7% with a good linear correlation ($r > 0.99$)

in each case.

The rate constants for the retinylidene iminium salts were obtained similarly with the following exceptions. The NMR tubes were sealed since CD_2Cl_2 is a relatively volatile solvent. Irradiation at 350 nm at -78°C produced the 11-cis isomer in each case. The peak heights of the singlet resonances corresponding to the methyl group at C20 were used to quantitate the reaction. The ratio of the 11-cis isomer to the total iminium salt was determined and $\ln(\text{ratio})$ plotted against time. The slopes of these plots were equal to the first-order rate constant for the reaction. The difference in rate constants was less than 5% and each run produced a good linear correlation ($r > 0.99$).

The rate measurements for the isomerization of protonated (using FSO_3H or $\text{CF}_3\text{SO}_3\text{H}$) 2,4-hexadienal, **96**, were determined using a Varian EM390 NMR spectrometer. Each spectrum was scanned twice and the extent of reaction determined by the average of integrations of methyl resonances of each species. Each rate constant was determined in duplicate with an error of less than 7% and linear correlations of greater than 0.99.

Single Crystal X-Ray Crystallography

Crystal Selection and Handling

Single crystals of iminium salts **51** and **52** suitable for x-ray diffraction studies were obtained from distillation of diethyl ether into an acetonitrile solution of each salt at -20°C .

Data Collection, Structure Solution and Refinement

N-t-butyl Retinylidene Iminium Perchlorate, 51.

A red plate crystal was mounted on a glass fiber on a Rigaku AFC5R diffractometer with graphite monochromated Cu K α radiation and a 12 KW rotating anode generator. Cell constants and an orientation matrix for data collection, obtained from a least-squares refinement using the setting angles of 24 carefully centered reflections in the range $47.04 < 2\theta < 81.43^\circ$ corresponded to a monoclinic cell. The data were collected at a temperature of $23 \pm 1^\circ\text{C}$. Based on the systematic absences of $h0l: l \neq 2n$, $0k0: k \neq 2n$ and the successful solution and refinement of the structure, the space group was determined to be $P2_1/c$.

Of the 5609 reflections which were collected, 3242 were unique; equivalent reflections were merged. The intensities of three representative reflections which were measured after every 150 reflections remained constant throughout data collection indicating crystal and electronic stability (no decay correction was applied). The linear absorption coefficient for Cu K α is 15.7 cm^{-1} . An empirical absorption correction, based on azimuthal scans of several reflections, was applied which resulted in transmission factors ranging from 0.84 to 1.00. The data were corrected for Lorentz and polarization effects.

The structure was solved by direct methods.¹⁴⁴ The oxygen atoms of the perchlorate ion were found to be disordered in a 0.7:0.3 ratio. All non-hydrogen atoms were, with the exception of two of the disordered oxygen atoms O5 and O7, refined

anisotropically. The final cycle of full-matrix least-squares refinement was based on 1854 observed reflections and 297 variable parameters. Plots of $\Sigma w (|F_o| - |F_c|)^2$ versus $|F_o|$, reflection order in data collection, $\sin \theta/\lambda$, and various classes of indices showed no unusual trends. All calculations were performed using the TEXSAN crystallographic software package of Molecular Structure Corporation.¹⁴⁴

Information pertinent to the data collection and final structure solution of **51** is comprehensively listed in Table 6-3. Table 6-1 lists final non-hydrogen positional parameters. Hydrogen atom positional parameters and isotropic temperature factors, anisotropic temperature factors for all non-hydrogen atoms and F_o/F_c values for **51** are tabulated in the Appendix section.

N-t-butyl Retinylidene Iminium Triflate, 52.

A red plated crystal was mounted in a glass capillary. All measurements were made on a Rigaku AFC6R diffractometer with graphite monochromated Cu K α radiation and a 12 KW rotation anode generator. Cell constants and an orientation matrix for data collection, obtained from a least-squares refinement using the setting angles of 17 carefully centered reflections in the range $21.19 < 2\theta < 26.07^\circ$ corresponded to a monoclinic cell. The data were collected at a temperature of $23 \pm 1^\circ\text{C}$. Based on the systematic absences of $0k0: k \neq 2n$ packing considerations, a statistical analysis of intensity distribution, and the successful solution and refinement of the space group was determined to be $P2_1$.

Of the 2229 reflections which were collected, 2078 were unique ($R_{int} = 0.065$). The intensities of three representative reflections which were measured after every 150 reflections remained constant throughout data collection indicating crystal and electronic stability (no decay correction was applied). The linear absorption coefficient for Cu $K\alpha$ is 14.1 cm^{-1} . An empirical absorption correction using the program DIAB¹⁴⁴ was applied which resulted in transmission factors ranging from 0.64 to 1.20. The data were corrected for Lorentz and polarization effects.

The structure was solved by direct methods.¹⁴⁴ The non-hydrogen atoms were refined anisotropically. The final cycle of full-matrix least-squares refinement was based on 1330 observed reflections and 297 variables. Plots of $\sum w (|F_o| - |F_c|)^2$ versus $|F_o|$, reflection order in data collection, $\sin \theta/\lambda$, and various classes of indices showed no unusual trends. All calculations were performed using the TEXSAN crystallographic software package of Molecular Structure Corporation.¹⁴⁴

Information pertinent to the data collection and final structure solution of 52 is comprehensively listed in Table 6-3. Table 6-2 lists final non-hydrogen positional parameters. Hydrogen atom positional parameters and isotropic temperature factors, anisotropic temperature factors for all non-hydrogen atoms and F_oF_c values for 52 are tabulated in the Appendix section.

Table 6-1
Atomic Coordinates for 51.

Atom	x	y	z	Occupancy
Cl	0.15527(10)	-.75906(24)	0.40008(10)	
O1	0.1353(7)	-.6184(12)	0.3469(6)	0.7
O2	0.1679(10)	-.6950(26)	0.4785(8)	0.7
O3	0.2191(5)	-.8273(21)	0.3936(7)	0.7
O4	0.1049(7)	-.8854(15)	0.3945(6)	0.7
O5	0.0910(21)	-.7583(58)	0.3711(27)	0.3
O6	0.1536(17)	-.7426(51)	0.4785(17)	0.3
O7	0.1734(18)	-.6448(54)	0.3500(28)	0.3
O8	0.1662(18)	-.9137(25)	0.3565(15)	0.3
N	0.0837(2)	-.6528(5)	0.1712(3)	
C1	0.3815(3)	0.6587(7)	0.3945(3)	
C2	0.4190(4)	0.7973(8)	0.4511(5)	
C3	0.4126(4)	0.9774(9)	0.4175(4)	
C4	0.4416(3)	0.9842(7)	0.3404(5)	
C5	0.4196(3)	0.8352(7)	0.2819(4)	
C6	0.3908(3)	0.6854(7)	0.3046(3)	
C7	0.3680(3)	0.5545(6)	0.2437(3)	
C8	0.3328(3)	0.4042(7)	0.2495(3)	
C9	0.3123(3)	0.2784(6)	0.1846(3)	
C10	0.2805(3)	0.1338(7)	0.2035(3)	
C11	0.2531(3)	-.0099(7)	0.1500(3)	
C12	0.2253(3)	-.1510(7)	0.1781(4)	
C13	0.1900(3)	-.2906(6)	0.1311(3)	
C14	0.1594(3)	-.4168(7)	0.1689(3)	
C15	0.1143(3)	-.5446(7)	0.1320(3)	
C16	0.4104(3)	0.4817(8)	0.4278(4)	
C17	0.3064(4)	0.6672(9)	0.4014(4)	
C18	0.4350(3)	0.8686(7)	0.1978(5)	
C19	0.3277(3)	0.3133(7)	0.1007(3)	
C20	0.1870(3)	-.2887(7)	0.0389(4)	
C21	0.0314(3)	-.7884(6)	0.1396(3)	
C22	0.0664(3)	-.9633(7)	0.1423(4)	
C23	-.0005(3)	-.7433(8)	0.0521(4)	
C24	-.0199(3)	-.7830(8)	0.1974(4)	

Table 6-2
Atomic Coordinates for 52.

Atom	x	y	z
S1	-.7135(3)	-1.4740(1)	0.6197(1)
F1	-.6403(8)	-1.550(1)	0.7531(3)
F2	-.747(1)	-1.744(1)	0.6880(4)
F3	-.5257(9)	-1.683(1)	0.6826(5)
O1	-.8460(7)	-1.407(1)	0.6382(4)
O2	-.7332(8)	-1.575(1)	0.5564(4)
O3	-.5950(8)	-1.357(1)	0.6266(4)
N	-.1557(8)	-1.401(1)	0.5785(4)
C1	0.289(1)	-.135(2)	0.8816(6)
C2	0.392(1)	-.003(2)	0.9206(7)
C3	0.329(2)	0.167(2)	0.9113(8)
C4	0.185(2)	0.179(2)	0.9438(6)
C5	0.083(1)	0.032(2)	0.9231(5)
C6	0.126(1)	-.109(1)	0.8904(5)
C7	0.014(1)	-.237(1)	0.8704(5)
C8	0.020(1)	-.379(1)	0.8353(5)
C9	-.097(1)	-.505(1)	0.8149(5)
C10	-.063(1)	-.646(1)	0.7824(5)
C11	-.161(1)	-.783(1)	0.7577(5)
C12	-.114(1)	-.917(1)	0.7270(5)
C13	-.205(1)	-1.051(1)	0.6938(5)
C14	-.143(1)	-1.169(1)	0.6571(5)
C15	-.219(1)	-1.290(1)	0.6115(5)
C16	0.298(1)	-.132(2)	0.8018(6)
C17	0.350(1)	-.298(2)	0.9152(7)
C18	-.070(1)	0.060(2)	0.9398(5)
C19	-.245(1)	-.465(2)	0.8325(6)
C20	-.366(1)	-1.048(2)	0.6968(6)
C21	-.219(1)	-1.527(1)	0.5269(5)
C22	-.129(1)	-1.515(2)	0.4659(5)
C23	-.378(1)	-1.488(2)	0.4956(5)
C24	-.203(1)	-1.694(2)	0.5628(6)
C25	-.656(1)	-1.619(2)	0.6896(7)

Table 6-3
Crystallographic Data for 51 and 52.

Compound	51	52
Formula	$C_{24}H_{38}O_4NCl$	$C_{25}H_{38}NO_3F_3S$
F.W.	440.02	489.64
Crystal Size (mm)	0.010x0.100x0.300 red, plate	0.100x0.001x1.000 red, plate
Systematic Absences	h0l: $l \neq 2n$ 0k0: $k \neq 2n$	0k0: $k \neq 2n$
Space Group	$P2_1/c$	$P2_1$
Unit Cell (\AA and $^\circ$)	a=20.179(3) b=7.585(1) c=16.556(7) $\beta=99.12(2)$	a=9.068(3) b=7.919(3) c=19.243(9) $\beta=99.87(3)$
Volume (\AA^3)	2502(2)	1361.5(9)
Z	4	2
ρ_{calc} (g cm^{-3})	1.168	1.194
μ (cm^{-1})	15.68	14.11
F_{000}	952	524
$2\theta_{max}$ ($^\circ$)	100.3	121.1
Temperature ($^\circ\text{C}$)	23	23
No. unique reflectns	3242	2078
No. total reflectns	5609	2229
Residuals: R; R_w	0.059; 0.072	0.057; 0.039
Max Shift in Final Cycle	0.15	0.03
Max. Peak in Final Diff. Map ($\text{e}/\text{\AA}^3$)	0.30	0.19
Min. Peak in Final Diff. Map ($\text{e}/\text{\AA}^3$)	-0.20	-0.17
Least-squares Weights	$4F_o^2/\sigma(F_o)^2$	$4F_o^2/\sigma^2(F_o^2)$

$$R = \frac{\sum ||F_o| - |F_c||}{\sum |F_o|}; R_w = \left[\frac{\sum w(|F_o| - |F_c|)^2}{\sum w F_o^2} \right]^{1/2}$$

$S = [\sum w(|F_o| - |F_c|)^2 / (N_o - N_v)]^{1/2}$ where N_o is the number of observations and N_v is the number of variables.

Appendix

Table A-1: Bond lengths (Å) Involving Hydrogen Atoms in 51 and 52.

Atom	Atom	51 Length	52 Length
N	H	0.952	0.954
C2	H21	0.953	0.948
C2	H22	0.946	0.941
C3	H31	0.948	0.944
C3	H32	0.952	0.959
C4	H41	0.950	0.959
C4	H42	0.951	0.948
C7	H7	0.950	0.946
C8	H8	0.945	0.959
C10	H10	0.954	0.953
C11	H11	0.954	0.951
C12	H12	0.951	0.951
C14	H14	0.952	0.954
C15	H15	0.950	0.948
C16	H161	0.951	0.940
C16	H162	0.955	0.957
C16	H163	0.948	0.955
C17	H171	0.953	0.949
C17	H172	0.955	0.953
C17	H173	0.952	0.947
C18	H181	0.953	0.950
C18	H182	0.948	0.952
C18	H183	0.950	0.951
C19	H191	0.949	0.955
C19	H192	0.949	0.951
C19	H193	0.952	0.963
C20	H201	0.949	0.955
C20	H202	0.949	0.950
C20	H203	0.956	0.952
C22	H221	0.948	0.958
C22	H222	0.950	0.948
C22	H223	0.952	0.952
C23	H231	0.945	0.953
C23	H232	0.952	0.950
C23	H233	0.952	0.960
C24	H241	0.946	0.951
C24	H242	0.950	0.949
C24	H243	0.948	0.950

Table A-2
Hydrogen Atom Coordinates and Isotropic Thermal Parameters for 5I.

Atom	x	y	z	B
H	0.0952	-.6476	0.2291	5.3
H7	0.3793	0.5770	0.1910	4.2
H8	0.3209	0.3785	0.3012	4.3
H10	0.2747	0.1233	0.2594	5.3
H11	0.2558	-.0027	0.0931	4.7
H12	0.2291	-.1599	0.2359	5.2
H14	0.1690	-.4187	0.2271	5.2
H15	0.1063	-.5508	0.0740	4.5
H21	0.4014	0.7966	0.5012	9.6
H22	0.4650	0.7662	0.4612	9.6
H31	0.3668	1.0104	0.4063	9.4
H32	0.4363	1.0575	0.4558	9.4
H41	0.4287	1.0922	0.3133	7.4
H42	0.4892	0.9802	0.3539	7.4
H161	0.3880	0.3880	0.3965	6.8
H162	0.4571	0.4774	0.4239	6.8
H163	0.4050	0.4692	0.4834	6.8
H171	0.2882	0.7779	0.3817	7.9
H172	0.2827	0.5754	0.3696	7.9
H173	0.3004	0.6534	0.4570	7.9
H181	0.3944	0.8638	0.1595	7.4
H182	0.4651	0.7816	0.1844	7.4
H183	0.4546	0.9820	0.1958	7.4
H191	0.3114	0.2187	0.0656	6.4
H192	0.3069	0.4201	0.0804	6.4
H193	0.3750	0.3232	0.1030	6.4
H201	0.1594	-.3822	0.0150	6.8
H202	0.1694	-.1794	0.0173	6.8
H203	0.2312	-.3035	0.0260	6.8
H221	0.0843	-.9915	0.1972	6.6
H222	0.0352	-1.0516	0.1204	6.6
H223	0.1018	-.9577	0.1106	6.6
H231	-.0331	-.8290	0.0326	7.6
H232	-.0210	-.6302	0.0517	7.6
H233	0.0333	-.7406	0.0181	7.6
H241	0.0010	-.8157	0.2505	7.8
H242	-.0373	-.6668	0.1984	7.8
H243	-.0553	-.8625	0.1785	7.8

Table A-3
Hydrogen Atom Coordinates and Isotropic Thermal Parameters for 52.

Atom	x	y	z	B
H	0.0491	-1.4009	0.5895	5.5
H7	-.0812	-.2147	0.8826	5.9
H8	0.1146	0.4034	0.8217	5.7
H10	0.0378	-.6568	0.7754	5.7
H11	-.2634	-.7765	0.7631	5.6
H12	-.0089	-.9258	0.7275	5.2
H14	-.0361	-1.1711	0.6632	5.6
H15	-.3249	-1.2898	0.6046	4.8
H21	0.4078	-.0288	0.9694	10.2
H22	0.4831	-.0038	0.9036	10.2
H31	0.3982	0.2476	0.9330	10.3
H32	0.3023	0.1922	0.8620	10.3
H41	0.2126	0.1805	0.9941	9.4
H42	0.1331	0.2805	0.9290	9.4
H161	0.3975	-.1435	0.7953	8.9
H162	0.2390	-.2231	0.7788	8.9
H163	0.2572	-.0283	0.7817	8.9
H171	0.3451	-.2957	0.9640	8.7
H172	0.2919	-.3898	0.8935	8.7
H173	0.4509	-.3112	0.9090	8.7
H181	-.0636	0.0811	0.9888	9.6
H182	-.1149	0.1549	0.9139	9.6
H183	-.1297	-.0371	0.9270	9.6
H191	-.2443	-.3571	0.8543	10.8
H192	-.3201	-.4666	0.7913	10.8
H193	-.2713	-.5481	0.8650	10.8
H201	-.4098	-.9463	0.6754	9.0
H202	-.4144	-1.1420	0.6723	9.0
H203	-.3806	-1.0508	0.7446	9.0
H221	-.0249	-1.5363	0.4836	8.0
H222	-.1638	-1.5959	0.4307	8.0
H223	-.1380	-1.4048	0.4459	8.0
H231	-.3844	-1.3806	0.4729	8.5
H232	-.4170	-1.5720	0.4621	8.5
H233	-.4387	-1.4851	0.5319	8.5
H241	-.2560	-1.6938	0.6012	8.8
H242	-.2415	-1.7795	0.5301	8.8
H243	-0.0997	-1.7154	0.5799	8.8

atom	U11	U22	U33	U12	U13	U23
Cl	0.0850(13)	0.0740(12)	0.0523(10)	-0.0043(11)	0.0126(9)	0.0098(11)
O(1)	0.177(11)	0.082(6)	0.090(6)	0.000(7)	-0.040(7)	0.060(5)
O(2)	0.241(16)	0.221(14)	0.054(10)	-0.064(11)	-0.004(9)	-0.050(9)
O(3)	0.121(9)	0.264(15)	0.156(10)	0.086(9)	0.065(8)	0.026(10)
O(4)	0.176(10)	0.116(7)	0.121(8)	-0.075(8)	-0.008(8)	0.031(7)
O(6)	0.159(26)	0.204(31)	0.054(23)	0.105(25)	0.083(20)	0.081(22)
O(8)	0.190(29)	0.075(13)	0.165(23)	0.020(16)	0.071(23)	-0.048(14)
N	0.071(3)	0.042(3)	0.053(3)	-0.013(3)	0.011(3)	-0.0029(25)
C(1)	0.074(4)	0.047(3)	0.043(3)	-0.003(3)	0.007(3)	-0.010(3)
C(2)	0.151(8)	0.056(4)	0.089(5)	-0.010(4)	0.004(5)	-0.022(4)
C(3)	0.149(8)	0.070(5)	0.071(5)	-0.028(5)	-0.003(5)	-0.023(4)
C(4)	0.081(5)	0.038(4)	0.109(6)	-0.015(3)	-0.001(5)	0.000(4)
C(5)	0.042(3)	0.036(3)	0.073(4)	0.001(3)	0.004(3)	-0.003(3)
C(6)	0.039(3)	0.041(3)	0.058(4)	-0.000(3)	0.005(3)	-0.005(3)
C(7)	0.054(4)	0.034(3)	0.042(3)	-0.000(3)	0.011(3)	-0.002(3)
C(8)	0.046(4)	0.052(4)	0.032(3)	-0.006(3)	0.004(3)	-0.006(3)
C(9)	0.051(3)	0.034(3)	0.058(4)	-0.002(3)	0.010(3)	-0.005(3)
C(10)	0.061(4)	0.049(3)	0.053(3)	-0.011(3)	0.006(3)	-0.003(3)
C(11)	0.043(3)	0.048(4)	0.056(4)	-0.005(3)	0.003(3)	-0.004(3)
C(12)	0.055(4)	0.048(3)	0.061(4)	-0.008(3)	0.001(3)	-0.002(3)
C(13)	0.045(3)	0.047(3)	0.047(3)	-0.005(3)	0.005(3)	0.000(3)
C(14)	0.061(4)	0.048(3)	0.053(4)	-0.007(3)	-0.000(3)	-0.004(3)
C(15)	0.061(4)	0.041(3)	0.043(3)	-0.007(3)	0.014(3)	-0.002(3)
C(16)	0.086(5)	0.070(4)	0.060(4)	0.010(4)	0.005(4)	0.004(4)
C(17)	0.107(6)	0.093(5)	0.061(4)	0.013(4)	0.039(4)	0.007(4)
C(18)	0.074(5)	0.051(4)	0.117(6)	-0.002(3)	0.045(4)	0.021(4)
C(19)	0.101(5)	0.056(4)	0.046(3)	-0.012(3)	0.013(4)	-0.010(3)
C(20)	0.080(5)	0.068(4)	0.071(4)	-0.029(3)	0.029(4)	-0.015(4)
C(21)	0.053(4)	0.044(3)	0.049(3)	-0.006(3)	0.013(3)	-0.003(3)
C(22)	0.091(5)	0.043(3)	0.076(5)	0.000(3)	0.021(4)	-0.005(3)
C(23)	0.076(5)	0.078(4)	0.084(5)	-0.030(4)	-0.003(4)	0.005(4)
C(24)	0.076(5)	0.078(5)	0.101(5)	-0.021(4)	0.041(4)	-0.023(4)

Table A-5: Anisotropic Temperature Factors for the Non-Hydrogen Atoms in 51.

ATOM	U11	U22	U33	U12	U13	U23
S(1)	0.056(2)	0.060(1)	0.073(2)	-0.000(2)	0.009(1)	0.003(2)
F(1)	0.145(7)	0.137(7)	0.071(5)	0.012(6)	0.011(5)	-0.008(5)
F(2)	0.22(1)	0.098(6)	0.128(7)	-0.048(7)	0.045(7)	0.021(6)
F(3)	0.133(7)	0.18(1)	0.18(1)	0.086(8)	0.026(7)	0.017(8)
O(1)	0.058(5)	0.121(8)	0.129(7)	0.029(5)	0.009(5)	-0.007(6)
O(2)	0.116(6)	0.082(6)	0.067(6)	-0.009(5)	0.008(5)	-0.017(5)
O(3)	0.082(5)	0.078(6)	0.140(8)	-0.025(5)	0.030(6)	-0.013(6)
N(1)	0.045(5)	0.077(6)	0.058(6)	0.002(5)	0.007(4)	-0.012(5)
C(1)	0.073(8)	0.072(9)	0.080(9)	-0.020(7)	0.008(7)	-0.007(7)
C(2)	0.12(1)	0.07(1)	0.13(1)	-0.016(9)	-0.018(9)	-0.010(9)
C(3)	0.12(1)	0.07(1)	0.14(1)	-0.03(1)	-0.020(1)	-0.00(1)
C(4)	0.18(1)	0.053(8)	0.064(9)	-0.01(1)	-0.01(1)	-0.013(7)
C(5)	0.103(8)	0.064(7)	0.032(6)	0.00(1)	0.009(5)	-0.008(7)
C(6)	0.100(9)	0.048(6)	0.040(7)	-0.004(6)	0.009(6)	-0.001(6)
C(7)	0.075(7)	0.063(7)	0.047(7)	0.005(6)	0.007(5)	-0.010(6)
C(8)	0.052(6)	0.070(7)	0.065(7)	0.003(6)	0.016(5)	0.005(7)
C(9)	0.058(6)	0.065(8)	0.048(6)	0.005(6)	0.017(5)	-0.011(6)
C(10)	0.055(6)	0.077(8)	0.058(7)	0.003(6)	0.015(6)	-0.021(7)
C(11)	0.061(7)	0.058(7)	0.056(7)	0.011(6)	0.002(6)	-0.010(6)
C(12)	0.050(6)	0.058(7)	0.058(7)	-0.001(5)	0.010(5)	-0.001(6)
C(13)	0.051(6)	0.058(6)	0.056(7)	0.005(6)	0.009(5)	-0.001(6)
C(14)	0.038(6)	0.081(8)	0.065(7)	0.002(6)	0.017(5)	-0.011(7)
C(15)	0.046(6)	0.062(6)	0.050(7)	-0.012(5)	0.013(5)	-0.005(6)
C(16)	0.11(1)	0.10(1)	0.08(1)	-0.020(8)	0.015(8)	0.007(8)
C(17)	0.075(8)	0.073(9)	0.13(1)	-0.008(7)	-0.012(8)	-0.006(9)
C(18)	0.18(1)	0.07(1)	0.067(8)	0.01(1)	0.050(9)	-0.010(7)
C(19)	0.091(8)	0.11(1)	0.14(1)	-0.01(1)	0.017(8)	-0.05(1)
C(20)	0.078(8)	0.09(1)	0.13(1)	0.003(8)	0.033(8)	-0.043(9)
C(21)	0.066(7)	0.057(7)	0.045(6)	-0.008(5)	0.011(5)	-0.015(5)
C(22)	0.080(7)	0.12(1)	0.068(8)	-0.018(8)	0.033(6)	-0.025(8)
C(23)	0.071(7)	0.12(1)	0.082(8)	-0.012(9)	0.009(6)	-0.04(1)
C(24)	0.14(1)	0.061(8)	0.08(1)	-0.011(8)	0.017(8)	-0.011(8)
C(25)	0.10(1)	0.08(1)	0.08(1)	0.010(9)	0.026(9)	-0.001(9)

Table A-6: Anisotropic Temperature Factors for the Non-Hydrogen Atoms in 52.

Table A-6: Observed and Calculated Structure Factors for 51.
 F_o , F_c and sig values have been multiplied by 10.

k	l	Fo	Fc	sigF	k	l	Fo	Fc	sigF	k	l	Fo	Fc	sigF
^^^^^^	h =	0	^^^^^^		3	-7	0	5	24*	7	-2	276	278	13
					3	-6	370	356	11	7	-1	169	165	4
0	2	675	629	13	3	-5	294	280	10	7	6	107	108	5
0	4	1684	1590	26	3	-4	472	462	11					
0	6	0	32	22*	3	-3	255	245	5	^^^^^^	h =	1	^^^^^^	
0	8	120	62	3	3	-2	57	54	4					
0	10	217	222	7	3	-1	129	113	6	-7	-3	48	74	20*
0	12	132	104	5	3	12	133	136	5	-7	4	0	7	29*
0	14	265	260	6	4	-13	111	135	21	-7	5	0	9	18*
0	16	61	64	18*	4	-12	26	28	19*	-6	-2	13	21	18*
1	-16	32	41	20*	4	-11	100	108	5	-6	4	108	120	8
1	-15	100	97	7	4	-10	45	12	24*	-6	5	124	118	4
1	-14	223	206	11	4	-9	0	36	21*	-6	6	188	185	5
1	-13	0	16	19*	4	-8	79	91	8	-6	7	51	82	19*
1	-12	159	161	4	4	-7	247	238	6	-6	8	48	25	15*
1	-11	11	8	18*	4	-6	123	154	7	-6	9	0	45	19*
1	-10	146	136	6	4	-5	37	36	25*	-5	-8	0	49	20*
1	-9	37	29	13*	4	-4	334	320	7	-5	4	179	176	14
1	-8	110	96	3	4	-3	347	321	10	-5	5	108	106	9
1	-7	49	27	17*	4	-2	500	516	9	-5	6	116	107	4
1	-6	536	530	11	4	-1	15	13	14*	-5	7	68	70	6
1	-5	234	240	8	4	0	314	305	6	-5	8	33	29	19*
1	-4	423	416	9	5	-12	144	141	14	-5	9	97	124	11
1	-3	94	99	2	5	-11	29	24	19*	-5	10	253	254	17
1	-2	34	27	3	5	-10	48	39	25*	-5	11	110	141	18
1	-1	62	68	2	5	-9	52	44	12	-5	12	96	109	9
1	14	229	206	6	5	-8	274	301	13	-4	-11	310	295	8
2	-15	4	20	18*	5	-7	54	60	7	-4	4	44	82	10
2	-14	252	250	6	5	-6	23	36	18*	-4	5	131	136	6
2	-13	21	56	15*	5	-5	81	72	4	-4	6	0	36	26*
2	-12	185	174	6	5	-4	128	133	6	-4	7	0	11	23*
2	-11	213	230	11	5	-3	0	33	29*	-4	8	76	66	9
2	-10	474	505	9	5	-2	135	132	3	-4	9	93	88	15
2	-9	28	40	17*	5	-1	113	106	3	-4	10	40	13	18*
2	-8	160	129	10	5	8	299	301	8	-4	11	154	160	4
2	-7	357	368	10	5	10	29	39	17*	-4	12	0	24	25*
2	-6	38	61	22*	6	-9	108	119	10	-4	13	51	65	24*
2	-5	59	58	8	6	-8	113	130	16	-3	-11	117	125	5
2	-4	7	39	17*	6	-7	12	25	17*	-3	4	221	241	8
2	-3	325	330	6	6	-6	133	109	7	-3	5	201	164	10
2	-2	489	521	8	6	-5	78	72	13	-3	6	60	80	21*
2	-1	111	117	3	6	-4	54	49	21*	-3	7	52	16	24*
2	0	1172	1169	19	6	-3	108	118	6	-3	8	64	72	7
3	-14	99	80	5	6	-2	79	76	14	-3	9	35	70	26*
3	-13	0	42	29*	6	-1	154	155	4	-3	10	182	189	4
3	-12	140	136	9	6	0	114	111	12	-3	11	142	125	4
3	-11	112	118	4	7	-6	74	108	20*	-3	12	9	50	40*
3	-10	146	141	4	7	-5	22	6	17*	-3	13	144	150	7
3	-9	45	57	22*	7	-4	34	21	21*	-3	14	152	154	4
3	-8	215	222	5	7	-3	86	84	13	-2	-11	257	249	7

Table A-6 (con't)

k	l	Fo	Fc	sigF	k	l	Fo	Fc	sigF	k	l	Fo	Fc	sigF
-2	4	49	78	8	1	-7	270	254	9	3	13	138	150	5
-2	5	549	548	11	1	-6	453	476	10	4	-13	122	121	4
-2	6	424	430	10	1	-5	203	199	8	4	-12	260	268	11
-2	7	0	61	24*	1	-4	72	77	5	4	-11	279	295	14
-2	8	231	227	6	1	-3	27	5	13*	4	-10	244	247	14
-2	9	148	141	4	1	-2	690	671	11	4	-9	141	135	4
-2	10	89	108	4	1	-1	218	228	4	4	-8	349	341	12
-2	11	187	210	7	1	0	581	563	9	4	-7	237	226	9
-2	12	256	255	7	1	1	95	101	6	4	-6	303	291	11
-2	13	0	33	27*	1	2	553	540	11	4	-5	38	51	23*
-2	14	85	92	20	1	3	63	70	7	4	-4	52	77	5
-2	15	81	92	13	1	14	184	185	5	4	-3	299	298	11
-1	-10	387	390	8	2	-15	55	62	26*	4	-2	50	58	9
-1	4	989	986	16	2	-14	160	176	9	4	-1	153	151	4
-1	5	348	339	9	2	-13	178	168	8	4	0	159	150	3
-1	6	53	35	7	2	-12	37	35	11*	4	1	49	45	5
-1	7	0	28	18*	2	-11	241	249	12	4	2	9	24	19*
-1	8	462	487	8	2	-10	112	119	4	4	3	277	262	7
-1	9	99	113	4	2	-9	107	119	4	5	-12	102	74	26*
-1	10	155	152	4	2	-8	172	177	4	5	-11	130	151	7
-1	11	180	177	7	2	-7	174	163	7	5	-10	62	75	30*
-1	12	81	94	5	2	-6	0	12	22*	5	-9	89	88	10
-1	13	195	209	8	2	-5	264	306	9	5	-8	0	49	30*
-1	14	180	185	8	2	-4	103	131	5	5	-7	26	30	17*
-1	15	98	105	22	2	-3	250	264	5	5	-6	120	112	20
0	-16	34	40	18*	2	-2	183	164	4	5	-5	0	39	29*
0	-14	176	159	5	2	-1	511	510	8	5	-4	204	214	9
0	-12	282	340	10	2	0	885	874	13	5	-3	182	175	5
0	-10	236	226	9	2	1	68	71	4	5	-2	23	52	17*
0	-8	974	922	24	2	2	602	628	11	5	-1	140	141	10
0	-6	1047	1002	17	2	3	381	392	9	5	0	203	200	4
0	-4	2314	2161	35	3	-15	33	31	27*	5	1	30	80	17*
0	-2	142	139	3	3	-14	111	105	13	5	2	150	140	8
0	2	698	641	11	3	-13	55	49	20*	5	3	77	83	4
0	4	435	408	9	3	-12	301	294	10	5	9	119	124	5
0	6	299	266	9	3	-11	95	125	11	6	-9	75	65	12
0	8	254	200	14	3	-10	310	331	15	6	-8	0	19	19*
0	10	87	52	15	3	-9	75	71	4	6	-7	41	46	24*
0	12	146	145	4	3	-8	220	222	5	6	-6	0	24	18*
0	14	101	142	6	3	-7	64	73	9	6	-5	68	87	10
0	16	72	78	7	3	-6	52	94	15*	6	-4	175	182	14
1	-16	154	147	9	3	-5	320	301	10	6	-3	67	74	17
1	-15	64	67	9	3	-4	0	18	22*	6	-2	30	21	27*
1	-14	19	11	19*	3	-3	11	9	12*	6	-1	69	82	6
1	-13	3	30	20*	3	-2	193	208	5	6	0	283	279	6
1	-12	394	398	8	3	-1	381	362	12	6	1	146	154	8
1	-11	40	22	13*	3	0	108	119	4	6	2	149	146	4
1	-10	366	390	12	3	1	76	73	3	6	3	265	264	7
1	-9	179	182	7	3	2	117	131	3	7	-6	191	190	11
1	-8	160	133	4	3	3	692	706	17	7	-5	72	60	33*

Table A-6 (con't)

k	l	Fo	Fc	sigF	k	l	Fo	Fc	sigF	k	l	Fo	Fc	sigF
7	-4	0	11	19*	-2	10	362	368	7	1	0	1612	1601	24
7	-3	69	74	31*	-2	11	35	3	18*	1	1	103	99	3
7	-2	0	25	22*	-2	12	120	132	9	1	2	1082	1089	37
7	-1	147	142	6	-2	13	31	30	20*	1	3	167	168	4
7	0	191	184	5	-2	14	225	214	9	2	-15	42	11	29*
7	1	195	209	16	-2	15	45	49	26*	2	-14	53	57	31*
7	2	99	96	15	-1	4	422	444	9	2	-13	109	116	10
7	3	98	111	36*	-1	5	559	539	11	2	-12	259	257	6
^^^^^^	h =	2	^^^^^^		-1	6	39	33	17*	2	-11	147	146	6
					-1	7	511	492	12	2	-10	75	74	19*
					-1	8	423	439	12	2	-9	124	121	4
-6	-9	0	32	20*	-1	9	109	111	3	2	-8	151	151	4
-6	-8	151	143	5	-1	10	349	384	7	2	-7	194	184	7
-6	-1	116	118	4	-1	11	49	41	7	2	-6	463	474	11
-6	8	162	156	4	-1	12	0	10	37*	2	-5	119	113	6
-6	9	63	44	7	-1	13	123	134	28	2	-4	32	39	21*
-5	8	131	166	14	-1	14	78	66	6	2	-3	0	8	19*
-5	9	179	186	10	-1	15	94	118	8	2	-2	1105	1141	17
-5	10	76	57	6	0	-16	125	113	4	2	-1	421	402	7
-5	11	55	59	22*	0	-14	58	48	10	2	0	364	354	7
-4	-2	46	30	5	0	-12	424	427	8	2	1	48	26	14*
-4	-1	154	169	4	0	-10	313	316	7	2	2	528	552	8
-4	0	199	181	8	0	-8	38	40	12*	2	3	268	260	9
-4	5	278	251	11	0	-6	468	422	10	3	-15	29	33	19*
-4	6	0	3	26*	0	-4	143	142	6	3	-14	54	61	8
-4	8	286	291	9	0	-2	423	463	7	3	-13	5	89	33*
-4	9	0	28	26*	0	0	349	322	5	3	-12	73	69	6
-4	10	117	115	7	0	2	501	528	8	3	-11	86	99	7
-4	11	36	23	19*	0	4	385	378	9	3	-10	78	75	9
-4	12	199	194	5	0	6	97	106	6	3	-9	161	159	4
-4	13	0	2	20*	0	8	609	613	13	3	-8	68	54	5
-3	-13	92	89	6	0	10	119	107	4	3	-7	192	188	8
-3	4	394	421	10	0	12	178	187	5	3	-6	313	351	10
-3	5	0	15	23*	0	14	334	319	8	3	-5	391	353	10
-3	6	63	84	16*	1	-16	95	120	7	3	-4	110	146	6
-3	7	504	545	12	1	-15	64	70	19*	3	-3	222	219	5
-3	8	114	133	4	1	-14	102	105	4	3	-2	87	25	3
-3	9	190	196	5	1	-13	38	73	22*	3	-1	87	71	13
-3	10	297	330	7	1	-12	69	71	9	3	0	4	19	11*
-3	11	193	198	5	1	-11	0	8	17*	3	1	104	103	3
-3	12	119	148	21	1	-10	173	157	4	3	2	436	431	7
-3	13	38	84	32*	1	-9	94	81	28*	3	3	521	528	23
-3	14	147	148	15	1	-8	166	130	5	3	13	98	84	5
-2	-15	20	11	19*	1	-7	618	613	12	4	-13	56	77	26*
-2	4	614	618	12	1	-6	333	328	9	4	-12	231	225	8
-2	5	82	90	7	1	-5	297	268	8	4	-11	43	33	15*
-2	6	149	149	6	1	-4	743	728	13	4	-10	55	45	20*
-2	7	165	156	8	1	-3	265	272	5	4	-9	172	176	16
-2	8	256	284	6	1	-2	774	773	16	4	-8	140	146	4
-2	9	64	57	5	1	-1	164	172	5	4	-7	59	53	5

Table A-6 (con't)

k	l	Fo	Fc	sigF	k	l	Fo	Fc	sigF	k	l	Fo	Fc	sigF
4	-6	40	50	24*	6	7	64	71	6	0	-14	26	25	27*
4	-5	0	37	24*	7	-6	46	32	14*	0	-12	70	81	10
4	-4	45	46	6	7	-5	0	25	24*	0	-10	93	54	7
4	-3	19	10	12*	7	-4	205	184	13	0	-8	25	3	15*
4	-2	0	30	24*	7	-3	332	323	37	0	-6	1124	1028	18
4	-1	160	169	8	7	-2	183	191	15	0	-4	343	333	8
4	0	190	181	4	7	-1	260	259	14	0	-2	1767	1754	27
4	1	272	263	6	7	0	125	130	4	0	0	236	213	4
4	2	76	75	4	7	1	21	1	19*	0	2	246	223	35
4	3	137	138	4	7	2	110	100	5	0	4	879	890	15
4	4	66	66	4	7	3	103	105	14	0	6	39	41	20*
4	6	0	3	18*	7	4	58	43	15*	0	8	374	376	7
4	7	74	57	5	7	5	83	80	12	0	10	197	183	13
5	-12	0	7	26*						0	12	0	72	20*
5	-11	43	47	17*	^^^^^^	h = 3	^^^^^^			0	14	31	31	21*
5	-10	0	66	23*						1	-16	36	28	21*
5	-9	81	73	29*	-6	-8	59	87	7	1	-15	28	61	29*
5	-8	245	250	6	-5	-11	121	139	5	1	-14	101	110	20
5	-7	0	12	27*	-5	-8	120	122	5	1	-13	100	82	13
5	-6	107	114	5	-4	-12	29	30	21*	1	-12	247	276	15
5	-5	193	180	7	-4	-9	104	106	4	1	-11	61	54	11
5	-4	218	225	5	-4	5	0	11	22*	1	-10	263	284	6
5	-3	29	35	22*	-4	12	0	15	41*	1	-9	21	1	19*
5	-2	81	75	10	-4	13	33	38	28*	1	-8	435	432	8
5	-1	138	134	6	-3	4	401	446	11	1	-7	130	116	6
5	0	42	56	11	-3	5	441	428	11	1	-6	139	172	7
5	1	18	18	15*	-3	6	168	174	8	1	-5	92	101	5
5	2	281	289	18	-3	7	49	10	17*	1	-4	856	881	14
5	3	86	98	13	-3	12	160	182	10	1	-3	304	304	5
5	4	22	6	22*	-3	13	66	68	7	1	-2	2002	1976	30
5	5	124	135	9	-3	14	0	14	36*	1	-1	213	216	4
5	6	246	255	6	-2	-13	184	204	5	1	0	104	94	3
5	7	19	38	19*	-2	4	324	319	9	1	1	600	610	10
6	-10	0	14	28*	-2	5	205	198	9	1	2	2626	2523	62
6	-9	75	32	19*	-2	6	520	489	12	1	3	547	542	9
6	-8	110	143	11	-2	7	168	189	8	1	8	118	109	3
6	-7	0	16	31*	-2	12	32	9	34*	1	9	0	64	21*
6	-6	60	54	6	-2	13	62	67	18*	1	10	108	67	15
6	-5	176	175	5	-2	14	39	10	19*	1	11	97	96	20
6	-4	51	20	16*	-2	15	54	49	7	2	-15	95	102	26*
6	-3	62	55	12	-1	-15	49	61	9	2	-14	244	232	18
6	-2	228	224	9	-1	4	367	384	9	2	-13	195	204	9
6	-1	106	118	9	-1	5	180	191	9	2	-12	204	198	5
6	0	63	72	12	-1	6	185	112	9	2	-11	172	163	4
6	1	65	59	24*	-1	7	148	164	7	2	-10	283	301	11
6	2	353	348	13	-1	12	459	450	9	2	-9	38	38	12*
6	3	156	165	9	-1	13	0	15	21*	2	-8	266	260	7
6	4	7	10	15*	-1	14	27	33	34*	2	-7	112	113	6
6	5	0	5	21*	-1	15	0	3	24*	2	-6	171	182	7
6	6	0	4	20*	0	-16	150	150	4	2	-5	0	62	23*

Table A-6 (con't)

k	l	Fo	Fc	sigF	k	l	Fo	Fc	sigF	k	l	Fo	Fc	sigF
2	-4	91	78	5	4	2	0	18	15*	6	8	28	5	17*
2	-3	380	379	6	4	3	28	14	20*	6	9	34	33	19*
2	-2	396	426	7	4	4	145	145	4	7	-5	81	81	6
2	-1	144	157	6	4	6	340	340	7	7	-4	39	48	19*
2	0	47	39	6	4	7	124	113	4	7	-3	0	20	30*
2	1	149	153	5	4	8	123	124	5	7	-2	89	96	31*
2	2	302	311	5	4	9	0	28	23*	7	-1	126	131	10
2	3	72	71	3	4	10	290	296	7	7	0	0	12	16*
2	8	351	349	10	4	11	95	84	5	7	1	0	15	19*
2	9	93	87	7	5	-12	186	204	5	7	2	99	85	4
2	10	99	90	4	5	-11	86	139	22*	7	3	135	140	4
2	11	0	21	18*	5	-10	98	79	15	7	4	36	46	27*
3	-15	30	36	26*	5	-9	108	117	5	7	5	0	29	28*
3	-14	0	32	20*	5	-8	103	122	10					
3	-13	209	203	9	5	-7	69	83	9	^^^^^^	h =	4	^^^^^^	
3	-12	152	155	8	5	-6	42	34	11*					
3	-11	68	71	6	5	-5	56	68	26*	-7	-4	140	144	5
3	-10	46	57	11	5	-4	201	209	6	-7	-1	112	103	5
3	-9	325	319	7	5	-3	23	20	20*	-7	0	135	143	11
3	-8	239	245	6	5	-2	89	89	21	-6	-9	19	37	20*
3	-7	298	285	11	5	-1	152	157	10	-6	-7	97	97	5
3	-6	96	124	7	5	0	141	142	5	-6	-5	32	62	20*
3	-5	164	157	7	5	1	26	26	17*	-6	-3	118	114	5
3	-4	152	166	8	5	2	113	110	4	-6	0	68	84	6
3	-3	144	145	4	5	3	132	125	4	-5	-11	93	101	5
3	-2	621	611	10	5	4	35	20	24*	-5	-10	131	134	5
3	-1	65	73	3	5	5	77	75	5	-5	-9	179	174	5
3	0	125	114	3	5	6	111	105	4	-5	-6	71	84	5
3	1	251	246	11	5	7	41	34	19*	-5	-3	100	105	4
3	2	395	404	8	5	8	40	60	12*	-5	-2	120	129	4
3	3	157	161	4	5	9	0	39	20*	-4	-8	98	100	5
3	8	91	140	13	5	10	55	79	23*	-4	-6	139	145	4
3	9	36	10	18*	5	11	93	96	20	-4	-4	66	89	5
3	10	144	155	7	6	-9	108	124	18	-4	1	53	42	19*
3	11	32	40	12*	6	-8	0	87	28*	-4	3	147	145	7
4	-13	30	39	19*	6	-7	0	22	18*	-3	-15	56	33	7
4	-12	51	30	32*	6	-6	141	140	9	-3	-11	38	45	21*
4	-11	37	31	33*	6	-5	0	9	40*	-3	4	242	268	10
4	-10	50	61	15*	6	-4	186	184	4	-3	5	217	170	10
4	-9	96	106	9	6	-3	55	44	9	-3	6	22	57	26*
4	-8	242	256	5	6	-2	0	16	33*	-3	7	138	148	7
4	-7	127	147	10	6	-1	118	129	21	-2	4	216	226	10
4	-6	264	279	11	6	0	149	147	3	-2	5	157	134	8
4	-5	39	17	23*	6	1	82	96	12	-2	6	164	124	8
4	-4	19	17	14*	6	2	228	221	8	-2	7	46	33	22*
4	-3	300	289	6	6	3	165	175	4	-1	4	376	402	9
4	-2	297	315	12	6	4	260	257	9	-1	5	147	121	7
4	-1	134	149	5	6	5	34	47	17*	-1	6	341	298	10
4	0	141	135	3	6	6	56	19	23*	-1	7	0	66	23*
4	1	30	42	7	6	7	78	85	8	-1	15	64	66	37*

Table A-6 (con't)

k	l	Fo	Fc	sigF	k	l	Fo	Fc	sigF	k	l	Fo	Fc	sigF
0	-16	36	66	29*	2	-8	260	251	6	4	-8	91	100	11
0	-14	332	353	8	2	-7	78	80	8	4	-7	0	41	18*
0	-12	146	132	7	2	-6	40	57	18*	4	-6	140	145	6
0	-10	295	277	7	2	-5	104	104	6	4	-5	76	77	9
0	-8	473	480	8	2	-4	163	202	6	4	-4	0	89	27*
0	-6	351	338	10	2	-3	58	52	3	4	-3	118	99	3
0	-4	569	618	11	2	-2	214	235	5	4	-2	286	264	6
0	-2	1175	1203	18	2	-1	564	584	9	4	-1	295	305	6
0	0	1365	1348	21	2	0	178	179	6	4	0	87	87	3
0	2	1296	1311	20	2	1	351	350	6	4	1	42	42	15*
0	4	227	208	8	2	2	63	69	5	4	2	489	484	15
0	6	495	527	11	2	3	57	58	7	4	3	151	145	4
0	8	107	127	8	2	8	113	130	11	4	4	141	148	5
0	10	140	159	5	2	9	172	179	9	4	5	17	13	17*
0	12	239	229	6	2	10	241	245	5	4	6	276	290	7
0	14	59	63	8	2	11	62	50	7	4	7	54	67	9
1	-16	108	102	21	2	12	227	245	6	4	8	76	81	32*
1	-15	35	45	37*	2	13	136	142	5	4	9	0	23	27*
1	-14	17	37	42*	2	14	55	29	19*	4	10	108	116	8
1	-13	69	94	9	3	-15	0	33	30*	4	11	32	22	21*
1	-12	175	172	5	3	-14	45	52	17*	4	12	28	72	26*
1	-11	29	22	16*	3	-13	121	128	5	5	-12	137	141	11
1	-10	314	336	7	3	-12	234	238	6	5	-11	55	101	27*
1	-9	123	125	6	3	-11	0	45	27*	5	-10	74	134	32*
1	-8	310	265	6	3	-10	229	211	18	5	-9	173	174	8
1	-7	134	142	6	3	-9	182	180	5	5	-8	199	186	7
1	-6	449	426	10	3	-8	43	40	16*	5	-7	63	54	6
1	-5	0	42	20*	3	-7	130	124	7	5	-6	53	84	27*
1	-4	0	50	20*	3	-6	285	281	11	5	-5	40	31	12*
1	-3	350	349	6	3	-5	139	127	6	5	-4	88	81	13
1	-2	1127	1121	17	3	-4	238	228	10	5	-3	98	105	8
1	-1	109	104	3	3	-3	0	29	15*	5	-2	111	129	7
1	0	1066	1083	16	3	-2	26	36	26*	5	-1	14	16	15*
1	1	729	742	11	3	-1	414	398	19	5	0	157	157	3
1	2	199	188	5	3	0	268	279	5	5	1	105	114	4
1	3	671	660	10	3	1	241	235	6	5	2	306	309	7
1	8	197	192	5	3	2	395	396	8	5	3	0	24	21*
1	9	63	58	17*	3	3	36	18	9*	5	4	9	21	18*
1	10	155	143	15	3	8	116	124	4	5	5	141	141	4
1	11	46	66	18*	3	9	194	194	5	5	6	128	123	4
1	12	69	68	8	3	10	134	116	15	5	7	117	100	9
1	13	114	140	6	3	11	15	13	23*	5	8	60	56	6
1	14	96	91	5	3	12	36	70	21*	5	9	123	146	16
2	-15	15	30	18*	3	13	36	53	30*	5	10	202	186	15
2	-14	175	181	9	3	14	63	67	20*	5	11	0	20	22*
2	-13	53	50	14*	4	-13	0	2	31*	6	-9	0	37	28*
2	-12	211	205	5	4	-12	83	97	11	6	-8	158	152	5
2	-11	0	6	25*	4	-11	117	125	10	6	-7	61	97	32*
2	-10	291	277	12	4	-10	296	273	14	6	-6	0	62	25*
2	-9	49	46	5	4	-9	100	111	7	6	-5	59	62	22*

Table A-6 (con't)

k	l	Fo	Fc	sigF	k	l	Fo	Fc	sigF	k	l	Fo	Fc	sigF
6	-4	167	169	4	-2	7	116	156	8	2	-15	113	120	4
6	-3	109	114	10	-2	14	94	88	10	2	-14	159	178	9
6	-2	36	8	22*	-1	-9	162	163	4	2	-13	101	108	7
6	-1	62	55	7	-1	4	167	175	7	2	-12	70	80	6
6	0	78	84	7	-1	5	168	186	8	2	-11	37	7	19*
6	1	167	169	10	-1	6	328	351	11	2	-10	133	137	7
6	2	95	97	5	-1	7	26	6	24*	2	-9	89	64	10
6	3	130	148	5	0	-16	48	45	37*	2	-8	30	16	17*
6	4	40	46	26*	0	-14	111	129	5	2	-7	41	57	24*
6	5	103	109	9	0	-12	115	108	31*	2	-6	0	62	22*
6	6	78	60	5	0	-10	0	42	16*	2	-5	205	192	9
6	7	102	85	13	0	-8	201	205	5	2	-4	84	134	6
6	8	5	39	21*	0	-6	541	531	11	2	-3	209	220	9
7	-5	156	159	18	0	-4	222	216	8	2	-2	388	398	7
7	-4	130	144	9	0	-2	1082	1112	16	2	-1	242	227	6
7	-3	0	3	18*	0	0	1014	1026	15	2	0	597	559	9
7	-2	250	239	10	0	2	236	223	5	2	1	214	216	5
7	-1	112	103	8	0	4	484	499	11	2	2	206	195	5
7	0	122	143	9	0	6	213	247	10	2	3	156	139	7
7	1	34	25	22*	0	8	141	126	4	2	8	298	329	17
7	2	200	193	14	0	10	83	80	5	2	9	303	318	7
7	3	0	4	25*	0	12	262	249	14	2	10	0	26	24*
7	4	121	113	4	0	14	85	55	6	2	11	94	97	5
1	-16				1	-16	40	52	23*	2	12	372	373	8
1	-15				1	-15	0	30	26*	2	13	0	13	32*
1	-14				1	-14	251	245	6	2	14	111	88	5
1	-13				1	-13	20	12	28*	3	-15	73	83	16
1	-12				1	-12	93	79	5	3	-14	220	204	6
1	-11				1	-11	25	38	31*	3	-13	0	21	23*
1	-10				1	-10	341	342	7	3	-12	0	2	29*
1	-9				1	-9	155	163	7	3	-11	373	344	8
1	-8				1	-8	141	114	4	3	-10	265	259	7
1	-7				1	-7	100	89	6	3	-9	203	213	5
1	-6				1	-6	32	44	20*	3	-8	20	12	19*
1	-5				1	-5	295	290	9	3	-7	34	69	27*
1	-4				1	-4	37	37	13*	3	-6	37	29	22*
1	-3				1	-3	181	174	4	3	-5	362	364	11
1	-2				1	-2	426	415	7	3	-4	216	224	10
1	-1				1	-1	1353	1361	20	3	-3	356	340	7
1	0				1	0	870	886	13	3	-2	219	264	17
1	1				1	1	1205	1210	22	3	-1	200	176	5
1	2				1	2	513	511	8	3	0	291	283	5
1	3				1	3	22	31	12*	3	1	153	158	5
1	4				1	4	23	62	17*	3	2	0	43	15*
1	5				1	5	183	212	5	3	3	351	354	7
1	6				1	6	180	195	5	3	4	15	22	17*
1	7				1	7	192	186	8	3	5	90	108	9
1	8				1	8	209	207	11	3	6	82	76	5
1	9				1	9	77	92	6	3	7	242	247	6
1	10				1	10	65	76	20*	3	8	103	84	17
1	11				1	11				3	9			
1	12				1	12				3	10			
1	13				1	13				3	11			
1	14				1	14				3	12			

***** h = 5 *****

Table A-6 (con't)

k	l	Fo	Fc	sigF	k	l	Fo	Fc	sigF	k	l	Fo	Fc	sigF
3	12	148	154	5	5	10	245	237	7	-4	-2	112	110	4
3	13	0	36	25*	6	-9	0	24	27*	-4	1	105	99	7
4	-13	24	24	18*	6	-8	136	132	11	-4	7	44	48	27*
4	-12	64	60	6	6	-7	32	62	18*	-3	-8	67	66	5
4	-11	35	73	18*	6	-6	49	57	18*	-3	4	262	256	11
4	-10	0	44	32*	6	-5	35	31	11*	-3	5	150	160	7
4	-9	164	188	8	6	-4	135	153	6	-3	6	0	31	26*
4	-8	160	145	16	6	-3	108	109	10	-2	-10	279	283	7
4	-7	155	151	4	6	-2	78	86	5	-2	1	340	328	9
4	-6	393	373	21	6	-1	59	41	6	-2	4	817	852	15
4	-5	130	121	6	6	0	51	67	21*	-2	5	347	317	11
4	-4	213	251	6	6	1	337	347	7	-2	6	55	51	19*
4	-3	216	191	5	6	2	44	35	10*	-2	7	230	225	12
4	-2	194	191	9	6	3	193	201	13	-1	-16	80	53	6
4	-1	80	58	9	6	4	214	193	9	-1	-13	48	58	9
4	0	336	290	8	6	5	120	127	6	-1	1	27	9	21*
4	1	176	169	6	6	6	109	113	5	-1	3	37	59	21*
4	2	91	122	7	6	7	57	57	8	-1	4	34	11	19*
4	3	92	86	10	6	8	150	146	4	-1	5	209	216	11
4	4	219	216	5	7	-5	91	104	5	-1	6	36	25	24*
4	5	204	201	5	7	-4	31	38	26*	-1	7	0	61	26*
4	6	90	84	5	7	-3	60	47	6	-1	8	108	105	8
4	7	0	26	24*	7	-2	16	17	25*	0	-16	129	123	4
4	8	87	105	19	7	-1	36	76	32*	0	-14	132	128	22
4	9	35	18	19*	7	0	93	87	11	0	-12	33	50	19*
4	10	97	102	18	7	1	0	28	23*	0	-10	277	266	7
4	11	43	58	16*	7	2	44	50	17*	0	-8	718	666	25
4	12	19	11	19*	7	3	40	40	19*	0	-6	755	734	14
5	-12	38	29	13*						0	-4	450	453	10
5	-11	72	73	10	^^^^^^	h =	6	^^^^^^		0	-2	694	691	11
5	-10	62	66	24*						0	0	134	134	3
5	-9	39	41	31*	-7	-3	66	79	6	0	2	128	141	5
5	-8	73	91	39*	-7	1	26	69	29*	0	4	149	142	7
5	-7	0	39	21*	-7	2	42	32	29*	0	6	56	97	20*
5	-6	32	21	17*	-6	-8	162	150	5	0	8	103	85	33*
5	-5	0	8	18*	-6	-6	0	26	21*	0	10	0	15	20*
5	-4	227	243	10	-6	0	483	472	9	0	12	127	151	35*
5	-3	23	26	26*	-6	3	0	21	30*	0	14	341	337	8
5	-2	84	87	4	-6	4	137	153	8	1	-16	65	53	17*
5	-1	0	9	15*	-6	6	0	52	28*	1	-15	0	25	29*
5	0	98	99	3	-6	7	59	9	23*	1	-14	253	257	6
5	1	86	105	31*	-5	-9	0	65	17*	1	-13	60	58	22*
5	2	184	186	5	-5	-2	150	140	4	1	-12	146	140	5
5	3	272	277	11	-5	3	77	77	21*	1	-11	49	34	7
5	4	166	167	5	-5	5	85	94	11	1	-10	28	24	18*
5	5	252	246	7	-4	-12	39	45	10*	1	-9	157	147	4
5	6	197	184	8	-4	-10	374	358	9	1	-8	219	188	6
5	7	68	64	13	-4	-7	107	107	4	1	-7	89	83	7
5	8	23	36	19*	-4	-6	120	113	4	1	-6	57	44	8
5	9	47	42	9	-4	-3	153	155	4	1	-5	314	315	9

Table A-6 (con't)

k	l	Fo	Fc	sigF	k	l	Fo	Fc	sigF	k	l	Fo	Fc	sigF
1	-4	37	36	16*	3	-5	45	30	21*	5	-3	0	15	17*
1	-3	665	647	14	3	-4	384	400	13	5	-2	138	140	7
1	-2	617	619	10	3	-3	50	56	5	5	-1	82	74	13
1	-1	331	323	7	3	-2	114	112	3	5	0	0	28	17*
1	0	867	849	13	3	-1	121	108	8	5	1	24	29	17*
1	1	26	9	14*	3	0	27	12	11*	5	2	154	150	4
1	2	93	106	3	3	1	156	169	6	5	3	69	77	6
1	3	49	59	4	3	2	40	48	8	5	4	171	169	4
1	8	115	105	4	3	3	50	57	5	5	5	99	94	5
1	9	42	22	15*	3	7	31	8	17*	5	6	290	310	18
1	10	272	264	7	3	8	287	293	8	5	7	0	8	20*
1	11	44	38	23*	3	9	123	114	6	5	8	0	21	30*
1	12	84	62	26*	3	10	196	203	5	5	9	0	15	26*
1	13	0	25	19*	3	11	71	72	9	5	10	0	20	23*
1	14	0	14	20*	3	12	131	127	4	6	-9	67	69	18*
2	-15	27	5	14*	3	13	0	25	19*	6	-8	140	150	9
2	-14	28	9	19*	4	-13	58	46	7	6	-7	167	182	11
2	-13	76	61	9	4	-12	64	45	27*	6	-6	64	26	27*
2	-12	0	9	41*	4	-11	34	24	27*	6	-5	112	104	20
2	-11	73	67	5	4	-10	365	358	13	6	-4	0	17	22*
2	-10	288	283	12	4	-9	160	168	9	6	-3	219	229	22
2	-9	107	109	5	4	-8	155	145	9	6	-2	52	60	10
2	-8	61	76	4	4	-7	95	107	10	6	-1	80	88	10
2	-7	196	174	8	4	-6	116	113	7	6	0	453	472	12
2	-6	415	403	11	4	-5	111	93	6	6	1	201	190	10
2	-5	72	68	7	4	-4	0	32	24*	6	2	188	176	6
2	-4	143	151	7	4	-3	134	155	7	6	3	45	21	16*
2	-3	212	208	5	4	-2	118	110	6	6	4	174	153	5
2	-2	620	632	10	4	-1	98	88	14	6	5	26	40	18*
2	-1	191	212	5	4	0	235	246	5	6	6	35	52	12*
2	0	1069	1074	16	4	1	109	99	4	6	7	25	9	18*
2	1	315	328	6	4	2	134	132	3	7	-4	126	130	5
2	2	318	298	6	4	3	8	5	16*	7	-3	54	79	30*
2	3	139	144	5	4	4	87	84	5	7	-2	34	26	20*
2	8	30	57	15*	4	5	23	25	17*	7	-1	20	23	18*
2	9	31	16	21*	4	6	10	8	27*	7	0	0	8	18*
2	10	51	41	15*	4	7	29	48	20*	7	1	81	69	5
2	11	134	158	24	4	8	21	16	18*	7	2	0	32	18*
2	12	51	41	35*	4	9	39	33	10					
2	13	38	15	19*	4	10	140	148	12	^^^^^^	h =	7	^^^^^^	
2	14	16	12	19*	4	11	10	25	18*					
3	-14	135	123	8	4	12	96	93	5	-7	-1	59	58	6
3	-13	253	263	20	5	-11	23	22	29*	-7	1	0	29	30*
3	-12	160	163	8	5	-10	23	28	19*	-6	-8	133	134	5
3	-11	272	286	11	5	-9	39	65	31*	-6	-7	165	175	5
3	-10	50	53	16*	5	-8	206	194	15	-6	-6	43	39	8
3	-9	0	30	18*	5	-7	89	93	6	-6	-5	42	35	18*
3	-8	0	66	27*	5	-6	62	65	6	-6	-1	166	159	4
3	-7	66	81	9	5	-5	145	152	4	-6	2	0	86	31*
3	-6	98	108	7	5	-4	149	152	14	-6	4	62	33	33*

Table A-6 (con't)

k	l	Fo	Fc	sigF	k	l	Fo	Fc	sigF	k	l	Fo	Fc	sigF
-5	-8	153	144	5	1	-12	299	293	13	3	-13	23	16	20*
-5	-7	0	13	20*	1	-11	75	57	11	3	-12	154	141	13
-5	-4	78	81	5	1	-10	86	75	6	3	-11	40	1	16*
-5	0	31	9	31*	1	-9	110	108	4	3	-10	238	220	9
-4	-13	18	31	15*	1	-8	49	38	5	3	-9	78	69	10
-4	-7	94	107	5	1	-7	151	135	7	3	-8	333	333	12
-4	-3	41	48	6	1	-6	399	445	11	3	-7	172	171	9
-4	0	267	263	6	1	-5	88	74	6	3	-6	66	91	10
-4	1	101	119	n	1	-4	32	2	20*	3	-5	137	127	6
-4	5	40	29	29*	1	-3	122	118	3	3	-4	88	82	4
-3	-9	72	69	6	1	-2	80	78	6	3	-3	335	322	16
-3	-8	360	333	8	1	-1	96	103	3	3	-2	33	34	24*
-3	1	236	268	11	1	0	316	321	5	3	-1	59	77	27*
-3	2	149	157	7	1	1	91	79	6	3	0	297	275	6
-3	4	402	416	12	1	2	124	108	3	3	1	234	268	6
-3	5	166	156	7	1	3	68	66	4	3	2	157	157	4
-2	-15	49	62	9	1	8	113	109	5	3	3	173	171	4
-2	-12	141	146	5	1	9	26	38	26*	3	6	206	181	5
-2	2	278	265	10	1	10	213	212	9	3	7	115	111	23
-2	4	359	382	11	1	11	2	46	20*	3	8	219	247	9
-2	5	46	54	25*	1	12	109	89	6	3	9	0	3	34*
-2	6	109	99	8	1	13	87	76	8	3	10	101	112	14
-2	8	130	137	9	1	14	242	224	8	3	11	33	46	12*
-1	-13	124	120	5	2	-15	48	62	26*	3	12	111	124	24
-1	-11	66	57	6	2	-14	241	237	7	4	-13	34	31	24*
-1	2	115	108	6	2	-13	129	133	4	4	-12	72	69	15
-1	4	0	34	22*	2	-12	146	146	8	4	-11	0	33	22*
-1	5	129	117	6	2	-11	0	18	18*	4	-10	41	30	18*
-1	6	230	219	12	2	-10	280	265	13	4	-9	45	39	43*
-1	7	108	93	8	2	-9	17	8	16*	4	-8	89	87	16
0	-16	97	128	5	2	-8	324	324	21	4	-7	90	107	9
0	-14	70	74	13	2	-7	113	92	7	4	-6	20	10	22*
0	-12	142	112	10	2	-6	378	359	11	4	-5	139	113	9
0	-10	303	312	13	2	-5	143	157	7	4	-4	208	223	8
0	-8	416	402	11	2	-4	82	112	6	4	-3	5	48	23*
0	-6	46	33	10	2	-3	42	62	5	4	-2	101	116	5
0	-4	126	125	6	2	-2	325	305	6	4	-1	34	56	23*
0	-2	408	438	7	2	-1	186	200	10	4	0	255	263	12
0	0	1004	1017	15	2	0	298	326	8	4	1	111	119	4
0	2	50	78	14*	2	1	218	203	16	4	2	271	265	11
0	4	195	209	10	2	2	292	265	6	4	3	0	36	18*
0	6	117	142	7	2	3	414	390	16	4	4	162	138	5
0	8	190	155	15	2	7	237	231	5	4	5	41	29	16*
0	10	190	186	5	2	8	130	137	4	4	6	258	256	6
0	12	10	38	30*	2	9	174	167	11	4	7	51	69	16*
0	14	140	146	5	2	10	0	33	37*	4	8	109	101	8
1	-16	0	70	34*	2	11	35	26	18*	4	9	35	18	28*
1	-15	0	0	30*	2	12	33	79	23*	4	10	82	82	6
1	-14	101	98	8	2	13	40	52	22*	4	11	47	80	27*
1	-13	103	120	10	3	-14	108	95	17	5	-11	0	21	32*

Table A-6 (con't)

k	l	Fo	Fc	sigF	k	l	Fo	Fc	sigF	k	l	Fo	Fc	sigF
2	11	83	64	6	4	8	214	202	11	-5	-8	125	114	5
2	12	238	236	6	4	9	96	83	17	-5	-2	181	171	5
2	13	101	115	5	4	10	40	24	18*	-5	-1	81	88	5
3	-14	99	107	13	4	11	43	49	13*	-5	3	65	13	27*
3	-13	149	126	12	5	-11	0	7	22*	-5	5	0	39	28*
3	-12	197	182	10	5	-10	105	86	18	-4	-9	243	252	6
3	-11	53	77	22*	5	-9	0	53	32*	-4	-8	64	48	6
3	-10	47	13	14*	5	-8	44	33	29*	-4	4	89	73	23*
3	-9	81	84	42*	5	-7	59	73	22*	-4	6	131	132	8
3	-8	72	96	23*	5	-6	178	168	10	-4	8	194	208	8
3	-7	34	11	22*	5	-5	44	15	24*	-3	-14	76	71	5
3	-6	178	154	9	5	-4	168	170	8	-3	-11	103	86	5
3	-5	59	71	26*	5	-3	57	23	21*	-3	-9	60	62	7
3	-4	314	315	7	5	-2	33	79	18*	-3	-7	118	130	4
3	-3	242	230	9	5	-1	162	168	18	-3	-6	199	175	5
3	-2	0	9	23*	5	0	168	172	8	-3	-1	33	32	16*
3	-1	261	261	6	5	1	102	100	22	-3	0	350	341	7
3	0	353	346	6	5	2	80	42	34*	-3	2	294	290	12
3	1	70	64	6	5	3	332	340	8	-3	3	150	142	7
3	2	198	188	5	5	4	42	42	20*	-3	8	0	11	28*
3	3	148	138	4	5	5	164	166	10	-2	-15	147	137	4
3	5	40	29	14*	5	6	140	136	5	-2	-9	137	133	4
3	6	124	131	4	5	7	0	8	24*	-2	3	0	7	26*
3	7	38	53	13*	5	8	98	108	25*	-2	4	148	162	7
3	8	230	228	6	5	9	51	27	16*	-2	5	49	100	27*
3	9	45	34	20*	6	-8	60	65	18*	-1	-13	0	13	20*
3	10	97	96	11	6	-7	0	7	30*	-1	-8	249	224	7
3	11	26	10	18*	6	-6	64	56	28*	-1	4	188	194	9
3	12	42	20	19*	6	-5	144	154	9	-1	5	220	227	9
4	-13	70	99	10	6	-4	113	116	35*	-1	6	252	234	9
4	-12	119	122	10	6	-3	184	193	17	0	-14	78	57	17
4	-11	139	143	9	6	-2	76	79	19*	0	-12	280	269	31
4	-10	0	7	22*	6	-1	0	18	27*	0	-10	139	145	13
4	-9	85	59	12	6	0	49	38	16*	0	-8	110	118	4
4	-8	262	242	6	6	1	40	5	16*	0	-6	120	119	6
4	-7	0	68	26*	6	2	36	24	18*	0	-4	280	276	10
4	-6	34	27	22*	6	3	18	11	17*	0	-2	309	325	6
4	-5	204	207	8	6	4	85	88	6	0	0	145	157	5
4	-4	117	115	4	6	5	33	24	19*	0	2	0	35	24*
4	-3	41	52	12*	6	6	139	129	5	0	4	65	16	17*
4	-2	271	269	12						0	6	59	55	17*
4	-1	83	73	11	^^^^^^	h =	9	^^^^^^		0	8	58	26	18*
4	0	7	22	36*						0	10	219	214	6
4	1	159	146	6	-6	-7	31	73	17*	0	12	194	187	5
4	2	114	117	4	-6	-5	27	47	20*	1	-15	0	41	19*
4	3	0	17	28*	-6	-1	75	60	5	1	-14	106	101	10
4	4	273	256	7	-6	1	139	158	10	1	-13	0	13	28*
4	5	78	86	10	-6	2	77	101	20*	1	-12	179	179	23
4	6	111	100	4	-6	5	110	106	9	1	-11	31	39	23*
4	7	114	111	5	-5	-9	115	126	5	1	-10	41	42	17*

Table A-6 (con't)

k	l	Fo	Fc	sigF	k	l	Fo	Fc	sigF	k	l	Fo	Fc	sigF
1	-9	106	108	4	3	-10	31	73	19*	5	-5	198	207	5
1	-8	221	224	9	3	-9	49	62	21*	5	-4	134	123	30
1	-7	0	18	25*	3	-8	345	345	11	5	-3	205	225	11
1	-6	158	162	7	3	-7	112	130	8	5	-2	146	171	8
1	-5	20	97	26*	3	-6	178	175	9	5	-1	71	88	23*
1	-4	553	585	12	3	-5	61	54	27*	5	0	0	7	16*
1	-3	357	337	7	3	-4	309	312	20	5	1	235	229	6
1	-2	191	151	11	3	-3	0	18	25*	5	2	435	442	23
1	-1	377	349	12	3	-2	135	125	10	5	3	47	13	16*
1	0	259	245	5	3	-1	67	32	17*	5	4	171	175	8
1	1	195	198	5	3	0	339	341	7	5	5	41	39	19*
1	2	406	421	7	3	1	134	116	6	5	6	41	8	16*
1	3	51	68	10	3	2	296	290	7	5	7	24	63	21*
1	7	124	129	21	3	3	154	142	4	5	8	39	29	26*
1	8	160	160	7	3	4	43	48	15*	6	-7	35	73	32*
1	9	41	51	23*	3	5	102	95	19	6	-6	22	31	18*
1	10	0	24	23*	3	6	96	86	9	6	-5	43	47	29*
1	11	62	67	31*	3	7	132	132	4	6	-4	35	49	32*
1	12	0	60	22*	3	8	0	11	21*	6	-3	140	144	22
1	13	34	29	20*	3	9	118	134	5	6	-2	102	107	8
2	-15	118	137	10	3	10	0	5	19*	6	-1	69	60	21*
2	-14	0	8	19*	3	11	45	53	34*	6	0	61	56	5
2	-13	68	70	31*	4	-12	198	193	6	6	1	166	158	5
2	-12	109	98	9	4	-11	211	221	5	6	2	92	101	5
2	-11	182	145	9	4	-10	130	126	5	6	3	84	80	5
2	-10	69	68	29*	4	-9	256	252	13	6	4	114	104	4
2	-9	121	133	9	4	-8	40	48	31*	6	5	104	106	5
2	-8	108	101	8	4	-7	107	94	14	6	5	104	106	5
2	-7	93	111	8	4	-6	170	166	11	^^^^^^	h = 10	^^^^^^		
2	-6	0	36	25*	4	-5	69	64	5					
2	-5	57	59	9	4	-4	0	9	16*	-6	-6	126	121	4
2	-4	50	93	19*	4	-3	0	8	16*	-6	-4	3f	26	20*
2	-3	368	390	22	4	-2	46	42	9	-6	-2	0	30	20*
2	-2	487	487	16	4	-1	0	15	21*	-6	-1	6	43	21*
2	-1	683	646	11	4	0	112	114	6	-6	1	67	73	11
2	0	152	166	8	4	1	29	4	21*	-6	2	27	10	29*
2	1	519	514	9	4	2	35	15	24*	-5	-10	65	72	7
2	2	295	315	14	4	3	138	142	4	-5	-7	80	87	6
2	3	0	7	18*	4	4	85	73	5	-5	-6	159	156	5
2	6	38	38	23*	4	5	38	37	16*	-5	-5	42	4	15*
2	7	43	67	16*	4	6	136	132	5	-5	-1	0	7	20*
2	8	212	208	5	4	7	0	30	20*	-5	1	87	100	13
2	9	43	47	21*	4	8	196	208	5	-4	-5	0	9	17*
2	10	209	199	6	4	9	61	79	10	-4	-4	160	169	4
2	11	76	77	13	4	10	0	9	23*	-4	-3	160	156	5
2	12	82	94	12	5	-10	89	73	4	-4	-2	0	11	17*
3	-14	85	71	22*	5	-9	105	126	10	-4	1	110	122	8
3	-13	123	127	4	5	-8	121	114	9	-4	9	0	12	35*
3	-12	145	139	7	5	-7	0	21	31*	-3	-11	32	43	22*
3	-11	65	86	27*	5	-6	0	48	20*	-3	-10	28	72	22*

Table A-6 (con't)

k	l	Fo	Fc	sigF	k	l	Fo	Fc	sigF	k	l	Fo	Fc	sigF
-3	-7	136	120	4	1	12	153	135	4	3	10	0	3	19*
-3	0	50	44	12	2	-14	122	116	9	3	11	0	12	21*
-2	-14	122	116	5	2	-13	0	52	24*	4	-12	35	38	19*
-2	-10	338	320	8	2	-12	30	9	21*	4	-11	111	124	5
-2	-8	137	140	4	2	-11	155	156	15	4	-10	119	104	18
-2	-3	46	63	6	2	-10	300	320	14	4	-9	44	23	16*
-2	4	112	118	8	2	-9	0	8	21*	4	-8	164	153	6
-2	7	45	49	27*	2	-8	122	140	8	4	-7	36	40	26*
-1	-10	31	35	11*	2	-7	110	114	22	4	-6	61	55	10
-1	4	193	172	9	2	-6	177	190	9	4	-5	57	9	21*
-1	5	57	57	27*	2	-5	144	137	8	4	-4	125	169	8
0	-14	83	53	6	2	-4	67	92	17*	4	-3	127	156	8
0	-12	0	31	18*	2	-3	0	63	25*	4	-2	46	11	23*
0	-10	27	51	24*	2	-2	0	40	15*	4	-1	60	43	10
0	-8	310	282	17	2	-1	148	159	9	4	0	135	144	4
0	-6	405	382	12	2	0	187	182	4	4	1	112	122	4
0	-4	158	172	6	2	1	0	24	21*	4	2	17	15	25*
0	-2	58	52	4	2	2	442	445	20	4	3	28	47	30*
0	0	83	87	4	2	3	115	103	10	4	4	248	236	20
0	2	188	183	4	2	5	48	29	7	4	5	32	25	21*
0	4	29	11	23*	2	6	337	340	7	4	6	54	55	9
0	6	175	169	4	2	7	46	49	16*	4	7	37	16	21*
0	8	142	124	15	2	8	36	40	21*	4	8	66	51	12
0	10	24	24	31*	2	9	50	25	20*	4	9	0	12	20*
0	12	301	301	12	2	10	130	119	18	5	-10	34	72	25*
1	-15	89	89	25*	2	11	0	37	23*	5	-9	190	203	6
1	-14	94	117	10	2	12	91	86	5	5	-8	0	15	19*
1	-13	71	69	37*	3	-13	78	100	5	5	-7	73	87	25*
1	-12	273	263	7	3	-12	266	259	6	5	-6	145	156	9
1	-11	89	98	7	3	-11	60	43	22*	5	-5	0	4	28*
1	-10	48	35	24*	3	-10	73	72	24*	5	-4	0	32	18*
1	-9	51	70	12	3	-9	151	158	14	5	-3	0	27	18*
1	-8	493	479	19	3	-8	79	73	28*	5	-2	247	261	26
1	-7	59	21	17*	3	-7	107	120	8	5	-1	0	7	27*
1	-6	244	243	11	3	-6	176	185	11	5	0	202	203	11
1	-5	79	95	9	3	-5	229	230	18	5	1	116	100	5
1	-4	154	161	7	3	-4	264	272	16	5	2	96	105	34*
1	-3	0	40	15*	3	-3	70	71	7	5	3	58	58	9
1	-2	324	347	13	3	-2	86	98	12	5	4	199	192	5
1	-1	27	41	18*	3	-1	182	188	14	5	5	71	69	9
1	0	66	10	9	3	0	48	44	13*	5	6	0	21	19*
1	1	229	228	10	3	1	237	227	8	5	7	65	70	6
1	2	501	491	9	3	2	135	142	6	6	-6	106	121	10
1	3	127	123	5	3	3	120	133	19	6	-5	25	35	21*
1	6	40	85	15*	3	4	98	88	18	6	-4	35	26	25*
1	7	202	182	10	3	5	0	4	26*	6	-3	59	59	7
1	8	0	14	23*	3	6	130	139	9	6	-2	0	30	32*
1	9	22	50	20*	3	7	98	98	6	6	-1	77	43	20*
1	10	172	174	7	3	8	237	236	6	6	0	140	139	7
1	11	79	77	7	3	9	0	33	25*	6	1	74	73	6

Table A-6 (con't)

k	l	Fo	Fc	sigF	k	l	Fo	Fc	sigF	k	l	Fo	Fc	sigF
6	2	0	10	19*	0	8	134	141	29	2	7	45	40	14*
6	3	28	8	25*	0	10	206	193	5	2	8	33	19	19*
6	4	27	41	26*	0	12	63	70	8	2	9	0	24	33*
^^^^^^^^	h = 11	^^^^^^^^			1	-14	156	153	8	2	10	85	88	5
					1	-13	39	59	19*	2	11	0	28	21*
					1	-12	124	112	12	3	-13	0	21	31*
-6	-3	39	61	10*	1	-11	16	46	20*	3	-12	69	53	21*
-6	-2	161	143	4	1	-10	126	113	4	3	-11	160	174	9
-6	-1	14	13	17*	1	-9	61	58	7	3	-10	275	264	7
-5	-9	26	23	20*	1	-8	0	53	27*	3	-9	277	296	14
-5	-8	53	62	18*	1	-7	46	60	31*	3	-8	150	137	11
-5	-7	56	54	8	1	-6	192	209	9	3	-7	89	108	9
-5	-4	186	189	5	1	-5	134	149	7	3	-6	82	94	13
-5	-2	42	64	19*	1	-4	190	188	8	3	-5	111	129	8
-5	0	0	28	25*	1	-3	54	51	14*	3	-4	71	79	8
-5	2	45	17	29*	1	-2	0	54	25*	3	-3	135	139	10
-5	6	87	59	23*	1	-1	259	276	10	3	-2	41	42	14*
-4	-11	151	144	5	1	0	371	360	9	3	-1	0	7	20*
-4	-10	134	118	5	1	1	107	109	3	3	0	261	294	23
-4	-7	94	81	5	1	2	112	112	4	3	1	33	41	21*
-4	-6	89	83	5	1	3	183	187	6	3	2	137	146	7
-4	-2	239	233	6	1	4	120	126	16	3	3	47	27	7
-4	2	228	230	10	1	5	157	135	10	3	4	292	312	7
-4	3	0	34	32*	1	6	187	177	5	3	5	155	147	5
-4	5	172	175	8	1	7	63	84	7	3	6	22	35	23*
-3	-13	25	21	18*	1	8	87	63	10	3	7	130	131	26
-3	-12	41	53	20*	1	9	136	118	6	3	8	31	59	25*
-3	-11	183	174	5	1	10	261	252	9	3	9	41	49	26*
-3	-9	310	296	8	1	11	0	39	20*	3	10	149	153	5
-3	-7	100	108	5	2	-14	174	173	5	4	-11	136	144	9
-3	-5	130	129	4	2	-13	36	6	25*	4	-10	105	118	11
-3	0	278	294	7	2	-12	35	48	14*	4	-9	0	11	18*
-3	5	160	147	8	2	-11	44	38	16*	4	-8	78	62	30*
-2	-13	0	6	20*	2	-10	64	54	7	4	-7	79	81	11
-2	2	0	33	26*	2	-9	44	71	15*	4	-6	65	83	26*
-1	-8	34	53	11*	2	-8	51	26	13*	4	-5	103	103	9
-1	-3	61	51	5	2	-7	53	59	12	4	-4	172	170	21
-1	-2	60	54	5	2	-6	161	169	4	4	-3	95	82	17
-1	-1	276	276	6	2	-5	66	60	9	4	-2	207	233	10
0	-14	35	49	19*	2	-4	147	160	7	4	-1	70	82	9
0	-12	102	117	5	2	-3	177	178	11	4	0	0	13	14*
0	-10	0	36	18*	2	-2	413	437	21	4	1	88	95	15
0	-8	36	24	17*	2	-1	386	366	9	4	2	247	230	6
0	-6	0	28	26*	2	0	89	95	5	4	3	46	34	18*
0	-4	378	421	12	2	1	124	141	9	4	4	43	44	19*
0	-2	37	29	18*	2	2	44	33	7	4	5	189	175	5
0	0	103	102	3	2	3	0	20	24*	4	6	143	143	4
0	2	67	75	5	2	4	60	62	6	4	7	182	186	8
0	4	69	90	22*	2	5	79	100	10	4	8	112	106	18
0	6	144	141	4	2	6	87	90	7	4	9	51	80	16*

Table A-6 (con't)

k	l	Fo	Fc	sigF	k	l	Fo	Fc	sigF	k	l	Fo	Fc	sigF
5	-9	0	23	32*	-1	-11	66	55	6	2	-5	122	129	15
5	-8	37	62	32*	-1	-10	36	44	20*	2	-4	183	173	21
5	-7	0	54	31*	-1	0	221	227	5	2	-3	116	115	9
5	-6	150	135	18	0	-14	74	54	5	2	-2	301	309	38
5	-5	67	78	6	0	-12	239	243	6	2	-1	286	356	13
5	-4	176	189	9	0	-10	165	174	22	2	0	108	103	10
5	-3	0	9	20*	0	-8	330	320	27	2	1	166	159	4
5	-2	71	64	30*	0	-6	195	209	9	2	2	159	141	4
5	-1	255	237	25	0	-4	298	303	12	2	3	0	19	23*
5	0	0	28	24*	0	-2	379	372	11	2	4	33	30	18*
5	1	199	197	11	0	0	367	367	11	2	5	99	118	5
5	2	0	17	19*	0	2	204	193	7	2	6	0	17	27*
5	3	20	12	18*	0	4	185	165	5	2	7	0	12	21*
5	4	107	98	17	0	6	42	30	15*	2	8	35	45	14*
5	5	41	48	16*	0	8	61	72	7	2	9	37	24	19*
5	6	74	59	6	0	10	123	145	22	2	10	28	15	31*
6	-5	188	187	19	1	-14	120	114	18	3	-12	32	78	24*
6	-4	97	88	6	1	-13	75	79	13	3	-11	34	57	23*
6	-3	0	61	29*	1	-12	180	156	16	3	-10	122	112	7
6	-2	123	143	9	1	-11	63	55	18*	3	-9	102	87	15
6	-1	0	13	29*	1	-10	0	44	30*	3	-8	59	75	13
6	0	41	22	9	1	-9	169	163	22	3	-7	33	26	24*
6	1	43	23	14*	1	-8	106	82	25	3	-6	0	40	18*
6	2	67	75	6	1	-7	190	164	16	3	-5	10	3	17*
					1	-6	68	47	14	3	-4	172	187	17
					1	-5	55	67	29*	3	-3	219	221	31
^^^^^^ h = 12 ^^^^^^^					1	-4	77	130	24*	3	-2	0	15	17*
-6	-3	40	11	19*	1	-3	61	66	17*	3	-1	75	106	20*
-6	-1	56	50	7	1	-2	51	51	5	3	0	237	226	8
-5	-8	44	34	15*	1	-1	96	103	4	3	1	298	305	8
-5	-7	64	81	6	1	0	216	227	13	3	2	65	82	6
-5	-5	0	49	21*	1	1	122	113	4	3	3	246	257	6
-5	-2	151	143	5	1	2	195	202	9	3	4	80	75	6
-5	-1	46	32	17*	1	3	54	48	8	3	5	11	14	19*
-5	2	0	63	33*	1	4	57	41	10	3	6	117	103	5
-4	-9	21	14	18*	1	5	55	43	12	3	7	54	34	7
-4	-8	75	50	6	1	6	227	230	14	3	8	95	92	5
-4	-4	44	49	15*	1	7	38	4	19*	3	9	43	47	18*
-4	-2	265	256	8	1	8	22	29	20*	4	-11	39	41	21*
-4	-1	330	324	8	1	9	70	69	7	4	-10	137	142	12
-4	6	0	37	31*	1	10	32	53	23*	4	-9	50	14	26*
-3	-8	55	75	8	1	11	68	76	7	4	-8	77	50	19*
-3	-1	96	106	5	2	-13	16	4	18*	4	-7	130	132	10
-3	1	324	305	13	2	-12	46	56	27*	4	-6	235	237	15
-3	3	224	257	11	2	-11	56	52	30*	4	-5	186	185	25
-3	6	109	103	11	2	-10	173	187	22	4	-4	68	49	20*
-3	7	60	34	23*	2	-9	33	25	12*	4	-3	72	72	19*
-2	-7	127	136	4	2	-8	11	22	18*	4	-2	230	256	10
-2	-1	375	356	8	2	-7	117	136	8	4	-1	249	324	11
-2	5	89	118	23*	2	-6	301	324	37	4	0	146	134	10

Table A-6 (con't)

k	l	Fo	Fc	sigF	k	l	Fo	Fc	sigF	k	l	Fo	Fc	sigF
4	1	105	108	5	-1	-9	165	171	5	2	-3	73	65	7
4	2	44	60	24*	-1	-4	0	25	17*	2	-2	32	52	18*
4	3	261	249	29	-1	3	51	55	29*	2	-1	63	66	18*
4	4	275	257	7	0	-14	177	176	5	2	0	273	270	13
4	5	82	84	6	0	-12	198	192	13	2	1	40	88	15*
4	6	41	37	20*	0	-10	255	286	42	2	2	69	84	31*
4	7	64	47	11	0	-8	0	37	20*	2	3	49	63	16*
4	8	0	7	28*	0	-6	260	282	16	2	4	250	236	6
5	-8	54	34	30*	0	-4	132	134	9	2	5	45	49	17*
5	-7	0	81	34*	0	-2	107	108	8	2	6	85	106	6
5	-6	34	6	17*	0	0	232	252	6	2	7	100	102	9
5	-5	19	49	32*	0	2	71	61	10	2	8	44	9	15*
5	-4	0	7	22*	0	4	128	130	4	2	9	16	25	21*
5	-3	39	56	17*	0	6	180	200	13	3	-12	78	62	6
5	-2	71	143	31*	0	8	285	292	7	3	-11	33	43	28*
5	-1	56	32	30*	0	10	187	168	6	3	-10	63	51	40*
5	0	210	220	4	1	-13	0	32	17*	3	-9	86	105	26*
5	1	0	5	17*	1	-12	134	129	4	3	-8	157	156	8
5	2	64	63	6	1	-11	99	90	15	3	-7	140	138	32
5	3	0	13	36*	1	-10	44	31	8	3	-6	20	61	29*
5	4	95	108	6	1	-9	114	171	10	3	-5	0	21	27*
5	5	36	48	37*	1	-8	52	53	12	3	-4	0	20	27*
6	-3	58	11	23*	1	-7	87	78	45*	3	-3	120	142	22
6	-2	70	58	7	1	-6	142	160	15	3	-2	127	130	27
6	-1	0	50	33*	1	-5	72	71	5	3	-1	84	88	12
6	0	0	12	16*	1	-4	30	25	21*	3	0	41	64	14*
6					1	-3	29	17	21*	3	1	180	174	5
6					1	-2	51	49	27*	3	2	29	28	16*
6					1	-1	50	49	5	3	3	0	66	20*
6					1	0	93	76	12	3	4	223	226	6
6					1	1	180	181	5	3	5	42	18	18*
6					1	2	75	76	5	3	6	192	189	5
6					1	3	45	55	9	3	7	53	53	14*
6					1	4	81	86	5	3	8	88	78	7
6					1	5	84	57	14	4	-10	134	142	7
6					1	6	40	11	24*	4	-9	95	134	13
6					1	7	24	62	23*	4	-8	60	41	23*
6					1	8	163	163	4	4	-7	166	168	13
6					1	9	0	11	31*	4	-6	104	108	9
6					1	10	16	26	30*	4	-5	120	135	9
6					2	-13	30	27	33*	4	-4	60	45	22*
6					2	-12	36	60	25*	4	-3	26	36	19*
6					2	-11	59	57	7	4	-2	26	58	25*
6					2	-10	245	248	17	4	-1	87	87	17
6					2	-9	0	20	18*	4	0	38	48	22*
6					2	-8	0	51	29*	4	1	84	65	17
6					2	-7	159	149	22	4	2	48	72	17*
6					2	-6	181	198	28	4	3	0	3	19*
6					2	-5	78	90	9	4	4	142	147	10
6					2	-4	11	40	18*	4	5	86	82	18

^^^^^^ h = 13 ^^^^^^^

Table A-6 (con't)

k	l	Fo	Fc	sigF	k	l	Fo	Fc	sigF	k	l	Fo	Fc	sigF
-4	-4	32	21	18*	2	-11	75	86	6	5	-1	67	32	21*
-4	-3	154	153	5	2	-10	93	88	20					
-4	-2	208	201	6	2	-9	118	144	9	^^^^^^	h = 16	^^^^^^		
-4	-1	140	135	5	2	-8	48	58	34*					
-4	0	0	12	22*	2	-7	230	231	12	-4	-6	113	109	5
-3	-9	27	17	20*	2	-6	35	31	18*	-4	-4	76	60	6
-3	-4	283	284	8	2	-5	72	61	10	-4	-3	19	38	18*
-3	-3	142	134	4	2	-4	46	55	7	-4	2	67	77	23*
-3	-2	103	111	5	2	-3	0	5	15*	-3	-8	160	154	4
-3	-1	38	81	10*	2	-2	112	114	29*	-3	-7	105	98	5
-3	0	123	111	17	2	-1	60	61	6	-3	-4	130	120	5
-3	4	0	14	32*	2	0	71	68	4	-3	-1	222	209	6
-2	-9	139	144	5	2	1	44	31	9	-3	3	0	12	35*
-2	1	24	31	31*	2	2	50	54	16*	-3	4	0	17	28*
-2	3	23	56	31*	2	3	65	56	7	-3	5	82	87	27*
-1	-12	96	92	5	2	4	112	105	11	-2	-10	0	13	21*
-1	1	30	4	27*	2	5	15	17	30*	-2	-7	115	107	5
-1	7	87	76	22*	2	6	38	26	18*	-2	-1	0	3	20*
0	-12	0	46	31*	2	7	0	27	27*	-2	0	122	123	4
0	-10	253	238	10	3	-10	23	29	19*	-2	1	49	23	25*
0	-8	87	90	21	3	-9	0	17	28*	-2	6	0	29	30*
0	-6	45	39	34*	3	-8	164	182	17	-1	2	78	63	10
0	-4	121	97	13	3	-7	93	89	11	0	-10	150	148	4
0	-2	138	157	21	3	-6	55	58	14*	0	-8	27	17	18*
0	0	159	158	16	3	-5	0	36	26*	0	-6	57	49	19*
0	2	239	246	9	3	-4	250	284	11	0	-4	112	100	22
0	4	202	221	5	3	-3	122	134	9	0	-2	39	23	8
0	6	122	112	18	3	-2	101	111	10	0	0	28	45	18*
0	8	56	63	15*	3	-1	0	81	30*	0	2	12	16	33*
1	-12	90	92	26*	3	0	109	111	5	0	4	56	53	14
1	-11	66	73	6	3	1	258	276	6	0	6	42	76	18*
1	-10	145	134	6	3	2	45	61	18*	1	-11	0	2	17*
1	-9	58	60	7	3	3	0	6	18*	1	-10	48	45	19*
1	-8	166	179	12	3	4	0	14	21*	1	-9	65	68	8
1	-7	14	59	23*	3	5	26	43	20*	1	-8	137	161	16
1	-6	164	165	29	3	6	28	57	29*	1	-7	0	19	17*
1	-5	93	78	16	4	-8	48	47	26*	1	-6	27	40	21*
1	-4	174	182	23	4	-7	131	151	9	1	-5	48	62	14*
1	-3	84	78	25*	4	-6	56	54	30*	1	-4	89	97	14
1	-2	0	34	18*	4	-5	28	15	27*	1	-3	25	11	15*
1	-1	91	111	24*	4	-4	0	21	28*	1	-2	137	137	22
1	0	175	172	15	4	-3	135	153	8	1	-1	31	29	21*
1	1	36	4	17*	4	-2	178	201	9	1	0	73	74	8
1	2	127	126	5	4	-1	123	135	9	1	1	17	53	24*
1	3	80	74	6	4	0	42	12	18*	1	2	63	63	7
1	4	106	111	5	4	1	51	68	18*	1	3	73	81	6
1	5	0	36	20*	4	2	257	243	6	1	4	120	130	12
1	6	31	10	37*	4	3	86	96	6	1	5	0	8	19*
1	7	76	76	7	4	4	47	20	15*	1	6	46	64	32*
1	8	40	5	18*	5	-2	0	39	31*	1	7	38	37	18*

Table A-6 (con't)

k	l	Fo	Fc	sigF	k	l	Fo	Fc	sigF	k	l	Fo	Fc	sigF
2	-10	43	13	29*	-3	1	72	60	26*	3	-7	0	26	28*
2	-9	84	92	7	-3	3	71	93	26*	3	-6	0	27	28*
2	-8	125	122	5	-2	-9	0	38	19*	3	-5	58	94	24*
2	-7	90	107	12	-2	-7	31	12	18*	3	-4	33	35	15*
2	-6	42	49	17*	-2	0	113	105	13	3	-3	92	92	5
2	-5	129	138	25	-2	2	0	73	34*	3	-2	65	55	28*
2	-4	149	156	11	-1	-7	42	36	18*	3	-1	65	98	28*
2	-3	30	43	24*	-1	-5	37	34	20*	3	0	66	42	15
2	-2	57	65	7	0	-10	80	85	5	3	1	60	60	7
2	-1	0	3	28*	0	-8	0	15	18*	3	2	121	106	21
2	0	128	123	27	0	-6	119	119	25	3	3	87	93	5
2	1	13	23	20*	0	-4	147	154	4	4	-3	53	48	30*
2	2	60	54	6	0	-2	224	235	8	4	-2	134	143	9
2	3	50	44	8	0	0	142	144	3					
2	4	92	88	17	0	2	0	20	29*	^^^^^^	h = 18	^^^^^^		
2	5	19	7	23*	0	4	41	38	10					
2	6	28	29	19*	0	6	33	50	24*	-3	-4	0	35	19*
3	-9	88	92	12	1	-10	82	90	6	-3	-3	106	107	5
3	-8	138	154	8	1	-9	0	20	20*	-3	-2	69	55	6
3	-7	93	98	11	1	-8	44	50	17*	-3	0	186	187	5
3	-6	45	39	15*	1	-7	0	36	28*	-2	-4	141	133	5
3	-5	0	15	28*	1	-6	178	176	18	-2	-2	111	108	5
3	-4	119	120	9	1	-5	49	34	25*	-1	-5	105	113	5
3	-3	69	66	6	1	-4	46	47	8	-1	4	109	118	10
3	-2	77	82	12	1	-3	25	16	25*	0	-8	43	47	21*
3	-1	199	209	9	1	-2	0	11	22*	0	-6	117	141	19
3	0	53	60	12	1	-1	0	29	27*	0	-4	123	121	5
3	1	175	192	5	1	0	179	173	5	0	-2	38	38	18*
3	2	97	108	10	1	1	0	21	19*	0	0	22	28	16*
3	3	36	12	19*	1	2	58	56	36*	0	2	85	73	5
3	4	0	17	20*	1	3	0	5	19*	0	4	47	56	17*
3	5	95	87	5	1	4	103	108	13	1	-9	42	39	8
4	-6	72	109	26*	1	5	34	40	30*	1	-8	0	20	29*
4	-5	30	1	25*	1	6	131	147	5	1	-7	102	98	22
4	-4	70	60	13	2	-9	0	38	30*	1	-6	44	29	16*
4	-3	0	38	27*	2	-8	50	53	27*	1	-5	88	113	12
4	-2	103	94	21	2	-7	60	12	23*	1	-4	8	9	31*
4	-1	51	36	20*	2	-6	0	3	22*	1	-3	16	22	17*
4	0	65	65	5	2	-5	32	59	20*	1	-2	0	17	23*
4	1	33	39	24*	2	-4	180	173	12	1	-1	25	25	15*
4	2	87	77	6	2	-3	46	54	15*	1	0	120	125	13
4					2	-2	68	80	36*	1	1	29	36	29*
4					2	-1	0	43	18*	1	2	70	63	5
4					2	0	106	105	12	1	3	35	38	16*
4					2	1	0	9	32*	1	4	122	118	5
4					2	2	64	73	7	2	-8	96	86	22
4					2	3	0	26	26*	2	-7	89	75	9
4					2	4	76	77	6	2	-6	93	114	8
4					2	5	30	18	18*	2	-5	29	15	18*
4					3	-8	65	43	11	2	-4	111	133	10
4					3	-7								
4					3	-6								
4					3	-5								
4					3	-4								
4					3	-3								
4					3	-2								
4					3	-1								
4					3	0								
4					3	1								
4					3	2								
4					3	3								
4					3	4								
4					3	5								
4					3	6								
4					3	7								
4					3	8								
4					3	9								
4					3	10								
4					3	11								
4					3	12								
4					3	13								
4					3	14								
4					3	15								
4					3	16								
4					3	17								
4					3	18								
4					3	19								
4					3	20								
4					3	21								
4					3	22								
4					3	23								
4					3	24								
4					3	25								
4					3	26								
4					3	27								
4					3	28								
4					3	29								
4					3	30								
4					3	31								
4					3	32								
4					3	33								
4					3	34								
4					3	35								
4					3	36								
4					3	37								
4					3	38								
4					3	39								
4					3	40								
4					3	41								
4					3	42								
4					3	43								
4					3	44								
4					3	45								
4					3	46								
4					3	47								
4					3	48								
4					3	49								
4					3	50								
4					3	51								
4					3	52								
4					3	53								
4					3	54								
4					3	55								
4					3	56								
4					3	57								
4					3	58								
4					3	59								
4					3	60								
4					3	61								
4					3	62								
4					3	63								
4					3	64								
4					3	65								
4					3	66								
4					3	67								
4					3	68								
4					3	69								
4					3	70								
4					3	71								
4					3	72								
4					3	73								
4					3	74								
4					3	75								
4					3	76								
4					3	77								
4					3	78								
4					3	79								
4					3	80								
4					3	81								
4					3	82								
4					3	83								
4					3	84								
4					3	85								
4					3	86								
4					3	87								
4					3	88								
4					3	89								
4					3	90								
4					3	91					</			

Table A-7: Observed and Calculated Structure Factors for 52.
 F_o , F_c and sig values have been multiplied by 10.

k	l	Fo	Fc	sigF	k	l	Fo	Fc	sigF	k	l	Fo	Fc	sigF
***** h = -5 *****					***** h = -1 *****					1	-8	183	185	5
										1	-7	331	332	4
-7	9	28	47	7*	-8	4	17	26	12*	1	-6	458	455	4
-7	10	18	33	12*	-8	9	15	28	9*	1	-5	802	803	3
-6	10	0	12	15*	-7	12	0	23	8*	1	-4	932	949	3
-6	13	36	38	5	-7	13	32	39	4	1	-3	503	518	3
-5	-9	0	24	12*	-6	13	18	32	9*	1	-2	818	794	2
-5	15	0	25	14*	-6	15	0	16	12*	1	1	339	351	2
-4	15	54	55	8	-5	16	0	18	14*	1	15	105	103	5
-4	17	0	11	19*	-5	17	23	15	16*	1	16	19	22	18*
***** h = -4 *****					-4	-16	81	85	5	1	17	0	32	20*
					-4	19	0	56	20*	1	18	67	51	7
-7	7	65	63	5	-3	-17	62	61	5	1	20	47	40	9*
-7	11	25	20	5*	-3	20	25	18	13*	2	-20	60	55	6
-6	-8	15	36	9*	***** h = 0 *****					2	-19	0	20	17*
-6	14	21	35	8*						2	-17	14	16	16*
-5	-11	19	8	12*	-8	9	7	25	9*	2	-13	83	88	5
-5	16	41	50	8*	-6	13	41	41	4	2	-12	82	77	5
-4	-13	42	12	10*	-6	15	14	15	13*	2	-11	246	237	6
-4	18	41	23	9*	-5	16	0	24	17*	2	-10	81	81	4
***** h = -3 *****					-3	-18	30	35	6*	2	-9	545	530	5
					-3	19	0	18	16*	2	-8	182	181	5
-8	6	25	29	7*	0	-21	20	19	10*	2	-6	160	159	4
-8	8	34	42	4	0	-20	21	36	12*	2	-1	334	328	3
-7	-6	16	16	6*	0	-18	0	5	14*	2	0	498	512	3
-7	12	0	15	11*	0	-17	31	13	9*	2	2	414	426	3
-6	12	0	60	9*	0	-15	33	38	17*	2	3	301	306	3
-6	15	46	48	4	0	-14	86	82	5	2	4	393	396	4
-5	-13	46	32	6	0	-13	188	184	6	2	5	305	313	4
-5	17	28	28	16*	0	-11	61	54	6	2	7	232	225	5
-4	-14	0	26	18*	0	-10	68	58	5	2	14	68	63	6
-4	18	31	13	17*	0	-9	11	16	15*	2	15	31	21	18*
-3	-16	134	103	5	0	-8	142	140	5	2	16	16	39	16*
-3	19	64	69	7	0	2	185	197	2	2	18	26	29	17*
***** h = -2 *****					0	3	141	136	3	3	-17	32	19	17*
					0	4	504	526	3	3	-16	85	91	5
-8	5	62	67	4	0	5	351	362	3	3	-15	92	91	5
-8	9	0	33	9*	0	6	255	268	4	3	-11	89	92	4
-7	-8	15	19	5*	0	7	306	323	4	3	-9	230	229	5
-7	13	15	33	11*	0	12	0	56	18*	3	-8	48	43	5
-5	16	19	38	10*	0	16	162	158	6	3	-6	165	163	5
-5	17	49	38	7	0	19	17	5	17*	3	-5	363	347	4
-4	-15	86	79	5	1	-19	31	32	16*	3	-3	91	86	3
-4	19	40	39	9*	1	-14	151	153	7	3	-1	274	285	4
-3	-17	62	60	6	1	-13	19	18	16*	3	2	315	313	4
-3	20	0	10	17*	1	-12	124	120	5	3	4	182	189	4
					1	-11	180	172	6	3	7	128	131	6
					1	-10	142	126	6	3	10	32	60	17*
					1	-9	254	251	5	3	12	67	77	6
					1					3	13	0	47	18*

Table A-7 (con't)

k	l	Fo	Fc	sig*	k	l	Fo	Fc	sigF	k	l	Fo	Fc	sigF
3	14	98	96	5	7	-11	35	42	5	0	4	356	354	3
4	-17	43	43	8*	7	-7	34	12	7*	0	5	173	182	4
4	-16	76	65	5	7	-3	101	95	5	0	6	84	90	4
4	-15	56	58	7	7	-2	150	140	6	0	7	148	117	5
4	-14	99	104	5	7	1	56	51	5	0	8	367	360	5
4	-13	152	142	5	7	4	35	37	8*	0	9	60	58	5
4	-12	0	11	16*	7	5	82	76	5	0	10	257	250	6
4	-11	20	30	13*	7	6	56	50	5	0	11	128	136	5
4	-3	90	92	4	7	8	44	49	6	0	12	0	8	17*
4	-1	106	111	4	7	9	0	32	14*	0	13	153	147	5
4	0	145	124	5	7	10	27	32	15*	0	14	178	173	7
4	2	113	107	6	7	12	16	41	17*	0	15	63	66	7
4	4	200	185	5	7	13	0	7	15*	0	16	27	7	18*
4	5	139	152	5	8	-8	48	40	5	0	17	107	91	5
4	6	93	104	4	8	-6	53	37	5	0	18	0	20	19*
4	7	85	86	4	8	0	0	16	15*	0	19	0	20	17*
4	8	53	56	6	8	1	33	13	8*	0	20	9	29	14*
4	9	145	142	5	8	2	43	43	7	1	-21	0	15	15*
4	10	28	21	17*	8	3	55	45	6	1	-20	7	23	13*
4	18	31	44	13*	8	4	86	80	4	1	-19	2	14	15*
5	-14	51	43	7	8	5	0	19	15*	1	-18	26	26	14*
5	-9	44	42	6	8	7	31	14	8*	1	-17	78	81	5
5	-8	93	85	4						1	-16	70	71	5
5	-6	55	62	5	*****	h =	1	*****		1	-15	43	43	8*
5	-5	105	105	4						1	-14	27	41	16*
5	-2	55	62	5	0	-21	25	19	9*	1	-13	150	155	6
5	-1	0	40	15*	0	-20	38	46	7*	1	-12	96	83	4
5	3	20	27	14*	0	-19	0	10	16*	1	-11	133	128	6
5	4	34	37	7*	0	-18	66	69	6	1	-10	96	93	5
5	7	81	79	4	0	-17	40	45	8*	1	-9	216	216	5
5	10	101	89	4	0	-16	105	107	5	1	-8	385	386	4
5	11	199	182	7	0	-15	189	201	7	1	-7	177	178	4
5	12	96	63	5	0	-14	70	71	5	1	-6	438	446	4
5	13	66	49	6	0	-13	0	3	17*	1	-5	198	199	3
5	15	53	45	7	0	-12	0	15	16*	1	-4	550	544	3
5	17	5	20	14*	0	-11	62	77	6	1	-3	930	927	3
6	-14	0	18	15*	0	-10	48	16	6	1	-2	366	368	2
6	-12	17	22	14*	0	-9	55	62	5	1	-1	585	573	2
6	-11	27	23	15*	0	-8	205	203	5	1	0	105	87	3
6	-10	62	55	5	0	-7	295	283	4	1	1	322	312	3
6	-9	54	65	6	0	-6	245	253	4	1	2	678	681	3
6	-5	57	66	5	0	-5	293	308	3	1	3	1059	1075	3
6	-2	67	66	5	0	-4	488	499	3	1	4	242	234	3
6	-1	95	89	4	0	-3	1055	1055	2	1	5	579	593	4
6	0	99	96	5	0	-2	68	91	3	1	6	175	177	4
6	3	0	38	16*	0	-1	145	142	2	1	7	245	257	4
6	4	99	102	4	0	0	325	330	2	1	8	253	262	5
6	6	92	98	4	0	1	678	677	2	1	9	9	42	16*
6	7	195	191	6	0	2	214	212	2	1	10	220	200	6
6	8	75	79	4	0	3	202	206	3	1	11	129	129	5

Table A-7 (con't)

k	l	Fo	Fc	sigF	k	l	Fo	Fc	sigF	k	l	Fo	Fc	sigF
1	12	163	154	7	3	-19	33	9	9*	4	-6	178	178	5
1	13	154	149	5	3	-18	84	73	5	4	-5	202	200	5
1	14	43	31	8*	3	-17	45	48	8*	4	-4	129	134	6
1	15	126	116	6	3	-16	99	100	5	4	-3	125	130	5
1	16	136	133	6	3	-15	69	74	5	4	-2	217	207	5
1	17	46	61	9*	3	-14	40	57	8*	4	-1	82	70	4
1	18	35	31	17*	3	-13	111	118	5	4	0	214	206	5
1	19	0	20	18*	3	-12	134	136	5	4	1	75	77	4
1	20	40	25	9*	3	-11	37	16	7*	4	2	235	233	5
2	-20	43	33	8*	3	-10	156	153	6	4	3	73	59	4
2	-19	24	17	13*	3	-9	135	150	6	4	4	59	80	5
2	-18	12	13	16*	3	-8	148	155	5	4	5	191	197	5
2	-17	36	43	9*	3	-7	209	217	5	4	6	95	100	4
2	-16	93	108	5	3	-6	301	299	4	4	7	80	81	4
2	-15	94	105	5	3	-5	33	40	6*	4	8	3	16	14*
2	-14	109	114	4	3	-4	428	420	4	4	9	43	41	7
2	-13	64	56	5	3	-3	229	248	4	4	10	119	119	5
2	-12	130	136	6	3	-2	115	110	5	4	11	197	187	7
2	-11	127	132	6	3	-1	64	60	3	4	12	104	103	5
2	-10	150	156	6	3	0	175	169	4	4	13	25	17	17*
2	-9	385	386	5	3	1	88	87	4	4	14	108	108	5
2	-8	182	176	5	3	2	70	76	3	4	15	76	70	6
2	-7	396	395	4	3	3	185	192	4	4	17	29	24	15*
2	-6	325	320	4	3	4	409	404	4	4	18	50	50	7
2	-5	227	219	4	3	5	337	330	4	5	-15	16	44	13*
2	-4	339	347	3	3	6	239	241	5	5	-14	0	50	17*
2	-3	212	223	3	3	7	179	176	5	5	-13	37	16	7*
2	-2	473	485	3	3	8	194	206	6	5	-12	41	47	6
2	-1	119	118	4	3	9	112	105	5	5	-11	69	81	5
2	0	206	222	3	3	10	45	58	8*	5	-10	36	33	6*
2	1	81	84	3	3	11	114	104	5	5	-9	4	31	13*
2	2	474	473	3	3	12	199	208	7	5	-8	107	106	4
2	3	407	427	3	3	13	70	78	6	5	-7	120	126	5
2	4	535	541	4	3	14	77	75	5	5	-6	74	65	4
2	5	243	234	4	3	15	0	60	19*	5	-5	69	73	5
2	6	375	376	4	3	16	101	100	5	5	-4	137	136	6
2	7	450	451	4	3	18	56	75	8	5	-3	14	23	14*
2	8	358	349	5	3	19	66	63	6	5	-2	115	107	4
2	9	189	179	5	4	-18	19	40	18*	5	-1	26	24	9*
2	10	208	215	6	4	-17	0	44	17*	5	0	89	78	4
2	11	85	91	5	4	-16	34	11	9*	5	1	66	56	4
2	12	46	39	7	4	-15	43	58	8*	5	2	148	147	5
2	13	52	44	7	4	-14	59	52	6	5	3	119	107	6
2	14	91	103	5	4	-13	56	49	6	5	4	100	98	5
2	15	73	62	6	4	-12	122	133	5	5	5	78	75	4
2	16	30	49	18*	4	-11	147	152	7	5	6	21	32	14*
2	17	36	14	10*	4	-10	0	47	12*	5	7	53	52	6
2	18	27	29	17*	4	-9	51	54	5	5	8	143	141	7
2	19	61	45	7	4	-8	80	82	4	5	9	143	143	6
2	20	61	64	6	4	-7	74	80	4	5	10	115	114	5

Table A-7 (con't)

k	l	Fo	Fc	sigF	k	l	Fo	Fc	sigF	k	l	Fo	Fc	sigF
5	11	72	63	5	7	3	116	107	4	0	-1	1431	1414	3
5	12	29	47	18*	7	4	73	71	4	0	0	848	834	3
5	13	49	33	7	7	5	60	73	5	0	1	308	301	3
5	14	31	27	18*	7	6	0	15	14*	0	2	21	34	12*
5	15	0	24	17*	7	7	0	4	15*	0	3	152	151	4
5	16	13	2	16*	7	8	47	45	6	0	4	194	199	4
5	17	21	9	16*	7	9	55	42	5	0	5	384	381	4
6	-14	0	8	16*	7	10	0	9	15*	0	6	25	4	14*
6	-12	0	26	15*	7	11	24	12	15*	0	7	150	148	5
6	-11	33	68	18*	7	12	40	31	7*	0	8	25	20	15*
6	-10	40	44	7*	8	-8	0	17	14*	0	9	35	62	9*
6	-9	74	68	5	8	-7	45	46	6	0	10	46	35	7*
6	-8	95	104	4	8	-6	56	39	5	0	11	31	20	16*
6	-7	91	93	4	8	-5	55	44	5	0	12	115	120	5
6	-6	31	44	8*	8	-3	74	69	4	0	13	138	133	5
6	-5	25	19	9*	8	-2	95	85	4	0	14	7	67	19*
6	-4	37	11	6*	8	-1	43	42	5	0	15	72	81	6
6	-3	97	103	4	8	0	41	25	6	0	16	80	85	6
6	-2	40	40	7*	8	1	132	127	6	0	17	34	16	10*
6	-1	43	36	6	8	2	76	64	4	0	18	8	8	17*
6	0	77	80	4	8	3	49	49	6	0	19	14	28	15*
6	1	97	103	5	8	4	7	11	14*	1	-21	0	29	14*
6	2	53	46	5	8	5	22	32	12*	1	-20	62	58	6
6	3	145	158	6	8	6	0	21	14*	1	-19	20	54	20*
6	4	117	120	4	8	7	48	26	5	1	-18	73	77	5
6	5	94	84	4	8	8	36	16	6*	1	-17	54	49	6
6	6	135	140	6	8	9	0	24	13*	1	-16	85	92	5
6	7	108	111	4						1	-15	83	91	6
6	8	0	8	16*						1	-14	53	58	7
6	9	39	35	8*						1	-13	77	79	5
6	10	74	74	5	0	-21	22	38	15*	1	-12	31	55	18*
6	11	57	60	6	0	-20	0	58	19*	1	-11	143	134	6
6	12	23	33	15*	0	-19	0	4	16*	1	-10	170	166	6
6	13	0	11	16*	0	-18	29	24	17*	1	-9	241	255	5
6	14	0	14	18*	0	-17	105	118	5	1	-8	68	53	4
6	15	0	5	16*	0	-16	94	87	5	1	-7	220	222	4
7	-11	18	22	10*	0	-15	0	9	16*	1	-6	363	350	4
7	-10	0	14	12*	0	-14	117	107	5	1	-5	318	319	3
7	-9	0	37	11*	0	-13	70	74	5	1	-4	320	311	3
7	-8	20	24	14*	0	-12	117	131	5	1	-3	447	446	3
7	-7	0	12	15*	0	-11	93	95	4	1	-2	427	418	3
7	-6	0	13	13*	0	-10	47	62	6	1	-1	146	150	4
7	-5	123	123	5	0	-9	63	60	4	1	0	383	369	3
7	-4	71	74	5	0	-8	39	31	6	1	1	326	336	3
7	-3	56	56	5	0	-7	259	254	4	1	2	406	403	3
7	-2	100	105	5	0	-6	359	346	3	1	3	478	485	3
7	-1	146	143	6	0	-5	49	53	4	1	4	259	267	4
7	0	67	68	5	0	-4	159	156	4	1	5	228	240	4
7	1	105	114	5	0	-3	59	57	3	1	6	286	295	4
7	2	83	91	4	0	-2	281	277	3	1	7	183	186	5

Table A-7 (con't)

k	l	Fo	Fc	sigF	k	l	Fo	Fc	sigF	k	l	Fo	Fc	sigF
1	8	41	34	6	2	18	21	32	14*	4	-7	51	68	6
1	9	64	69	5	2	19	49	38	6	4	-6	64	56	5
1	10	188	178	6	3	-19	0	11	16*	4	-5	177	180	6
1	11	88	96	5	3	-18	79	74	5	4	-4	95	95	4
1	12	19	15	17*	3	-17	33	40	10*	4	-3	95	106	5
1	13	116	111	5	3	-16	0	13	14*	4	-2	175	175	5
1	14	154	144	7	3	-15	59	48	6	4	-1	209	195	5
1	15	0	28	18*	3	-14	52	60	6	4	0	220	219	5
1	16	34	25	10*	3	-13	50	49	6	4	1	162	171	5
1	17	23	14	17*	3	-12	56	55	6	4	2	68	75	4
1	18	40	15	8*	3	-11	112	133	5	4	3	110	117	4
1	19	30	28	11*	3	-10	170	172	6	4	4	124	118	6
2	-20	30	29	17*	3	-9	122	103	6	4	5	122	130	6
2	-19	28	22	11*	3	-8	43	42	6	4	6	118	104	4
2	-18	36	41	11*	3	-7	50	47	5	4	7	107	102	5
2	-17	54	52	7	3	-6	203	200	5	4	8	148	154	6
2	-16	10	36	17*	3	-5	97	84	4	4	9	81	88	5
2	-15	34	46	9*	3	-4	63	53	4	4	10	0	55	18*
2	-14	0	23	15*	3	-3	68	69	4	4	11	67	75	6
2	-13	49	47	7	3	-2	161	164	4	4	12	0	12	17*
2	-12	115	122	5	3	-1	285	285	4	4	13	166	165	7
2	-11	121	128	4	3	0	180	179	4	4	14	27	70	21*
2	-10	149	156	6	3	1	442	435	4	4	16	23	42	16*
2	-9	0	35	14*	3	2	243	237	4	4	17	29	46	17*
2	-8	13	15	14*	3	3	177	173	5	5	-15	0	61	14*
2	-7	131	125	5	3	4	232	234	5	5	-14	60	70	5
2	-6	61	63	4	3	5	250	253	5	5	-13	54	58	6
2	-5	36	31	5	3	6	12	72	15*	5	-12	81	101	5
2	-4	146	144	4	3	7	105	99	5	5	-11	138	144	7
2	-3	73	69	3	3	8	142	126	6	5	-10	103	101	5
2	-2	125	126	4	3	9	64	70	5	5	-9	51	55	5
2	-1	195	201	4	3	10	19	52	15*	5	-8	57	63	6
2	0	141	129	4	3	11	107	111	5	5	-7	103	103	5
2	1	239	244	4	3	12	71	72	6	5	-6	146	140	6
2	2	55	34	4	3	13	60	54	6	5	-5	56	48	5
2	3	419	418	4	3	14	86	86	5	5	-4	77	81	5
2	4	213	223	4	3	15	55	50	6	5	-3	114	120	5
2	5	196	206	4	3	16	40	35	8*	5	-2	44	33	6
2	6	240	232	5	3	18	23	37	15*	5	-1	69	77	4
2	7	337	341	5	4	-18	35	51	9*	5	0	103	103	5
2	8	316	329	5	4	-17	22	27	13*	5	1	61	60	5
2	9	94	90	4	4	-16	0	16	15*	5	2	106	101	4
2	10	76	88	5	4	-15	0	61	18*	5	3	107	105	4
2	11	35	33	8*	4	-14	109	106	5	5	4	103	111	5
2	12	124	124	5	4	-13	83	81	5	5	5	150	144	6
2	13	72	72	5	4	-12	54	43	6	5	6	145	143	6
2	14	55	51	6	4	-11	3	17	14*	5	7	52	49	6
2	15	72	60	5	4	-10	79	79	4	5	8	120	117	5
2	16	43	21	8*	4	-9	138	145	6	5	9	110	119	5
2	17	21	19	15*	4	-8	53	47	5	5	10	165	171	6

Table A-7 (con't)

k	l	Fo	Fc	sigF	k	l	Fo	Fc	sigF	k	l	Fo	Fc	sigF
5	11	28	9	15*	7	2	0	39	14*	0	2	38	28	5
5	12	0	23	15*	7	3	62	64	5	0	3	54	42	4
5	13	55	43	6	7	4	77	70	4	0	4	26	24	8*
5	14	65	44	5	7	5	66	68	4	0	5	0	9	13*
5	15	0	51	17*	7	6	48	45	5	0	6	141	144	5
5	16	0	8	16*	7	7	0	7	14*	0	7	68	61	5
6	-15	0	25	12*	7	9	34	28	7*	0	8	53	69	6
6	-14	0	43	16*	7	10	0	27	14*	0	9	29	37	16*
6	-13	0	25	13*	7	11	0	8	15*	0	10	0	11	16*
6	-12	41	62	7	8	-8	13	7	12*	0	11	32	45	10*
6	-11	22	44	12*	8	-7	0	26	14*	0	12	103	109	5
6	-10	0	31	16*	8	-6	0	29	13*	0	13	173	174	7
6	-9	104	103	4	8	-4	31	17	7*	0	14	0	26	17*
6	-8	137	150	6	8	-3	22	25	14*	0	15	0	46	19*
6	-7	18	26	14*	8	-2	20	34	14*	0	16	0	27	18*
6	-6	74	71	5	8	-1	12	12	13*	0	17	39	42	9*
6	-5	146	145	6	8	0	0	29	13*	0	18	44	27	7*
6	-4	141	139	6	8	1	25	37	9*	0	19	68	57	5
6	-3	77	80	4	8	2	21	42	14*	1	-21	38	29	7*
6	-2	47	40	6	8	3	21	38	13*	1	-20	0	25	17*
6	-1	13	34	14*	8	4	35	33	6*	1	-19	63	54	6
6	0	92	92	4	8	5	0	15	13*	1	-18	43	48	9*
6	1	89	90	4	8	6	33	32	6*	1	-17	40	26	9*
6	2	79	75	4	8	7	16	4	11*	1	-16	14	30	17*
6	3	23	42	15*						1	-15	68	67	7
6	4	127	131	4	*****	h =	3	*****		1	-14	107	106	5
6	5	96	97	5						1	-13	58	55	7
6	6	54	54	6	0	-21	27	25	16*	1	-12	81	68	5
6	7	39	56	8*	0	-20	31	20	16*	1	-11	47	48	7
6	8	77	89	4	0	-19	32	23	11*	1	-10	201	190	6
6	9	76	64	4	0	-18	0	2	18*	1	-9	80	90	4
6	10	27	32	10*	0	-17	86	91	6	1	-8	96	87	4
6	11	55	58	6	0	-16	97	106	5	1	-7	39	39	6
6	12	28	49	15*	0	-15	94	89	5	1	-6	153	153	5
6	13	44	17	6	0	-14	49	47	7	1	-5	63	70	4
6	14	0	18	15*	0	-13	54	47	7	1	-4	93	104	4
7	-12	57	51	5	0	-12	0	22	15*	1	-3	49	59	4
7	-11	66	41	5	0	-11	31	6	16*	1	-2	355	352	4
7	-10	32	26	8*	0	-10	249	232	6	1	-1	337	332	4
7	-9	0	21	15*	0	-9	246	246	5	1	0	230	215	4
7	-8	57	55	5	0	-8	268	267	5	1	1	98	83	3
7	-7	27	53	15*	0	-7	24	41	10*	1	2	326	314	4
7	-6	41	29	6	0	-6	96	95	4	1	3	155	156	4
7	-5	83	94	4	0	-5	45	19	5	1	4	67	69	4
7	-4	64	62	4	0	-4	88	75	4	1	5	75	82	4
7	-3	61	63	5	0	-3	468	447	3	1	6	53	52	5
7	-2	90	92	4	0	-2	253	258	3	1	7	188	186	5
7	-1	107	103	5	0	-1	442	449	3	1	8	43	55	7
7	0	66	63	4	0	0	96	102	5	1	9	130	121	6
7	1	56	49	5	0	1	234	237	4	1	10	62	62	6

Table A-7 (con't)

k	l	Fo	Fc	sigF	k	l	Fo	Fc	sigF	k	l	Fo	Fc	sigF
1	11	50	51	7	3	-15	54	60	7	4	1	83	91	4
1	12	61	68	6	3	-14	74	75	5	4	2	216	210	5
1	13	91	91	5	3	-13	97	99	5	4	3	137	127	6
1	14	71	80	5	3	-12	19	42	17*	4	4	117	123	4
1	15	103	107	4	3	-11	144	138	7	4	5	153	151	6
1	16	0	59	21*	3	-10	221	230	6	4	6	121	134	5
1	17	83	73	5	3	-9	98	105	4	4	7	53	56	6
1	18	30	10	18*	3	-8	25	14	13*	4	8	51	55	6
2	-20	19	26	18*	3	-7	87	83	4	4	9	105	111	4
2	-19	32	25	10*	3	-6	66	74	5	4	10	68	79	5
2	-18	0	36	17*	3	-5	150	143	5	4	11	112	113	5
2	-17	60	61	7	3	-4	180	183	5	4	12	53	47	6
2	-16	124	117	6	3	-3	141	136	5	4	13	57	52	6
2	-15	149	158	7	3	-2	250	249	5	4	15	57	55	6
2	-14	85	72	5	3	-1	190	204	5	4	16	39	32	6
2	-13	76	86	6	3	0	355	347	4	5	-16	58	42	6
2	-12	102	103	5	3	1	180	165	5	5	-15	33	23	8*
2	-11	60	65	6	3	2	59	47	5	5	-14	0	25	15*
2	-10	108	106	5	3	3	167	168	5	5	-13	59	67	6
2	-9	72	75	5	3	4	272	282	5	5	-12	21	33	16*
2	-8	233	236	5	3	5	76	81	4	5	-11	54	59	6
2	-7	249	252	5	3	6	56	46	5	5	-10	54	64	6
2	-6	138	143	5	3	7	174	178	5	5	-9	129	150	5
2	-5	54	44	5	3	8	154	147	6	5	-8	121	127	5
2	-4	63	56	4	3	9	93	90	4	5	-7	22	34	14*
2	-3	299	304	4	3	10	57	65	6	5	-6	103	105	5
2	-2	362	344	4	3	11	122	134	5	5	-5	109	107	5
2	-1	117	109	5	3	12	0	17	16*	5	-4	45	49	6
2	0	138	146	5	3	13	58	39	5	5	-3	42	38	7
2	1	261	255	4	3	14	20	25	16*	5	-2	63	53	5
2	2	174	167	4	3	15	0	45	19*	5	-1	56	55	5
2	3	73	69	4	3	17	66	50	5	5	0	11	49	14*
2	4	336	323	4	4	-17	0	17	17*	5	1	0	32	14*
2	5	292	287	5	4	-16	29	32	15*	5	2	107	103	4
2	6	276	268	5	4	-15	92	89	5	5	3	69	72	5
2	7	26	28	15*	4	-14	94	96	5	5	4	35	37	6*
2	8	105	99	5	4	-13	67	58	5	5	5	20	51	16*
2	9	74	86	5	4	-12	118	135	5	5	6	115	123	5
2	10	53	52	6	4	-11	79	84	5	5	7	168	164	6
2	11	92	96	4	4	-10	38	37	8*	5	8	62	56	5
2	12	24	44	13*	4	-9	22	35	12*	5	9	35	46	8*
2	13	115	98	5	4	-8	175	168	6	5	10	0	7	15*
2	14	18	49	17*	4	-7	150	160	7	5	11	27	38	11*
2	15	0	44	15*	4	-6	107	110	5	5	12	26	30	15*
2	16	49	30	6	4	-5	165	162	6	5	14	0	17	16*
2	17	19	22	15*	4	-4	130	123	6	5	15	34	13	6*
2	18	73	60	5	4	-3	133	122	6	6	-14	0	9	16*
3	-18	22	43	17*	4	-2	86	79	4	6	-13	0	23	16*
3	-17	70	77	6	4	-1	164	158	5	6	-11	46	65	6
3	-16	0	37	18*	4	0	92	88	4	6	-10	52	60	6

Table A-7 (con't)

k	l	Fo	Fc	sigF	k	l	Fo	Fc	sigF	k	l	Fo	Fc	sigF
6	-9	10	60	15*	8	0	65	64	4	1	-18	58	54	7
6	-8	48	49	6	8	1	50	47	4	1	-17	82	82	6
6	-7	58	56	5	8	2	45	41	4	1	-16	77	67	6
6	-6	63	63	5	8	3	17	25	11*	1	-15	0	15	20*
6	-5	0	45	15*	8	4	0	10	12*	1	-14	30	10	18*
6	-4	85	82	.	8	5	33	27	5	1	-13	63	57	7
6	-3	0	67	17*	8	6	28	28	4	1	-12	114	122	5
6	-2	33	29	7*						1	-11	71	71	6
6	-1	23	18	14*	h = 4					1	-10	226	216	6
6	0	78	75	4						1	-9	83	84	5
6	1	134	124	6	0	-20	31	14	18*	1	-8	54	64	5
6	2	83	84	4	0	-19	6	2	19*	1	-7	201	215	5
6	3	0	32	14*	0	-18	88	70	6	1	-6	286	267	5
6	4	45	28	5	0	-17	108	113	6	1	-5	125	137	5
6	5	87	89	4	0	-16	0	12	16*	1	-4	168	167	5
6	6	101	108	5	0	-15	77	57	6	1	-3	234	256	4
6	7	10	9	15*	0	-14	132	129	6	1	-2	270	269	4
6	8	42	44	6	0	-13	82	59	5	1	-1	68	66	4
6	9	37	41	7*	0	-12	120	103	5	1	0	158	164	5
6	10	56	53	5	0	-11	134	130	5	1	1	300	296	4
6	11	0	24	16*	0	-10	0	47	17*	1	2	322	306	4
6	12	26	13	14*	0	-9	27	13	14*	1	3	183	192	5
6	13	26	30	14*	0	-8	0	39	16*	1	4	0	41	15*
7	-11	11	1	12*	0	-7	345	346	5	1	5	32	26	8*
7	-10	27	27	9*	0	-6	332	336	4	1	6	25	26	10*
7	-9	36	41	7*	0	-5	158	154	5	1	7	71	69	5
7	-8	37	46	7*	0	-4	68	75	4	1	8	138	138	6
7	-7	0	42	16*	0	-3	294	295	4	1	9	149	146	6
7	-6	50	59	6	0	-2	86	78	4	1	10	108	113	5
7	-5	58	59	5	0	-1	233	258	4	1	11	60	71	6
7	-4	31	39	8*	0	0	195	187	4	1	12	28	10	10*
7	-3	22	33	15*	0	1	163	155	4	1	13	31	38	16*
7	-2	70	70	4	0	2	93	93	4	1	14	50	66	7
7	-1	61	72	5	0	3	90	88	4	1	15	61	57	6
7	0	70	77	4	0	4	227	238	5	1	16	40	25	7
7	1	34	29	7*	0	5	146	160	5	1	17	30	22	9*
7	2	82	80	4	0	6	39	67	7*	2	-20	32	34	16*
7	3	81	87	4	0	7	56	56	5	2	-19	34	18	17*
7	4	25	32	13*	0	8	0	5	16*	2	-18	83	75	6
7	5	17	21	14*	0	9	26	26	13*	2	-17	70	53	7
7	7	25	33	13*	0	10	24	11	12*	2	-16	0	50	19*
7	8	45	42	5	0	11	0	16	12*	2	-15	73	70	6
7	9	17	23	13*	0	12	165	164	7	2	-14	135	132	6
7	10	29	19	6*	0	13	110	116	5	2	-13	61	45	7
8	-7	22	18	12*	0	14	0	36	17*	2	-12	79	79	5
8	-5	9	24	13*	0	15	44	31	8*	2	-11	31	20	16*
8	-4	41	45	5	0	16	53	45	6	2	-10	0	15	16*
8	-3	52	47	4	0	17	12	15	15*	2	-9	0	35	16*
8	-2	49	56	4	1	-20	0	24	19*	2	-8	57	54	5
8	-1	53	46	4	1	-19	93	88	5	2	-7	70	68	5

Table A-7 (con't)

k	l	Fo	Fc	sigF	k	l	Fo	Fc	sigF	k	l	Fo	Fc	sigF
2	-6	75	76	4	3	7	52	60	6	5	-7	106	106	5
2	-5	187	202	5	3	8	151	148	6	5	-6	97	94	4
2	-4	159	158	5	3	9	24	16	10*	5	-5	47	41	6
2	-3	62	51	4	3	10	116	122	5	5	-4	99	96	4
2	-2	286	289	4	3	11	47	43	6	5	-3	151	143	6
2	-1	172	163	5	3	12	28	13	15*	5	-2	70	64	5
2	0	189	194	5	3	13	50	57	6	5	-1	25	12	15*
2	1	76	71	4	3	14	21	38	12*	5	0	17	36	13*
2	2	118	115	5	3	15	34	26	7*	5	1	163	156	6
2	3	77	72	4	3	16	42	28	6	5	2	173	174	6
2	4	88	86	4	4	-17	29	12	15*	5	3	68	74	5
2	5	92	94	4	4	-16	0	37	16*	5	4	103	111	4
2	6	121	111	4	4	-15	46	46	7	5	5	76	73	4
2	7	96	98	5	4	-14	50	64	7	5	6	62	77	5
2	8	80	73	4	4	-13	83	80	5	5	7	86	84	4
2	9	68	75	5	4	-12	56	50	5	5	8	70	73	5
2	10	72	75	5	4	-11	59	57	6	5	9	99	98	4
2	11	92	90	5	4	-10	110	120	5	5	10	47	48	6
2	12	87	90	5	4	-9	108	105	5	5	12	0	16	15*
2	13	56	60	6	4	-8	102	101	4	5	13	16	31	14*
2	14	32	18	9*	4	-7	136	129	7	5	14	15	19	13*
2	15	11	35	16*	4	-6	142	137	6	6	-13	0	4	14*
2	16	0	4	14*	4	-5	54	55	6	6	-12	28	23	15*
2	17	0	4	15*	4	-4	158	154	6	6	-11	40	31	7*
3	-19	46	51	7	4	-3	100	107	4	6	-10	64	71	5
3	-18	12	10	13*	4	-2	134	119	6	6	-9	53	69	6
3	-17	30	21	17*	4	-1	171	177	6	6	-8	64	65	5
3	-16	33	44	11*	4	0	93	96	4	6	-7	65	75	5
3	-15	0	38	18*	4	1	55	53	5	6	-6	73	83	5
3	-14	0	32	20*	4	2	140	144	6	6	-5	141	140	7
3	-13	40	36	9*	4	3	166	176	6	6	-4	83	76	4
3	-12	132	151	5	4	4	143	124	6	6	-3	12	12	14*
3	-11	70	90	6	4	5	20	45	14*	6	-2	0	40	14*
3	-10	85	95	5	4	6	78	87	4	6	-1	109	115	5
3	-9	93	96	4	4	7	85	78	4	6	0	8	19	14*
3	-8	152	150	6	4	8	89	90	4	6	1	21	23	9*
3	-7	161	168	6	4	9	61	66	5	6	2	78	72	4
3	-6	30	27	15*	4	10	29	33	15*	6	3	97	97	5
3	-5	91	83	4	4	11	16	39	16*	6	4	35	32	7*
3	-4	154	148	6	4	12	100	103	5	6	5	0	15	13*
3	-3	305	297	5	4	14	38	41	7*	6	6	46	59	5
3	-2	76	95	4	4	15	41	28	5	6	7	78	74	4
3	-1	122	113	6	5	-15	0	37	15*	6	9	22	23	11*
3	0	170	179	5	5	-14	0	20	17*	6	10	0	36	15*
3	1	107	96	4	5	-13	34	40	10*	6	11	25	32	15*
3	2	92	80	4	5	-12	119	133	5	7	-10	0	6	13*
3	3	145	145	6	5	-11	22	40	14*	7	-9	0	47	15*
3	4	79	78	4	5	-10	27	11	16*	7	-8	48	29	5
3	5	83	81	4	5	-9	0	32	16*	7	-6	63	62	5
3	6	53	51	5	5	-8	84	79	5	7	-5	27	47	14*

Table A-7 (con't)

k	l	Fo	Fc	sigF	k	l	Fo	Fc	sigF	k	l	Fo	Fc	sigF
7	-4	44	44	5	0	4	73	76	4	2	-19	24	9	13*
7	-3	98	106	5	0	5	113	109	5	2	-18	56	52	7
7	-2	46	36	5	0	6	0	22	15*	2	-17	30	43	16*
7	-1	34	35	6*	0	7	45	45	6	2	-16	102	98	6
7	0	16	40	12*	0	8	68	70	5	2	-15	25	42	19*
7	1	39	36	5	0	9	0	22	16*	2	-14	55	47	8
7	2	0	29	13*	0	10	25	7	15*	2	-13	52	69	9*
7	3	0	31	12*	0	11	125	129	5	2	-12	60	66	7
7	4	36	31	5	0	12	76	73	5	2	-11	130	138	6
7	5	43	32	4	0	13	0	8	17*	2	-10	70	75	6
7	6	29	28	6*	0	14	38	15	8*	2	-9	183	188	6
7	7	0	13	12*	0	15	24	21	15*	2	-8	133	146	5
7	8	31	31	5	0	16	0	1	14*	2	-7	125	145	5
8	-6	21	29	12*	1	-20	0	39	16*	2	-6	68	69	4
8	-5	32	35	5	1	-19	16	24	14*	2	-5	212	203	5
8	-4	0	17	11*	1	-18	65	52	6	2	-4	196	193	5
8	-3	0	6	12*	1	-17	54	52	8	2	-3	156	154	6
8	-2	27	31	6*	1	-16	38	16	9*	2	-2	30	26	8*
8	-1	16	27	10*	1	-15	54	66	9	2	-1	98	97	4
8	0	18	28	11*	1	-14	121	107	6	2	0	155	166	5
8	1	16	9	12*	1	-13	53	47	8	2	1	50	37	5
8	2	0	28	10*	1	-12	36	44	10*	2	2	20	21	15*
8	3	17	32	11*	1	-11	46	71	9*	2	3	140	142	4
					1	-10	37	43	9*	2	4	199	191	6
					1	-9	45	36	7	2	5	176	173	5
					1	-8	87	98	5	2	6	126	121	6
					1	-7	48	34	6	2	7	76	81	5
					1	-6	170	159	6	2	8	0	51	15*
					1	-5	148	145	6	2	9	28	21	14*
					1	-4	93	94	4	2	10	39	31	7*
					1	-3	64	67	4	2	11	11	17	14*
					1	-2	370	363	5	2	12	69	72	5
					1	-1	197	179	5	2	13	57	56	5
					1	0	41	35	6	2	14	47	40	6
					1	1	75	78	4	2	15	14	17	15*
					1	2	78	88	4	3	-18	62	46	6
					1	3	49	66	5	3	-17	48	27	7
					1	4	53	44	5	3	-16	0	10	17*
					1	5	87	93	4	3	-15	90	90	5
					1	6	49	58	6	3	-14	52	49	8
					1	7	37	42	8*	3	-13	64	53	6
					1	8	37	56	9*	3	-12	88	101	5
					1	9	65	54	5	3	-11	179	198	7
					1	10	33	15	8*	3	-10	88	79	5
					1	11	56	55	6	3	-9	102	93	5
					1	12	56	47	6	3	-8	0	30	16*
					1	13	0	33	14*	3	-7	102	92	5
					1	14	31	51	16*	3	-6	142	141	6
					1	15	58	70	6	3	-5	214	212	6
					1	16	13	33	12*	3	-4	95	81	5

Table A-7 (con't)

k	l	Fo	Fc	sigF	k	l	Fo	Fc	sigF	k	l	Fo	Fc	sigF
3	-3	63	82	5	5	-13	22	19	16*	7	-5	18	7	10*
3	-2	135	127	6	5	-12	56	71	6	7	-4	38	29	5
3	-1	218	211	5	5	-11	46	36	7	7	-3	0	3	14*
3	0	144	136	6	5	-10	89	87	5	7	-2	42	45	5
3	1	77	90	4	5	-9	95	99	5	7	-1	30	36	6*
3	2	84	79	4	5	-8	59	59	6	7	0	17	27	10*
3	3	190	188	6	5	-7	18	39	16*	7	1	17	13	12*
3	4	0	57	18*	5	-6	94	104	5	7	2	49	49	4
3	5	94	95	4	5	-5	46	55	7	7	3	49	46	4
3	6	71	78	5	5	-4	0	42	15*	7	4	46	38	4
3	7	149	147	6	5	-3	0	50	16*	7	5	14	12	9*
3	8	79	79	4	5	-2	127	135	5	7	6	27	16	5*
3	9	28	44	9*	5	-1	87	90	4					
3	10	61	48	5	5	0	50	49	5	*****	h = 6	*****		
3	11	66	63	4	5	1	27	49	15*					
3	12	0	7	14*	5	2	72	70	4	0	-19	21	25	15*
3	13	41	37	7	5	3	60	57	4	0	-18	66	65	6
3	14	54	52	5	5	4	48	42	5	0	-17	0	27	18*
3	15	45	49	5	5	5	50	60	5	0	-16	41	10	9*
4	-16	46	42	7	5	6	96	94	5	0	-15	103	112	5
4	-14	31	32	10*	5	7	34	47	8*	0	-14	86	87	5
4	-13	91	99	5	5	8	17	39	15*	0	-13	95	85	5
4	-12	69	77	6	5	10	26	38	14*	0	-12	20	10	15*
4	-11	106	106	5	5	11	33	22	7*	0	-11	122	138	5
4	-10	0	22	16*	5	12	22	37	15*	0	-10	101	91	4
4	-9	138	146	6	6	-12	0	33	15*	0	-9	105	73	5
4	-8	0	57	16*	6	-11	33	17	7*	0	-8	48	40	6
4	-7	130	132	5	6	-9	45	40	6	0	-7	40	42	7
4	-6	12	49	12*	6	-8	26	10	15*	0	-6	0	11	14*
4	-5	111	108	4	6	-7	61	57	5	0	-5	128	126	6
4	-4	34	15	7*	6	-6	72	67	4	0	-4	48	50	6
4	-3	161	161	6	6	-5	28	20	9*	0	-3	216	208	5
4	-2	91	90	4	6	-4	75	79	4	0	-2	218	217	5
4	-1	0	3	11*	6	-3	42	16	6	0	-1	128	118	6
4	0	143	147	6	6	-2	42	54	6	0	0	0	28	14*
4	1	130	131	5	6	-1	54	50	5	0	1	113	107	5
4	2	24	30	13*	6	0	112	126	4	0	2	133	127	6
4	3	101	103	5	6	1	0	14	13*	0	3	71	72	5
4	4	156	162	6	6	2	16	7	12*	0	4	28	10	15*
4	5	148	146	6	6	3	36	37	6	0	5	0	7	16*
4	6	29	29	9*	6	4	89	82	4	0	6	0	40	16*
4	7	21	7	12*	6	5	57	69	4	0	7	57	58	6
4	8	56	50	5	6	6	23	23	8*	0	8	0	37	17*
4	9	79	82	4	6	7	20	19	13*	0	9	46	34	7
4	10	45	51	6	6	8	23	18	13*	0	10	0	9	16*
4	11	0	17	14*	6	9	45	40	5	0	11	175	170	7
4	12	33	26	7*	6	10	45	33	4	0	12	78	78	5
4	13	41	49	6	7	-8	17	20	13*	0	13	39	5	7*
4	14	35	34	6*	7	-7	0	9	13*	0	14	37	47	8*
5	-14	32	43	10*	7	-6	24	42	13*	1	-19	9	16	16*

Table A-7 (con't)

k	l	Fo	Fc	sigF	k	l	Fo	Fc	sigF	k	l	Fo	Fc	sigF
1	-18	12	52	16*	2	-1	56	51	5	4	-13	49	54	8
1	-17	87	80	5	2	0	120	117	4	4	-12	77	81	5
1	-16	0	26	15*	2	1	146	148	6	4	-11	0	11	16*
1	-15	57	51	7	2	2	152	145	6	4	-10	99	97	5
1	-14	56	48	7	2	3	84	81	4	4	-9	91	87	4
1	-13	42	44	9*	2	4	44	24	6	4	-8	94	107	4
1	-12	84	72	6	2	5	105	121	5	4	-7	11	26	16*
1	-11	118	110	5	2	6	130	138	5	4	-6	162	148	6
1	-10	77	54	5	2	7	52	53	5	4	-5	26	38	16*
1	-9	79	78	5	2	8	36	32	7*	4	-4	0	69	16*
1	-8	157	148	7	2	9	55	44	5	4	-3	59	56	5
1	-7	105	97	5	2	10	46	53	6	4	-2	145	144	6
1	-6	10	18	14*	2	11	71	73	5	4	-1	69	77	5
1	-5	26	61	16*	2	12	0	34	15*	4	0	81	73	4
1	-4	169	164	6	2	13	0	9	13*	4	1	75	74	4
1	-3	46	59	6	2	14	0	26	13*	4	2	130	126	6
1	-2	108	93	4	3	-17	0	16	15*	4	3	59	59	5
1	-1	133	133	6	3	-16	67	46	5	4	4	41	42	6
1	0	77	74	4	3	-15	67	64	6	4	5	47	53	6
1	1	141	135	6	3	-14	31	19	16*	4	6	72	71	4
1	2	73	76	4	3	-13	51	39	7	4	7	64	67	5
1	3	87	92	4	3	-12	83	64	5	4	8	0	5	14*
1	4	43	31	7	3	-11	89	87	5	4	9	0	12	14*
1	5	83	92	4	3	-10	73	68	5	4	10	40	38	6
1	6	46	58	6	3	-9	101	101	4	4	11	0	33	14*
1	7	116	114	5	3	-8	144	152	6	4	12	19	15	10*
1	8	114	117	5	3	-7	12	28	15*	5	-14	0	21	16*
1	9	108	113	5	3	-6	59	73	5	5	-13	69	60	5
1	10	53	52	6	3	-5	134	132	7	5	-12	22	15	15*
1	11	0	7	17*	3	-4	129	134	4	5	-11	25	18	16*
1	12	30	36	9*	3	-3	55	55	6	5	-10	25	25	15*
1	13	50	31	5	3	-2	67	62	5	5	-9	0	32	18*
1	14	44	46	6	3	-1	24	28	12*	5	-8	66	64	5
2	-18	0	19	15*	3	0	135	145	6	5	-7	35	44	8*
2	-17	0	21	18*	3	1	25	22	15*	5	-6	55	51	6
2	-16	0	28	18*	3	2	122	127	4	5	-5	0	38	15*
2	-15	71	69	7	3	3	79	81	5	5	-4	122	124	5
2	-14	0	53	20*	3	4	98	95	5	5	-3	57	40	5
2	-13	32	24	17*	3	5	42	49	6	5	-2	23	44	16*
2	-12	65	66	7	3	6	16	26	14*	5	-1	80	81	4
2	-11	58	46	7	3	7	89	91	4	5	0	130	120	6
2	-10	67	56	6	3	8	67	60	5	5	1	110	109	4
2	-9	142	122	7	3	9	14	43	16*	5	2	71	66	4
2	-8	18	23	16*	3	10	42	52	6	5	3	90	94	4
2	-7	22	41	13*	3	11	28	17	8*	5	4	29	32	8*
2	-6	72	71	4	3	12	0	30	14*	5	5	0	52	13*
2	-5	57	43	5	3	13	29	3	6*	5	6	24	30	10*
2	-4	38	41	8*	4	-16	0	8	14*	5	7	0	24	13*
2	-3	169	177	6	4	-15	24	24	15*	5	8	17	25	13*
2	-2	147	137	6	4	-14	24	56	17*	5	9	62	58	4

Table A-7 (con't)

k	l	Fo	Fc	sigF	k	l	Fo	Fc	sigF	k	l	Fo	Fc	sigF
5	10	19	22	11*	0	1	26	30	15*	2	-9	67	75	6
6	-11	30	34	7*	0	2	53	60	6	2	-8	0	41	16*
6	-10	8	25	13*	0	3	0	5	16*	2	-7	26	37	16*
6	-9	51	45	5	0	4	124	133	5	2	-6	79	91	5
6	-8	0	21	15*	0	5	19	29	17*	2	-5	133	150	6
6	-7	67	76	5	0	6	21	6	16*	2	-4	84	79	4
6	-6	70	66	5	0	7	0	29	15*	2	-3	122	121	4
6	-5	69	69	5	0	8	148	123	7	2	-2	106	116	5
6	-4	29	15	8*	0	9	0	3	15*	2	-1	129	132	6
6	-3	60	61	5	0	10	72	77	5	2	0	81	87	5
6	-2	0	17	13*	0	11	52	38	6	2	1	84	86	4
6	-1	45	43	5	0	12	0	15	13*	2	2	23	42	13*
6	0	19	20	10*	1	-17	47	52	7	2	3	43	40	7
6	1	0	42	13*	1	-16	0	12	17*	2	4	117	129	5
6	2	33	19	6*	1	-15	22	39	17*	2	5	88	96	4
6	3	52	43	4	1	-14	24	47	18*	2	6	25	22	13*
6	4	48	55	6	1	-13	54	30	7	2	7	18	24	12*
6	5	51	40	4	1	-12	25	25	16*	2	8	65	61	5
6	6	63	60	4	1	-11	34	24	8*	2	9	18	34	15*
6	7	59	55	3	1	-10	54	45	6	2	10	0	23	14*
7	-6	0	19	12*	1	-9	53	53	6	2	11	40	33	6
7	-5	34	29	5	1	-8	83	75	4	2	12	0	24	13*
7	-4	45	39	4	1	-7	111	107	5	3	-16	23	38	16*
7	-3	28	41	6*	1	-6	161	171	6	3	-15	30	29	10*
7	-2	16	11	11*	1	-5	95	101	5	3	-14	53	49	7
7	-1	0	13	11*	1	-4	0	21	14*	3	-13	26	54	17*
7	0	19	20	9*	1	-3	62	55	5	3	-12	51	48	6
7	1	38	34	4	1	-2	115	123	5	3	-11	84	66	5
7	2	16	8	10*	1	-1	110	114	5	3	-10	68	71	5
.....	h = 7	1	0	38	44	7*	3	-9	20	49	14*
.....	1	1	48	49	6	3	-8	65	51	5
.....	1	2	129	122	6	3	-7	122	125	5
.....	1	3	139	152	6	3	-6	148	144	7
0	-17	0	2	14*	1	4	38	35	7*	3	-5	23	46	14*
0	-16	23	5	12*	1	5	67	77	5	3	-4	55	58	6
0	-15	0	16	18*	1	6	30	16	16*	3	-3	77	67	4
0	-14	32	59	11*	1	7	0	17	16*	3	-2	59	54	5
0	-13	43	60	9*	1	8	58	68	6	3	-1	141	142	6
0	-12	73	70	5	1	9	0	10	16*	3	0	47	55	6
0	-11	5	29	15*	1	10	58	62	5	3	1	120	127	4
0	-10	0	13	15*	1	11	0	9	14*	3	2	104	107	4
0	-9	78	76	4	1	12	13	31	15*	3	3	96	109	5
0	-8	54	54	5	2	-17	0	57	17*	3	4	55	55	5
0	-7	0	5	16*	2	-16	0	12	17*	3	5	50	55	6
0	-6	207	194	5	2	-15	47	55	8*	3	6	54	59	5
0	-5	176	207	6	2	-14	0	16	18*	3	7	14	43	15*
0	-4	81	79	4	2	-13	59	59	6	3	8	25	3	13*
0	-3	25	41	10*	2	-12	91	99	5	3	9	27	20	8*
0	-2	126	133	4	2	-11	68	62	6	3	10	34	30	6*
0	-1	105	96	5	2	-10	61	56	6	3	11	0	23	14*

Table A-7 (con't)

k	l	Fo	Fc	sigF	k	l	Fo	Fc	sigF	k	l	Fo	Fc	sigF
4	-14	0	22	15*	6	-2	0	15	9*	1	-1	69	67	5
4	-13	59	58	5	6	-1	0	18	12*	1	0	99	100	4
4	-12	69	62	5	6	0	20	31	11*	1	1	42	49	7
4	-11	6	34	14*	6	1	40	31	4	1	2	62	61	5
4	-10	36	25	8*	6	2	9	22	10*	1	3	29	22	15*
4	-9	49	63	6	6	3	0	42	12*	1	4	70	74	5
4	-8	46	53	7						1	5	90	85	4
4	-7	0	8	17*	***** h = 8 *****					1	6	25	28	14*
4	-6	52	43	6						1	7	73	84	5
4	-5	57	43	6	0	-16	40	36	6	1	8	68	70	5
4	-4	76	82	4	0	-15	54	73	6	1	9	46	33	5
4	-3	85	98	4	0	-14	57	55	5	1	10	29	21	7*
4	-2	16	23	12*	0	-13	34	6	8*	2	-15	43	27	6
4	-1	97	101	5	0	-12	40	43	7*	2	-14	34	25	8*
4	0	103	101	4	0	-11	81	94	5	2	-13	0	18	15*
4	1	19	29	12*	0	-10	92	98	4	2	-12	0	10	16*
4	2	40	35	6	0	-9	55	70	5	2	-11	0	19	16*
4	3	68	65	4	0	-8	29	35	9*	2	-10	96	86	5
4	4	62	65	5	0	-7	66	65	4	2	-9	54	67	7
4	5	0	12	14*	0	-6	23	20	14*	2	-8	26	19	10*
4	6	18	9	10*	0	-5	0	28	13*	2	-7	0	23	14*
4	7	0	23	13*	0	-4	56	69	5	2	-6	68	70	5
4	8	44	46	5	0	-3	99	104	4	2	-5	90	103	4
4	9	0	17	12*	0	-2	71	69	4	2	-4	0	38	15*
5	-12	0	15	15*	0	-1	110	110	4	2	-3	53	60	5
5	-11	0	36	16*	0	0	56	53	6	2	-2	67	70	5
5	-10	53	50	5	0	1	72	74	4	2	-1	83	90	4
5	-9	50	47	6	0	2	71	58	5	2	0	11	29	15*
5	-8	27	14	9*	0	3	21	41	15*	2	1	79	85	4
5	-7	27	53	15*	0	4	36	37	8*	2	2	92	97	4
5	-6	24	28	11*	0	5	128	119	5	2	3	16	39	14*
5	-5	16	12	11*	0	6	78	67	5	2	4	62	63	5
5	-4	58	70	5	0	7	0	5	12*	2	5	65	58	4
5	-3	63	67	5	0	8	28	33	16*	2	6	51	57	6
5	-2	0	3	13*	0	9	53	30	5	2	7	17	5	11*
5	-1	47	50	5	0	10	83	82	4	2	8	27	24	13*
5	0	40	38	6	1	-15	0	14	15*	2	9	0	30	14*
5	1	40	24	6	1	-14	48	38	6	3	-13	32	39	9*
5	2	26	35	13*	1	-13	59	67	6	3	-12	14	35	16*
5	3	40	38	5	1	-12	55	52	6	3	-11	0	16	17*
5	4	21	6	11*	1	-11	29	36	16*	3	-10	62	61	5
5	5	0	13	12*	1	-10	25	40	13*	3	-9	49	40	5
5	6	25	41	9*	1	-9	89	94	4	3	-8	20	11	12*
5	7	31	27	5*	1	-8	91	99	4	3	-7	22	25	15*
6	-8	33	29	6*	1	-7	55	66	5	3	-6	0	48	16*
6	-7	37	27	5	1	-6	37	39	7*	3	-5	8	10	14*
6	-6	0	10	13*	1	-5	64	79	5	3	-4	64	65	5
6	-5	0	15	13*	1	-4	126	112	6	3	-3	54	54	6
6	-4	0	9	13*	1	-3	50	34	5	3	-2	14	18	14*
6	-3	0	21	13*	1	-2	51	53	5	3	-1	24	7	14*

References

1. W. Stoeckenius and R. Rowen, *J. Cell Biol.* 34, 65(1962).
2. G. Wald, *Science*, 162, 230(1968).
3. H. Larsen, *Adv. Microbiol.* 1, 97(1967).
4. D. Oesterhelt, W. Stoeckenius, *Nature New Biol.* 233, 149(1971).
5. G. S. Harbison, S. O. Smith, J. A. Pardoen, C. Winkel, J. Lugtenburg, J. Herzfeld, R. Mathies and R.G. Griffin, *Proc. Natl. Acad. Sci. USA* 81, 1706(1984).
6. R. H. Lozier, R. A. Bogomolni and W. Stoeckenius, *Biophys. J.* 15, 907(1975).
7. M. C. Kung, D. Devault, B. Hess and D. Oesterhelt, *Biophys. J.* 15, 907(1975).
8. R. A. Mathies, C. H. Brito-Cruz, W. T. Pollard, C. V. Shank, *Science*, 240, 777(1988).
9. A. V. Sharkov, A. V. Pakulev, S. V. Chekalin, Y. A. Matveetz, *Biochim. Biophys. Acta.* 808, 94(1985).
10. R. R. Birge, T. M. Cooper, *Biophys. J.* 42, 61(1983).
11. M. Braiman, R. Mathies, *Proc. Natl. Acad. Sci. USA*, 79, 403(1982).
12. S. O. Smith, A. B. Myers, J. A. Pardoen, C. Winkel, P. P. J. Mulder, J. Lugtenburg, R. Mathies, *Proc. Natl. Acad. Sci. USA* 81, 2055(1984).

13. D. L. Narva, R. H. Callender, T. G. Ebrey, *Photochemistry and Photobiology* **33**, 567(1981).
14. J. B. Ames, S. P. S. Fodor, R. Gebhard, J. Raap, E. M. M. van den Berg, J. Lugtenburg and R. A. Mathies, *Biochemistry* **28**, 3681(1989).
15. S. P. A. Fodor, W. T. Pollard, R. Gebhard, E. M. M. van den Berg, J. Lugtenburg, R. A. Mathies, *Proc. Natl. Acad. Sci. USA* **85**, 2156(1988).
16. S. O. Smith, J. A. Pardoen, P. P. J. Mulder, B. Curry, J. Lugtenburg, R. A. Mathies, *Biochemistry* **22**, 6141(1983).
17. J-M. Fang, J. D. Carriker, V. Balogh-Nair and K. Nakanishi, *J. Am. Chem. Soc.* **105**, 5162(1983).
18. E. Kolling, W. Gartner, D. Oesterhelt and L. Ernst, *Angew. Chem. Int. Ed. Engl.* **23**, 81(1984).
19. B. Aton, A. Doukas, R. Callender, B. Becker and T. Ebrey, *Biochemistry* **16**, 2995(1977).
20. D. Ort and W. Parson, *J. Biol. Chem.* **253**, 6158(1978).
21. R. Govindjee, T. Ebrey and A. Crofts, *Biophys. J.* **30**, 231(1980).
22. Q-Q. Li, R. Govindjee, T. G. Ebrey, *Proc. Natl. Acad. Sci. U.S.A.* **81**, 7079(1984).
23. S. O. Smith, A. B. Myers, R. A. Mathies, J. A. Pardoen, C. Winkel, E. M. M van den Berg and J. Lugtenburg, *Biophys. Soc.* **47**, 653(1985).
24. M. J. Pettei, A. P. Yudd, K. Nakanishi, R. Henselman and W.

- Stoeckenius, *Biochemistry* 16, 1955(1977).
25. G. S. Harbison, P. P. J. Mulder, H. Pardoën, J. Lugtenburg, J. Herzfeld and R. G. Griffin, *J. Am. Chem. Soc.* 107, 4809(1985).
 26. B. Curry, A. Broeck, J. Lugtenburg and R. Mathies, *J. Am. Chem. Soc.* 104, 5274(1982).
 27. K. J. Kaufmann, P. M. Rentzepis, W. Stoeckenius and A. Lewis, *Biochem. Biophys. Res. Comm.* 68, 1109(1976).
 28. T. Hamanaka, T. Mitsui, T. Ashida and M. Kakudo, *Acta Cryst.* B28, 214(1972).
 29. B. Honig, B. Hudson, B. D. Sykes and M. Karplus, *Proc. Natl. Acad. Sci. USA* 68, 1289(1971).
 30. P. Tavan, K. Schulten and D. Oesterhelt, *Biophys. J.* 415(1985).
 31. B. Santarsiero, M. James, M. Mahendran and R. F. Childs, *J. Am. Chem. Soc.* 112, 9416(1990).
 32. H. G. Khorana, G. E. Gerber, W. C. Herlitz, C. P. Gray, R. J. Anderegg, K. Nihei, K. Biemann, *Proc. Natl. Acad. Sci. U.S.A.* 76, 5046(1979).
 33. P. N. T. Unwin and R. Henderson, *J. Mol. Biol.* 94, 425(1975).
 34. B. A. Lewis, G. S. Harbison, J. Herzfeld and R. G. Griffin, *Biochemistry* 24, 4671(1985).
 35. R. Henderson, J. M. Baldwin, T. A. Ceska, F. Zemlin, E. Beckmann and K. H. Downing, *J. Mol. Biology* 213, 899(1990).

36. T. Marti, S. J. Rosselet, H. Otto, M. P. Heyn and H. G. Khorana, *J. Biol. Chem.* 266, 18674(1991).
37. P. E. Blatz, J. H. Mohler and V. Navangul, *Biochemistry* 11, 848(1972).
38. A. Allerhand, P. Schleyer, *J. Am. Chem. Soc.* 85, 1233(1963).
39. P. E. Blatz and J. H. Mohler, *Biochemistry* 11, 3240(1972).
40. B. Honig, A. D. Greenberg, H. Dinur and T. G. Ebrey, *Biochemistry* 15, 4593(1976).
41. K. Nakanishi, V. Balogh-Nair, M. Arnaboldi, K. Tsujimoto and B. Honig, *J. Am. Chem. Soc.* 102, 7945(1980).
42. M. G. Motto, M. Sheves, K. Tsujimoto, V. Balogh-Nair and K. Nakanishi, *J. Am. Chem. Soc.* 102, 7947(1980).
43. A. M. Schaffer, T. Yamaoka, R. S. Becker, *Photochem. Photobiol.* 21, 297(1975).
44. U. Dinur, B. Honig, K. Schulten, *Chem. Phys. Lett.* 72, 493(1980).
45. S. Harbison, S. Smith, J. Pardoen, J. Courtin, J. Lugtenburg, J. Herzfeld, R. Mathies and R. Griffin, *Biochemistry* 24, 6955(1985).
46. J. Lugtenburg, M. Muradin-Szweykowska, C. Heeremans, J. A. Pardoen, G. S. Harbison, J. Hersfeld, R. G. Griffin, S. O. Smith and R. A. Mathies, *J. Am. Chem. Soc.* 108, 3104(1986).
47. R. Van der Steen, P. L. Biesheurel, R. A. Mathies and J. Lugtenburg, *J. Am. Chem. Soc.* 108, 6410(1986).

48. M. Sheves, T. Baasov and N. Friedman, *J. Chem. Soc. Chem. Commun.*, 77(1983).
49. T. Baasov, M. Sheves, *Israel J. Chem.* 25, 53(1985).
50. S. Seltzer and R. Zuckermann, *J. Am. Chem. Soc.* 107, 5523(1985).
51. K. Ohno, Y. Takenchi and M. Yashida, *Biochem. Biophys. Acta.* 462, 575(1977).
52. F. Merenji, G. Nettermark and B. Roos, *Chem. Phys.* 1, 340(1973).
53. S. Seltzer, *J. Am. Chem. Soc.* 109, 1627(1987).
54. D. Lukton and R. R. Rando, *J. Am. Chem. Soc.* 106, 258(1980).
55. D. Lukton and R. R. Rando, *J. Am. Chem. Soc.* 106, 4525(1984).
56. R. F. Childs and B. D. Dickie, *J. Am. Chem. Soc.* 105, 5041(1983).
57. S. Seltzer, *J. Am. Chem. Soc.* 112, 4477(1990).
58. R. F. Childs, G. S. Shaw and C. J. L. Lock, *J. Am. Chem. Soc.* 111, 5424(1989).
59. R. R. Birge, L. P. Murray, R. Zidovetzki and H. M. Knapp, *J. Am. Chem. Soc.* 109, 2090(1987).
60. R. F. Childs, G. S. Shaw and R. E. Wasylishen, *J. Am. Chem. Soc.* 109, 5362(1987).
61. D. Cossette and D. Vocelle, *Can. J. Chem.* 65, 1576(1987).
62. A. Albeck, N. Livnah, H. Gottlieb and M. Sheves, *J. Am. Chem. Soc.* 114, 2400(1992).

63. M. Pankratz and R. F. Childs, *J. Org. Chem.*, 30, 4553(1985).
64. I. Gupta, K. Suzuki, N. R. Bruce, J. J. Krepinsky and P. Yates, *Science* 225, 521(1984).
65. R. F. Childs, M. Mahendran, S. D. Zweep, G. S. Shaw, S. K. Chadda, N. A. D. Burke, B. E. George, G. Faggiani and C. J. L. Lock, *Pure and Appl. Chem.* 58, 111(1986).
66. R. F. Childs, R. Faggiani, C. J. L. Lock, M. Mahendran, S. D. Zweep, *J. Am. Chem. Soc.* 108, 1692(1986).
67. R. F. Childs, M. D. Kostyk, C. J. L. Lock and M. Mahendran, *J. Am. Chem. Soc.* 112, 8912(1990).
68. M. D. Kostyk, PhD. Thesis, McMaster University, 1992.
69. R. F. Childs, M. D. Kostyk, C. J. L. Lock and M. Mahendran, *Can. J. Chem.* 69, 2024(1991).
70. G. A. Olah, Y. Halpern, Y. K. Mo, G. Liang, *J. Am. Chem. Soc.* 94, 3554(1972).
71. R. F. Childs, E. F. Lund, A. G. Marshall, W. J. Morrissey and C. V. Rogerson, *J. Am. Chem. Soc.* 98, 5924(1976).
72. J. Griffiths and H. Hart, *J. Am. Chem. Soc.* 90, 5296(1968).
73. H. Hart and T. Takino, *J. Am. Chem. Soc.* 93, 720(1971).
74. R. J. Gillespie and T. E. Peel, *J. Am. Chem. Soc.* 95, 5173(1973).
75. C. Blackburn and R. F. Childs, *J. Chem. Soc. Chem. Commun.*,

- 812(1984).
76. E. L. Eliel in "Stereochemistry of Carbon Compounds", McGraw-Hill, New York, N.Y., 1962, p236.
 77. K. Mullen, E. Kotzamani, H. Schmickler and B. Frei, *Tett. Lett.* 25, 5623(1984).
 78. R. F. Childs and M. E. Hagar, *Can. J. Chem.* 58, 1788(1980).
 79. D. Cremer, J. Gauss, R. F. Childs and C. Blackburn, *J. Am. Chem. Soc.* 107, 2435(1985).
 80. C. Blackburn, R. F. Childs, D. Cremer and J. Gauss, *J. Am. Chem. Soc.* 107, 2442(1985).
 81. D. M. Brouwer, J. A. van Doorn and A. A. Kiffen, *Recl. Trav. Chem. Pays-Bas.* 94, 198(1975).
 82. R. F. Childs and G. S. Shaw, *J. Chem. Soc. Chem. Commun.*, 261(1983).
 83. B. C. L Weedon and R. J. Woods, *J. Chem. Soc.*, 2687(1951).
 84. N. J. Leonard and J. V. Paukstelis, *J. Org. Chem.* 28, 3021(1963).
 85. P. E. Blatz and J. H. Mohler, *Biochemistry* 14, 2304(1975).
 86. G. S. Shaw, PhD. Thesis, McMaster University, 1988.
 87. C. Pattaroni and J. Lauterwein, *Helv. Chim. Acta.* 64, 1969(1981).
 88. R. F. Childs and B. D. Dickie, *J. Chem. Soc. Chem. Commun.*, 1268(1981).
 89. S. J. Opella and M. H. Frey, *J. Am. Chem. Soc.* 101, 5854(1979).

90. H. Kobayshi, Y. Vanagawa, H. Osada, S. Minami and M. Shiziwa, Bull. Chem. Soc. Japan 46, 1471(1972).
91. F. H. Allen, O. Kennard, D. G. Watson, L. Brammer, A. G. Orpen and R. Taylor, J. Chem. Soc. Perkin. Trans. II S1(1987).
92. L. M. Trefonas, R. L. Flurry Jr, R. Majeste, E. A. Meyers and R. F. Copeland, J. Am. Chem. Soc. 88, 2145 (1966)
93. R. F. Childs, B. D. Dickie, R. Faggianni, C. A. Fife, C. J. L. Lock and R. E Wasylshen, J Cryst. Spec. Res. 15, 23(1985).
94. R. F. Childs, G. S. Shaw and C. J. L. Lock, J. Am. Chem. Soc. 111, 5424(1989).
95. P. E. Blatz and D. L. Pippert, J. Am. Chem. Soc. 90, 1296(1968).
96. S. S. Malhotra and M. C. Whiting, J. Chem. Soc., 3812(1960).
97. J-O. Lundgren, Acta. Cryst. B35, 1027(1979).
98. V. H. Hartl, Acta. Cryst. B31, 1781(1975).
99. A. J. Serewicz, B. K. Robertson and E. A. Meyers, J. Phys. Chem. 69, 1915(1965).
100. R. Taylor and O. Kennard, J. Am. Chem. Soc. 104, 5063(1982).
101. G. R. Desiraju, Acc. Chem. Res. 24, 290(1991).
102. W. Suenger, Angew. Chem. Int. Ed. Engl. 12, 591(1973); G. A. Jeffrey, H. Maluszynska, Int. J. Bio. Macromol. 4, 173(1982).
103. G. S. Harbison, S. Smith, J. Pardoen, J. Courtin, J. Lugtenburg, J. Herzfeld, R.

- Mathies, R. Griffin, *Biochemistry* 24, 6955(1985).
104. L. Mukherjee, *J. Phys. Chem.* 62, 1311(1958); T. Baasov and M. Sheves, *Biochemistry* 25, 5249(1986).
105. K. J. Rothschild and H. Marrero, *Proc. Natl. Acad. Sci. U.S.A.* 79,4045(1982).
106. F. Derguini, D. Dunn, L. Eisenstein, K. Nakanishi, K. Odashima, V. J. Rao, L. Sastry and J. Termini, *Pure and Appl. Chem.* 58, 719(1986).
107. R. F. W. Bader, *Can. J. Chem.* 64, 1036(1986).
108. B. Honig, B. Hudson, B. D. Sykes and M. Karplus, *Proc. Natl. Acad. Sci. U.S.A.* 68, 1289(1970).
109. J. Langlet, B. Pullman and H. Berthod, *J. Mol. Structure*, 6, 139(1970).
110. M. Engelhard, K. Gerwert, B. Hess, W. Krentz and F. Siebert, *Biochemistry* 24, 400(1985); M. Braiman, T. Mogi, T. Marti, L. Stern, H. Khorana and K. Rothschild, *Biochemistry* 27, 8516(1988); K. Gerwert, B. Hess, J. Soppa and O. Oesterhelt, *Proc. Natl. Acad. Sci. U.S.A.* 86, 4943(1989).
111. T. E. Hogen-Esch and J. Smid, *J. Am. Chem. Soc.* 88, 307(1966).
112. J. B. Grutzner, J. M. Lawlor and L. M. Jackman, *J. Am. Chem. Soc.* 94, 2306(1972).
113. P. C. Mowery and W. Stoeckenius, *J. Am. Chem. Soc.* 101, 414(1979).
114. M. Sheves and T. Baasov, *J. Am. Chem. Soc.* 106, 6840(1984).

115. R. F. Childs and G. S. Shaw, *J. Am. Chem. Soc.* 110, 3013(1988).
116. S. J. Milder, *Biophys. J.* 60, 490(1991).
117. G. A. Olah, G. K. S. Prakash and J. Sommer in "Superacids", Wiley-Interscience, N.Y., 1985, p34.
118. P. W. Atkins in "Physical Chemistry", W. H. Freeman and Co., San Francisco, 1982, p932.
119. J. B. Milne in "The Chemistry of Non-Aqueous Solvents", J. J. Lagowski, Ed., Academic Press, New York, 1978, Vol VB, p1-52.
120. N. C. Baird, *Tetrahedron*, 28, 2355(1972).
121. M. Yato, T. Ohwada and K. Shudo, *J. Am. Chem. Soc.* 113, 691(1991).
122. R. D. Gilliom in "Introduction to Physical Organic Chemistry", W. R. Moore and F. D. Greene, Eds., Addison-Wesley Publishing Co., Reading Ma., 1970, p121.
123. D. M. Brouwer, E. L. Mackor and C. Maclean, *Rec. Trav. Chim.* 85, 114(1966).
124. R. F. Childs, M. Mahendran, C. Blackburn and G. Antoniadis, *Can. J. Chem.* 66, 1355(1988).
125. R. M. Orgias, MSc. Thesis, McMaster University, Hamilton, Ontario, 1989.
126. T-L Ho and S-H Liu, *Chem. Ind.(London)* 11, 371(1982).
127. J. C. Gilbert and K. R. Smith, *J. Org. Chem.* 41, 3883(1976).

128. N. C. Deno and C. U. Pittman Jr., *J. Am. Chem. Soc.* 86, 1871(1964).
129. T. S. Sorensen, *Can. J. Chem.* 42, 2768(1964).
130. T. S. Sorensen and R. Z. Bladec, *Can. J. Chem.* 50, 2806(1972).
131. R. B. Woodward and R. Hoffmann, *J. Am. Chem. Soc.* 87, 395(1965).
132. N. W. K. Chiu and T. S. Sorensen, *Can. J. Chem.* 51, 2776(1973).
133. I. N. Nazarov, I. I. Zaretskaya and T. I. Sorkina, *Zhur. Obsheei Khim.* 30, 746(1960).
134. D. Kurkland, PhD. Thesis, Harvard University, 1967.
135. R. Lehr, PhD. Thesis, Harvard University, 1968.
136. G. Ohloff, K. H. Schulte-Elte and E. Demole, *Helv. Chim. Acta.* 54, 2813(1971).
137. G. J. Karabatsos and J. L. Fry in "Carbonium Ions" Vol II, G.A. Olah and P. von R. Schleyer, Eds., Wiley-Interscience, New York, 1970, p521.
138. R. F. Childs, T. Diclemente, E. F. Lund-Lucas, T. J. Richardson and C. V. Rogerson, *Can. J. Chem.* 61, 856(1983).
139. H. Hart and A. F. Naples, *J. Am. Chem. Soc.* 94, 3256(1972).
140. A. R. de Lera, W. Reischl and W. H. Okamura, *J. Am. Chem. Soc.* 111, 4051(1989).
141. W. L. Earl, D. L. Vander Hart, *J. Magn. Res.* 48, 35 (1982).
142. L. P. Hammett in "Physical Organic Chemistry", McGraw-Hill, New York, 1970, p. 263-313.

143. J. W. Moore and R. G. Pearson in "Kinetics and Mechanism", 3rd ed, Wiley: New York, 1981, pg. 304.
144. MITHRIL: C. J. Gilmore; an integrated direct methods computer program. J. Appl. Cryst. 47, 42-46, Univ. of Glasgow, Scotland, 1984.

DIRDIF: P. T. Beurskens; direct methods for difference structures - an automatic procedure for phase extension and refinement of difference structure factors. Technical Report 1984/1 Crystallography Laboratory, Toernooiveld, 6525 Ed Nijmegen, Netherlands.

D. T. Cromer and J. T. Waber; "International Tables for X-ray Crystallography", Vol. IV, The Kynoch Press, Birmingham, England, Table 2.2 A (1974).

J. A. Ibers and W. C. Hamilton, Acta. Cryst. 17, 781(1964).

D. T. Cromer, "International Tables for X-ray Crystallography", Vol IV, The Kynoch Press, Birmingham, England, Table 2.3.1 (1974).

TEXSAN - TEXRAY Structure Analysis Package, Molecular Structure Corporation (1985).